New perspectives to undestand the lipid packing recognition by the curvature sensor ALPS (amphipathic lipid packing sensor) : molecular dynamics studies

Paula Gonzalez-Rubio Garrido

THESE DE DOCTORAT

DE L'UNIVERSITÉ PIERRE ET MARIE CURIE PARIS - VI

Spécialité

Sciences de la vie

École Doctorale Interdisciplinaire pour le vivant (ED 387)

Présenté par

M.S Paula Gonzalez-Rubio Garrido

Pour obtenir le grade de

Docteur de l'Université de Pierre et Marie curie

Nouvelles perspectives pour comprendre la reconnaissance des défauts d'empaquetage lipidique par le senseur de courbure membranaire ALPS (Amphipathic Lipid Packing Sensor): études par dynamique moléculaire.

Soutenue le 27.11.2009

devant le jury composé de :

Rapporteurs:

Monique Genest

James Sturgis

Examinateurs:

Guillaume Drin

Julie Ménétrey

Germain Trugnan

Directrice de thèse: Catherine Etchebest

Co-Directeur de thèse: Patrick Fuchs

NEW PERSEPCTIVES TO UNDERSTAND THE LIPID PACKING RECOGNITION BY THE CURVATURE SENSOR ALPS (AMPHIPATHIC LIPID PACKING SENSOR): MOLECULAR DYNAMICS STUDIES

Paula González-Rubio Garrido

27 novembre 2009

DSIMB INSERM UMR S-665 INTS,
6 rue Alexandre Cabanel 75015 Paris FRANCE.

Résumé

La recherche concernant les processus de la modulation de la courbure membranaire est un fascinant domaine en émergence. Récemment, plusieurs domaines de liaison aux lipides ont été identifiés impliqués dans la génération et reconnaissance de la courbure membranaire. La plupart des études intéressés à ces phénomènes ont été amenés principalement à comprendre la génération de courbure et donc la recherche sur sa reconnaissance a été moins étudiée. Cependant, ce deux processus sont étroitement liés. Des motifs structuraux largement impliqués dans les processus de modulation de la courbure membranaire sont les hélices amphipathiques. Parmi eux, un senseur de la courbure exhibant des propriétés particulières a été identifiée récemment et il a été appelé ALPS (ArfGAP1 Amphipathic lipid packing sensor). Ce motif se plie en hélice au contact avec les membranes positivement courbées, sa face polaire est riche en serines/threonines et sa face hydrophobe contient plusieurs résidus aromatiques. Il a été montré que son interaction avec la membrane était indépendante des charges électrostatiques et en conséquence, un rôle prépondérant a été attribué aux résidus hydrophobes. En effet, le modèle actuel suggère que ces résidus hydrophobes soient les responsables de l'ancrage d'ALPS à la membrane en reconnaissant les défauts d'empaquetage lipidique. Nous avons réalisé des simulations par dynamique moléculaire du motif ALPS et une de ces mutants, qui expérimentalement compromet la reconnaissance de la courbure membranaire, liés à l'interface solvant/lipides des membranes de composition simple et mixte. Nous montrons que les particularités dans la séquence d'ALPS, exhibant un motif répétitif Bulky-small&polar-Bulky, lui permet de (1) avoir une considérable liberté conformationnelle et structurelle, (2) les serines /threonines participent dans des interactions hydrogènes importantes pour la reconnaissance de défauts d'empaquetage aux niveaux des têtes polaires et (3) les résidus aromatiques hydrophobes lui permettent d'explorer les défauts d'empaquetage au niveau des chaînes aliphatiques. Également, nous montrons que la déformabilité et flexibilité d'ALPS dépendent du contexte membranaire et donc des défauts d'empaquetage lipidique intrinsèques à la membrane. Finallement, nous proposons des nouvelles perspectives au niveau atomique de la reconnaissance des défauts d'empaquetage lipidique par ALPS où la déformabilité et flexibilité structurale ainis que les propriétés dynamiques et physiques de la membrane jouent un rôle prépondérant.

Mot clés

Dynamique Moléculaire ; Hélices amphipathiques ; Senseur de courbure ; Défauts d'empaquetage Lipidique ; ALPS ; Courbure membranaire ; ArfGAP1 ; Membrane simulations

Abstract

The research about membrane-shape related processes is a new fascinating field. Recently an increasing number of lipid-binding domains that sculpt or sense the shape of the membrane have been identified. Most of the studies about membrane-shape have been focus on the generation of the curvature and less attention has been put on the mechanism of curvature sensing. Thus, this fascinating subject remains less understood. Recently, a general motif for sensing membrane curvature was proposed based on the properties of ALPS (ArfGAP1 Amphiphatic Lipid packing Sensor). This motif folds in an amphipathic α-helix once bound to the interface of membranes, has a populated serine/threonine polar face and hydrophobic aromatic residues rich hydrophobic face. Its membrane interaction depends on the recognition of defects in lipid packing and not in electrostatic charges. We performed molecular dynamics simulations of the amphipathic helical peptide ALPS, and a triple-mutant that experimentally compromises the sensitivity of ALPS to the membrane curvature. Both peptides were embedded at the water/lipid interface of explicit simple and mixed phosphatidylcholine membranes and simulations over 300 ns were run. In this thesis, we propose a novel atomistic view of ALPS curvature sensor lipid-packing recognition, where the dynamics and plasticity of both, ALPS and the membrane, act and adapt in a perfect synchony. We propose that ALPS is able to adapt to these inhomogeneities of the membrane thanks to the conformational deformability and structural flexibility that allow it to explore the lipid packing defects at the level of the polar heads and the acyl chains. This deformability is favor by a bulky-small&polar-bulky pattern that dispose the bulky hydrophobic residues and the small polar residues in a way that favors peptide-lipid interactions. Moreover we suggest that ALPS can induce adaptative dynamic response of the membrane that leads to a bilayer-coupling effect and a reciprocal orchestrated adaptation process. We show how the absence of lipid-packing defects avoid ALPS deformability and structural flexibility, affecting in consequence important intra-peptide and lipid-peptide interactions. Our results show that the deformability and structural flexibility of ALPS and the presence of lipid-packing defaults in the membrane are correlated. We also propose that the deformability is environment-dependent whereas the structural flexibility depends on the particularities of the sequence. Hence, ALPS plasticity must be of relevance for its curvature sensitivity. We advance that this could imply a concertated mechanism to recognize curved membranes. The partitioning of ALPS at the interfacial phosphate/glycerol level, suggest an adaptive interplay between the peptide-sequence geometrical and space restrictions, the lipids conformations and the physical forces that shape the membrane.

Key Words

Molecular dynamics ; Amphipathic helix ; Curvature sensor ; Lipid packing defects ; ALPS ; Membrane curvature ; ArfGAP1 ; Membrane simulations

Contents

Chapter 1

The sense of shaping and sensing the membrane

"When you are describing A shape, or sound, or tint;
Don't state the matter plainly, but put it in a hint;
And learn to look at all things With a sort of mental squint"

Lewis Carroll

The cell is the scenario of a complex interplay of biophysical and biochemical processes that make possible its survival. Cells interact with their environment in various ways, by secreting, for instance a great variety of molecules to modify their surroundings. They are also able to protect themselves by producing extracellular matrices or cell walls, and more importantly, they interact with other cells to share information, control cellular populations or to preserve multicellular organisms. Cells can be assigned to one of three domains based on their biophysical, biochemical and phylogenetic characteristics: Eukaryota, Archaea and Bacteria. These three types of cells are in constant interaction with their surroundings and the major cellular structure that make this possible is the plasmatic membrane that delimits individual cells. The nature of the lipid components of Eukaryota and Bacteria membrane is the same whereas Archaea membranes differ from the other life domains. These differences have been explained by two opposed hypothesis, in the first one Archaea would have completely replaced their plasmatic membrane by changing their lipid metabolic pathways (Lopez-Garcia and Moreira, 2004), having at some point a mixed membrane, in the second hypothesis the last universal common ancestor (LUCA)(Delaye *et al.*, 2005; Forterre *et al.*, 2005; Jekely, 2006) was not yet delimited by a lipid membrane, and archaeal and bacterial/eukaryal membranes emerged independently afterwards (Koonin and Martin, 2005). Phylogenetic analyses of the enzymes involved in the lipid metabolic pathways of archaea and bacteria have showed that these life domains share highly divergent but homologous enzymes. Researches have therefore confirmed that the plasmatic membranes have always been a crucial condition for life through its multiple shape manifestations (Fig.1.1).

During the second half of the 19th century, while Charles Darwin was preparing its masterpiece 'On the Origin of Species', C. Naegeli and C. Cramer described for the first time the cell membranes, as essential barriers to maintain osmosis equilibrium in plant cells. Indeed, before the advent of modern cell biology, pioneered by Albert Claude in the 1940s, many biologists viewed the cell as a mere "bag of enzymes" or a "biochemical bog" filled with formless protoplasm and devoid of inner structure. These ideas started to change with the discovery, in the late 19th century, by light microscopy staining techniques, of internal organelles such as the chloroplast, the mitochondria and the Golgi apparatus. However, the real breakthrough was 60 years ago, when Albert Claude, Keith Porter and Ernest Fullam published the first picture of an intact cell taken with an electron microscope (Edidin, 2003). Since then, and thanks to the advances in electron microscopy during the last decades, we have been able to look inside the eukaryotic cell to find many specialized membrane-delimited compartments, as well as complex intracellular dynamic processes through which there is a constant flow of vesicles scaffolded by an internal cytoskeleton (Fig.1.1). Moreover the intricate scaffold constituted by the cytoskeleton and the vesicles transport, determines the global form and dynamics of the cell, the organelles and the endomembranes.

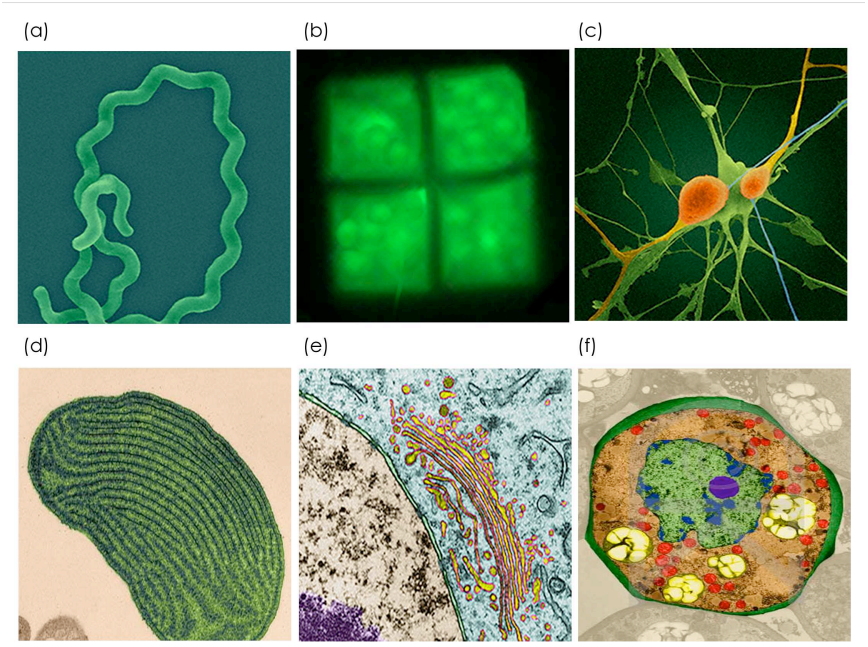

Figure 1.1: Membranes sculpt different shapes in nature.(a) Bacteria: *Spirochetes sp,* (b)Arquaea: *Haloquadratum walsbyi*, (c) Eukaryote: Neuron, (d) Chloroplast and its inner membranes (thilachoids), (e) Internal membranes in an eukaryot cell. In yellow the Golgi apparatus, in green the nuclear envelope and in bleu other endomembranes systems, (f) Plant cell showing endomembane systems such as vacuoles in yellow, mitochondria in red and nucleous in bleu. (Microscopy Photographs taken from the website http://www.denniskunkel.com/)

1.1 Membranes can adopt numerous shapes

Biological membranes constitute the surface of all living organisms and they determine the shape cells can adopt. The principal components of membranes, the phospholipids, spontaneously form spherical or laminar shaped structures in aqueous solution. The laminar forms can bend creating different degrees of membrane curvature and allowing organisms to adopt a great variety of shapes, spherical, oval, discoid, rod, spiral sheath, stalk, filamentous, square, star, spindle, lob, and pleomorphic[1] (Zimmerberg and Kozlov, 2006). Each shape represents a different life strategy. The biological membrane is an interface between inside and outside environments, which the cell (or cell organelles) can modulate specifically in order to fulfill the cellular requirements and to respond to a wide range of external influences. For example the biconcave disc-like shape of erythrocytes guarantees the optimal surface-to-volume ratio that is necessary for fast oxygen exchange between hemoglobin and the outside medium.

The shape of all inner-cellular membrane compartments also depends on the different forms a membrane can adopt: tubes, vesicles, invaginations, protrusions. Organelles such as lysosomes and peroxisomes have a basic shape that is relatively spherical. Other organelles, on the other hand, have more complex shapes. Mitochondria and chloroplast have outer limiting membranes and complex networks of internal tubular membranes, cristae and thylacoides respectively. Golgi apparatus and endoplamic reticulum (ER) contain regions that form elaborate networks of interconnected cisternae, tubules and fenestrations which dynamic modulation (i.e budding and forming vesicles) is crucial for the secretory pathways[2]. During endocytosis, cells deform their membranes to engulf molecules such as proteins that cannot pass through the membrane. This process can be macropinocytosis, caveolae, or receptor-mediated endocytosis (Doherty and McMahon, 2009). Endocytosis is also used to introduce other cells or viruses, by phagocitosis. During this precise cellular event the shape of the particle that will be internalized determines the deformation of the engulfing membrane. These membrane-dependent processes are tightly regulated by specific molecular mechanisms and depend, on their turn, on the membrane curvature and on the physcial forces that govern membrane dynamics (Veiga and Cossart, 2006).

The shape of most organelles is highly conserved across species. Moreover, different organelles can have subdomains that resemble to each other in shape and architecture. Electron tomography studies have shown tubules with similar diameters in numerous cell types (approximately 60 nm and 30 nm in diameter for ER (Voeltz *et al.*, 2006)and inner mitochondrial membranes tubules (IMM), respectively). As the physical principles underlying shape formation and the sensing of this shapes (curvature-sensing) must be universal not matter the biological system, the inter-species organelle shape conservation indicates that specific shapes play an important role for the organelle proper functions (Voeltz, 2007).

It has now been clear for a long time that a complex interplay of factors determines organelle morphology. However, so far, nobody knows how this is produced and how this is recognized. Are there any lipid-protein domains present exclusively in the Golgi apparatus, for instance, that would stabilize

[1] Variable in shape

[2] The secretory pathway is the process of exocytosis that involves a complex dynamic of endomembrane shape modulations to direct the secretory vesicles carring the cell products to the extracellular environement.

the strange fenestration and interconnection of the Golgi stacks? How the mechanical and biophysical properties of the membrane influence the shape deformation? What is the identity of those proteins involved in all these processes? How the membrane curvature is controlled and sensed for the correct feedback and distinction of multiple regions in the same organelles?

These are great times for the research on membrane-shape related processes. Our knowledge on structure and dynamics of the cell, organelles, membranes and proteins increases steadily along with the technical developments. For example, last-generation biophysical techniques allow to track single-molecule functions or manipulate membranes and molecular motors in synchrony (i.e pulling tubes from giant unilamellar vesicles (GUV) with kinesines (Roux *et al.*, 2005; Sorre *et al.*, 2009). Moreover, we have seen great advances in biochemistry and cell biology, which methods have become more sophisticated. The imaging techniques such as atomic force and electron micrography, X-ray diffraction, solid-state NMR, fluorescence resonance energy transfer and simple direct fluorescence measurements of probes in model membranes, have played a crucial role in the evolution of our understanding of many cellular or biochemical processes that, in many cases, have been explained at the atomic level. This last point have also been possible thanks to the increase in computational power, which incidentally have allowed to perform longer and realistic computer simulations using macromolecular complexes and membranes-protein assembles.

1.2 Outlook

Given this overview about the multiple membrane shapes and their importance in macro and micro scale biological processes, in the follow chapters I will develope a discourse to understand our study subjet : the curvature sensor Amphiphatic helical Lipid-Packing Sensor (ALPS).

The research about membrane-shape related processes is a new fascinating field. In order to explore and answer some of its fundamental questions, we must first accept that membrane curvature is generated as a result of a complex interplay between membrane proteins, membrane lipids and the physical forces that modulate this multi-dimensional assembly. Just an integral perspective which includes the dynamics of the membranes and of the membrane-proteins will importantly contribute to understand this amazing natural setting of sensors, sculptors and malleable matter. In the following chapters you will find some of the most important details about theses actors in the membrane-shape related process.

Among an increasing number of lipid-binding domains, that sculpt or sense the shape of the membrane, ALPS is a particular interesting case. Biochemical studies on these motifs have revealed the importance of the amphipathic helix, which potentially intercalates into the lipid bilayer to sense membrane curvature. A combination of bioinformatics with structural analyses has been identifying an increasing number of novel families of lipid-binding domains or potential candidates. Most of the studies related to membrane-shape related proteins have been focus in the generation of the curvature and less attention has been put on the mechanism of curvature sensing. Thus, this fascinating subject remains less studied and less understood. In this thesis, we propose a novel atomistic view of ALPS curvature sensor lipid-packing recognition, where the dynamics and plasticity of both, ALPS and the

membrane, act and adapt in a perfect synchony. We advance that this could be of relevance as a concertated mechanism to recognize curved membranes. To contextualize the atomical models we explain here and to develope my discouse about these aspects,

In chapter 2 *Membranes are complex and dynamic systems*, I describe some of the most important knowledge about the membrane componentes (phospholipids and membrane-proteins), highlighting the most important contributions of the Molecular Dynamics Simulations. I talk about the structure of the membranes an the determinants of the membrane-proteins structures, such as partitioning and aminoacid propensities to form their secondary structure, considering mostly the case of the alpha-helices. I will focus the las part of the chapter to discuss about the amphipathic alpha-helices in particular.

In chapter 3 *Remodelling and sensing the membrane,* I discuss the membrane mechanical and physical foces that contribute to shape the membranes. I also develope an overview of the state of the art regarding the mechanism of generation, regulation and sensing of the membrane curvature. I explain the differnt lipid-binding domains or proteins that scult or recognize the membrane shape by different but complementing mechanisms. As in chapter 2, I constantly underline the contribution of the Molecular dynamics simulatioons to understand these remodelling processes.

Chapter 4 *Regulation of vesicular transport by membrane curvature*, is dediated to explain the biological context of ALPS function, the secretory pathway. I make a resume of the most importante stages of the pathway and I focus on the role of ALPS sensor in the regulations of the vesicular transport. I also described the discovery of ALPS sensors and the research done about them in the recent years.

In Chapter 5 *Molecular Dynamic Simulations,* I resume the main principles in Molecualr Dynamic Simulations and I describe the methology use in this thesis. I also discuss about force fields and today simualtion capabilities in membrane systems.

Chapter 6 to 8 comprise all the results of my work. In chapter 6 I focus on the structural aspects of ALPS in comparison with a mutant that is inefficent as curvature sensor. In chapter 7, I explain all the effects induced in a DOPC membrane by ALPS. And in chapter 8, I evaluate the effect of different lipid-packing defaults in the structural properties of ALPS.

To conclude, in chapter 9 I discuss all my results. I propose a novel perspective to understand ALPS fuction and the posibility to extend my explanations to other membrane-curvature sensing contexts. I also propose further experiments and simulations.

Chapter 2

Membranes are complex and dynamic systems

Our first conception of the cell membranes is thanks to Hooke and his discovery of the plant cells in the 16th century. But our knowldge about these biological membranes rather goes back to the end of the 19th century when, when Hugo de Vries found that the cell membrane was permeable for ammonia and glycerol. Ten years later, Walther Nernst developed the theory of electrical potentials based on diffusion of ions in solution. During those same years, Charles Overton proposed for the first time that lipid membranes enclosed animal and plant cells. Moreover, he introduced the hypothesis in which the exchange of external Na^+ for internal K^+ ions was performed by an active membrane transport that required metabolic energy, and it was not until 1930s when J.R. Danielli and H. Davson proposed that proteins formed also part of the cellular membrane (Campbell and Mitchell., 1999).

The membrane was for long time perceived as just a barrier which served as the support for membrane proteins. Nowadays, this vision has deeply evolved. Computer simulations have turned out to be particularly important to address key questions on this research area and to substantially change our old perceptions. This new era on membrane research began in 1985 with the first X-ray low-resolution structure of a membrane protein, the bacterial reaction center (1PRC, PDBcode), by M. Diesenhofer, R. Huber, H. Michel, and then after the determination of the bacterial K^+ channel at the beginning of this century by Doyle and MacKinnon (Doyle *et al.*, 1998), the amount of structural information about membrane-proteins increase constantly. Computer simulations have taken advantages of these crystallographic structures in order to analyze the dynamics and behaviors of proteins inside the membrane at atomic level. For the time being, these researches have provided valuable insights on the role of membranes, not just as a support-based structure, but rather as a key active actor for protein functions.

Although it is still difficult to obtain crystallographic structures of membrane proteins, the scientific community has overcome this specific handicap by increasing the interplay between solid-state NMR studies and computer simulations. Thanks to the constant growing in computer power and more efficient simulation softwares, today it is becoming possible to analyze and understand different membranes

states as well as other lipid aggregates, systems that otherwise would be extremely difficult to study experimentally. Among this, we found simulations of small hydrophobic molecules diffusion (Shaitan *et al.*, 2008a; MacCallum and Tieleman, 2006; Xiang and Anderson, 1998b), aminoacid chains analogues (MacCallum *et al.*, 2008) or oligopeptides (Shaitan *et al.*, 2008b) through the membranes, as well as simulations of many membrane-proteins and the membrane lipids behavior and assembly (Gumbart *et al.*, 2005; Chandler *et al.*, 2008; Yefimov *et al.*, 2008; Kandt *et al.*, 2006; Oloo *et al.*, 2006; Sansom *et al.*, 2002; Shepherd *et al.*, 2003; Woolf and Roux, 1994; Nina *et al.*, 2000).

Modulation of membranes, as I mentioned in the first chapter, is possible thanks to the complex interplay between all their components. In this chapter I would like to discuss the nature of these membrane components and some of the membrane structural properties. Once these aspects introduced I will discuss in the next chapter about the forces that shape the membrane. It is almost impossible to cover here all the researches that have been performed on this vast subject, however I will develop in the following sections the most important findings that are relevant for the understanding of the scope of this thesis.

2.1 A glance at membrane lipids

Lipids, the main component of biological membranes, provide a complex, dynamic and active support for integral membrane proteins, and at the same time, represent a varied functional relevant surface for the interaction of soluble amphitropic[1] proteins. The large repertoire of lipids makes biological membranes a highly diverse system depending on both, the type of cell and the inner-cellular organelle. Furthermore, the large diversity of lipid structures produces a broad spectrum of chemical and physical properties that influence protein functions and their organization. That is, the ability of lipids to form subdomains of unique composition provides a physical mechanism to compartmentalize proteins by confining them in a specific and reduced membrane microdomain or raft (Rajendran and Simons, 2005). These lipid-protein rafts could play an important role, for instance in protein regulation and efficient signal transductions. Lipid patches found in organelles may also form microdomains, whose distinct physiochemical properties are a mere reflect of both, the stereochemical and electrostatic characteristics of the lipids shaping these organelles (McIntosh, 2007). Therefore, the structure and chemical properties of cellular membranes and their microdomains are rather difficult to define, especially since these microdomains are highly dynamic (Risselada and Marrink, 2008; Niemela *et al.*, 2009). The study of lipids and their links to cellular physiology and cellular pathology have become a major research target. Technological advances in mass spectrometry have boosted up these studies creating in recent times the field of "lipidomics" (Han and Gross, 2003)).

[1] Having both lipotropic and hydrotropic characteristics

2.1.1 Lipids structure

The works performed by Overton showed for the first time, at the end of the 19th century, that phospholipids were the principal components of biological membranes (Edidin, 2003). Phospholipids are amphipathic[2] molecules, which hydrophilic and hydrophobic moieties induce the formation of lipid bilayers. I will detail this in the next sections, for the moment lets talk about their structure.

The basic structure of phospholipids consists of a headgroup or polarhead (HG) (the hydrophilic moiety) and two acyl chains (AC) (the hydrophobic moiety). The polarhead is composed of a glycerol molecule and one of the different derivatives of the phosphoric acid. The nature of these phosphoric acid derivatives allows to differentiate and classify the phospholipids. Among some of the most abundant phospholipids we find the phosphatidylcholine (PC), the phosphatidylserine (PS), the phosphatidylethanolamine (PE), the phosphatidylinositol (PI), and the phosphatidic acid (PA) (Fig.2.1(b)). Whereas PC and PE are neutral zwitterions, PS, PI, and PA bear a net negative charge. The acyl chains are derivatives of saturated and unsaturated fatty acids, such as palmitic acid and the oleic acid respectively (Fig.2.1(a)). Therefore, acyl chains can be also saturated or unsaturated, this nature can be useful to classify the lipids based on the global form of the lipid, the arrangements they can form, and their influence in the fluidity of the membrane. The most studied lipids in model membranes are the PC phospholipids, such as dimyristoylphosphatidylcholine (DMPC), dipalmitoylphosphatidilcholine (POPC) and dioleoylphosphatidilcholine (DOPC)[3] (Fig.2.1). As mention above, biological membranes are built by a great diversity of lipids, other than phospholipids. For instance, cholesterol accumulates transiently in membranes and cause changes in the physical properties of the bilayer, influencing deeply the membrane fluidity. On their turn, diacylglycerols (DAG), which can be regrouped in restricted portions of the membrane and by doing this, they induce changes on the membrane curvature that facilitate membrane fission[4] and fusion[5]. I will discuss these aspects in detail in chapter 3.

2.1.2 Lipid packing and the membrane shape

Phospholipids, as many other lipids, are able to form spontaneous fluid crystalline structures, which are entropy favored. The resulting structure depends on the shape of the lipid molecules. Lipids associate in different arrangements that reduce the contacts between their hydrophobic part and the solvent. The organization that lipids may adopt depends on the relative size of their hydrophilic and hydrophobic

[2] Or amphiphilic, pertains to a molecule containing both polar (water-soluble, hydrophilic) and nonpolar (water-soluble, hydrophobic) portions in its structure.

[3] These are the lipids used on this work.

[4] Membrane fission occurs in eukaryotic cells whenever a vesicle is produced or a larger subcellular compartment is divided into smaller discrete units. During endocytosis, cell membranes bud and then pinch off smaller sack-like "vesicles." This process is possible because the protein dynamin, forms a short "collar" of proteins around a bit of the membrane that has emerged from the "parent" membrane, and then squeezes it tight, cleanly separating the new "daughter" vesicle. Recent evidence suggests this fission event is promoted by enzymes that generate phosphatidic acid and thereby cause a distortion of the lipid bilayer.

[5] Cellular membrane fusion is one of the most common ways for molecules to enter or exit cells, in processes such as fertilization and viral infection, for example. When two cells fuse together, their membranes come together at one location and create a connection between the cells that allows the exchange of material between them. The protein complex SNARE is implicated in this fusion proces. Eventually, the two membranes form one single, continuous membrane surrounding the contents of both cells.

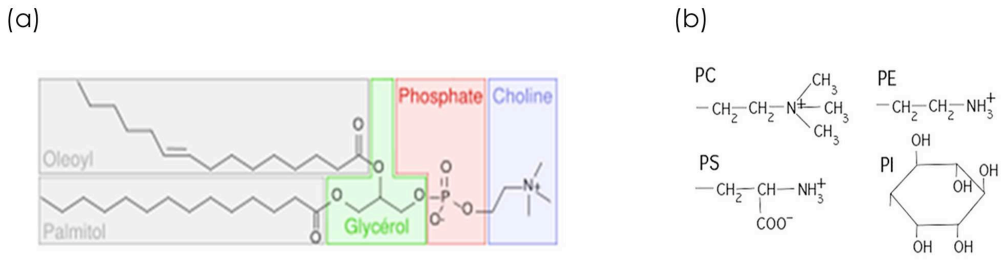

Figure 2.1: Exemple of lipid structure (a) shows the acyl chains (one saturated (Palmitoyl) and the other one monounsaturated (Oleoyl) of palmitoyloleoylphosphadidylcholine, and its headgroup with the glycerol and the derivative of phosphatidic acid, phosphadidylcholine. (b) Representations of those derivatives that can be found as polar heads of the most common phospholipids in biologicla systems.

moieties.

Gorter and Grendel, at the dawn of the 20th century, discovered that cell membranes are in fact structured by a lipid bilayer (Gortel and Grendel, 1925), but it was Robertson who, in the 1950s, argued that all cell membranes have the same common structure (Robertson, 1959). This phospholipid bilayer is arranged by two phospholipid leaflets that form a hydrophobic interior (the hydrophobic core [HC]), which is stabilized by the contacts between the hydrophobic acyl chains of the phospholipids. The phospholipids headgroups of each leaflet form the interior and exterior surfaces of the bilayer that are in contact with the aqueous environment.

A useful measure that allows the distinction of lipid molecules, from the point of view of their organization, is the dimensionless packing parameter (PP) (or shape factor), which is defined as the ratio of the cross-section area of the headgroup (HG) to that of the acyl chain (AC), i.e. HG/AC (De Krujiff, 1985). Consequently, large values of the PP (HG/AC $>$ 1) correspond to molecules of large head group section area and small acyl chain section, inversed conical shape. On the other hand, if HG/AC $<$ 1 then both sections are close (this usually being the case of lipid molecules with two acyl chains as the POPC in Fig.2.1) and the molecules can be represented as a cylinder (Przestalski *et al.*, 2000) (Fig.2.2). I will discuss this in more detail in chapter 3, for the moment keep in mind that these cylindrical lipids tend to form lamellar structures, which can additionally form lipid bilayers separated by water layers, as commonly occur in biological membranes. This particular observation has been use as a central argument to speculate that in the early stages of life, the spontaneous formation of lipid bilayers gave rise to the development of biological membranes (Tien, 2000). In some pioneering works, Marrink and co-workers have been recently able to simulate the spontaneous formation of bilayers. These works demonstrated that even processes that involved hundreds of lipids can be simulated obtaining realistic intermediate stages (de Vries *et al.*, 2004a; Marrink *et al.*, 2001).

I will give in the further sections the details about the bilayer composition and global bilayer structure.

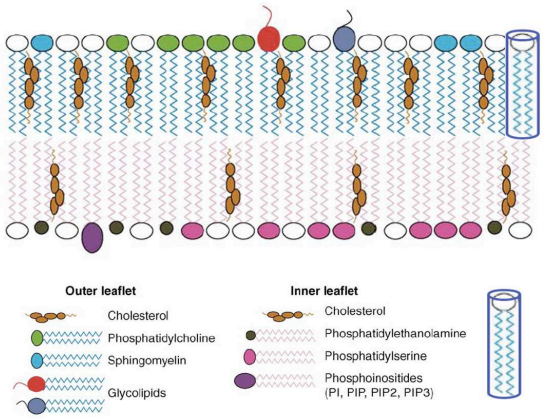

Figure 2.2: Lipid shape determine the organization in bilayers. Bilayers can be asymmetric in lipid composition (Modified from (Janmey and Kinnunen, 2006a)).

2.1.3 Membrane composition

The chemical composition of the two leaflets of the lipid bilayer is different (Fig.2.2). For example, in eukaryotes, nearly only anionic lipids face towards the cytoplasm, whereas most lipids with large glycosylated headgroups are exposed to the extracellular environment. Differences in bilayer asymmetry between eukaryotic and prokaryotic membranes are essential for the activity of endogenous antimicrobial factors that break bacterial membranes but are harmless to eukaryotic cells ((Sevcsik *et al.*, 2007; Sato and Feix, 2006).

The chemical composition of the bilayer affects its mechanical properties and conversely, the use of physical forces on membranes alters their chemical composition. The bilayer asymmetry is highly dynamic and different cell types as well as organelles and cells at different states of activity are likely to change the lipid distribution. Moreover, the bilayer trasversal asymmetry have important consequences in the spontaneous curvature of the membrane (Devaux, 2000). I will explain in more detail all these bilayer mechanical properties in chapter 3.

The formation of microdomains and the presence of mixed bilayers induce lateral asymmetry. In these bilayers, the differences in lipid shapes (cylinders, cones, etc.) between both bilayers create lipid mismatches, known as lipid packing defects. These packing inhomogeneities can also appear by an increase in the membrane curvature. This particular phenomenon will be also discussed in the following chapter. Complicated mixtures have proven to be difficult to simulate for the moment. However, there exist few exemples of simulations made on bilayer with a simple (2 or 3 different lipids) mixed lipid compostion. However they have been able to describe some important atomic feature related with the bilayer properties (Chiu *et al.*, 2002; de Joannis *et al.*, 2006b,a).

2.1.4 Lipid dynamics and membrane fluidity

Besides their shapes and lipids physicochemical properties, lipid dynamics are essential features of membranes and are crucial for its biological viability. As you probably guess at this point, lipid dynamics is affected by the shape and physichochemical properties, and on its turn, dynamics can play an important role in bilayer asymmetry and many mechanical properties that I will discuss in the next chapter. I chosed to mention here this aspects to start to prepared the reader to have a perspective of membranes as very dynamic entities, none of the interactions or processes that take place in the biological membranes are static.

We know that lipids can display many movements, however, our understanding of lipids dynamics is very limited. The chemical structure of lipids influences their kinetic behavior: the presence and nature of the polar head, the length of the lipid, the degree of saturation or instauration of the acyl chains, *etc.* define and delimit the behavior that a certain lipid may adopt (Kusumi and Suzuki, 2005; Tristram-Nagle and Nagle, 2004; Marrink *et al.*, 2009a). Moreover, the surrounding environment of the lipid molecules introduces additional parameters to this behavior and movement, such as the interaction of the polar head with the aqueous medium and ions, and with the membrane proteins, which also exert an influence on lipids.

Membrane fluidity is first of all determined by the lipid composition and depending on it the membrane will exhibit a particular lamellar fluid state known as lamellar phase. The lamellar phases can vary as a function of the lipid content or with the temperature, leading to different phases exemplified in Figure 2.3. This phases can be disordered or ordered depending on the orientations of the lipids acyl chains with respect to the normal of the bilayer. As an exemple, if the acyl chains are almost parallel to the bilayer normal the lamellar phase is ordered, this is the case of saturated acyl chains; the disorder in the bilayer can be induce by many factors (Feigenson, 2006). The biological membrane correspond to a lamellar liquid-disordered phase. In order to understand the dynamics of this biological relevant phase and the effect of lipid dynamics on membrane the global membrane structure, I will next explain these aspects in more detail.

Two main lipid movements are rotation and oscillation. Both of them are implicated in the lipid transport. Additionally, lipids display many other important movements for the membrane function, which has been assessed by MD simulations (Marrink *et al.*, 2009a): the lateral diffusion[6] in the plane of the membrane, the transversal diffusion from one layer to the second one. This diffusion can be partial, concerning solely one fragment of the acylchains, or can be total, that is when the transversal diffusion concern the entire lipid that has passed from one leaflet to the opposite one (process known as flip-flop)[7](Holthuis and Levine, 2005). The bilayer asymmetry discussed in section 2.1.3 is dependent

[6]The lipids can difusse in a membrane covering an area from 0,1 to 1 microm^{2}s^{-1} in a cell membrane. However, lipid diffusion can vary in function of the lipid nature and the environment surrounding it.

[7]In model membranes, the flip-flop is very slow for lipids with polar heads compared with lipids without polar heads (Bai & Pagano, 1997). For some membranes such as the reticulum endoplamic, the expansion of the membrane is very important and depends on the flip-flop of lipids at a high rate. This is possible thanks to the proteins called flipases (Buton et al. , 1996) that assure the transversal diffusion from one leaflet to another at a high rate. In the case of plasmatic membranes that have to mantain an asymmetric composition, the ATP-dependent flipases, make possible the traslocation of PS or PE phospholipids (Seigneuret & Devaux, 1984).

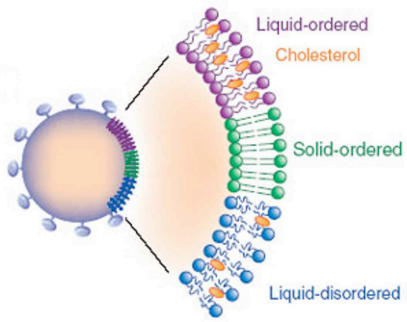

Figure 2.3: Liquid phases in biological membranes that determine the fluidity and order/disorder of the lipids. (Modified from (Veatch, 2008)

of this last process.

The range of phospholipid motions are correlated with the acyl chain orientation and movements. Lipid order inside membranes reflects their rotational motion and the average orientation of the acyl chains C-C bond with respect to the normal to the membrane which can be measured with the Order Parameter (see section 5.7.1.2)(Takaoka *et al.*, 2000). For instance, if we consider a fully saturated phospholipid below the phase transition temperature, the acyl chains are in the extended all-trans conformation and are closely packed (ordered), in this case the range of motion is small. However, above the phase transition temperature, the chains contain a number of gauche configurations, which makes the packing of the chains looser and the range of motion of the acyl chains higher (disordered). The presence of different types of lipid molecules in a cell membrane decreases the order in the bilayer, and produces the different lamellar phases we just described (Feigenson, 2006) (Fig2.3).

Among other important factors that influence the lipids order are the volume and ratio of the polar head and the acyl chains, as well as the nature of the polar head, the saturation of the fatty acyl chains, and the number of *trans* and *gauche* positions of the C-C bonds in the chain. In saturated PC membranes, the increase of acyl chain lengths also increases their order but decreases their reorientation motion (Kusumi and Suzuki, 2005; Subczynski *et al.*, 1992, 1993). The introduction of unsaturations in the PC acyl chains generates packing defects in the lipid bilayer and affects deeply the narrow lipid packing and the membrane order. For instance, the presence of a *cis* double bonds introduces a bend in the unsaturated acyl chain that would create some non-conformability between chains and increase chain disorder, leading to the lipid packing defects we discuss previously. Additionally, the presence of either *cis* or *trans* double bonds in the acyl chain would reduce the dynamics of the chain around the rigid double bonds.

If we consider the example of the introduction of cholesterol in a PC bilayer, it has a prominent

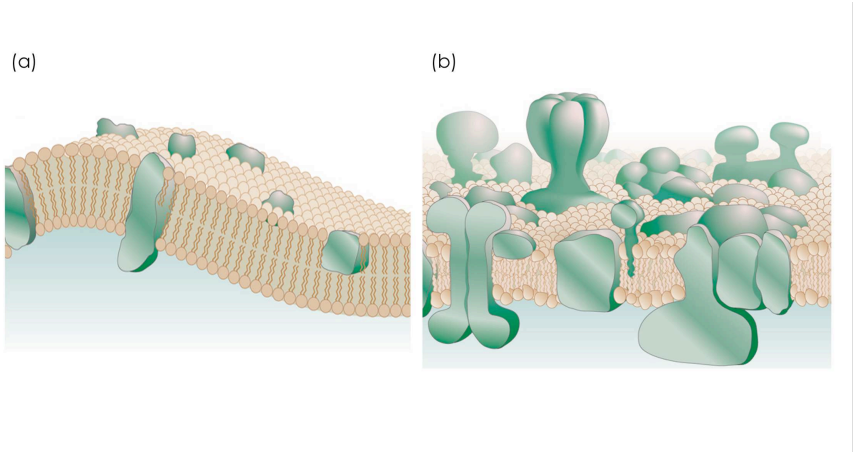

Figure 2.4: (a) Singer & Nicholson Mosaic-fluid membrane model. (b) Engelman model of a membrane more mosaic than fluid. (Taken from (Engelman, 2005)).

influence in already highly ordered saturated membranes since it is capable to increase even more the membrane rigidity (Chiu *et al.*, 2002; Pasenkiewicz-Gierula *et al.*, 1990). On the other hand, the introduction of unsaturated acyl chains in these rigid membranes, as in any other membrane, increases greatly the fluidity and the disorder of the membrane. The "fluidizing" effect of unsaturated chains observed in biological membranes moderates and counteracts the "rigidifying" effect of cholesterol (as well as the effect of any other rigid-membrane modifiers).

The proteins embedded in the membrane can cause dramatic changes in this fluid states structure of the lipid bilayer, since the size, structure and composition of these proteins may restrict lipid movements or increase lipid disorder (Sanderson, 2005; Salnikov *et al.*, 2009b,a). All these effects in the lipid bilayer are going to modify the order and the diffusion of each lipid. Moreover, these effects are specific of the lipid structure, its environment and the lapse of time the lipids spend in that environment. In order to clarify these dynamic aspects, I will discuss now the structure of the biological membrane. Remember nonetheless, that since the biological membrane is a mixture of many elements, its behavior is far from the ideal liquid structures we illustrate in Figure 2.3.

2.2 Membrane structure is a complex target

Almost forty years ago Singer and Nicholson proposed the first structural model for the biological membrane, the fluid-mosaic model (Singer and Nicolson, 1972). This first model proposed an initial vision of static proteins, which at low concentrations were embedded in the fluid membrane. The membrane, on the other hand, was not perturbed by the presence of proteins nor by its direct contact with the solvent. All the functional properties were attributed to the membrane-proteins embedded in it. Nowadays, this vision has become more complex. We now know that the biological membrane is a highly dynamic system whose components are in continuous change and movement. The membrane, by

it-self, is starting to be recognized as an important actor of many membrane-protein related functions. The plasmatic membrane is composed of regions showing different and specific structures and functions (Engelman, 2005) (Fig.2.4). The most important of these specialized membrane structures are the lipid rafts (Rajendran and Simons, 2005; McIntosh, 2007). These lipid specific regions modulate the membrane fluidity by restricting the directions lipids can follow (Kusumi and Suzuki, 2005). Moreover, the thickness of these membrane regions can also change according to the lipid composition and as a function of the length[8] of the proteins that are embedded in these membrane regions (Mitra *et al.*, 2004). The prevailing model suggests that the membrane is more mosaic than fluid (Engelman, 2005). This change of vision became possible thanks to the development of new methodologies and technologies such as the electron microscopy, NMR and the fluorescence spectroscopy. Finally, in recent times, the computer simulations have started to play an important role in the construction of these new perspectives of the biological membranes (Marrink *et al.*, 2009a; Gumbart *et al.*, 2005; Risselada and Marrink, 2009; Niemela *et al.*, 2009).

2.2.1 Structure

Since cellular membranes should remain in a fluid state for normal cell functions, it is exactly this fluid structure (Lα-phase) (Fig.2.3) of the bilayer that is relevant for the understanding of membrane-peptide interactions at a molecular level. Unfortunately, the disorder found in fluid bilayers prevents high atomic-resolution. Useful low-resolution structural information can nevertheless be obtained by diffraction methods using multilamellar bilayers (liquid crystals), which have been dispersed in water or placed on surfaces, and whose structure along the bilayer normal is highly periodic. This one-dimensional crystallinity shows a distribution of matter along the bilayer normal that can be hence determined from combined X-ray and neutron diffraction measurements ((White SH, 1996). The dynamic structure of the fluid (Lα-phase) bilayer that results from such measurements is a collection of time-averaged spatial distributions (Gaussians) of the principal structural groups of the lipid (carbonyls, phosphates, etc.) and the water projected to the normal axis of the bilayer plane (Wiener and White, 1991a,b) (Fig.2.5)). Using this technique White and co-workers determined for the first time the structure of a DOPC bilayer (Wiener *et al.*, 1991). Inspired by these works, Tristram-Nagle and colleagues refined and completed the structural properties of DOPC (and other phospholipids) bilayers fully hydrated (Tristram-Nagle *et al.*, 1998). This structure, which computer simulations can reproduce (Berger *et al.*, 1997; Feller, 2007; Tieleman *et al.*, 2006; Martinez-Seara *et al.*, 2008a,b), revealed several features of great importance (Fig.2.5):

1. The DOPC bilayer has a highly disordered structure. This great amount of disorder is revealed by the width of the probability densities.

2. The crosssectional area per lipid is ~72 Å^2.

[8] Known as hydrophobic mismatch. Membrane hydrophobic mismatch is the difference between the hydrophobic length of α helices of the integral proteins and the hydrophobic thickness of the membrane they span. Under the consideration of energy requirement, in order to avoid unfavorable exposure of hydrophobic surfaces to a hydrophilic environment, the hydrophobic length of the integral proteins is supposed to be approximately equal to the hydrophobic bilayer thickness.

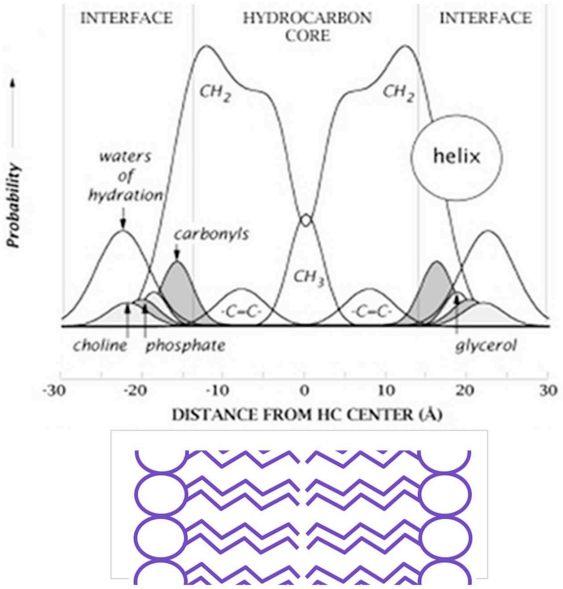

Figure 2.5: DOPC bilayer structure density profile obtained by X-ray Scattering (modified from

3. The optimal membrane thickness depends on the chain length, the degree of saturation and the angle of tilt of the acyl chain within the membrane. The thcikness of the hydrophobic core (HC) is around 20 Å and the combined thickness of the interfacial regions (those covered by the density distribution of the waters of hydration) is around 30 Å thickness of the entire bilayer. The thickness of a single interface (15 Å) can easily accommodate unfolded and folded polypeptide chains such as an amphipathic α-helix with diameter ~10 Å (typical of TM helices in membrane proteins).

4. The interface is chemically heterogeneous; they can have multiple possibilities for non-covalent interactions with peptides. Since these interfaces are the sites where proteins have their first membrane contact (typical of interfacial amphipathic helices in membrane-proteins as we will discuss in section 2.4), they are especially important in the folding and insertion of peripheral proteins or non-constitutive membrane proteins such as toxins.

5. The interface, besides being chemically heterogeneous, is also regions where dramatic changes in polarity occur over small distances.

2.2.2 Partitioning

How the small molecules can pass through the complex structure of the membrane? How the proteins fold and insert in the membrane? These are two of the most studied questions in the membrane field. The answers are not clear since the ability of molecules to cross the membrane or to get embedded in it

depend on their partitioning behavior a fascinating and difficult problem. Therefore, and before I talk about membrane proteins, I would like to mention some aspects about the partitioning .

Many essential biomolecules such as water, oxygen, and carbon dioxide move across the cell membrane by passive diffusion (Bemporad *et al.*, 2004; Xiang and Anderson, 1998a,b; Marrink *et al.*, 1996; Tieleman, 2006) Additionally, many drug molecules are also capable to enter the cell through passive diffusion across the cell membrane. This means that their partitioning within lipid bilayers has important implications for their pharmacokinetics (Pohorille *et al.*, 1998). Finally, the protein folding adopted inside a membrane is determined by the partitioning behavior of the amino acid side chains (Ulmschneider and Ulmschneider, 2008; Ulmschneider, 2009; White *et al.*, 1998; White and Wimley, 1999; Wimley *et al.*, 1998, 1996b,a; MacCallum *et al.*, 2008, 2007), based on the thermodynamics of lipid-side chain interactions. The partitioning has, in consequence, different energetic costs.

The structure of the bilayer and the gradient of polarity in the direction normal to the membrane, govern the behavior of polar and charged residues when they are moved into the hydrocarbon core by a large range of opposing tendencies, including hydrogen bonding, hydrophobic effects, and the energetic costs of membrane deformation and transfer of charges and dipoles in a low dielectric environment (White, 1994; White and Wimley, 1998; White, 2007). Numerous experimental studies have addressed the question of partitioning of amino acid side chains in lipid bilayers with significant success, finding unexpected behaviors for all polar and charged amino acids when they are confronted to the large range of opposing tendencies (White, 2007). However, most of the results from these experiments have limited spatial resolution. In particular, it is difficult to control the local environment of a side chain due to the inhomogeneous nature and the deformability of the bilayer. These two factors also prevent the prediction of side chain partitioning behaviors.

White and co-workers (Wimley and White, 1996) determined some hydrophobic scales for whole-residues by a combination of experiments that determined the free energies of transfer for each amino acid in POPC membranes (and n-octanol)[9]. These scales are essential for understanding the energetics of protein-bilayer interactions. The most important feature of White and co-workers practical scales is that they decided to include in their calculations the contributions of the peptide backbone bonds in the free-energies of the different transfers, instead of limiting their research to just the side-chains. By including whole-residues, these data have become of great value to understand some partitioning issues and have turned out to be crucial to perform more realistic peptide-membrane simulations.

The atomistic computer simulations may provide a level of detail that is not accessible with other kind of experiments. Consistently, molecular dynamics simulations can give a complementary view of side-chain partitioning to experimental macroscopic measurements, and to elaborate predictions. Some simulations of the designed pentapeptides used by White and co-workers (Aliste and Tieleman, 2005; Ahumada *et al.*, 2003) and of side-chains in bilayers (MacCallum *et al.*, 2007, 2008) have provided a molecular interpretation of the thermodynamic measurements that form the basis of the hydrophobicity scales (Wimley and White, 1996; Wimley *et al.*, 1996b,a) (Fig.2.6). On the other hand, the partitioning of side chain between water and hydrophobic solvents has been used to test and parameterize the force

[9]Many experiemental and simulation research in membrane partitioning sometimes use hydrophobic solvents that mimic the HC of the membrane. In these environments, is not possible to asses the effect of the interface.

Calculated Side Chain Transfer Free Energies

Residue	Water to DOPC Interface (kJ/mol)	Water to Center of DOPC Membrane (kJ/mol)
Leu	−14.1	−15.2
Ile	−20.6	−22.1
Val	−12.2	−13.8
Phe	−14.9	−12.8
Ala	−0.8	−8.4
Trp	−21.6	−4.9
Met	−10.5	−4.4
Cys	−0.6	−3.4
Tyr	−14.0	6.6
Thr	−4.2	13.9
Ser	−0.7	15.8
Gln	−8.9	20.2
Lys	−18.6[a]	19.9[b]
Asn	−6.5	23.9
Glu	−1.68[b]	21.1[b]
Asp	1.9[b]	31.0[b]
Arg	−21.2[a]	58.1[c]

[a]Residue is charged at this location.
[b]Residue is neutral at this location.
[c]Charged and neutral forms are equally likely.

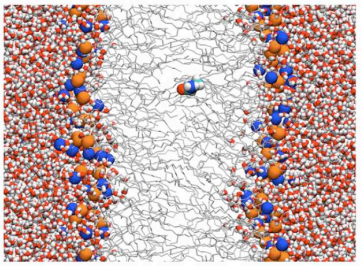

Figure 2.6: Transfer free energies calculated by MD simulations (right) and an example snapshot of a side-chain inside the bilayer :acyl chains in grey, phosphate level (bleu), glycerol level (orange) and water (red).

field used in molecular dynamics (Tieleman *et al.*, 2006; MacCallum *et al.*, 2007; MacCallum and Tieleman, 2003; Oostenbrink *et al.*, 2004). Finally, several computational studies have also addressed the distribution of specific small molecules in lipid bilayers, finding the basic atomic characteristics of this phenomenon highly dependent on bilayer properties and solute volume, size, and cross-sectional area (Bemporad *et al.*, 2004; MacCallum *et al.*, 2008; MacCallum and Tieleman, 2006; Marrink *et al.*, 1996; Norman and Nymeyer, 2006). Marrink and co-workers have recently simulated the insertion of an entire peptide in the membrane, and demonstrate that even with long times of simulations, this process, highly energetically expensive, cannot be succesfully simulated (Yesylevskyy *et al.*, 2009).

2.2.2.1 Partitioning-folding-coupling mechanism

In order to get inside the membrane bilayer, a single peptide pass througth different stages: (i) partitioning of an unfolded protein fragment chain into the bilayer interface, (ii) the formation of secondary structure in the interface, (iii) insertion of the secondary structure element across the membrane, followed by the association of the secondary structure elements within the membrane (Fig.2.7).

The folding of membrane-proteins in the bilayer environment is a difficult experimental and simulation problem, some studies in both fields have addressed this question indirectly, traditionally using small peptides that are unfolded in aqueous solution but are fully structured upon partitioning into the interface. White and co-workers have called this process partitioning-folding coupling mechanism, based on their works with an amphipathic helical peptide, the antimicrobial melittin (Hristova *et al.*, 2001). They suggest then that the stages (i) and (ii) are coupled. They established that the energetic cost of transferring an unfolded state (a virtual unfolded state calculated from the hydrophobicity scales) to the interface environment was higher than transferring a folded state. Therefore, the partitioning-folding coupling implies that secondary structure formation is driven by lipid-peptide interactions and the subsequent H-bond formation that accompanies the partitioning of the peptides. Numerous studies have studied the thermodynamics of this process (Seelig, 2004) and some MD simulations have addressed the question of membrane folding and insertion with results that have provided some promising insights

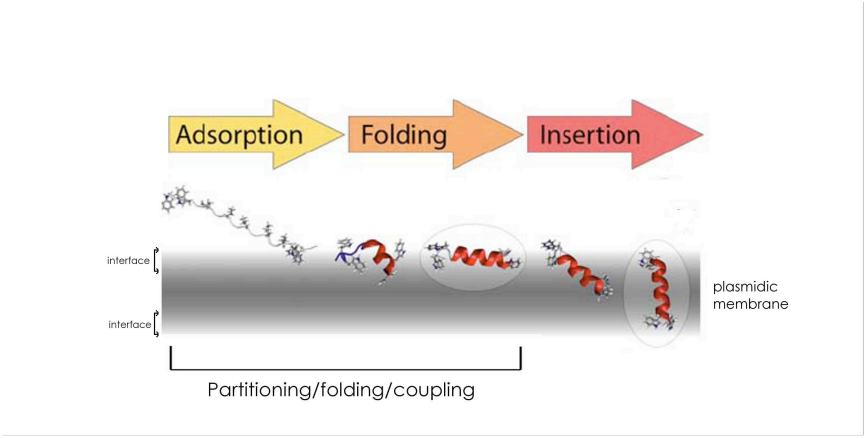

Figure 2.7: Insertion of a peptide in the bilayer showing the partitioning-folding coupling process (Modified from (Ulmschneider and Ulmschneider, 2008)

about this complicated problem (Chipot *et al.*, 1999; Tieleman *et al.*, 2001a; Ulmschneider and Ulmschneider, 2008; Yesylevskyy *et al.*, 2009). It is just recently that Ulmschneider (Ulmschneider, 2009) has achieved the folding of a TM peptide in explicit model membranes using high temperatures though.

In eukaryots, the energetic cost of folding and translocating an entier membrane-protein is counteract by the translocon machinary [10]. I consider now apropiated to talk about the membrane-proteins and the different interactions they can establish with the peptides. In particular, I will discuss the amphipathic α-helix, which is a conspicuos membrane-binding motif, that we already slightly mentioned in this last section.

2.3 A Glimpse of Membrane proteins

Membrane proteins represent 30% of the Open Reading Frames (ORFs) identified in complete sequenced genomes (Stevens and Arkin, 2000), which makes more than 10,000 protein molecules. From the last sections and given this number, it is possible toi infer that our current understanding on the structure of membrane protein and protein-lipid interactions is rather limited. There are two mayor reason for this: one, the difficulties to obtain high-resolution structures of membrane proteins, and two, the disordered nature of the lipid environment with its strong gradients of density, chain order, and polarity. Even if the structures of membrane proteins has increased steadily in the PDB database during the last years, they remain under-represented, and in many cases, only the soluble sub-domains are known. This technical difficulty to obtain the membrane-embedded protein sub-domains has become a serious challenge for the molecular dynamics and structural prediction sciences. Nowadays, the available structures of membrane-embedded protein sub-domains are modeled *in silico* inside artificial membranes, in order to evaluate the role of lipid dynamics in the protein function and structure (Appelt *et al.*, 2005; Blood *et al.*, 2008;

[10]The translocon (commonly known as a translocator or translocation channel) is the complex of proteins associated with the translocation of nascent polypeptides across membranes.

Chen *et al.*, 2002; Durrieu *et al.*, 2009; Efremov *et al.*, 2004; Lee, 2009). These molecular dynamics simulations expect to understand the atomic structural and dynamical bases of the protein-membrane interactions that will help overcome the technological problems confronted in the *in vitro* experiments.

2.3.1 Membrane-proteins determin membrane topology

Membrane proteins play a major role in membranes. They display an orientational asymmetry with respect to the membrane normal that, together with the lipid asymmetries and membrane discontinuities, define membrane topology. This spatial organization contributes to the interactions of the membrane components with most of the biological proteins soluble in water.

Membrane proteins are classified in two groups, depending on their localization in the membrane: integral proteins, those inserted in the bilayer, and peripheral proteins, those that establish transitive interactions with the membrane using both electrostatic and hydrophobic interactions or thanks to membrane-protein partners. According to the interactions the membrane proteins establish with the membrane, two main categories of membrane-protein interaction can be distinguished (Sanderson, 2005)(Fig.2.8):

- The polytopic interaction (i.e. transmembrane (TM) proteins) typical of integral proteins
- The monotopic interaction (i.e non-TM proteins) typical of proteins that are only inserted in one leaflet of the membrane, and peripheral proteins.

Polytopic transmembrane interactions are typical of those proteins that span the membrane one or many times. These proteins can be divided in two groups based on the two more frequent secondary structure elements that conform them: the α-helix TM interaction, with one or more hydrophobic helices spanning the membrane (from 1 to more than 20 helices) (Ubarretxena-Belandia and Engelman, 2001) and the β-sheets TM interaction, a succession of anti-parallel β-stands (8 to 22 strands) forming a β-barrel (Schulz, 2002) (Fig. 2.8). The α-helix and β-sheets of TMs are in contact with each other, with the bilayer hydrophobic core, the bilayer interface, and, of course, the water. This is the reason of the importance of non-random amino acid distributions on those secondary structures.

As in soluble proteins, the interiors of polytopic proteins are comprised of internally H-bonded α-helix and/or β-sheets (Fig.2.8). Moreover, the major portions of their masses are buried inside the HC of the membrane, and are arranged in such a manner that allows their outer surfaces to face acyl chains that conform the HC(Schulz, 2002; Ubarretxena-Belandia and Engelman, 2001). Although the average hydrophobicity of the membrane proteins interior is the same compared to soluble proteins, the amino acids of the outer surfaces are more hydrophobic (Samatey *et al.*, 1995). The outside of an integral membrane protein is lipid-exposed. Its sub-domains are rich in hydrophobic amino acids, which are entirely matched by the lipid tails that make up about 40% of the thickness of the bilayer.

The average lengths of the TM α-helix and β-strands are greater than those observed in soluble proteins, so the 20 Å thick bilayer HC core can be spanned: α-helix are generally longer than 20 amino acids (1.5 Å /residue), and β-strands are longer than 10 amino acids (3.3 Å /residue). The TM

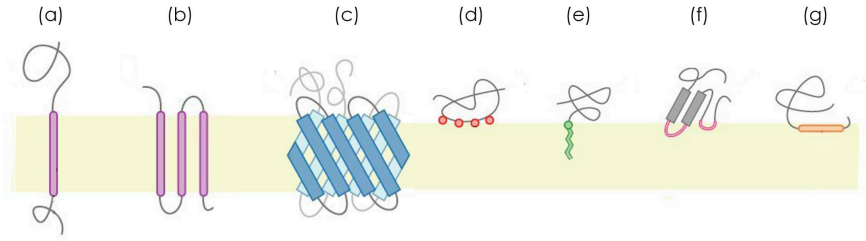

Figure 2.8: Schematics of the topology of the membrane depending on membrane-proteins interactions.(a-c) Correspond to integral proteins with polytopic interactions (a and b) with α-helices and (c) with β-sheets as the main secondary structures present. (d-g) Correspond to monotopyc interactions and they represent groups 1,2,3 and 4 described in the text, respectively.

proteins helices can tilt in order to make their length match the bilayer thickness, this is known as the hydrophobic-mismatch (Ozdirekcan *et al.*, 2007; de Planque and Killian, 2003; Sparr *et al.*, 2005; Debret *et al.*, 2008). At the same time, the bilayer thickness can change in the proximities of the proteins as we will discuss in the next chapter. Because of the length and the highly non-polar character of TM helices, hydropathy plots (Engelman *et al.*, 1986; White, 1994) have proven to be useful and remarkably accurate for predicting the topology of α-helical transmembrane proteins.

In turn, monotopic non-transmembrane protein-membrane interactions are characteristic of proteins that get in contact with only one leaflet of the lipid bilayer. They can be divided in four groups Lomize 2007 (Fig. 2.8):

- The first group includes those proteins that bind the membrane thanks to post-translational modification. Here, a covalent bond between the protein and a hydrophobic component is formed; most of the time this component is the Glycosyl-Phosphatidyl-Inositol (GPI) (Sangiorgio *et al.*, 2004) or prenylations in the proteins (Resh, 2006).

- The second group consists in proteins that interact with the membrane thanks to hydrophobic loops in their surfaces. This segments, can insert deeply into the membrane interface. (i.e. cardiotoxine (Efremov *et al.*, 2004))

- The third group corresponds to proteins that display electrostatic protein-membrane interactions. For example, the annexine V is capable to interact with the membrane thanks to a salt bridge formed between a Ca^{++} ion, the protein and the phospholipids negative charges (Mukhopadhyay and Cho, 1996).

- The fourth group includes proteins that interact with the membrane thanks to one or many interfacial amphipatic α-helices, which remain parallel to the plane of the membrane (IPM helix for In-Plane Membrane) (Sapay, 2006). Sapay and Gautier have develop new approaches in order

to predict this kind of interactions (Sapay *et al.*, 2006a; Gautier *et al.*, 2008). In the section 2.4 we will describe this group with greater detail. Before I will mention some aspects related with the secondary structure determinants in membrane proteins.

2.3.2 Membrane-proteins secondary structure

As we discussed before, the structure of the membrane determines the partitioning and folding of the membrane proteins in the bilayer. However, the three-dimensional structure of membrane proteins is governed by the same rules that define globular proteins structure. The proteins structure is stabilized inside the membrane by non-covalent interactions such as electrostatic, H-bonds, and hydrophobic interactions. That is, the polypeptidic chains folds in order to expose the polar residues toward the polar environments (solvent or headgroups), forming the polar domains, and keeping the hydrophobic residues in the interior of the protein or exposed to the hydrophobic environment (the acyl chains), forming the hydrophobic domains (Ubarretxena-Belandia and Engelman, 2001; Samatey *et al.*, 1995; Schulz, 2002).

The most predominant secondary structures in transmembrane proteins are α-helix and β-sheets. Some crystallographic structures of membrane proteins as well as numerous molecular dynamics simulations have started to highlight the importance of flexibility on these structures for the correct function of membrane proteins (Debret *et al.*, 2008; Stelzer *et al.*, 2008; Deupi *et al.*, 2009; MS and H., 2000).

Several experimental and simulation studies have analyzed the propensities of different amino acids to form particular secondary structures in solution (Petukhov *et al.*, 1999, 2002; Ramirez-Alvarado *et al.*, 1999; Viguera and Serrano, 1999; Chakrabartty *et al.*, 1994, 1993b,a, 1991; Pace and Scholtz, 1998). Hydrogen bonds play a role in stabilizing the α-helix and β-barrel conformation. However, the size and charges of sidechains are also important factors. This turned out to be relevant in the description of different aminoacid propensities to form helices in an aqueous environment. Different amino-acid sequences have different propensities to form α-helical structure. Met, Ala, Leu, uncharged Glu, and Lys, have especially high helix-forming propensities, whereas Pro, Gly and Asp have poor helix-forming propensities. Pro tends to break or kink helices because it cannot form a hydrogen bond (having no amide hydrogen), and because its sidechain interferes sterically. However, Pro is often seen as the first residue of α-helix, presumably due to its structural rigidity. In contrast, Gly, which also tends to disrupt helices, has a high conformational flexibility that becomes entropically too expensive to stay in the relatively constrained α-helical structure. Ser and Thr have also been identified as helix breakers or mostly in loop regions since they introduce flexibility to the soluble proteins. Other residues such as Val and Ile (well known as β-sheets formers) also break the α-helices .

The folding and packing of the membrane proteins is a major issue. I already discuss the influence of the partitioning in the folding. This is correlated with the individual amino acids propensities to form specific secondary structures. Thus, it is not surprising, that the structural propensities of different residues in the membranes are not yet well defined. Some clues have been revealed though. The experimentalists have tried to understand the propensities for a particular folding by examining its secondary structure stability and oligomerization. Some of these studies have been performed using

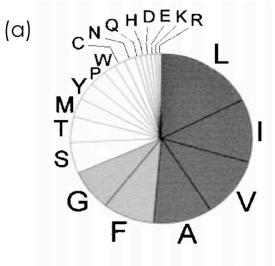

(b)

θ_{222nm} in CD spectra is used as a measure of helicity. Values reported are based on triplicate measurements, with a standard deviation of ±1%. Peptide concentrations were 30 μM.

Rank order	In *n*-butanol		In Aq.
	X residue ($-\theta_{222} \times 10^{-4}$)	*X* residue [P_a (TM)]	*X* residue ($-\theta_{222} \times 10^{-4}$)
1	I (3.88)	I (2.69)	E (2.25)
2	L (3.84)	L (2.53)	A (2.06)
3	V (3.82)	V (2.32)	L (1.80)
4	F (3.78)	A (1.86)	I (1.54)
5	A (3.72)	F (1.63)	D (1.47)
6	M (3.67)	G (1.36)	R (1.35)
7	G (3.44)	M (1.26)	M (1.33)
8	Y (3.33)	C (0.76)	Q (1.19)
9	C (3.28)	T (0.70)	Y (1.16)
10	T (3.27)	S (0.63)	W (1.13)
11	W (3.20)	W (0.45)	F (1.12)
12	S (2.99)	Y (0.39)	K (1.12)
13	H (2.90)	P (0.30)	V (1.03)
14	Q (2.87)	H (0.27)	C (0.91)
15	R (2.84)	Q (0.11)	T (0.90)
16	N (2.82)	N (0.10)	H (0.79)
17	D (2.66)	R (0.08)	S (0.79)
18	K (2.65)	K (0.08)	N (0.59)
19	E (2.54)	D (0.06)	G (0.34)
20	P (1.70)	E (0.05)	P (0)

Figure 2.9: (a) Frequencies of residues in TM proteins. (b) Propensities to form alpha helices in hydrophobic and aqueous environment (Adapted from (Liu and Deber, 1998b)).

transmembrane synthetic peptides in hydrophobic environments, such as micelles and vesicles (Li and Deber, 1994a), whereas others has been made in bulk-hydrophobic solutions (Liu and Deber, 1998b) (Fig. 2.9). These works have shown that, in contrast to their conformational preferences in water, the helical proclivity of the non-charged amino acids inside membranes is governed by their side chain hydrophobicity, and by the hydropathy of the local peptide segments in which the residues reside (Li and Deber, 1994b; Li *et al.*, 1996; Liu and Deber, 1998b).

Gly, and β-branched residues, such as Ile, and Val (Li and Deber, 1992a) seem to have an environment-dependent role for the support and modulation of helices. In those examples, the helical propensity of hydrophobic segments with different composition, decrease in the following order: Ala-Leu-rich> Gly-Leu-rich> Gly-Ile(Val)-rich. These results suggest that these residues may provide, partially, the structural basis for conformational transitions within or adjacent to membrane domains (Landolt-Marticorena *et al.*, 1993). Indeed, it has been shown that the lipid hydrophobic effects can contribute to dimer stability and the affinity of motif-mediated helix-helix interactions to define helix-helix interfaces (Johnson *et al.*, 2006).

On the other hand, the ability of all naturally occurring amino acids to form a turn when placed in the middle of a transmembrane helix has recently been measured (M. *et al.*, 1999). The observed rank order for turn-stabilizing tendencies are Asn=Arg=Pro (1.7)>Asp=Glu=His=Lys=Gln=(1.6)>Gly (1.3)>Ser=Trp (0.7)>Cys=Ile=Tyr (0.6)>Ala=Met=Val (0.5)>Leu=Phe=Thr (0.4). Moreover statistical analysis have confirmed that clearly, there are two sets of residues with either high ($\geq$1.3) or low ($\leq$0.7) turn propensity. Charged or polar residues induce a turn ($\geq$1.3), whereas hydrophobic residues plus Ser, Thr, and Cys remain α-helical ($\leq$0.7) (Ballesteros *et al.*, 2000). Furthermore, it has been

shown that Ser and Thr play an important role in the modulation of Pro-kinked TM segments when they are in the vecinity of the Pro moderating the steric clash between the pyrrolidine ring and the O-C_{i-4} carbonyl oxygen by modifying the conformation of the N_{i-3}-H amide group (Deupi *et al.*, 2004). Besides the important role of Pro residues (MS and H., 2000), Ser and Thr residues also stabilize local helical distortions of possible functional importance. It has been shown that combinations of these residues can produce dramatic effects on the conformation of TM α-helices. Indeed Ser/Thr can induce small distortions that can be amplified by the neighbour residues. Their unusual distribution in TM segments further suggests a possible functional role as structural adapters (Ballesteros *et al.*, 2000; Deupi *et al.*, 2004, 2009)

Other studies have highlighted that cation-pi interactions, particularly between Lys and Trp, Tyr, or Phe, as well as weakly polar interactions between pairs of aromatic residues, significantly enhance the strength of oligomerization of these hydrophobic helices. The contribution of these forces to the tertiary structure formation in designed transmembrane segments suggests that similar forces may also be a significant factor in the folding and stability of native membrane proteins (Johnson *et al.*, 2007). Deber and co-workers proposed that the high frequency of occurrence in membranes of residues such as Leu, Val, Ile, and Phe derives not only from their hydrophobicity but also from their intrinsic propensity to form the α-helical conformation in the non-polar environments of membranes (Liu and Deber, 1998a), since the helical propensity for individual amino acids is correlated with non-random occurring frequency in protein TM helices (Landolt-Marticorena *et al.*, 1993).

In brief, all that has been discussed until now gives the first notions to reconstruct the scenario for the action of the membrane curvature sensor ALPS, our study subject. The specific features of ALPS will be discuss in detail in chapter 4, for the moment, is important to remind that ALPS is an interfacial amphipathic α-helix, which structure depends on its partitioning. The individual propensities of its amino acids to form an α-helix, most also be taken in account. However, less is known about this matter at the interface due to its chemical heterogeneougenisity. Hence, its is crucial to consider that many non-covalent interactions are taking place and the structural and dynamic properties of the membrane will have an impact on them.

2.4 Amphipathic alpha-helices

This type of interaction to the membrane was discoverd more recently that the other monotopic binding interactions. The first amphipathic helix motif was identified in the Penicillin Binding protein 5 (PBP5) in 1986 (M *et al.*, 1986), which coincidently, contributes to maintain the shape of the cell in *E.coli* (Nelson and Young, 2001). The first crystallographic structure of this kind of motif was from the protein Prostaglandin H2 synthase-1 in 1994 (D *et al.*, 1994). Since then, many exemples of this binding motif have been identified. The amphiphatic helix is a conspicuous motif in proteins that bind to the membranes. It can be found for instance in many small GTPAses (Sar1, Arp1, Arf1, *etc*) (Farsad and De Camilli, 2003) or in some of their activators (as ArfGAP1 (Bigay *et al.*, 2003)). It can be present in the sterol transporter Kes1p and nucleoporin Nup13, and the golgin GMAP-210 (Drin *et al.*, 2007),

or in other cytosolic proteins such as endophilin, amphiphysin, and epsin (Farsad and De Camilli, 2003; Farsad *et al.*, 2001; Zimmerberg and Kozlov, 2006) and Annexin II (Hong *et al.*, 2003). In some N-Bar domains and N-terminal amphipathic helix is allso founded (Blood *et al.*, 2008). All these proteins have a role in sensing or producing membrane curvature and I will discuss about them in chapter 4. However, not all the amphipathic helix found in proteins are interfacial binding proteins and not all them are involved in shape membrane regulation neither.

The amphipathic helix can also be the preferential structure of many antimicrobial peptides (Haney *et al.*, 2009) or as part of non-structural viral proteins (NS5A) (Sapay *et al.*, 2006b). Many works have been done in order to understand this kind of interaction with the membrane, experimentally and by molecular dynamics simulations (Mishra *et al.*, 2008; Kandasamy and Larson, 2004; Nina *et al.*, 2000; Berneche *et al.*, 1998; Lomize *et al.*, 2007; Hristova *et al.*, 2001; Khandelia *et al.*, 2008). However, they have been mostly focused on amphipathic antimicrobial peptides and less simulations have been performed on amphipathic helices implicated in the control and/or recognition of the shape of the membrane. These works will be discussed further for the moment, since this is the structure of relevance for the subject of this thesis, it is important now to know some of its features.

2.4.1 Alpha-helix structure

The α-helix is a right- or left-handed coiled conformation, in which every backbone N-H group donates a hydrogen bond to the backbone C=O group of the amino acid four residues earlier (*i+4* to *i* hydrogen bonding). An α-helix has therefore the following features (Fig.2.10) :

- Every 3.6 residues make one turn, that is each amino acid in a α-helix corresponds to a 100° turn in the helix and a rise of 1.5 Å (0.15 nm) along the helical axis
- The pitch of the α-helix (the vertical distance between two points (turns) on the helix) is 5.4 Å (0.54 nm), which is the product of 1.5 and 3,6.
- The N-H group of an amino acid forms a hydrogen bond with the C=O group of the amino acid four residues earlier; this repeated *i+4* to *i* hydrogen bonding defines an α-helix. Similar structures include the 3_{10} helix (*i+3* to *i* hydrogen bonding) and the π-helix (*i+5* to *i* hydrogen bonding). These alternative helices are relatively rare, although the 3_{10} helix is often found at the ends of α-helices, or as intermediates of membrane binding-motifs (Gao and Wong, 2001; Hong *et al.*, 2003).

Helices observed in proteins can range from four to over fourty residues long, but a typical helix contains about ten amino acids (about three turns). Short polypeptides generally do not exhibit much α-helical structure in solution, since the entropic cost associated with the folding of the polypeptide chain is not compensated by a sufficient amount of stabilizing interactions. The backbone hydrogen bonds of α-helices are generally considered slightly weaker than those found in β-sheets, and are readily attacked by the ambient water molecules. However, in more hydrophobic environments such as the

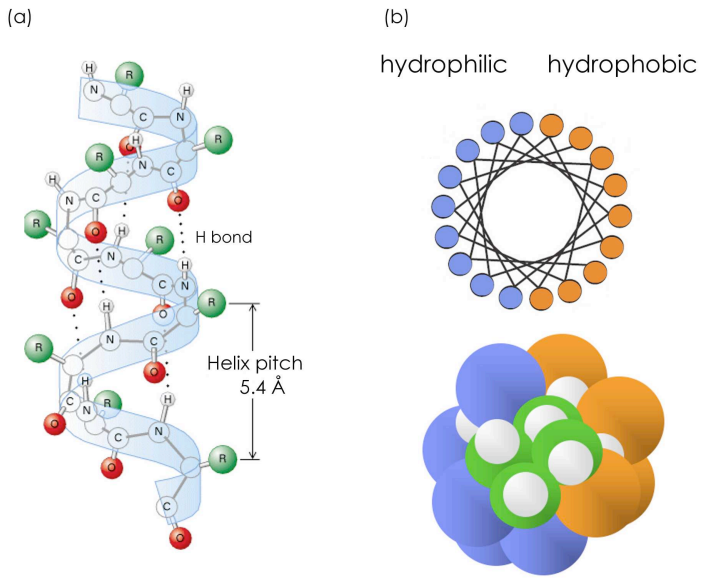

Figure 2.10: (a) α-helix structure. (b) show the faces of an amphipathic helix: (bleu) polar and (orange) hydrophobic. (upper) α-helix wheel diagram representation (bottom) α-helix vdw representation.

plasma membrane, or in the presence of co-solvents such as trifluoroethanol (TFE) (Myers *et al.*, 1998) oligopeptides readily adopt stable α-helical structure.

2.4.2 Amphipathic helices

In an amphipathic α-helix (AH), one side of the helix contains mainly hydrophilic amino acids and the other side contains mainly hydrophobic amino acids. The amino acid sequence of amphipathic α-helix alternates between hydrophilic and hydrophobic residues every 3 to 4 residues[11]. In most of the AHs, the interaction with the membrane strongly depends on charged electrostatic interactions between the positively charged residues of the polar face and the polar negatively charged headgroups of the membrane lipids. Moreover, many of the AH motifs that bind the membranes, are unfolded in solution and only fold in their appropriate α-helix once they bind to the membrane interface, following the partitioning-folding coupling mechanism described in section 2.2.2.

Mishra and colleagues made X-ray diffraction measurements on DOPC multilayers (liquid crystals) containing an ideally amphipathic α-helical peptide of 18 residues and determined the precise location of the α-helix within the bilayer (Fig.2.11).

Similar to the principal groups of the lipids that show a Gaussian transbilayer profile (Fig.2.11) (as a result of because of the thermal motion of the bilayer), the partitioning of the helix in the membrane

[11]Since the a helix makes a turn for every 3.6 residues.

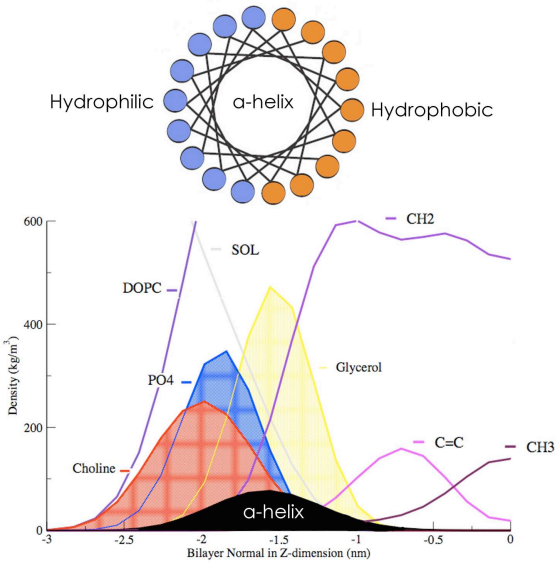

Figure 2.11: Partitioning of an amphipathic helix in the membrane interface (Density profile from a MD simulation)

can be seen as a Gaussian transbilayer profile too (Fig.2.11). The axis of the α-helix, which is parallel to the membrane surface, is located between the mean positions of the glycerol and carbonyl groups. White and co-workers showed that the surface of the helix penetrates and reaches the level of the double-bonds of the acyl chains, without causing major perturbations in the structure of the bilayer. It is worth to mention that since the membrane interface has a very steep decent of polarity that arises as the headgroup region gives way to the hydrocarbon region, the AH resides at approximately the mid-point where it can establish all kind of interactions with the membrane.

Another important property of almost all the amphipatic helix that interact with the membrane interface is their charged polar face. In consequence, the interaction with the membrane is mediated by charged electrostatic interactions with the polar heads of the phospholipids.

2.4.3 Amphipathic helices as mediators of the membrane interaction of amphitropic proteins and as modulators of bilayer physical properties

We mentioned that many membrane-shape related proteins have an amphipathic helical motif implicated in generate or sensing the membrane curvature. How this single motif can have both functions is still unknown, or how this processes are imbricated is yet unclear. The amphipathic helix is one of the most common secundary structure motifs in proteins. It is used by amphitropic[12] proteins to mediate weak, reversible binding to cell membrane surfaces. In these proteins this amphipathic motif share some

[12] a subclass of proteins that exhibit a regulated interconversion between two environments, aqueous and lipidic.

common features, some of them have already been pointed out (Cornell and Taneva, 2006):

1. All of them have net positive charge, with the exception of ALPS (our study subject)
2. they oil-water partitioning near to zero, consistent with their amphipathic nature
3. their peak hydrophobic moments range between 0.4-0.8 and their mean hydropathy is typical of surface seeking helices
4. their hydrophobic sectors are typically ~180°

Besides these physicochemical properties, this kind of amphipathic helix can have some or one of the following functional attributes (Cornell and Taneva, 2006):

1. **Sense membrane physical properties,**
   (a) As a response to the negative surface potential, binding selectively to anionic lipids. Their binding can have electrostatic and hydrophobic contributions. While the electrostatic attraction contributes to the binding, the hydrophobic character of the amphipathic helix is the key dterminant of the binding strength.
   (b) as a response to packing disorder (i.e. MinD interactions with polyunsaturated acyl chains rich vesicles) or to surface defects at phase boundaries (i.e. CTT or α-synuclein binding to lipid mixtures phase separations)
   (c) they also respond to negative curvature strain or
   (d) to the positive curvature of the membrane
2. **Bind membrane surfaces weakly and therefore their binding is subject to regulation**
   (a) some of them are subject to a control of the binding were the driving force is the partitioning-folding coupling process described in section 2.2.2, there exist some exception thougth.
   (b) low affinities are maintained by relatively low-specificity Van der Waals interactions, althougth some MD studies showed prevalent hydrogen bonding between peptides and lipids
   (c) the lipid composition, sorting and lipid concentration varaitions can also regulate their binding
   (d) some studies in CCT protein showed that the phosphorilation can antagonize the binding
   (e) the binding can be also regulated by the membrane curvature as in the case of some proteins implicated in the secretory pathways (I will discuss these aspects in chapter 4)
3. **AH motif can serve as an autoinhibitory domain in certain amphitropic proteins**
4. The insertion of AH helices at the membrane interface modulate bilayer physcial properties such as,

(a) neutralization of surface negative charge

(b) elimination of packing stress, by inserting in the lipid packing defects can alleviate the curvatures strain in vesicles of small radius and stabilize the high curvature

(c) generation of membrane curvature as is the case of Bar domains and other lipid-bindig motifs that we will mention in the next chapter.

Some of these attributes will be discussed in more detailed in the following chapters in order to offer the appropiate background to understand the amphiphatic sensor of our interest, ALPS. Our work could give insights about the particularities about this kind of particular sensors. To accomplish this aim, it is important to introduce some aspectes related with the generation of the curvature and all the forces implicated in the maintainance of the membrane structure.

It is noteworthy that there are different types of proteins that could be part of membrane-shape processes and different ways of being sensible to the environment. Membrane proteins functions are very diverse. Among their functions we find enzymes, structural components, molecular motors, etc. Integral proteins, that serve as an interface between both sides of the bilayer, can have other specific functions directly related with this favorable disposition: they can be transporters or receptors. The function of these membrane-proteins can be very sensitive to the changes in mechanical or physical membrane properties, such as the surface tension in the case of mechanosensitive channels (Yefimov *et al.*, 2008). Membrane proteins can also be the fixation points of surrounding structures such as the cytoskeleton or the extracellular matrix that turn out to be important in the adhesion of the tissues, cell migration or in endocytotic process, where the ability to sense the form or the geometry is important (Vogel and Sheetz, 2006; Cukierman *et al.*, 2001).

I will focus in the next chapter on those mechanical and physical properties of the membranes and on that fascinating kind of membrane-shape related proteins, which are able to act as remodelers or sensors of the membrane curvature.

Chapter 3

Remodelling and sensing the membrane

The research field of shape and remodeling of the biological membrane is rather recent and only multi-interdisciplinary researches have started to give proper answers about the processes that are involved. Several recent studies in biochemistry and cell biology have begun to identify and characterize proteins that are required for shaping some organelles and endomembrane systems (Zimmerberg and Kozlov, 2006; McMahon and Gallop, 2005). An elegant example of membrane reshaping mediated by membrane proteins is observed in the chromatophores of purple photosynthetic bacteria where the light harvesting complexes I and II (LH1 and LH2), the cytochrome$_{bc1}$, and possibly the ATP synthase are able to shape and maintain the chromatophore structure [1](Frese *et al.*, 2004, 2008; Bahatyrova *et al.*, 2004). Another example would be the F1F0-ATP synthase[2] (Paumard *et al.*, 2002; Giraud *et al.*, 2002; Everard-Gigot *et al.*, 2005) that maintains the tubular form of the inner mitochondial membranes, in the same way the reticulon and DP1/YOP1 (Voeltz *et al.*, 2006; Buton *et al.*, 1996) maintain the shape of the ER. The cytoskeleton, microtubules and actin filaments dynamics, play a key role maintaining Golgi stacks shapes (Egea *et al.*, 2006; Cole *et al.*, 1996) and to shape the mitochondria (De Vos *et al.*, 2005; Varadi *et al.*, 2004). These findings indicate general mechanisms of organelle shaping that are used throughout the cell (Voeltz, 2007). Physicist and mathematicians have also been recently interested in studing and modeling membrane deformations. They have been particularlly attracted by the formation of tubes that change the membrane topology[3] and progressively move the surface to higher levels of shape complexity. Additionally the researches have analyzed the mechanical forces

[1]Light harvesting dimers curvature effect has been simulated by Schulten and co-workers.

[2]F-ATPases (F1FO-ATPases) in mitochondria, chloroplasts and bacterial plasma membranes are the prime producers of ATP, using the proton gradient generated by oxidative phosphorylation (mitochondria) or photosynthesis (chloroplasts).

[3]In mathematics terms, topology is an area of study concerned with spatial properties that are preserved under continuous deformations of objects, for example deformations that involve stretching, but no tearing or gluing. It emerged through the development of concepts from geometry and set theory, such as space, dimension, and transformation. We must distinguish it from the term "membrane topology" used by the biochemists to make reference to the disposition and orientation of the proteins in the biological membranes.

implicated in the elastic, bending and tension properties of the bilayer. Their studies and models, together with molecular dynamics (MD) simulations of several membrane-shape related proteins, have provided invaluable elements to understand the role of biophysical properties of the lipids in shaping the membranes. Maintaining, sculpting and sensing the membranes are essential processes for the cell. In this chapter we will discuss both aspects.

3.1 Determinants of the membrane shape

3.1.1 Membrane tension

One important force in the membrane is the tension. The cell membrane tends to maintain a specific lipid packing density, an increase in the lipid spacing by osmotic swelling, leads to membrane rupture when the membrane is strained slightly above its optimal packing. Therefore, and in order to compensate the increase in the lipid spacing by osmotic swelling, several mechanosensitive ion channels adopt an open structure as a response to the generated surface tension (Yefimov *et al.*, 2008). Compression within the plane of the membrane would be also resisted, however the membrane buckles out of plane before significant compression occurs. Bucking events have a high energy barrier and occur rarely, but when a small membrane patch buckles between cytoskeleton anchors, this patch will grow to become a vesicle by drawing area from surrounding patches, which are also under compression. The vesicle will eventually pinch out off the membrane, thereby reducing the excessive area. The rate of buckling depends on the stress in the membrane, which is increased by cytoskeleton stiffening and decreased by vesicle shedding (Manneville *et al.*, 2008; Sens and Gov, 2007).

3.1.2 Spontaneous curvature

We already mention that cylindrical lipids such as PC tend to form lamellar structures. Since the biological membrane is a mixture of many lipids with different shape factors, the default shape for the membrane is not flat. Instead, each lipid shape that deviates from a cylinder contributes to a spontaneous curvature of the membrane. The curvature can be positive or negative. To define the curvature sign, we need to distinguish between the two sides of the surface. For a lipid monolayer, one surface is covered by the phospholipid polar headgroups, whereas the other is hydrophobic. By convention, monolayer bending from the heads to the tails produces positive curvature, whereas bending in the opposite direction results in negative curvature (Fig. 3.1 (c)). Lipids that have an overall inverted conical shape, such as lysophospholipids and polyphosphoinositides, favor the formation of structures with a positive curvature such as micelles (Fig.3.1 (d)). Lipid molecules that have an overall conical shape with a small hydrophilic cross-section area, such as DAG and PE, form structures with a negative curvature, for example the hexagonal phases of tubes with the head groups facing the inside and hydrophobic tails outside (Sprong *et al.*, 2001; Janmey and Kinnunen, 2006b)

The lipid composition favors different membrane curvatures (Fig.3.1), and lipid dynamics have important implications in the maintenance of curved structures that are essential for the shape of

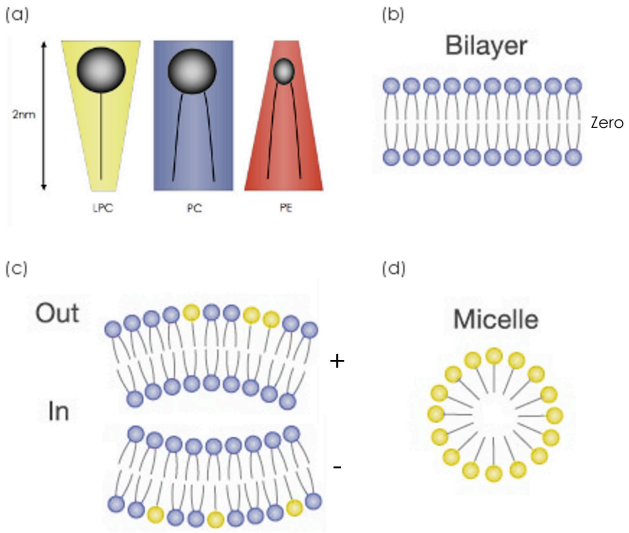

Figure 3.1: 3.1Lipid packing and spontaneous curvature. (a) Different lipid shapes: inversed cone (yellow), cylindric (bleu), conical (red). (b) the bilayer formed by cylindric lipids, (d) micelles formed by inversed cone lipids and (c) mixed bilayers with spontaneous curvature depending in lipid composition.

the cell, organelles and endomembrane systems. The importance of non-lamellar bilayer states (i.e. hexagonal phases) in biological systems has been substantially examined (Baumgart *et al.*, 2003). Lipid phases occur in a large number of processes, including pore formation, membrane genesis, and in intermediates of fusion or fission found in endocytosis, exocytosis and viral entry. In many of these processes the local membrane composition is far from homogeneous. Formation of non-lamellar phases is therefore intrinsically linked to the appearance of dynamical heterogeneities. In most cases, non-lamellar states are transient and only involve a fraction of the lipids in the aggregates. These results complicate experimental studies, however computer simulations are finding methodological procedures to deal with such problems (Marrink and Mark, 2004; Marrink and Tieleman, 2001; Marrink *et al.*, 2009b).

On the other hand, the local shape of a membrane depends on the type of lipids that are present and on their spatial distribution. Insertion or removal of lipids into the inner or outer leaflet leads to area mismatches that also alter curvature (Fig. 3.1). For entropic reasons, any bilayer, like any elastic material, exhibits temperature induced fluctuations called undulations (fluctuations in the average position of the bilayer surface). Besides, and as we mention before, a finite patch has a tendency to close upon itself (i.e. form a vesicle) in order to minimize the line tension arising at the bilayer edge. Undulations, are governed by the bending rigidity of the bilayer. Lindahl and Edholm (Lindahl and Edholm, 2000) were the first to show the spontaneous appearance of such undulations in their benchmark simulations study of a DPPC membrane (modeled at all-atom resolution).

Membranes resist bending because changing local curvature alters both, the head group spacing and

the entropy of the hydrophobic chains. The bending stiffness is strongly dependent on the nature of the lipids and their spatial distribution. The bending is characterized by two bending moduli, quantifying stiffness in the two possible orthogonal radii of curvature for a planar membrane (Janmey and Kinnunen, 2006b). For an initially flat membrane in the x–y plane, one bending direction can be visualized in the z direction along the x-axis and the other in the z direction along the y-axis (Zimmerberg and McLaughlin, 2004).

3.2 Forces within the lipid bilayer

The cell membrane can resist to deformation caused by forces applied in various directions. The magnitude of this resistance is characterized by several elastic constants that are defined by different geometries of deformation: shear, bending and stretching. These physical properties depend on the chemical composition of the bilayer and on the lateral and transverse asymmetries. Shear deformations within the plane of the fluid bilayer meet no elastic resistance because the lipids and TM proteins can flow over each other. Lipid bilayer membranes resist stretching and bending with elastic constants that are physiologically relevant (see below). The bilayer also strongly resists to stretching because the distance increase (on average) between head groups increases exposure of the hydrophobic core to water (Farsad and De Camilli, 2003; Janmey and Kinnunen, 2006b).

We mention in chapter 2 that the presence of TM proteins inside the bilayer induces transversal forces that can alter the membrane thickness. The transition from a thicker to a thinner membrane generates packing disorders that increase elastic energy (Risselda, Campelo). TM proteins also have a specified length of hydrophobic contour that can differ from the optimal hydrophobic thickness of the bilayer. This hydrophobic mismatch can lead to stretching or compression of lipids and proteins inside the membrane (Fig.3.2) (Turner and Sens, 2004) or to tilting of transbilayer helices to decrease the hydrophobic height (Ozdirekcan *et al.*, 2007). Insertion of different lipids or proteins in an isolated domain can also affect the thickness of the membrane (Bucki *et al.*, 2000).

The differences in lipid order and lipid packing can cause lateral pressures due to loss of chain entropy in the hydrophobic domain that creates compressive forces in the bilayer (Kung, 2005). The magnitude of the lateral pressure depends on bilayer thickness, lipid composition (the nature of the hydrophobic chains (e.g. saturated, unsaturated, single chains or sterols)), and the membrane curvature. In the bilayer, a compression force acts at the hydrophilic interface to crowd the head groups tightly to minimize exposure of the hydrophobic chains to water. These lateral forces are present even if no external force is applied to the membrane (see also section 3.3). However, external forces that deform the membrane – osmotic stress and membrane bending – affect directly these lateral forces and subsequently modify the membrane protein structure and interactions (Kung, 2005).

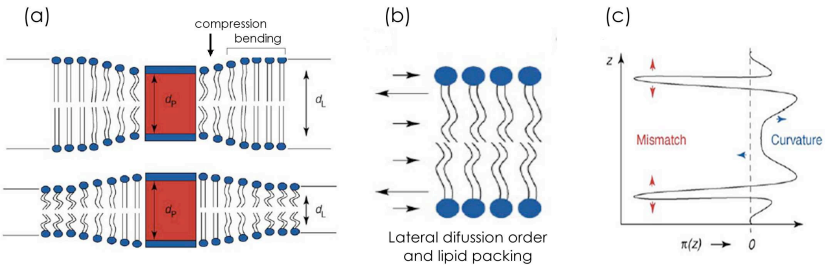

Figure 3.2: Schematic representation of the forces that shape the membrane (a) Transversal forces and the hydrophobic mismatch. The influence of the protein over the unperturbed d_L depends on the distance (b) lateral pressures (c) The blue arrows show how the bending of the membrane alters the pressure gradient within the bilayer, stretching and compression. (Modified from (Janmey and Kinnunen, 2006b)).

3.3 Membrane bending

The difference between the membrane sides according to their orientation with respect to the volume that is surrounded by the membrane, allows to distinguish between a positively or negatively curvature. This differentiation permits the characterization of membrane deformations. In the lipid bilayer, the hydrophobicity of the inner core guarantees that no membrane edges can be exposed to the aqueous solvent. Any membrane compartment in cells has therefore a continuous surface. Topological discontinuity between membranes can arise by the budding off of vesicles or the scission of tubules and sacks. Topologically segregated compartments have distinct membrane surfaces where the orientation of membrane lipids and proteins is typically inherited from the mother membrane (Jekely, 2007). If we take budding off of vesicles as an example, we observe that positive curvature bulgs towards the cytoplasm. At this moment of transition, that is, between the dome of the vesicle and the vesicle neck we find both, positive and negative curvature, in perpendicular directions. The positive curvature is present when the neck is still round, and negative curvature is present because a concave surface is formed (a longitudinal section of the budding vesicle). The neck is shaped like a cylinder with positive curvature in one direction but zero curvature in the other. Finally, once the vesicle is formed, its size is determined by the degree of positive curvature exhibited (small vesicles exhibit higher positive curvature) (McMahon and Gallop, 2005).

3.4 Proteins that bend membranes

Proteins that are capable to apply mechanical forces to the membrane can disturb the membrane inherent forces. There are two main mechanisms of membrane deformation, which are not mutually

exclusive, and where proteins participate: the extrinsic [4] and intrinsic[5] mechanisms (Fig.3.3)(Farsad and De Camilli, 2003). Several of the extrinsic forces applied to the membrane have been studied for a long time, as is the case of the cytoskeleton that deformes the membranes (Vale and Hotani, 1988; Lippincott-Schwartz *et al.*, 2000; Dabora and Sheetz, 1988) by pulling them to form tubules or to endow the membrane with resistance to shear and determine viscoelastic properties (Janmey and Kinnunen, 2006b) (Fig.3.3(b)). Many intracellular membrane tubules are generated by this process (Hirokawa, 1998; Allan and Schroer, 1999; Roux *et al.*, 2005). Recently, the role of other peripheral and integral proteins on membrane deformation has been identified and characterized, i.e. photosynthetic proteins in purple photosynthetic bacteria and chloroplast thylacoids, F1F0-ATP-synthase in mithocondrial crestae, reticulon and DP1/YOP1 in endoplasmic reticulum (Paumard *et al.*, 2002; Giraud *et al.*, 2002; Buton *et al.*, 1996; Voeltz *et al.*, 2006; Everard-Gigot *et al.*, 2005) However, most of today's knowledge on membrane deformation comes from the vesicle and tubules formation during trafficking events (Peter *et al.*, 2004; Blood and Voth, 2006; Durrieu *et al.*, 2009; Praefcke and McMahon, 2004; McMahon and Mills, 2004; Zimmerberg and McLaughlin, 2004; Nossal and Zimmerberg, 2002; Huttner and Zimmerberg, 2001; Coorssen *et al.*, 2003). This kind of event corresponds to the intrinsic mechanisms, which will be discussed in the following sections. The intrinsic mechanisms of membrane deformation (or bending) include: the lipid composition (already discussed), the scaffolding (by peripheral or integral proteins), and the helix insertion (Farsad and De Camilli, 2003; Miller and Krijnse-Locker, 2008; Voeltz, 2007).

3.4.1 Proteins actin by the scaffold mechanism

The scaffold mechanism assumes that proteins can function as scaffolds when the intrinsic curvature of the protein matches and impose higher curvature to the lipid bilayer (Farsad and De Camilli, 2003) (Fig.3.3 (c)). Such proteins must satisfy several criteria in order to bend lipid bilayers locally. Most importantly, the intrinsic shape of a protein, or protein network, must expose a curved interaction surface with the lipid bilayer. Such shape can result either from the tertiary protein structure or from a surface that is formed by protein–protein interactions. Furthermore, the protein or proteins should have sufficient intrinsic rigidity to counteract the tendency of the lipid bilayer to relax towards its state of spontaneous curvature (bending stiffness). Finally, peripheral proteins must have a sufficient affinity for the lipid polar headgroups in order to make the lipid bilayer fit the shape of the protein. The energy of protein–membrane binding has to exceed the membrane-bending energy.

According to the scaffold mechanism, all protein coats that cover the surface of membrane invaginations that bud along the membrane, function as scaffolds for membrane curvature. Three kind of vesicles coat proteins, COPI and COPII complexes and the clathrin–adaptor-protein, are able to oligomerize to promote budding and hence, they provide scaffolds for spherical curvatures (McMahon and Mills, 2004). Furthermore, two other proteins are involved in the scaffold mechanism: dynamin, a protein implicated in the fission of vesicles (Praefcke and McMahon, 2004; Hinshaw and Schmid, 1995), and the BAR

[4] Extrinsic forces on the membrane are exerced by peripheral or transiently associated membrane-proteins
[5] Intrinsic forces on the membrane are exerced by monotopic or integral polytopic membrane-proteins

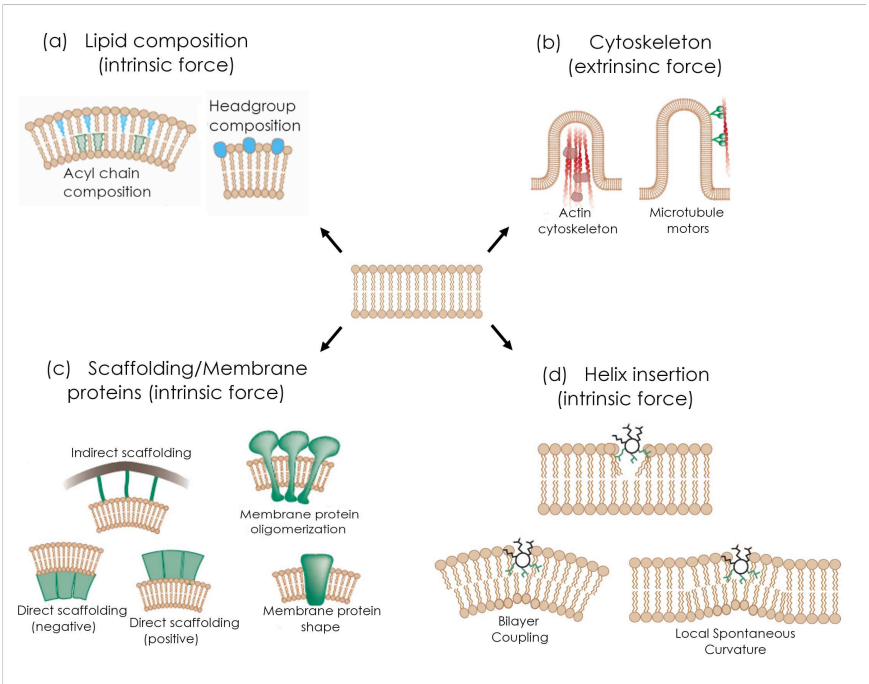

Figure 3.3: Membrane Bending mechanisms (Modified from (McMahon and Gallop, 2005; Zimmerberg and Kozlov, 2006)).

((Bin/amphiphysin/Rvs)-domain-containing proteins (Peter *et al.*, 2004; Dawson *et al.*, 2006; Gallop and McMahon, 2005), which wraps around membranes and provide scaffolds for cylindrical curvature (Zimmerberg and McLaughlin, 2004; McMahon and Gallop, 2005; Gallop and McMahon, 2005).

As scaffolding proteins, dynamin and Bar-domains have a high affinity for the membrane and their intrinsic curved shape counteracts the forces of the membrane and allows them to modify, by them selves, the membrane curvature (Zimmerberg and Kozlov, 2006). That is, the dynamin helix self-assembles in the absence of lipids into rings and helices (Hinshaw and Schmid, 1995). Then, dynamin binds to lipid membranes and forms cylindrical coats that have the same helical structure and cross-section radius as the pure dynamin helix (Sweitzer and Hinshaw, 1998). This means that the rigidity of the dynamin coat is greater than that of the lipid bilayer, and therefore, dynamin lipid-binding is sufficiently strong to allow the work of the scaffold mechanism in membrane shaping and membrane fission (Praefcke and McMahon, 2004; Kozlov, 1999, 2001). On the other hand, the BAR-domain has a banana-like shape (Peter *et al.*, 2004; Gallop and McMahon, 2005), and its concave surface binds the lipid membrane. This banana-like shape has a correct intrinsic shape to bind curved membranes. In addition, the BAR-domain has positively charged residues on its concave surface, which allows a strong interaction with negatively charged polar headgroups of the lipid molecules. In general, the electrostatic interaction between lipids and proteins is one of the important factors that determine membrane shape (Zimmerberg and McLaughlin, 2004). Although there are no data available regarding the intrinsic

rigidity of BAR-domains, presumably the bundling of the BAR-domain helices produces rigidity. The curvature of many membrane tubes that are covered by these domains have shapes that are close to the intrinsic curvature of the concave BAR-domain. The tubulation process induced by the BAR-domains has been elegantly simulated by molecular dynamics (Yin *et al.*, 2009; Blood *et al.*, 2008; Blood and Voth, 2006; Ayton *et al.*, 2007) showing, at an atomic level, how curved BAR-domains have a high affinity for curved membranes and their ability to induce greater shape deformations.

In turn, clathrin proteins have an intrinsically curved shape that allows them to form spheroid arrangements in the absence of lipids. Therefore one could expect that clathrin function by the scaffold mechanism. However, it has been demonstrated that clathrin proteins are not able to curve membranes by them self, and in consequence, they need to interact with other adaptor-proteins in order to modulate the degree of curvature generated (Nossal and Zimmerberg, 2002). Similarly, the structure of the one component (Sec23–Sec24) of the COPII coat complex has a concave surface that fits a circle with a 30-nm radius (Bi *et al.*, 2002), and under optimal conditions, Sec23–Sec24 and Sec13–Sec31 self-assemble into spheroids (Bi *et al.*, 2002). However, they need to act simultaneously in other associated proteins to curve the membranes (McMahon and Mills, 2004).

3.4.2 Proteins acting by the local spontaneous curvature mechanism

The helix insertion mechanism is tightly correlated with the local spontaneous curvature mechanism and the bilayer-coupling effect (Farsad and De Camilli, 2003; Zimmerberg and Kozlov, 2006) (Fig.3.3 (d)).

3.4.2.1 The local spontaneous curvature mechanism

The local spontaneous curvature mechanism has been essentially attributed to the local deformation of membranes that occurs when the amphipathic helical moieties of proteins become embedded in the lipid matrix. A shallow insertion of an amphiphatic protein helix into only the upper part of a membrane monolayer has the role of a wedge that perturbs the packing of the lipid polar headgroups and results in a local monolayer deformation (Campelo *et al.*, 2008) (Fig. 3.3 (d)).

The epsine protein is a classical example of this type of proteins (Ford *et al.*, 2002). It has been shown that the epsine is able to form small tubules when incubated with liposomes. The ENTH-domain has a high binding affinity for membranes when phosphatidylinositol-4,5-bisphosphate is present in the membrane. The epsine ability to curve membranes depends entirely on the insertion of its ENTH-domain amphipathic helix into the membrane bilayer by inducing a spontaneous curvature deformation (Stahelin *et al.*, 2003). Presumably, the amphipathic N-terminal region of endophilin functions in a similar fashion, independently of its putative enzymatic activity (Farsad and De Camilli, 2003). The small GTPase Sar1, which is one of the core COPII proteins, has been shown to curve lipid bilayers by membrane insertion of its N-terminal amphiphatic α-helix (Fath *et al.*, 2007; Lee *et al.*, 2005) and inducing local spontaneous deformations. Replacing hydrophobic residues in this α-helix with alanines, impaired the ability of Sar1 to tubulate membranes.

3.4.2.2 The bilayer-coupling mechanism and other distorsions of the membranes attributed to amphiphatic helices

The bilayer-coupling mechanism is tightly associated with the local spontaneous mechanism. Therefore, proteins involved in local spontaneous mechanism, which penetrate only one lipid monolayer, induce a curvature by the asymmetry between the membrane leaflets and the membrane.

The bilayer-coupling mechanism was initially popularized by Sheets and Singer in 1974. This mechanism postulates that the two leaflets of a closed lipid bilayer, by virtue of asymmetries between them, could have differential responses to various perturbations (Sheetz and Singer, 1974; Sheetz *et al.*, 1976). If the amphiphatic protein domains penetrate only one lipid monolayer, they can produce an area difference between the membrane leaflets and the membrane that will develop curvature to compensate for this area asymmetry (Campelo *et al.*, 2008) (Fig. 3.3 (d)). Moreover, the insertion of an amphipathic helix, depending on the depth of penetration can induce changes in the bilayer thickness as a result of the transversal diffusion of the surrounding lipids. If the helix has a superficial position the membrane get thick on its vecinity, whereas if the helix is near the center of the hydrophobic core, it gets thinner. These effects also account to both the bilayer-coupling and the local spontaneous curvature mechanisms (Campelo *et al.*, 2008; Devaux, 2000).

There are examples of proteins that have an N-terminal amphiphatic helix critical for membrane binding, which could potentially play a key role in budding. This is the clear case of ARF-family GTPases (Amor *et al.*, 1994; Bigay *et al.*, 2003; Antonny *et al.*, 2003), involved in the recruitment of coat proteins for vesicular trafficking along the secretory and endocytic pathways. Moreover, many monotopic proteins interact with the membrane using amphipatic helical motif[6] . Some examples are the Annexin B12 ((Fischer *et al.*, 2007), the Annexin II N-terminal tails (Hong *et al.*, 2003) or the amyloid proteins such as α-synuclein (Jao *et al.*, 2004), Prostaglandin H2 synthase (Fowler *et al.*, 2007) and IAPP, which are important in type-II or non-insulin-dependent diabetes mellitus (Jayasinghe and Langen, 2007). A huge number of amphiphatic helices that interact with the membranes are found in antimicrobial peptides (AMP) (Haney *et al.*, 2009). In all these proteins, the electrostatic interactions of the protein with the membrane play an important role in membrane binding.

An intriguing possibility could be that all proteins with amphiphatic peptide that are involved in local spontaneous bending and in bilayer coupling mechanisms, might share a common system for enabling membrane deformation through the interaction of their amphipatic α-helix with the lipid bilayer. Therefore, the identification of those mechanisms behind these protein-bilayer behaviors and regulations would be the key aspects to understand the dynamics of these processes. Most of the studies concerning the action of AMP, highlight the importance of an interfacial partitioning of the peptides prior to the pore formation. Many MD simulations demonstrate the importance of the insertion and interfacial positioning of amphipatic peptides in the membranes (Kandasamy and Larson, 2004; Nina *et al.*, 2000; Berneche *et al.*, 1998; La Rocca *et al.*, 1999).

[6] An amphipathic helix is a helical arrangement of polar residues in one face and hydrophobic residues in the other. This disposition matches well the properties of the membrane interface. See Fig.2.11

3.4.3 Simultaneous operation of bending mechanisms

It is unlikely that during the complex formation of vesicles and tubules each curvature-membrane mechanism operates independently. Instead, the interplay of different proteins guarantees the robustness of the membrane-deformation process. The budding machinery of endocytic vesicles needs clathrin–adaptor-protein complexes, which seem to be too flexible to bend membranes effectively by their own, and so, they are helped by epsin, which is able to induce membrane curvature using the local spontaneous curvature mechanism. The formation of membrane necks that connect clathrin-coated buds with the plasma membrane and the fission of these two elements, could be carried out by dynamin alone. However, within the cell, dynamin operates together with endophilin and amphiphysin. As mentioned before, endophilin possess one amphipathic helix that might function according to the local spontaneous curvature mechanism (Peter *et al.*, 2004; Farsad and De Camilli, 2003). Similarly, amphiphysin might also function according to the local spontaneous curvature mechanism by the insertion of one amphipathic helix into one leaflet of the lipid bilayer, and therefore the bilayer-coupling effect operates as well. Additionally, amphiphysin contains a N-BAR-domain that might induce membrane-curvature, and it was recently observed, by molecular dynamics simulations, that the N-terminal amphiphatic helix of this N-BAR domain is able to form tubules around the membrane by it self (Blood *et al.*, 2008). As discussed in section 3.4.1, the COP complexes are unlikely to provide a sufficiently rigid scaffold to bend intracellular membranes into small buds and vesicles. Therefore, membrane shaping by the COPII coat is most probably driven by the synergistic action of the Sec23–Sec24 plus Sec13–Sec31 scaffold and Sar1. All these elements act together to generate local spontaneous curvatures.

3.5 The importance of sensing shape

I have mentioned throughout the previous chapters that membrane-protein functions depend on their ability to sense biophysical properties of the membrane. Since formation of different membrane shapes are crucial for many biological processes, the ability to recognize and/or sense these shapes must be also indispensable to regionalize and regulate a great number of cellular functions. If we are aware of the existence of molecular mechanisms that induce membrane curvature, then there should also exist mechanism that would sense this curvature. Vogel and Sheetz have defined the concept of "geometry sensing" as the formation of signaling complexes produced by the recognition of shape changes in the surfaces (i.e. the geometrical shape of the surface) (Vogel and Sheetz, 2006). The latter is of great relevance as we see, for example, in cell adhesion, in tissues formation (Chen *et al.*, 1997), in morphogenesis or in cell migration (Schindler *et al.*, 2005), where the extracellular matrix plays a crucial role in recognizing different patterns in the substrate surfaces. But, how cells differentiate between a concave (positive) and a convex (negative) membrane curvature? This is a very relevant question with important implications in the understanding of endocytosis i.e. phagocytosis (in immunological responses by macrophages) and trafficking. The answer to this question is not obvious, and it has not yet been fully understood how the membrane curvature is recognized. However, several types of sensors have been identified that can either sense convex or concave curvatures (Vogel and Sheetz, 2006).

An interesting example of convex-curvature sensors is the case of certain K+ channels that adopt an opened structure when they are embedded in membranes with convex curvature (Patel *et al.*, 2001).

Among concave curvature sensors we can mention the membrane-anchor proteins (whose anchors can be acylchains covalently linked to the protein, such as in prenylated proteins (Resh, 2006) or an amphipathic helix motif) (Hatzakis *et al.*, 2009) and scaffold-peripheral proteins (such as BAR-domain proteins). On the other hand, lipids with asymmetric shape factors are predicted to sense the membrane curvature (Fig.3.3 (a)) (Farsad and De Camilli, 2003; Roux *et al.*, 2005). Recently Hatzakis proposed that "sensing" is predominantly mediated by a higher density of binding sites on curved membranes, instead of higher affinity of certain proteins to the membrane curvature. In their work, they proposed a model that is based on curvature-induced defects in lipid packing related to lipid sorting (Sorre *et al.*, 2009)l and accurately predicted the curvature sensor capacities of the membrane-anchored proteins. Based on the fact that unrelated structural motifs such as α-helices and acyl chains sense the membrane curvature, they suggested that membrane-curvature sensing is a generic property of curved membranes rather than a property of the anchoring molecules (Hatzakis *et al.*, 2009). They also put forward that membrane-curvature will promote the redistribution of proteins that are anchored in membranes through other types of hydrophobic moieties. Indeed, it has been shown that the fluidity of the membrane may induce the mechanical or diffusional separations of components. This phenomenon can have important biochemical consequences, for example, in the formation of the immune synapses where the spatial patterning of TM receptors regulates T-cell activation (Bromley *et al.*, 2001; Mossman *et al.*, 2005).

As I mentioned in section 3.4.1, proteins with a BAR-domain can recognize, using their intrinsic concave form, a positive membrane curvature and then induce higher degrees of curvature until tubulation (Dawson *et al.*, 2006; Yin *et al.*, 2009). Therefore, BAR-domains have a double role as a curvature sensor and as a membrane-bending protein (Peter *et al.*, 2004; Yin *et al.*, 2009). The extra bending induced by proteins like the Bar-containing-proteins might allow the recruitment of further protein partners (that may act based on the Hatzikis model) in order to form a multi-protein complex with a synergic bending force. Indeed, it has been shown that some of these proteins and amphipathic helices up-concentrate on areas of high membrane curvature (Peter *et al.*, 2004; Mesmin *et al.*, 2007; Cornell and Taneva, 2006). The BAR-domains of arfaptins for example can recruit some small GTPases (Tarricone *et al.*, 2001), and other BAR-domains have effects on cell motility (Carstanjen *et al.*, 2005).

Finally, amphipathic α-helices are one of the most important classes of membrane curvature sensors found in a wide range of proteins. Some examples are Annexin B12 N-terminal tail (Fischer *et al.*, 2007), and some trafficking proteins, which regulate, for instance, the protein coat assembly (GMAP 210, Sar1, Epsin) (Lee *et al.*, 2005; Drin *et al.*, 2007; Ford *et al.*, 2002) and the coat disassembly (ArfGAP1). ArfGAP1 and GMAP210 contain amphipathic α-helices called ALPS motif (Amphipatic Lipid Packing Sensor) (Bigay *et al.*, 2003; Drin *et al.*, 2007, 2008), which is the main interest of this thesis. The next chapter is dedicated to ALPS.

Chapter 4

Regulation of vesicular transport by membrane curvature

In the last chapters I discussed the membrane properties and forces involved in membrane-shape related process. I have also mentioned some aspects related to trafficking, endomembranes and some of the proteins implicated in these processes. In the following sections I will focus in more detail in the secretory pathway, which is the biological context of the subject of this thesis.

It has been shown that carriers located inside the membrane usually transport small molecules across the plasma membrane. However, the majority of secreted proteins and polysaccharides in eukaryotes are released into the medium by exocytosis. Eukaryotic cells evolved a complex secretory pathway, consisting of several membrane-bound compartments (endoplasmic reticulum, Golgi apparatus, vacuoles, vesicles, they are collectively termed the endomembrane system); each one of these compartments contains different sets of proteins. Upon insertion into the endoplasmic reticulum, proteins travel through this membrane system in order to reach other subsequent compartments and their final destination. At various steps, carbohydrates and lipids enter this pathway, many of which would be also secreted or act as regulators (McMahon and Mills, 2004). The secretory pathway (also known as the anterograde or biosynthetic pathway) is countered by an endocytotic pathway (also known as the retrograde pathway) that originates at the plasma membrane and whose major destination are the lysosomes (or vacuoles). Crossroads interconnects these two pathways at various steps. Thus, eukaryotic cells evolved a complex intracellular traffic system, in which vesicles are the major transport vehicles (Drin *et al.*, 2009).

Trafficking usually involves the generation of vesicles from a membrane precursor, followed by the transportation of these vesicles to their destination and, lastly, the fusion of these vesicles with the target compartment. Despite the enormous diversity of organelles in eukaryotes (including a broad range of sizes and shapes) , the basic reactions of the vesicles trafficking — budding and fusion — are carried out by multiprotein complexes that have been conserved throughout eukaryotic evolution (Bonifacino and Glick, 2004).

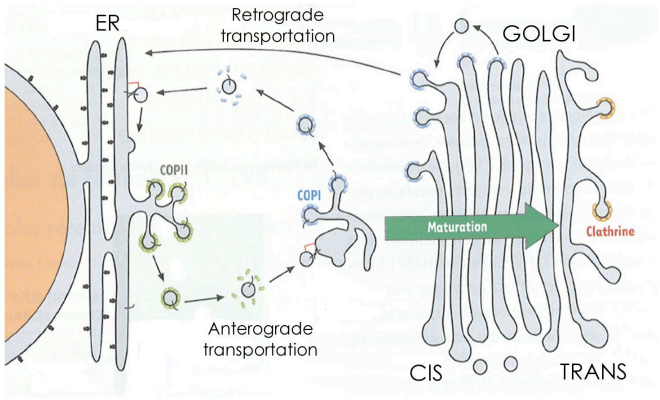

Figure 4.1: Schematics of the secretory pathway (Modified from (Drin *et al.*, 2009)).

4.1 The secretoy pathway and vesicle formation

The main goal of the secretory pathway is to transport the newly synthesized proteins from the ER to the Golgi complex, where they will undergo further modifications, before being released to their final destination at the cellular membrane. These proteins are specifically transported in vesicles that have a surrounded protein structure formed by COPII (Coat Protein Complex II) (McMahon and Mills, 2004; Smith *et al.*, 1998; Fotin *et al.*, 2004) (Fig.4.1 . COPII vesicles bud at the ER with several protein partners that allow them to target the pre-golgian compartements and eventually fused with them. Then, and according to the currently accepted model, the carried proteins transit through the Golgi apparatus in a process called "cisternae maturation" (Losev *et al.*, 2006). During this maturation, the proteins (and membranes) flow from the cis face to the trans face of the Golgi apparatus, undergoing post-translation modifications (Stagg *et al.*, 2008). In order for this model to work, it should exist a constant regeneration of cisternae, that is, the COPII vesicles must return to the ER to form more COPII vesicles. This recycling (retrograde transportation from the cis-golgi to the ER) is performed by the COPI vesicles (Rabouille and Klumperman, 2005). Finally, the carried proteins that have accomplished their correct maturation and have reached the trans-golgi are then transported by endosomes or lysosomes to the plasmatic membrane.

The vesicles formation is accomplished, as I discussed in the previous chapter, by the action of proteins that are capable of bending membranes. Vesicles of 50-70 nm in diameter are formed by the specific action of coat proteins: COPI, COPII and clathrin (McMahon and Mills, 2004). These coat proteins polymerize around the vesicle and complete the budding. On the other hand, the dynamin acts to pinch the vesicles out of the mother membrane (Praefcke and McMahon, 2004; Kozlov, 2001). These formed vesicles can then dismantle their coat and fuse to their target compartment delivering their cargo (Bonifacino and Glick, 2004). The formation of the COPII vesicles starts with the activation of Sar1

by Sec12. Sar1, as we mention in section 3.4, is able to bind the membrane thanks to its amphipathic α-helix, and hence, it is able to start the bending of the membrane. This initial membrane deformation allows the subsequent building of COPII coat, with the binding of Sec23/Sec24, which stabilize the curvature initiated by Sar1 and serve as anchor point for Sec13/31 heterotetramers. These oligomers form an icosahedric assembly, whose lattice is supported by Sec23/Sec24. The synergic action of this multiprotein complex accomplish the global deformation of the membrane to form and stabilize the vesicles (Fath *et al.*, 2007; Stagg *et al.*, 2008; Bi *et al.*, 2002).

Conversely, the formation of COPI vesicles starts with the activation of Arf1 by its exchange-factor-activator-GBF1 in the cis-Golgi. Arf1 activation leads to the formation of a coatomer made by several subunits, which polymerize as in the case of COPII, in order to bend the membrane and start the budding. The structure of the COPI coat is still unknown but microscopic studies show that it can deform the membrane in a similar manner as COPII coat does (McMahon and Mills, 2004).

4.2 Membrane-curvature regulates traffic

Since the coat is an obstacle for the fusion of the vesicle with the target membrane, the deactivation of Sar1 -in the case of COPII coats- and Arf1 -in the case of COPI coats- is essential to destabilize the coats. The active state of these GTPase proteins is in their GTP-bound form. GAP proteins (GTPase activating proteins) stimulate GTP to GDP hydrolysis, and therefore inhibit GTPase proteins (Sar1 and Arf1, for instance). The GAP protein ArfGAP1 inhibits Arf1 in a membrane-curvature dependent manner (Bigay *et al.*, 2003). Antonny and co-workers have shown that ArfGAP1 begins a rapid depolymerisation of the COPI coat when it is bound to liposomes of ~60 nm (Golgi vesicles size). In contrast, ArfGAP1 presents a reduced activity when it is incubated with larger liposomes (~180 nm) (Bigay *et al.*, 2003) (Fig. 4.2 (b)). The same research group showed that this was possible thanks to two motifs in ArfGAP1 , which they named ALPS (Amphipathic Lipid packing Sensor) (Fig. 4.2). As other amphipathic α-helices, they fold at the contact with the membrane (Bigay *et al.*, 2003; Mesmin *et al.*, 2007; Bigay *et al.*, 2005). Contrary to the Sar1 and Arf1 amphipathic α-helices, ALPS do not induce positive membrane curvature but rather recognizes it (however, we cannot neglect the role of the bilayer-coupling effect in this process) (Fig.4.2) . This recognition process is possible thanks to some intriguing features found in ALPS motifs that I will describe with greater detail in the next section. For the moment, it is important to mention that these special properties of ALPS helped the identification, by bioinformatic approaches, of other ALPS motifs. Among them the exemple of ALPS in the golgin GMAP-210 (Golgi microtubule associated protein) (Drin *et al.*, 2007; Gautier *et al.*, 2008) resulted extreamly interesting. Some golgines are known to bind COPI and COPII vesicles to their target membrane in order to help the vesicle-membrane fusion. For instance, GMAP-210 has a long coiled-coil of around 200 nm that is ideal to bridge the vesicle membrane (curved) and the target membrane (flat). Two ALPS motifs are in GMAP-210 at one extremity of the coiled-coil extremities where, as a dimer, they bind to highly positively curved membranes (Fig. 4.3). The other extremity has a GRAB domain (GRIP-related-Arf binding), which binds to the target membrane thanks to Arf1. As a result of these

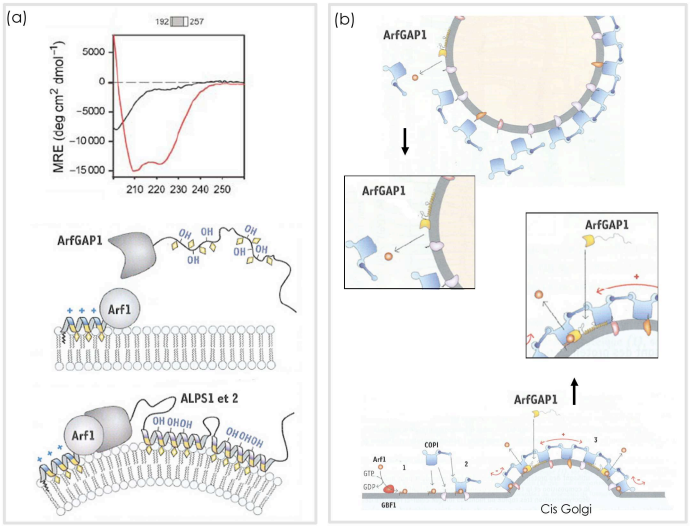

Figure 4.2: Membrane-curvature regulation of traffic by ArfGAP1 modified from Drin (Drin *et al.*, 2009).

two different extremities, GMAP-210 is able to link small liposomes to flat Arf1-containing membranes (Fig.4.3) (Drin *et al.*, 2008).

In the following sections I will discuss the nature of these ALPS motifs, their discovery and the features that make them such an special case of membrane curvature sensor.

4.3 ALPS, a membrane curvature sensor

ArfGAP1 is a 415 amino acid cytosolic protein that associates in a dynamic manner with the Golgi apparatus where it controls COPI coat cycling. The structure of the N-terminal region (1-128 aminoacids) has been already determined (3DWD,PDBcode). This region forms the GAP catalytic domain, which is built on a characteristic Zn-finger fold and promotes GTP hydrolysis on Arf1. Following this GAP domain, and up to the C-terminus, the protein contains two ALPS motifs (Bigay, mesmin). Based on sequence analyses and in vitro experiments, it was possible to characterize some of the ALPS special features that allow it to sense the curvature (Bigay *et al.*, 2003; Mesmin *et al.*, 2007) (Fig.4.4) :

- ALPS are amphipathic α—helical motifs that can expand from 25 up to 36 residues approximately
- Their polar face is rich in uncharged small polar residues, serine and threonine (contrary to most of the AH that bind the membranes)
- The hydrophobic face have mostly bulky aromatic residues
- Glycines can be found all along the sequence

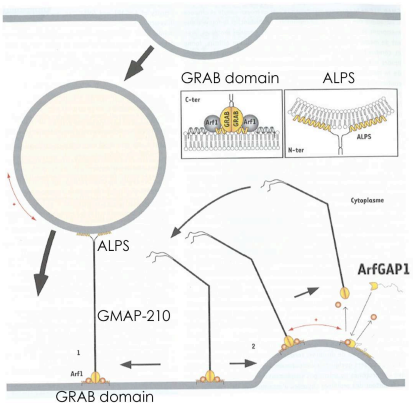

Figure 4.3: Membrane-curvature regulation of traffic by GMAP-210 (Modified from (Drin *et al.*, 2009)).

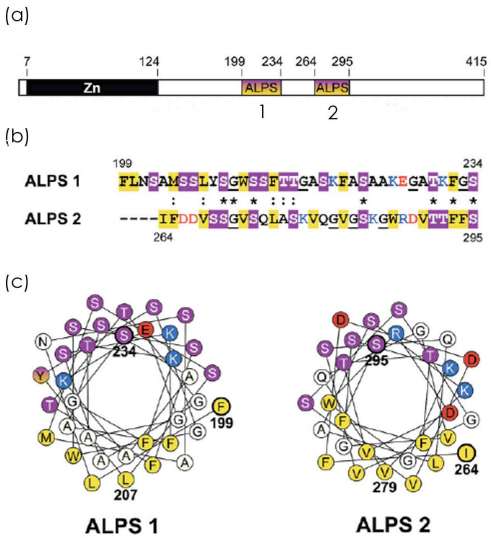

Figure 4.4: ALPS1 and ALPS2 (a) position in ArfGAP1 sequence, (b) amino acid composition, (c) helical wheels of their amphipathic α−helical structure (Taken from (Mesmin *et al.*, 2007))

- only few charged residues are present

4.3.1 ALPS discovery

Using liposomes with a lipid composition similar to that of the Golgi membranes (with DOPC as the predominant phospholipid), Antonny and colleagues showed that ArfGAP1 activity was optimal when it bound small vesicles (~60nm)(Bigay *et al.*, 2003). Therefore, they proposed that ArfGAP1 contains a region capable of recognizing vesicle curvatures. This specific recognition and binding will be followed by Arf1 inhibition and the disassembly of the COPI coat (liposomes with radius <50 nm)(Bigay *et al.*, 2003; Antonny *et al.*, 1997b) (Fig. 4.2 (b)). All these experiments led Bigay *et al* to identify the first ALPS motif (ALPS1).

The discovery of ALPS, and all subsequent experiments on this system, has been possible thanks to numerous experimental approaches that are currently applied in the field of liposomes research such as flotation assays, GTPAse activity measurements, different fluorescence assays based on marked liposomes, tryptophan fluroscence, circular dichroism (CD) experiments, *etc*. All ALPS features that I will describe in further sections are the fruit of these experiments. For clarity, I will only focus on those conclusions and experiments that are relevant for the discussion of my work.

4.3.1.1 Amphipathic alpha helix structure

Limited proteolysis experiments importantly contributed to the identification of the ArfGAP1 region responsible for the recognition and binding to curved membranes. Furthermore, CD experiments[1] on ArfGAP1 incubated with small liposomes showed that the central region of this protein undergoes a transition from an unfolded state in solution to an α-helical structure (Bigay *et al.*, 2005). Thus, it was suggested that ArfGAP1 recognizes curved membranes thanks to this central region that follows a coupled process of partitioning and folding (Bigay *et al.*, 2005) (Fig. 4.2 (a)).

4.3.1.2 Identification of ALPS2

Based on the physicochemical properties of ALPS1, Mesmin *et al* identified a second ALPS motif in ArfGAP1 (ALPS2) (Mesmin *et al.*, 2007). ALPS2 polar face is also very populated in serine and threonine residues, but its hydropbobic face does not have many aromatic bulky residues (Fig.4.4). When they compared the specificity and affinity of ALPS1 and ALPS2 to small liposomes, they observed that ALPS2 had a weaker binding for curved membranes. However, they noticed that ALPS2 presence renforces ALPS1 recognition of the curvature.

[1] The far-UV (170-250 nm) circular dichroism spectrum of helices exhibits a pronounced double minimum at ~208 nm and ~222 nm. This kind of structure measurement is of very low-resolution. The most reliable experimental methods for determining an α-helix involve an atomic-resolution structure provided by X-ray crystallography or NMR spectroscopy.

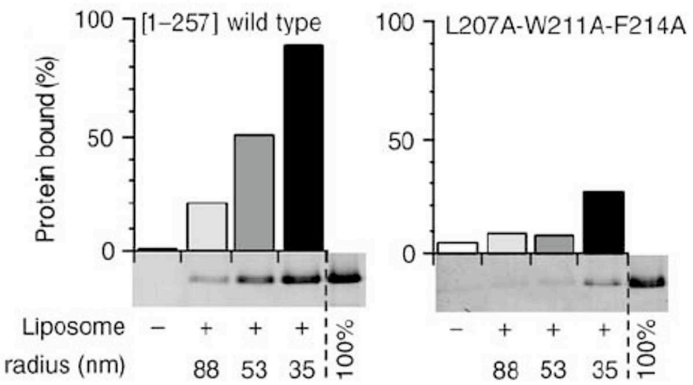

Figure 4.5: Binding of (a)ALPS$_{wt}$ and (b) the triple-mutant LWF-A to liposomes of different sizes (Taken from (Bigay *et al.*, 2005)).

4.3.2 Importance of hydrophobic residues on lipid packing recognition

As we mention in section 2.4, most amphiphatic helices interact with the membrane thanks to charged electrostatic interactions. Serine and threonine residues cannot establish charged electrostatic interactions with the polar headgroups of the lipids. Therefore, ALPS recognition of curved membranes might occur independently of these forces. Antonny and colleagues supposed that ALPS binding could be driven mostly by the hydrophophobic interactions (Antonny *et al.*, 1997a). To test this hypothesis, they substituted some conserved hydrophobic residues by alanines (L207A, W211A and F214A, corresponding to L12, W16, and F19 in this work). They found that individually, these mutations decreased the ALPS motif affinity to curved membranes, although liposome binding was not significantly depleted. Indeed, it was only the introduction of the three simultaneous mutations (L207A-W211A-F214A, the triple mutant LWF-A) that considerably decreased the affinity to highly positive curved liposomes, maintaining some degree of specificity though (Bigay *et al.*, 2005) (Fig.4.5) . This mutated version of ArfGAP1 showed to be mostly inactive whatever the liposome size. In consequence, it was suggested that ALPS curvature strongly depends on the hydrophobic interactions.

It is worth to mention that there is no available data using CD experiments with the LWF-A mutant. Thus, we do not know what would be the structure of the mutant in solution nor with liposomes. Even if it is expected to have a more helical content because of the presence of the alanines, this effect has not yet been confirmed experimentally.

4.3.3 ALPS binding does not depend on charged electrostatic interactions

To confirm the hypothesis that the hydrophobic residues were the principal responsible of ALPS curvature recognition, Drin *et al* performed some experiments using different mutants where the hydroxylated residues found in ALPS sequence (serine and threonines) were substituted by positively charged residues (lysines) (Drin *et al.*, 2007). The position of the mutations was guided by other studies on model membrane-absorbing amphipathic helices (Mishra *et al.*, 2008) and depending on the position of the residues on the amphipathic diagram wheel. This diagram suppose an amphiphatic helix as a rigid tube divided in two perfectly well differentiated polar and hydrophobic faces (Fig.2.10).

Four mutants were designed based on this perception of the amphipathic helix. The mutant 2Ki (S206K and T215K) and 4Ki (S206K, Y208K, S213K and T215K) include two and four lysines mutations respectively (Fig.4.6(a)) (placed in supposed favorable positions). These mutants were made based on the "snorkel model" (Mishra and Palgunachari, 1996). According to this model, a lysine at the border of the polar and hydrophobic face of the amphipathic helix is well suited for membrane interactions, as this combines both a favorable hydrophobic interaction through the long carbon chain of the lysine and a favorable electrostatic interaction through the ε-ammonium group. In a third mutant, the 2Kt (S205K and T216), the lysines were positioned at the center of the polar face, a location that should be less favorable for these residues to interact with the membrane. Finally, the 4Ki/4Et mutant includes four interfacial lysines (at the same positions as mutant 4Ki) as well as four glutamates in the center of the polar face (in the same positions as mutant 2Kt plus S209E and S212E) and has the design of an archetypal zwitterionic amphipathic helix[2]. The net charge of this helix is the same as that of the wild-type form, but the presence of numerous negative and positive residues could promote membrane interaction because these residues are distributed in a manner that matches the charge distribution at the membrane interface (Drin *et al.*, 2007) (Fig.4.6) .

As compared with the wild-type form, all mutants appeared less sensitive to liposome radius. Drin and co-workers attributed this decrease in affinity to their more efficient binding to large liposomes. The mutant 2Kt, which is the only mutant that contains no interfacial lysines, has a substantial affinity to liposome size whatever the assay considered. The 2Ki mutant showed to be almost totally insensitive to membrane curvature, whereas a weak effect on liposome size binding was observed on 4Ki and 4Ki/4Et (Fig.4.6(b)). All mutants showed an increase in helicity (compared to the soluble peptide) upon liposome binding, suggesting that their membrane adsorption is coupled to the folding of the ALPS motif into an α-helix. However, the CD spectra of the 2Ki and 4Ki/4Et mutants suggest some degree of α-helical content in solution and have less helical content than $ALPS_{wt}$ when they are bound to the liposomes (Fig,4.6(c)). They interpreted these results suggesting that the partial folding of these mutants may contribute with their insertion in the membrane. When the activity of ArfGAP mutants was tested, the difference observed in the rates of GTP hydrolysis and COPI disassembly between large and small liposomes was greatly reduced compared with the wild-type. However, the rates of the 2Ki, 4Ki and 4Ki/4Et mutants were difficult to compare (Drin *et al.*, 2007). We will discuss, at the light of the MD simulations I performed for this thesis, one of the possible reasons why this could have

[2]Based on the works of (Mishra *et al.*, 1995; Mishra and Palgunachari, 1996)

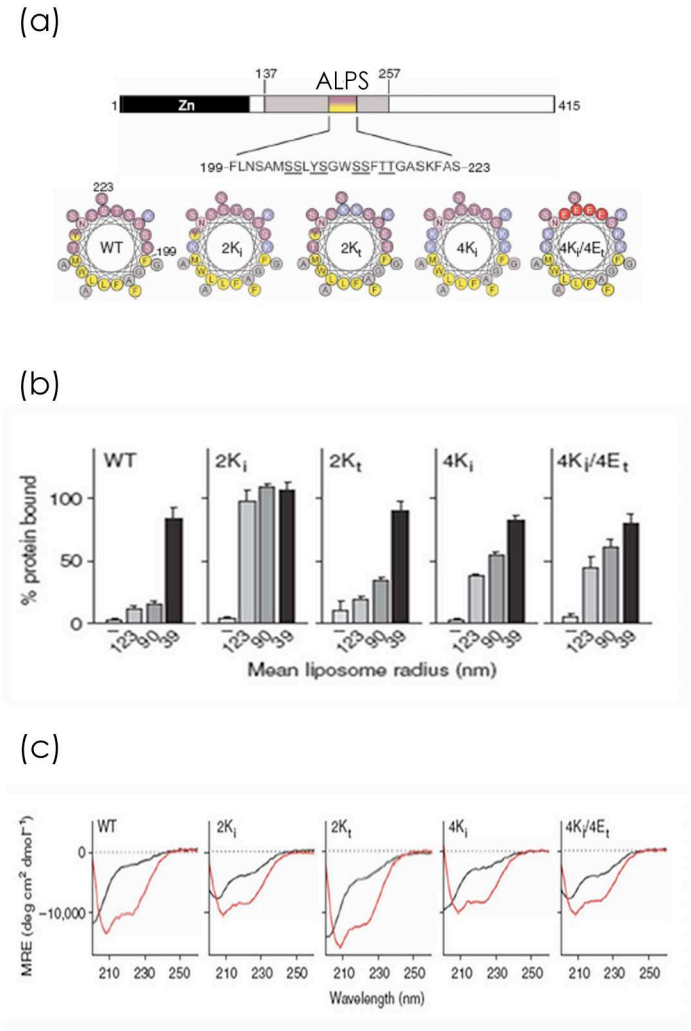

Figure 4.6: Experiments with different mutants of ALPS at the polar face showing (a) ALPS sequence and the wheel diagram of each of the mutants (b) the binding of each mutant to different liposome sizes and (c) the CD spectra of each mutant measured at teh binding to the liposomes. (Taken from (Drin *et al.*, 2007))

happened. Nonetheless, these mutations confirmed that the presence of charged residues in the polar face of ALPS decreases the specificity and affinity of binding to small liposomes (Drin *et al.*, 2007). Therefore it was clear that the introduction of lysines at the polar-non-polar interface of ALPS motif enhances the interaction of ArfGAP1 with large liposomes and consequently reduces the influence of membrane curvature. To summarize, ALPS motifs, compared to classical amphipathic helices, do not have a superior affinity for curved membranes but rather a unexistent adsorption to weakly-curved membranes. Indeed, the introduction of only two interfacial lysines (2Ki mutant) strongly decreases the specificity for curved liposomes. Therefore, the lack of positively charged residues in the polar face of ALPS motif seems to be the key to ensure an absolute low binding to flat, negatively charged membranes.

4.3.4 Dependence on lipid composition

As I mentioned previously, the curvature of the membrane depends also on the lipid composition. The binding of ArfGAP1 to model lipid membranes and its activity are remarkably sensitive to lipid composition. The key bilayer parameter governing the adsorption of ArfGAP1 to membranes is lipid packing, which is the physical parameter I discuss in sections 2.1.2 and 3.1.2, that depends on the shape of lipid molecules and on the curvature of the membrane.

A former research about ArfGAP1 function that used unilamellar vesicles, showed that ArfGAP1 (and Gcs1p, the yeast homologue) binding and activity improves with the presence of conical-shape or monounsaturated lipids (Antonny *et al.*, 1997b). These experiments showed that if a constant liposome radius is maintained using systematic variation of the vesicle composition and synthetic lipids of strictly defined acyl chains, then ArfGAP1 activity increases when the size of the polar head decreases (PC > PE > PA > DAG)[3] and when the number of monounsaturated acyl chains in DAG or in PC increases (C16:0-C16:0 > C16:0-C18:1 > C18:1-C18:1) (Fig.4.7(a and b) see de schematics of the size of polar heads and acyl chains at the bottom of the plots) . Therefore, if conical lipids (e.g. dioleolylglycerol) are introduced at the expense of cylindrical lipids (e.g. phosphatidylcholine or PC) ArfGAP1 binding to membranes is enhanced (Antonny *et al.*, 1997a). These results encouraged them to propose that ArfGAP1 is able to recognize the lipid packing defects that resulted from different membrane lipid compositions (Antonny *et al.*, 1997b). Conversely, when the liposome composition is kept constant, the activity of ArfGAP1 increases with liposome curvature (Bigay *et al.*, 2003). They concluded that ArfGAP1 recognizes the defects in lipid packing that appear when the curvature of the membrane exceeds its spontaneous curvature (Bigay *et al.*, 2003). Moreover, in further experiments, they showed that the presence of negatively charged headgroups of PS (at expenses of PC) did not enhance the recognition of highly curved membranes by ALPS (Bigay *et al.*, 2005) (Fig.4.7 (c)). This confirmed that ALPS recognition is independent of charged interactions. Additionally, Drin performed several experiments to test the activity of ArfGAP1 with all the lysine mutants under different lipid geometry conditions. He demonstrated that the changes on acyl chains monounsaturation content (replacing

[3]See Fig. 2.1 for guidance about the size of the polar head

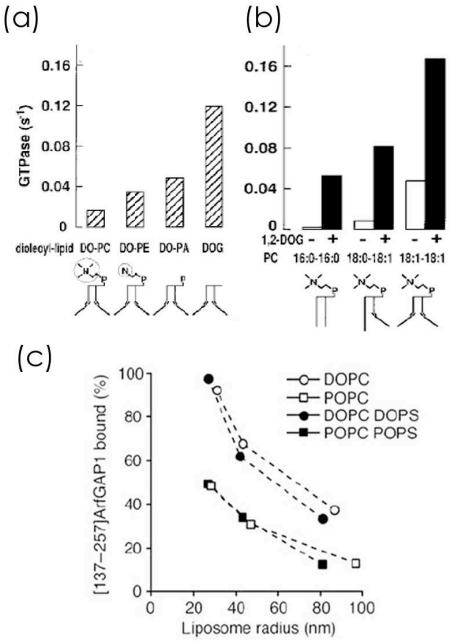

Figure 4.7: Lipid composition and packing affects ALPS binding and therefore ArfGAP1 function (a) GTPase activity of ArfGAP1 as a function of changes in the lipid packing at the level of (a) the polar heads and (b) the acyl chains (changes in degree of saturation). (c) Binding of ALPS to liposomes of different sizes in response to the introduction of negatively charged (PS) phospholipids. (Modified from (Antonny *et al.*, 1997b; Bigay *et al.*, 2005)).

POPC[4] by DOPC[5]) and/or the size of the headgroup (DOPC by DOPE[6]) (see Fig. 2.1 for guidance) enhanced the activity of ArfGAP1 and the mutants (Drin *et al.*, 2007). These experiments suggested that, when there is not possibility of establishing charged electrostatic interactions with the membrane -due to the lack of anionic lipids- , the lipid packing governs the adsorption of all mutants, making them potential sensors of membrane curvature.

4.4 Model of ALPS curvature recognition

In the current accepted model that explains ALPS curvature recognition, ALPS binds to highly positively curved membranes thanks to its hydrophobic residues (Fig.4.2 (a)). During this binding ALPS undergoes a partitioning-folding couplig process leading to an amphipathic α-helix once adsorbed in the membrane interface. Inserting its hydrophobic residues between lipids, ALPS is capable of recognize defects in lipid packing that result from the mismatch between the actual curvature of the membrane and lipid geometry (Drin *et al.*, 2007; Bigay *et al.*, 2003, 2005; Antonny *et al.*, 1997b). ALPS binding is mostly a consequence of hydrophobic interactions and that does not need the influence of charged electrostatic interactions. Indeed they low number in the sequence contribute to maintain the binding of ALPS to big liposomes at their minimal level. Hence, throuth this motif ArfGAP1 can recognize when a vesicle have reach its optimal size, an then activate Arf1 to start the coat depolymerization (See Fig.4.2) (Fig.4.2 (b)).

4.5 ALPS-like motifs are present in numerous proteins

Several proteins that use ALPS-like motifs to sense membrane curvature were found recently by screening the yeast and human sequence databases (Drin *et al.*, 2007; Gautier *et al.*, 2008). Gautier created a webserver, known as Heliquest (Gautier *et al.*, 2008), in order to identify sequences of approximately 18 amino acids that matched an α-helix structure and that showed the general features of ALPS motifs. To do so, the program calculates the hydrophobicity of the protein region, the hydrophobic moment (which quantifies the amphipathicity), the number of serine, threonine and glycine residues and the number of charged residues. To refine the search, some geometrical rules were added so the program can reject, for example, sequences that seem amphipathic according to the hydrophobic moment but that actually include a polar residue right in the middle of the hydrophobic face. A sequence can be selected when it meets all the parameters established on the basis of ALPS1 and ALPS2 compositions and structure. Thus, the Heliquest program would only select sequences containing a minimum of seven serines, threonines or glycines, a maximum of three arginines, lysines, aspartates or glutamates, and a net charge between –1 and +2. Glycines were considered with serines and threonines because they are small and neutral, and provide conformational flexibility. Since ALPS2 has also valines and

[4] with one monounsaturatedacyl chain
[5] with two monounsaturated chains
[6] conical lipid with small headgroup, ethalonamide

isoleucines in its sequence, Heliquest considered all hydrophobic amino acids and not only aromatic hydrophobic residues. After screening the yeast and human sequences database, around 200 putative ALPS motifs were detected. The motifs are present in proteins with a broad range of functions. Among these proteins, the golgin GMAP-210 (already mentioned in this chapter) (Drin *et al.*, 2007, 2008), the nucleoporin Nup133 and the sterol-binding protein Kes1p are the more notorious examples. Since amphipathic helices are frequently found in structural domains, probably ALPS-like motifs are over-estimated using this methodology and in fact, only few of these detected motifs truly correspond to motifs engaged in membrane interaction. Therefore, it would be suitable that the list of potential ALPS motifs is examined in detail using further structural and functional information.

4.6 Main interests of the present work

Among an increasing number of lipid-binding domains, a group that not only binds to membrane lipids but also changes and sense the shape of the membrane has been found. These domains can be characterized by their strong ability to transform liposomes as well as flat plasma membranes into elongated membrane tubules or can be extreamly efficient sensor of the different shapes. Biochemical studies on the structures of these proteins have revealed the importance of the amphipathic helix, which potentially intercalates into the lipid bilayer to induce and/or sense membrane curvature. Bioinformatics in combination with structural analyses has been identifying an increasing number of novel families of lipid-binding domains or potential candidates. Most of the studies related to these membrane-shape related proteins have been focus in the generation of the curvature and less attention has been put on the mechanism of curvature sensing. Thus, this fascinating subject remains less studied and less understood. However, recently its is becoming more evident the importance of adressing the question of curvature sensing. Given the form of the amphipathic helix, the increasing examples of amphipathic sensor motifs or the existence of many lipid-binding motifs of different nature also implicated in membrane curvature sensing, the question has been raised about if the curved membrane is responsable of the recruitment of different "adaptors" to its lipid-packing defects (as has been propose by Hatzakis (Hatzakis *et al.*, 2009), or if the proteins have special sensor capabilites. The increase in computational power would help to dilucidate these crucial questions in atomic detail using vesicles, for instance.

I believe, that we cannot set the problem in a simplistic way. The membranes are dynamic systems and the proteins as well. The adaptation of these two entities when they get in contact must be synergic. I profoundly dout that we will be able someday to discriminate one effect from the other. Moreover, the fact that curvature sensors with so special features, such as ALPS, may exist in a wide range of proteins, makes ALPS a very interesting and challenging research subject. Understanding the atomic details of ALPS and membrane interactions may provide unvaluable insights about ALPS properties and its way of action, as well as how the membranes respond to ALPS. How ALPS reacts to a lipid environment? What kind of interactions it establishes with the lipid polar heads and acyl chains? As we mentioned before, the composition of the bilayers determines the lipid packing, how is this affected by ALPS or how ALPS responds to the inhomogeneous landscape of the bilayer? And how the properties of the bilayer

are altered, or changed in a way that contribute to the sensor capacities. Is there generated a local curvature that potentiate the sensing power, of is the order and fluidity of the membrane contributing in some way also. Our research aimed at solving some of these essential questions using Molecular Dynamics simulations, and providing the atomic detail not yet accesible experimentally.

The story you are going to read in the further chapters was possible thanks to a bioinformatician, Romain Gautier, who works in Bruno Antonny's lab, an experimentalist environment. In the work they made together "A general amphipathic alpha-helical motif for sensing membrane curvature" (Drin *et al.*, 2007), Gautier designed the program that predicts ALPS-like motifs, which offered new possibilities to adress some essential questions about amphiphatic sensors. This also showed the relevance of an inter-disciplinary work between the experimentalist and the theoricians. Following this philosophy, Gautier proposed to Antonny a collaboration with our lab, aiming at pursuing molecular dynamics simulations on this kind of curvature sensors. This thesis is hence the beginning of a promising adventure using molecular simulations to understand ALPS and dilucidate some general aspectes of the amphipathic helices implicated in the sensing of the membrane curvature.

In the following chapter, I will discuss some methodological ascpects, the principles of Molecular Dynamics simulations. I will also exposed some considerations of today's capabilities in membrane simulations and the pertinence of the simulations described in this work.

Chapter 5

Molecular Dynamic Simulations

In theoretical chemistry, Molecular mechanics modeling is the discipline that allows accessing the atomic details of condensed phases thanks to the application of physical, mathematical and statistical representation models. This discipline includes different techniques such as the Stochastic Dynamics, and Molecular dynamics (MD). In the case of MD we construct a physical model based on experimental information (i.e high-resolution structures of the molecules, or using physical parameteres derived from experiments). The application of statistical physics to this model means that we try to link the reality to a simplified but accurate representation to explain that reality. Thus, the simulation of this model during time offer notions about the probablility of an event to succed. As an analogy, by doing MD we are like climatologists that predict a sunny day in Paris thanks to a complex model that represents the weather[1].

Molecular dynamics (MD) simulations numerically investigate the motions of a system of discrete particles under the influence of internal and external forces. The spectrum of possible applications based on this approach is broad, ranging from atoms in a molecule to stars in a galaxy (Karplus and Petsko, 1990). The underlying principles are the same: interactions of the respective particles are empirically described by a potential energy function from which the forces that act on each particle are derived. Knowing all these forces we can calculate the dynamic behavior of the system using classical equations of motion for all the atoms in the system.

5.1 Simulations of membranes systems

Thanks to computer simulations it is possible to support conceptual hypothesis such as the hydrophobic mismatch between lipids and TM segments of the proteins, or to construct interpretations and propose new predictions about different mechanism, such as the membrane bending or the curvature sensing. Computer simulations can also be very useful to propose new and more adapted experiments. Providing dynamics at an atomic level of detail, these simulations facilitate the interpretation of experimental data

[1] Some other predictions can be then be formulated, such as that all parcs will be crowded of people doing picnics!

and give access to information not easily obtained with *in vitro* experiments.

As I have made reference in the last chapters, today it is possible to simulate membrane systems at different scales. The space scale of the phenomena analyzed is correlated with the time necessary to simulate the event of interest. Computer simulations in membranes are very useful for the study of different phenomema that take place at different microscopic scales. Since their application to atomic systems by Alder in the late 1950s (Alder and Wainwright, 1959) and their first application to a protein structure by McCammon in the 1970s (McCammon and Karplus, 1977), MD simulations have become a common tool to investigate structure–activity relationships in biological macromolecules. Moreover, since the first simulation of a membrane-embedded peptide by Woof in 1994 (Woolf and Roux, 1994) and an integral membrane protein (the bacteriorhodopsin) by Edholm in 1995 (Edholm *et al.*, 1995), molecular dynamics simulations of membrane proteins have become an important research field.

In order to understand the general principles of membrane organization, it has been mandatory to perform simulations of phospholipid bilayers with a pure composition (i.e just DOPC) or simple mixtures and study the properties of the membrane alone without any proteins embedded on it. The former works on lipid bilayer simulations goes back to the early 1980s (Ploeg P van der, 1982; Berendsen *et al.*, 1986; Berendsen and C., 1987). During the last years, significant progress in this domain have allowed the simulations of membranes containing hundreds of lipids during simulation times on the order of hundreds of nanoseconds and to few microseconds.

The aim of Molecular dynamics simulations is to obtain an atomical scale representation of a phenomea of interest. This can be done in several ways that include the physical and physicochemical properties of the atoms that compose the molecules implicated in the process. These representations can mainly consist of all-atoms models, united-atoms models and coarse-grained models. In principle a model that include all the atoms will be more detailed than an united-atoms or coarse-grained model. The selection of each kind of model depends on the time scale at a particular phenomena take place, and the size of the system to simulate (Fig.5.1). I will explain this in mored detail in section 5.3. The first simulations of lipid bilayers were made with united-atoms models of the lipids where each aliphatic carbon with associated hydrogens is described by a single particle with the approximate physical characteristics of a methyl, methylene, or methine group (Berger *et al.*, 1997). This is a level of detail somewhere between fully atomistic descriptions and some of the coarse-grained approaches that have been developed over the years (Monticelli *et al.*, 2008; Marrink *et al.*, 2007; Clementi, 2008). When hydrogens are treated explicitly, the number of atoms per lipid approximately triples, and the number of pairwise interactions in the membrane becomes much higher. That is also the case when the coarse-grained models are use, where an amino acid can be represented by for instance a bead that represent the peptide bond, and another (or two depending on the size and properties) that represent the side chain. The computationally inexpensive united-atom lipids reproduce experimental behavior reasonably well. Ultimately, an all-atom force Field should be more accurate, but despite some discussion in the literature we do not have reached the point yet where the united-atom approximation is the limiting factor in accuracy for most purposes. Processes such as lipid autoassembly, lipid phases transitions, or vesicles, may need an enourmous quantity of atoms and long times of simulation. In consequence, the

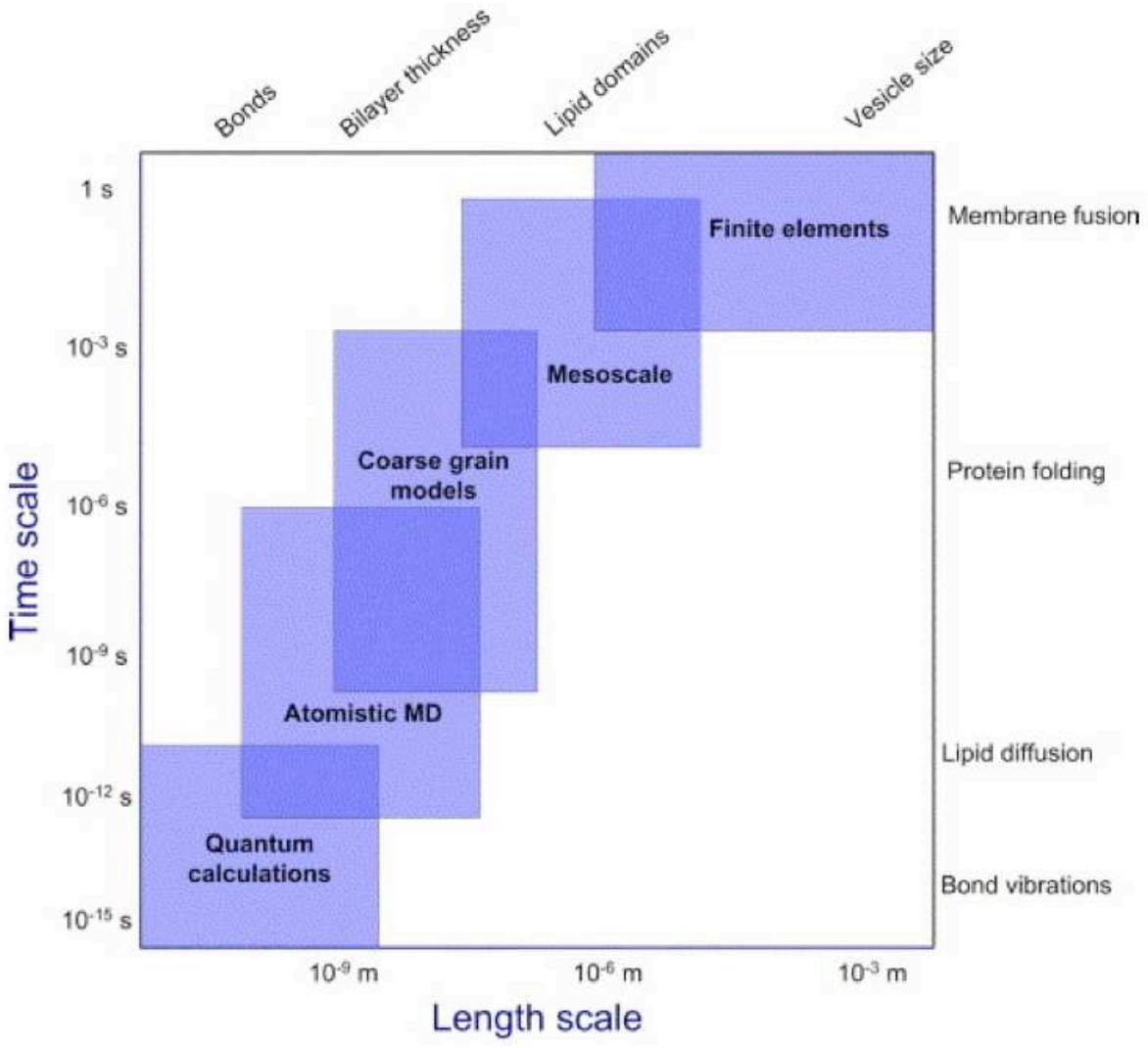

Figure 5.1: Simulation methods and the size of the phenome they can represent and the time of simulation necessary.

coarse grained models have became the optimal choise.

It has been therefore possible to calculate membrane parameters such as the lateral diffusion coefficient, which needs long times of simulations to equilibrates (Anezo *et al.*, 2003). Simulations on membranes of different sizes have provided a first view of phenomena like membrane undulation (Lindahl and Edholm, 2000). MD have turned out to be very useful to address questions related to larger scales process such as the autoassambly of membranes (Marrink *et al.*, 2001), the phase transition (Marrink and Tieleman, 2001), and the formation of rafts and lipid domains (Risselada and Marrink, 2009, 2008; Niemela *et al.*, 2009), or even, very recently, to the formation of vesicles (Risselada and Marrink, 2009; Yefimov *et al.*, 2008). Autoassembly of phospholipids to form a bilayer can take some dozens of nanoseconds (Marrink *et al.*, 2001), whereas the formation of some vesicles can take longer than 100ns ((de Vries *et al.*, 2004b). The formation of pores by the action of antimicrobial peptides or by the influence of an electric field or a mechanical stress has also been simulated (Monticelli *et al.*, 2004; Robertson and Tieleman, 2002; Tieleman *et al.*, 2001b; Yefimov *et al.*, 2008). The simulation of mixtures of lipids as we mentioned before is en emerging field as well.

5.2 When to use simulations

Prior to approach a specific problem in membrane-protein biology using simulations, it is worthwhile to think carefully to some primary questions, for instance, whether the problem to be investigated is accessible by MD and whether the simulations are practical or likely to deliver interesting and informative results. Other important questions are related to the time scale and the system size (mentioned in the previous section): in function of the size of the system and the computational power, one must wonder whether the time scales reachable by MD simulations are enough for the particular system of interest. Lastly, it is important to consider whether there is further experimental data available that can be used for validating simulation results.

If simulations seems an appropriate approach, additional questions arise related with the model[2] to use to simulate the system. Among them, whether there are appropriate starting structures available, or whether computational models of the lipids of interest exist, or do they have to be developed (useful, but a substantial effort). Another issue is whether there is a parameter set that adequately describes the lipids and protein of interest. Since many membrane proteins are sensitive to the lipid environment, they may be critically affected by the membrane model used (Feller and Gawrisch, 2005). Finally, the choice of the software to use depends on the problem at hand, the availability of local expertise, computational facilities, and other factors, such as whether there is enough computer time available for the planned simulations.

In our particular case we decided to use GROMACS version 3.3.3 (Spoel *et al.*, 2005; Berendsen, 1995; Lindahl, 2001), a popular, freely available, and relatively user-friendly set of programs for MD simulations (rather good scaling). We carried out our simulations using two (in-house) dual CPU (Quad

[2]the starting structure obtained from an structural database, by homology modeling, *etc.* and the way of representing the molecule (all-atoms, Coarse-grains).

Core Intel Xeon 2.0Ghz q) computers and at the « Mesocentre de Calcul – SIGAMM facility » (using 6 dual CPU (Quad Core Opteron 2.3 GHz) with Infiniband interconnects) at Observatoire de la Côte d'Azur, achieving approximately 4ns/day for a system size ~50,000 atoms.

5.2.1 Simulation capabilities on membrane systems

The studies about ALPS motifs are centered in the recently emerged domain of the membrane-curvature-related proteins. They represent a very interesting area of study from both cellular and MD perspectives. ALPS essential properties (recognition of curved membranes and the partitioning-folding coupling) denote some of the most challenging issues in today's molecular dynamics field.

Here I will quickly review what is the current state of MD simulations in membrane systems. Particle based simulation studies traditionally have been looking at small planar membrane patches artificially extended to quasi-infinite size by the use of periodic boundary conditions (see section5.4.1). This periodicity make possible the study of bulk systems facilitating calculations and avoiding vaccum in the system surroundings that will lead to unrealistic simulations. In a system with a finit size, particles moving towards the boundary of the shell experienced an attractive force, more they get close to the boundary and more they experience a repulsive force that creates surface tension at the boundaries affecting the membrane physical properties. Moreover, in membrane simulations under periodic boundary conditions, it is not possible to truncate the periodicity of these patches in order to curve them, using classical MD methods (Wang *et al.*, 2008). In order to observed for instance membrane undulations and bending, larged patches are need. The simulation engine is design to iterate periodic conditions by translations and therefore it is difficult to simulate a spherical symetrical system. Recently the simulations of vesicles is starting to be possible thanks to other ways of compensate the surface tension created at the boundaries of finite size systems, such as the Mean Field Force Potential. However, even the smallest vesicle simulation already needs near 1,000 lipids and substantially more water molecules per lipid than in bilayer systems, resulting in an until recently challenging number of particles. Furthermore, vesicles autoassembled are not necessarly equilibrated and hence, expensive simulations in time and in computational resources are needed. Even recent simulation studies using coarse-grained (see section 5.3) models on vesicles concern vesicle sizes not exceeding the limit size of the vesicles used in vitro with radius up to 30 nm (Yesylevskyy *et al.*, 2009; Yefimov *et al.*, 2008; Risselada and Marrink, 2009, 2008). This condition already restricts the possibility of simulate ALPS binding to vesicles of different radius.

Although some works exist where the partitioning-folding coupling process has been simulated in explicit lipids, are routinely not feasible due to a very high computational cost (Ulmschneider *et al.*, 2006, 2007; Ulmschneider and Ulmschneider, 2008, 2009). Moreover some of these works have proven to need long times of simulations at high temperature. Furthermore, the free energy of insertion of a single peptide into a membrane was estimated to be ~75 kJmol-1, which suggests that the spontaneous penetration of single peptides would require a timescale of at least seconds to minutes which is computationally unreachable, and thus free energy techniques like umbrella sampling are necessary (Yesylevskyy *et al.*, 2009). Moreover, today's most used coarse-grained force fields are not yet capable

to simulate conformational changes or folding process (Monticelli *et al.*, 2008; Marrink *et al.*, 2007), although some examples of protein folding coarse grain models are under development (Clementi, 2008).

In the next sections I would like to describe the decisions we made to simulate ALPS-membrane system and detail some important aspects for understanding the setting up and running of MD simulations.

5.3 Force Fields

The behavior of a particle system composed by atoms, nuclei, protons and electrons is in principle best described by quantum mechanics. All other descriptions at a superior level, as atoms or molecules instead of nuclei and electrons, where classical mechanics applies instead of the quantum mechanics, are approximations. These approximations can be classified based on the detail they make possible to assess, from the atom to the macroscopic scale. Each level of approximation makes possible to describe new properties of the system with a better calculation efficiency (calculation times) and traitability.

In MD models, a molecule consists on a group of spheres (the atoms) with mass, size and charge, linked by springs (covalent bonds) that get the bonds to their most stable length after a deformation. In molecular dynamics, three approximations are important, the velocity of the particles is weak compared to the light velocity, and the electron movements are faster than nuclei movements (Born-Oppenheimer approximation), therefore, the movement of atoms can be described by classical mechanics.

This ensemble of spheres and springs are characterized by the force field. All the properties of each atom in a force field are parameterized based on experimental data or *in silico* calculations by quantum mechanics. The physical interactions between the atoms (steric hindrance, hbonds, etc) are taken into account in the calculation of the potential energy.

When we model a system, three choices have to be made: the degrees of freedom that are going to be explicitly simulated and the degrees of freedom that will be implicitly incorporated in the function that describes the interactions between the explicit degrees of freedom; second, the choise of the integration function for the treatement of the interaction energy between the explicit degrees of freedom; and thirth, the choise of the method for the conformational sampling, for simulating the movement base on the explicit degrees of freedom (i.e. MC, MD, *etc.*).

The force field plays a very important role, since it represents the set of parameters that describe the model we want to simulate. So it can be considered as the primary assumption in MD simulations. There are many different force fields, but currently there are only four widely used force fields for simulating biological macromolecules: AMBER (Cornell *et al.*, 1995), CHARMM (Mackerell, 2004), GROMOS (Oostenbrink *et al.*, 2004) and OPLS (Jorgensen *et al.*, 1996). In the case of proteins all these force fields have been tested and compared yielding approximatly good agreements with experiments but despite remaining sampling issues, a number of distinct trends in the folding behavior of the peptides emerged. Pronounced differences in the propensity of finding prominent secondary structure motifs in the different applied force fields suggest that problems point in particular to the balance of the relative stabilities of helical and extended conformations. For instance, in AMBER force field the conformational

space was quickly explored and did not critically depend on the initial structure. The GROMOS96 force fields has revealed an underestimation of propensity for sampling α-helical conformations in the simulations. While the GROMOS43A1 version exhibit a significant disparity that is the considerable amount of π-helix, which was not found in the other force fields. The OPLS force field in turn, provided superior results when representing the folded state. However, the chosen initial conformations affected the sampled structural ensembles considerably. These remaining differences emphasize the importance of continuous force-field development and refinement (Matthes and de Groot, 2009).

Phospholipids are a subset of biomolecules that have received considerably less attention than proteins or nucleic acids. There are only two phospholipid force fields commonly used today, although additional sets have been developed recently (e.g. (Chandrasekhar *et al.*, 2003)). The first commonly used lipid force field is part of CHARMM; the second is based on an older version of OPLS and AMBER with some additional parameters from Berger *et al.* in combination with GROMOS rules(Berger *et al.*, 1997; Lukas D. Schuler, 2001). Some improvements have been done with CHARMM lipids force field making possible the simulation of membranes with out surface tension. These new properties have made it to approximate more accuratly the experimental data. However, parameters from Berger *et al.* in combination with GROMOS rules reproduce better the membrane properties even if neither of both force fields approximate the experimental data with the experimental error (Taylor et al., 2008).

Berger lipids are described by a united-atom force field as we previosly mentioned. However, recently Berger lipids have been reparametrized to represent all-atom models (Monticelli, Personal communication; Tieleman *et al.*, 2006). When hydrogen are treated explicitly, the number of atoms per lipid approximately triples, and the number of pairwise interactions in the membrane becomes much higher. Therefore, the consideration of all the atoms limits the possibilty to simulate large-scale phenomena. It would very long to simulate the formation of vesicles, for instance, with all-atoms lipids. The construction of force fields that consider for example an amino acid as a single bead, the called Coarse grained (CG) force fields, have proven to be very useful to simulate this and other large scale phenomena.

Significant progress has been made in developing modern protein force fields, based on a comparison with high-level quantum mechanics and high-resolution experiments on soluble proteins, but it is challenging to obtain accurate experimental data to validate and improve lipid models. There is also the problem to simulated mixtures of lipids. The situation is even more complex for lipid–protein interactions compared to pure lipids, because experiments on membrane proteins and peptides typically have a significantly lower resolution than in solution (i.e. to determine high-resolution structures of the membrane-proteins they are solved in detergents and not in lipids). In addition, from a simulation point of view, critical tests are difficult due to the long simulations required. For now, the most straightforward approach to membrane protein simulations involves directly combining mathematically compatible protein and lipid force fields, and this approach has yielded useful insights into membrane protein behavior (Ash *et al.*, 2004; Gumbart *et al.*, 2005).

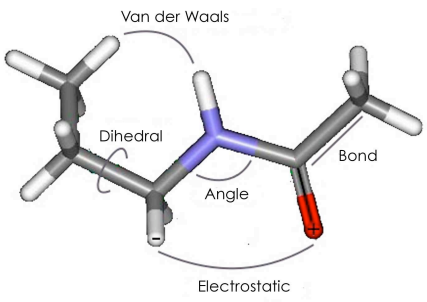

Figure 5.2: Parameters considered to asses the potential energy

5.3.1 Energies

I have already mentioned that the objective of molecular dynamics is to approximate the energy of a molecule applying mechanic laws. The principle of force field isto take into account the electronic motions implicitely and calculate the energy of a system as a function of the nuclear positions. The force field methods offer the possibility of assessing structural and thermodynamic properties of many molecules. The atoms are represented by punctual charged masses and the potential energy is in general expressed by the additive internal contributions between bond atoms, and external contributions of the non-bound atoms.

The potential energy role is to reproduce faithfully the interactions on the system. It is expressed as the addition of all the contributions (Fig.5.2) :

$$E_{pot} = E_{bond} + E_{angle} + E_{dihedral} + E_{improper} + E_{VdW} + E_{electrostatic} \tag{5.1}$$

The interactions between bond atoms correspond to the covalent energy of the system. It is applied to the atoms that are closer than 3 bonds. The interactions between the non-bound atoms include the van der Waals energy and the coulombic energies. The improper term correspond to the angles that allow to define a bond out of the plane (i.e. it maintains the atoms from a cycle in the same plane).

Two aspects are important for a force field in order to reproduce the interactions of the system:

1. Each force field needs accurate parameters for all the interactions in the system,

2. The force field needs an analytic expression (associated to the parameters) that allow the calculation of the potential energy.

Therefore, every force field is a set of parameters that define each atom and a set of equations that define how the energies must be calculated.

Many force fields are available as well as many ways to define the potential energy (E*pot*). In this work we decided to use the force field OPLS-all atoms (OPLS-aa)(Jorgensen *et al.*, 1996) (which

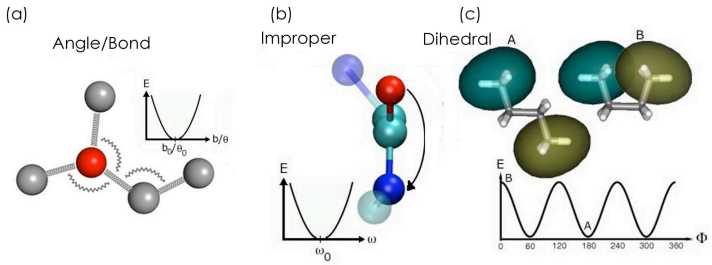

Figure 5.3: Schematics of the parameters that determined the bond interactions of the molecules

contains parameters for all the atoms of the proteins[3]) for simulate ALPS. For the lipids we used some parameters adapted from the Berger united atoms parameters (Berger *et al.*, 1997)[4], which have been modified in order to work in combination with the all-atom OPLS-AA force-field (Tieleman *et al.*, 2006). This force field allow the calculation of the potential energy according to the philosophy in the program Gromacs (Spoel *et al.*, 2005; Lindahl, 2001). Gromacs assess the E*pot* based on the positions of the atoms, expressed as a function of the bond length (*b*), the valence angles (θ), the dihedral angles (ω), the improper angles (Φ) and inter-atomic distances (r_{ij}). in the following way:

$$\begin{aligned} Etot = & \sum k_b(b-b_0)^2 \\ & + \sum k_\theta(\theta-\theta_0)^2 \\ & + \sum k_\omega(\omega-\omega_0)^2 \\ & + \sum k_\Phi(1+cos(n\Phi-\delta)^2 \\ & + \sum_i \sum_{j>i} (\frac{A_{ij}}{r_{ij}^{12}} - \frac{B_{ij}}{r_{ij}^{6}}) \\ & + \sum_i \sum_j (\frac{1}{4\pi\varepsilon_0}\frac{q_i q_j}{\varepsilon_r r_{ij}}) \end{aligned} \tag{5.2}$$

This expression allows to characterize the system based on their relative coordinates and not based on their orientation or position in space. The terms related to the covalent bonds and their angles are described by harmonic potentials, which consider the energetic cost of bond and angles deformations with respect to reference ideal values (Fig.5.3).

The electrostatic interactions, in turn, describe the interactions between charged particles, where the electric force of interaction is proportional to the value of each charge and inversely proportional to the distance that separate those charges (Fig.5.4 (b)). Finally, the van der Waals interactions correspond to dispersion forces. These forces consider that even for a mean neutral distribution of charges there exist

[3]compared to other force fields that have parameters for united-atoms or coarse grained force fields, which can represent an aminoacid, for instance as just one bead with specific properties

[4]Which were conceived to work with the force field Gromos

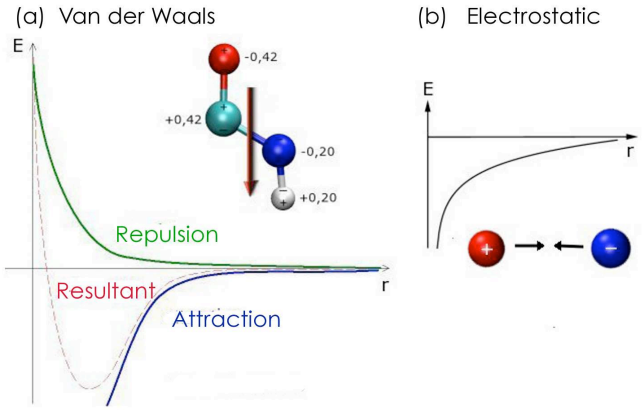

Figure 5.4: Schematics of the (a) vdw and (b) electrostatic parameters

instantaneous dipole moments associated to the temporary fluctuations of the electronic distributions. Those dipole moments generate induced dipoles in their surroundings. The instantaneous dipoles and the induced dipoles are then attracted by the law $\frac{1}{r^6}$. Nonetheless, this attraction is compensated by a strong short-distance repulsion ($\frac{1}{r^{12}}$). Both terms are combined in the Lennard-Jones potential (Fig.5.4(a)).

The force field used is pair-additive. This means that all non-bonded forces result from the sum of non-bonded pair interactions. Non pair-additive interactions, the most important example of which is interaction through atomic polarizability, are represented by effective pair potentials. Only average non pairadditive contributions are incorporated. This also means that the pair interactions are not valid for isolated pairs or for situations that differ appreciably from the test systems on which the models were parameterized. Inpractice the effective pair potentials are acceptable. But the omission of polarizability also means that electrons in atoms do not provide a dielectric constant as they should. For example, real liquid alkanes have a dielectric constant of slightly more than 2, which reduce the long-range electrostatic interaction between (partial) charges. Thus the simulations will exaggerate the long-range Coulomb terms. The application of long-range interactions cuttof compensate a little this effect, as I will discuss in section 5.4.3. The proper treatement of the long-range interactions can also be important when claculating the dielectric constant.

5.4 Principles of MD simulations

During MD simulations, based on a physical model defined by the parameter of the force field, and the representation of the selected potential energy, the Newton laws are applied in order to propagate the molecules in the phase space, defined by their positions and the velocities of their atoms.This way we obtain trajectories that we use to evaluate the statistical and dynamic properties temporally

(a)

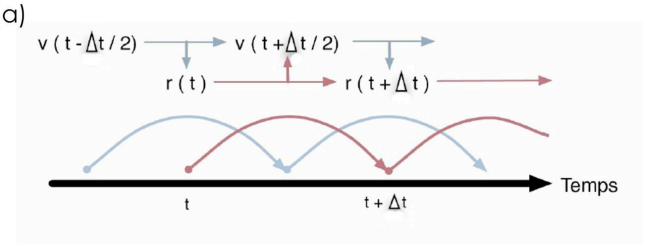

(b)

type de liaison	type de vibration	fréquence (cm^{-1})
C-H, O-H, N-H	étirement	3000-3500
C=C, C=O	étirement	1700-2000
H-O-H	flexion	1600
C-C	étirement	1400-1600
C-C-C	flexion	800-1000
O-H...O	libration	400-700
O-H...O	étirement	50-200

Figure 5.5: Leap-frog alghorithm representation (a) and typical vibrational frequencies in molecules (b).

averaged, that can coincide with the statistic averaged in simulation times, long enough to simulate the phenomena in question . For biomolecular systems, a discrete time step of few femtoseconds is used, with typical simulations consisting of millions of steps.

Molecular dynamics assess the forces exerted on each atom and provide divers information about their trajectories (position and velocity as a function of time). The force $F_i(t)$ exerted on an atom i with coordinates $r_i(t)$ in time t is determined by the deviation from the function of the potential energy V:

$$F_i(t) = -\frac{\partial V}{\partial r_i(t)} \tag{5.3}$$

$$F_i = m_i \frac{\partial^2 r_i}{\partial t^2},\ i = 1, \ldots,\ N. \tag{5.4}$$

Considering a small range of time, it is possible to integrate the equations of movement and obtain a trajectory of each atom over time. To do this, Gromacs uses the leap-frog algorithm (Hockney& Goel, 1974) (Fig.5.5) based on a Taylor expressioon. Knowing the position and the velocity of each atom at time t, it is possible to determine those values at time $t + \Delta t$. The size of Δt (time step) must allow to describe physical phenomena of the molecule such as bond vibrations: as Δt get shorter, the calculation is more accurate but it takes longer. In consequence it is imperative to find the good

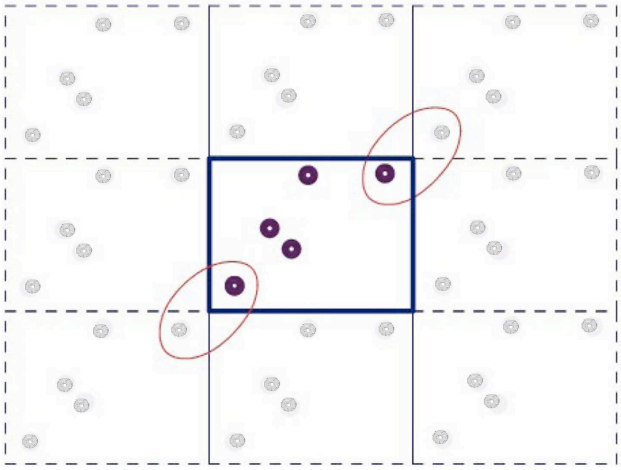

Figure 5.6: Schematics of the periodic conditions and minimum image convention

compromise between precision and rapidity (Fig.5.5). This implies that the time of steps of integration of the movement equations must be one order of magnitude (10 or 20 times) smaller than the highest frequencies of vibrations of the system. The time step is therefore between 1 and 2 fs (femtoseconds). Furthermore, the leap-frog algorithm needs to know the initial velocities in time $t = t_0 - \frac{\Delta t}{2}$. If these data are not available, random initial velocities are generated using a Maxwell distribution for a temperature T and assigned to each atom.

5.4.1 Periodic conditions

Since in MD the system is contained in a simulation box, it has a finite size that induces some problems related with the border effects at the interface with the vacuum surrounding it. That means that the molecules at the border of the box do not have the same environment than the other molecules. In order to minimize these effects, periodic conditions are applied that allow to simulate an environment of infinite size. Each box containing the system is surrounded by replicas of this same box, and everything that happens in one box, happens in the replicas. The movement calculations are only done in the central box but considering the interactions with the neighbor replicas (Fig.5.6). This is the minimum image convention that supposes that each atom interacts with at most one image of every atom and approximates isolated-molecule or cluster calculations . The periodicity allow the speed up of calculation of the interactions and therefore of static and dynamic properties of the system. Between the static properties are the elastic constant and the dielectric constant. At constant pressure there are forces on, for instance, two atoms and the unit cell as a whole. The interatomic forces within the cell give rise to “internal stress”. The elastic laws describe the behavior of a system under stress (defined as the force per unit area). The strains (the fractional change of the stres sin the dimension) on the lattice

are equal to the stress (Pressure static and applied) divided by the elastic constant matrix that relates the stress with the internal forces.

5.4.2 Pressure and temperature control

Two issues are of critical importance when dealing with membrane simulations, the way of controlling the pressure of the system and computing electrostatics Feller (2007). The pressure is a macroscopic propertie evaluated in a microscopic system. The pressure often fluctuates much more than quantities such as the total energy. This is expected beacuse the pressure is related to the virial (product of the positions and the derivative of the of the potential energy function), therefore the pressure calculation is dependent on the velocities and on the periodicity that allow to calculate the potential energy. The virial changes more quickly as a function od the distance than does the interanal energy, hence the greater fluctuation in the pressure.

Nowadays, membrane simulations are most of the time run under the so-called 'NPT' miicrocanonical ensemble, that is the number of molecules (N) is fixed and one weakly couple the system to a thermostat and barostat to get the temperature (T) and pressure (P) constant respectively; the other alternative is the use of the NPγT ensemble, where γ stands for constant surface tension. When coupling the system to a pressure "bath", the rate of pressure changes is given by:

$$\frac{dP\left(t\right)}{dt} = \frac{1}{\tau_p}\left(P_{bath} - P\left(t\right)\right) \tag{5.5}$$

where τ_{p} is the coupling constant (if τ is large then the coupling will be weak), P_{bath} is the pressure of the bath, and *P(t)* is the actual pressure at the time *t*. It basically needs to scale the volume scaling the dimensions of the box (x,y,z), which can be done using the same scaling factor for all directions (isotropic coupling), the same scaling factor for x and y directions but a different one for the z direction (semi-isotropic coupling), or independently in all directions (anisotropic coupling). In all these possibilities, it is recommended to use semi-isotropic coupling when simulating lamellar systems. Usually, the bilayer stands in the box along the xy plane (with the normal along z). Isotropic pressure coupling should be avoided because it creates an artificial surface tension due to the same scaling in the 3 dimensions. Anisotropic or semi-isotropic coupling are more correct in this respect since they allow an independent scaling of the z dimension. Last, anisotropic coupling can lead to a deformation of the box on long simulations, with the bilayer forming a rectangle instead of square. This can cause artifacts especially if there are not enough lipids next to the protein in the direction that was too much reduced. Thus it is recommended to use semi-isotropic coupling to handle pressure coupling on a membrane systems. One popular algorithm for applying pressure coupling is the one of Berendsen (Berendsen and Postma, 1984). This is the most widely used algorithm for pressure coupling in the precedent equation. Although it does not generate the strict NPT ensemble (the same holds for the thermostat), it is very efficient for equilibrating the density of a system in case of 'vacuum defects'. The algorithm shrinks the box until the correct density is reached, the ability to reproduce the correct density then depends primarily on the force field. This is of critical importance since reaching the correct density should give

the correct area per lipid. In turn, the temparture is calculated by scaling the velocities and therefore is related to the time average of the kinetic energy. The temperature is coupled using the same equation than before, such as the rate of change temperature is proportional to the difference in temperature between the bath and the system.

5.4.3 Electrostatic interactions calculations

The other important issue in membrane protein simulation is the way of computing electrostatics when evaluating the energy of the system. Non bonded interactions (including van der Waals and electrostatics) represent the most expensive computational burden. To alleviate the computing effort, various strategies were created in the early time of MD in the seventies and improved so far. They all rely on the so-called cutoff. This latter stands for an atom-atom distance beyond which the interaction is considered equal to 0; since both electrostatics and van der Waals are inverse power functions (of the distance between atoms) they quickly tend to 0 at long distances.

In GROMACS always uses a cutoff radius for long-range interactions the Lennard-Jones interactions and sometimes for the Coulomb interactions as well. Due to the minimum-image convention (only one image of each particle in the periodic boundary conditions is considered for a pair interaction), the cutoff range can not exceed half the box size. Although this approximation can be acceptable for simple systems, that is still pretty big for large systems, and trouble is only expected for systems containing charged particles. But then truly bad things can happen, like accumulation of charges at the cutoff boundary or very wrong energies. It has been demonstrated to cause numerous artifacts on highly charged systems such as ionic solutions. It leads to a wrong radial distribution of the ions, which tend to be separated by the cutoff distance while they should not. In membranes systems this effect cause important alterations on the membrane physical properties, such as the surface tension because of the high dielectric constant of the membrane interface. To circumvent this problem two main techniques/algorithms are used in biomolecular simulations, the particle-mesh-Ewald (PME)[5] (Darden *et al.*, 1993; Essmann *et al.*, 1995) and the reaction field not discussed here. On pure phospholipids, the use of cutoff gives the wrong area per lipid; they indeed tend to be too packed, thus the membrane thickness is overestimated (Anezo *et al.*, 2003). For simulations of membrane proteins (or peptides) within a bilayer of phospholipids, the use of cutoff has been shown to not affect directly the protein nor the water, but only the phospholipids (Cordomi, Edholm et al. 2007). Nonetheless, it is still highly recommended not to use cutoff schemes if one wants to avoid artifacts due to a wrong thickness/area per lipid, which may cause conformational consequences due to different matching/mismatching conditions of the environment around the protein (or peptide). Currently, PME is the most correct and most used technique for computing electrostatics on membrane systems (Anezo *et al.*, 2003).

[5]PME is a smart and fast way of evaluating the so-called Ewald summation, which is basically a method for calculating electrostatics in a crystal. When we use PME in biomolecular simulations, we thus consider the system as an infinite crystal, that is, we replicate the simulation box infinitely in all directions. Although this is the most correct way to handle electrostatics it has been shown to induce artificial periodicities on the system

5.5 System set up

In membrane MD simulations studies the set up of the initial system is very important and strongly influences the fate of the simulation. In addition to addressing general questions and choosing simulations parameters, setting up a membrane protein simulation system usually requires three major working steps: 1, preparation of the bilayer; 2, insertion and orientation of the protein; and 3, system equilibration.

We designed our experiments based on some of the peptide mutations and the lipid composition that influence ALPS curvature recognition and we perfomed simulations in flat membrane patches. FIrst, we designed a control ALPS-bilayer system in a favorable (for the membrane-curvature recognition) lipid composition: 1,2-diacyl-sn-glycerol-3-phosphorylcholine (DOPC) as the experimental data dictated (see sections 4.3.1 and 4.3.4). We also designed other systems for comparison in unfavorable (1,2-dimyristoyl-sn-glycerol-3-phosphocholine (DMPC) and 1-palmytoyl-2-oleoyl-sn-glycerol-3-phosphorylcholine (POPC)) and more favorable conditions (mixed bilayer of DOPC and dioleoyl-sn-glycerol (DOG)). We adressed the question of ALPS lipid-packing recognition from this two perspectives, the favorable ALPS sequence and the favorable lipid composition that determine ALPS-lipid interactions and the function of the motif.

From the perspective of the peptide, and based on the prevailing model of ALPS membrane-curvature recognition (see section 4.4), we focus first on the role of the hydrophobic interactions (see section 4.3.2). Hence, we used the the triple-mutant of ALPS, L12A-W16A-F19A (called LWF-A) inefficient curvature sensor (Fig.5.7) and we setted up an LWF-A-DOPC-system.

From the perspective of the membranes lipid composition, we decided to change the lipid environment based on the experimental results we described in section 4.3.4. Hence, we selected to perform simulations in different homogeneous (one lipid nature composition) and heterogenous (simple mix of two lipids) phospholipid bilayers that according to the experimental data affect ALPS efficiency.

In order to evaluate the role of the nature of the lipid acyl chains in ALPS behavior. We set up three different homogeneous bilayers, which increasingly enhance ALPS efficiency starting from: one composed of DMPC, which both acyl chains are saturated (C14:0, C14:0); the second, composed of POPC, with one monounsaturated acyl chain and the other saturated (C16:0, C18:1); and the third, composed by DOPC, which both acyl chains are monounsaturated (C18:1,C18:1) and one heterogeneous bilayer composed of 85% DOPC and 15% of its diacylglycerol (dioleoylglycerol DOG)) (Fig.5.8). In this way we aimed at test the effect of changing the lipid packing as a result of different acyl chains (homogeneous bilayers) and headgroups (heteogeneous bilayer).

The starting configuation for both peptides was in their α-helix folded state already embedded at the interface of the respective different flat bilayers. (Fig.5.9), it was possible to overcome the problem of folding/insertion -as has been done in other computational studies of amphipathic peptides (Dolan *et al.*, 2002; Jang *et al.*, 2006; Kandasamy and Larson, 2004; Blood *et al.*, 2008; Tieleman *et al.*, 1998)-, and it was possible as well to observe properties related to the lipid-peptide interactions once the peptides is in a lipidic environment.

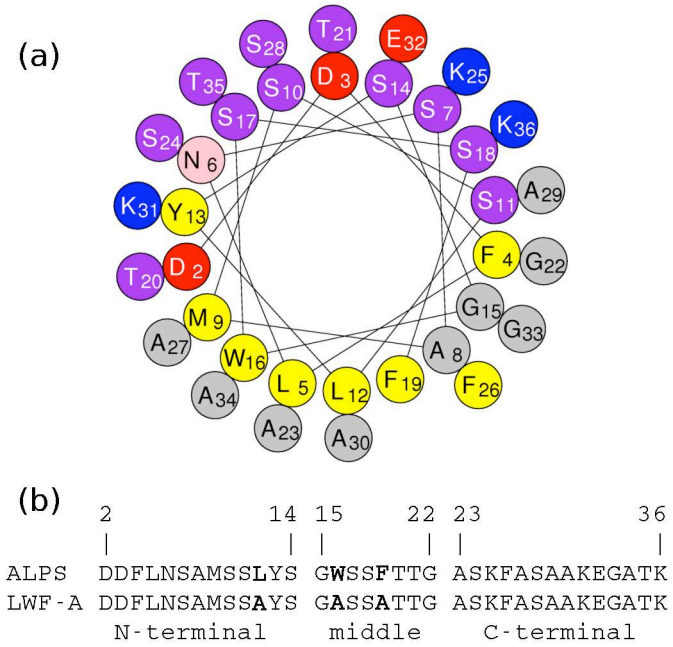

Figure 5.7: (a) ALPS helical wheel diagram. The color code of the wheel diagram is given as in ref. (Drin *et al.*, 2007) (yellow: bulky hydrophobic residues, purple: serines and threonines, gray: glycines and alanines, blue: positively charge residues, red: negatively charged residues). (b) Sequences of ALPS (up) and LWF-A (bottom) indicating the segmentation of both peptides for the N-terminal, middle and C-terminal segment.

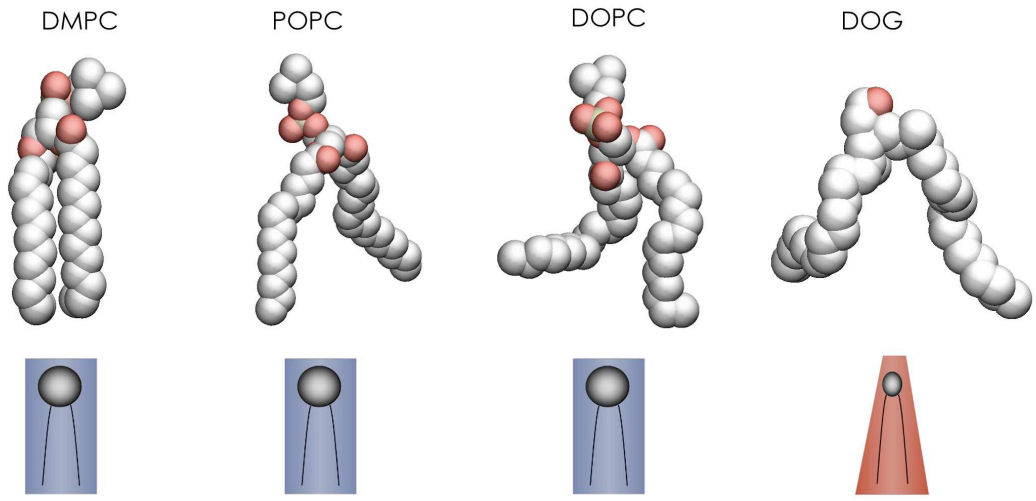

Figure 5.8: Lipids with different shapes used in this work

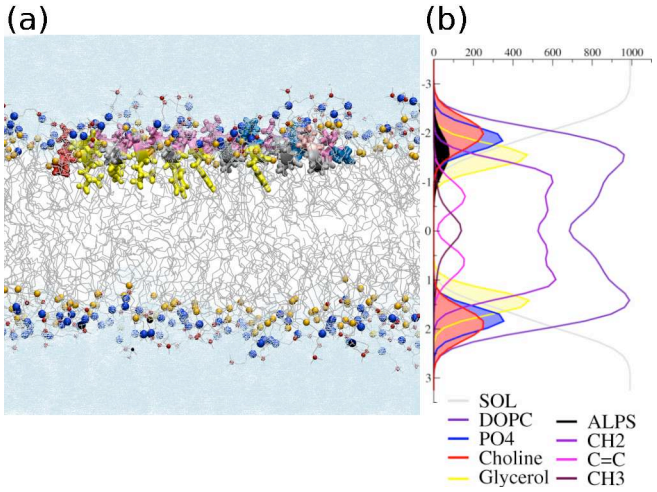

Figure 5.9: (a) Snapshot of the ALPS-DOPC system used as starting configuration for the different simulations. The peptide is in licorice representation with the polar face in purple, and the hydrophibic face in yellow. The detail of the color code is specified in Fig. 1. The lipids are in gray and the phosphate, glycerol and choline moieties are represented by colors dots with the same color code that in the density plot on the right. (b) Density plot of ALPS-DOPC system showing the partitioning of the peptide at the level of the phosphate/glycerol moieties.

1. **Preparation of the bilayers**. First, we needed a pure bilayer system where the peptides could be inserted. To carry out our simulations we used different pre-equilibrated starting patches of lipid bilayers (DOPC, POPC and DMPC (Fig.5.8). This patches were adapted from the work of Tieleman et al. (Tieleman *et al.*, 2006) (provided by L. Monticelli[6]) -in the case of DOPC and POPC bilayers, and we obtain the DMPC start patches form Tieleman's website. We expanded these patches from 128 to 300 lipids (150 per leaflet) and added 12,301 water molecules, distributed along the normal of the bilayer (Z-dimension). This latter operation allows an adequate distance between the peptide-bilayer system and its periodic image. We removed all the water molecules from the centre of the membrane keeping the headgroups well solvated. The ~40 water molecules/lipid ratio obtained was slightly superior than the hydration limit proposed by Nagle and Tristram-Nagle (Tristram-Nagle *et al.*, 1998). The pure lipid system was then energy-minimized using a steepest-descent algorithm and equilibrated under the NPT ensemble (see below the description of the simulations conditions). In order to build the heterogeneous composed by DOPC and dioleoylglycerol (DOG) (Fig.5.8) bilayers patches we randomly substituted 15% of the DOPC lipids by DOG (smae number on each leaflet) maintaining the same quantity of lipids in both leaflets. These patches were then solvatated, minimized and equilibrated as in the case of homogeneous systems. We had therefore 5 peptide-free systems. We considered that these peptide-free systems were well equilibrated when they successfully reproduce the membrane properties determined experimentally (Tristram-Nagle and Nagle, 2004) (i.e. area per lipid, bilayer

[6]Modified paramters that connect the double-bond (Martinez-Seara *et al.*, 2008a,b)

Peptide	control	Acyl chain variation	Headgroup variation
ALPS	DOPC	DMPC	DOPC(85%)-DOG(15%)
		POPC	
LWF-A	DOPC	POPC	DOPC(85%)-DOG(15%)

Table 5.1: Systems constructed and simulated (the simulation conditions were the same in all cases, as described in the text)

thickness and order parameter) (in the cases there exist experimental or simulation data for comparison).

2. **Construction and orientation of the peptides.** ALPS and LWF-A are 35 residues long α−helical models generated using CHARMM (Brooks *et al.*, 1983) in an ideal α−helix conformation. The side chains were repositioned in optimized conformations using SCWRL (Canutescu *et al.*, 2003) and the SCit web server (Gautier *et al.*, 2004). In order to generate the LWF-A peptide, we mutate, *in silico*, the ALPS L12, W16 and F19 residues to Alanine. Then the N-terminal was amidated and the C-terminal acetylated. An energy minimization procedure followed this construction. We used the final equilibrated pure bilayers to insert the peptides. This process was performed using the molecular visualization program PyMol (DeLano, 2002). We placed each amphipathic peptide oriented with its helical axis parallel to the lipid/water interface of one of the leaflets (hereafter referred to as the bound leaflet), taking care of adjusting the azimuthal rotation in order to have the hydrophobic moment in the right direction with respect of the hydrophobic core of the bilayer. Then, the peptide was translated at the position in the phosphate/glycerol region (Fig.5.9). We removed all the lipids in a 3Å radius around the peptide, the same number from both leaflets, ending with the same number of lipids on both sides of the bilayer and thus assuring that all the bilayer asymmetries observed afterward were due to the presence of the peptide. In order to neutralize the ionic charge of the system and at the same time to reach experimental salt concentration, we added 15 atoms of Na+ and Cl- that correspond to a concentration of approximately 60 mM of NaCl similar to the one used experimentally (Bigay *et al.*, 2003; Drin *et al.*, 2007; Mesmin *et al.*, 2007). The ions were placed in the most electrostatically favorable positions for the system, using the genion program from the GROMACS package.

3. **Equilibration.** We ended up with 8 "peptide-bound" systems (detailed in Table5.1) consisting of 1 peptide bound to a single leaflet, 250 DOPC lipids (125 per leaflet), 9,670 water molecules and 30 ions. We performed a last energy minimization procedure and applied a harmonic force constant of 1000 kJ/mol to the backbone of the peptide during a 10 ns position restraints dynamics. This led to a shrink of the box allowing thereby the closure of the hole created for the peptide and to the equilibration of the bilayer and the surrounding solvent. Finally, all restraints were released and standard MD simulations were performed for 120 ns in three different replicas for each peptide.

5.6 Simulations details

The simulations were then carried out using the force field described previously. The all-atom OPLS-AA force-field paramters for the peptide. For the DOPC lipids, we used the adapted Berger parameters in order to work in combination with the all-atom OPLS-AA force-field. These parameters include some corrections for the insaturation (cis double bond) of each acyl chain (Martinez-Seara *et al.*, 2008a). Although there exist some trends for each force-field (Sapay *et al.*, 2008) and their conformational sampling depends, to a certain extent, on the starting conformations as well as on the force field accuracy (Matthes and de Groot, 2009), the combination of Berger (modified) -OPLS force-field have proven to yield a good agreement between simulations and the available experimental data (Tieleman *et al.*, 2006). Additionally, the TIP3 water model (Jorgensen, 1982) was used as the solvent. For both the Na+ and the Cl−, we used the default ion parameters of the OPLS force field (Gurtovenko and Vattulainen, 2008, 2009).

Simulations were run under the NPT ensemble and periodic boundary conditions were applied in all three dimensions. We used the weak coupling algorithm of Berendsen described before, to maintain the system at a constant temperature of 313 K using a coupling constant of 0.1 ps (protein, lipid and water-ions separately). Pressure was held constant semi-isotropically (x and y dimensions were scaled by the same factor, whereas the z dimension was scaled independently from x and y) with the Berendsen algorithm at 1 atm with a coupling constant of 1 ps. Water molecules were kept rigid using the SETTLE algorithm (Miyamoto and Kollman, 1992). All other bond lengths were constrained with the LINCS algorithm (Hess *et al.*, 1997), with a 2 fs time step. We used a short-range coulombic and van der Waals cutoff of 10 Å and we calculated the long-range electrostatic interactions using the smooth particle mesh Ewald (PME) algorithm. For PME, we used a grid spacing of 1.2 Å and an interpolation order of 4. The neighbor list was updated every 10 steps. Molecular configurations were saved every picosecond for further analysis.

For the comparison between ALPS and LWF-A mutant, we performed a total of 7 simulations of 120 ns each: Three replica of ALPS-bound system, three of LWF-A system, and one peptide-free (pure bilayer) for each different type of bilayer system. For the comparison of ALPS in different bilayers we perfomed 11 additional simulations: three replicas for ALPS-DMPC of 70 ns each, three for ALPS-POPC of 120 ns each, and three for ALPS-DOPC-DOG systems of 120 ns, and the three respective pure peptide-ffree bilayers equilibrations.

5.7 Trajectory analysis

From the trajectories issued of MD simulations, it is possible to obtain an enourmous amount of information. We focus our analysis to the main properties of the bilayers, the confromational changes that can be observed in the peptides, and some aspects of lipid-peptide interactions. To do this, we used the GROMACS Package and some in-house python and C tools to analyze all peptide and membrane metrics.

5.7.1 Analysis of the lipid bilayer properties

5.7.1.1 Bilayer thickness

The total bilayer thickness is defined as the distance between the center of mass of the P atoms of each leaflet, projected in the Z-*axis* (normal to the bilayer plane). The center of mass of a group of atoms is defined by:

$$C_m = \frac{1}{N}\sum_{i}^{N} m_i r_i \tag{5.6}$$

,where m_i and r_i are respectively, the mass and the coordinates of the atom *i*.

We calculated the local bilayer thickness in function of the distance to the center of mass of every atom of the backbone of the peptide. We considered as close (associated) lipids those that were within a radius of 1 nm in the plane XY and far(non-associated lipids those that were outside this radius. A list of all the close lipids was updated every step of time. The bilayer thickness is calculated from the first aliphatic carbon of tha acyl chains.

5.7.1.2 Order Parameter

The orientation of the acyl chains of lipids can be assessed with the order parameter {Vermeer, 2007 #589}. This parameter allows us to obtain information about the dynamics and orientation of the lipids acyl chains. It is usually measured by ^{2}H solid state NMR by labeling the different carbons along the acyl chain, and depends on the orientation of each *C-D* bond compared to a reference axis (often the bilayer normal). The use of a united-atom force field does not give access to these angles, but it has been shown that it was possible to reconstruct each C_i-*D* bond from the best vector corresponding the $C_{i-1} - C_i - C_{i+1}$ {Egberts, 1994 #590}. Thus the order parameter S_{CD} for a given carbon Ci is calculated from the orientation of the vector that approximates the better the orientation of $C_{i-1} - C_i - C_{i+1}$ bonds in our simulations given the equation:

$$(S_n) = \frac{1}{2} < 3cos^2\theta_n - 1 > \tag{5.7}$$

,where $< >$ stands for a time and ensemble average, θ_n is the angle between the normal to the bilayer and the vector $C_{i-1} - C_i - C_{i+1}$of the carbon C_n. (S_n) is averaged over the simulation time and over the equivalent atoms of different lipids. High values (close to 1) correspond to ordered bond orientations whereas values close to 0 indicate disorder. The order parameter value of 0.5 corresponds to *trans* (extended) conformations and perpendicular to the normal of the bilayer. A value of 1 corresponds to a trans acyl chain conformation but parallel to the bilayer normal, and a value of 0 (it can go to -0.5) when there is no preferential orientation and therefore it represents the disorder that the acyl chains adopt during the simulation. The lower order in double bonds in the case of insaturated lipids is mostly the result of double bond *cis* geometry: double bonds oriented parallel to the bilayer normal have order parameters of zero (even in the absence of motions).We calculate the order parameter of the associated

and non-associated lipids applying the same criteria than for the calculation of the bilayer thickness.

5.7.2 Analysis of the peptide properties

5.7.2.1 Root mean square deviation (RMSd)

This value is useful to measure the geometric deviation of one structure compared to another one of reference once they have been superposed. In our analysis we used this parameter to evaluate the deviation of the peptides helical structure with respect to an ideal one (structure of reference) and to also evaluate the different conformation with respect to the initial model at $t = 0$ (another structure of reference). This value is given by:

$$RMSd = \sqrt{\frac{1}{N}\sum_{i=1}^{n} \mid r_i\,(t) - r_i\,(ref)\mid^2} \tag{5.8}$$

where N is the number of atoms in the system and $r_i\,(t)$the position of atom *i* in time *t*. The average RMSd is the sum of RMSd values at a time *t* divided by the number of time steps.

5.7.2.2 Root mean square fluctuations (RMSf)

This value allows to measure the fluctuations of each atom around their average position in a given structure. It is calculated:

$$RMSf_i = \sqrt{\frac{1}{N_t}\sum \mid r_{i(t)} - < r_i >\mid^2} \tag{5.9}$$

where (r_i) is the average position of atom *i* in the range of time simulated. The average RMSf is the sum of RMSf values at a time *t* divided by the number of time steps.

5.7.2.3 Secondary structure

We evaluated the secondary structure of the peptides using the DSSP program (Kabsch and Sander, 1983). The principle of this program is to assign secundary structre based on H-bond patterns present in the structure, for example between the atom i and $i+4$ in a α-helix. This is a rapid method that only depends in the presence of the H-bond. It considers that an H-bond exist when the distance between a donnor and an acceptor of H-bond (the atoms N and O respectively) are closer than 3.2 Å. It also apply an angle and energetic criteria.

From the secondary structure analysis we decided to define three different regions in the helices. Using this segmentation we applied the further anlayses to the peptide. Gromacs allowed us to compute all kind of helix properties.

5.7.2.4 Helix deformational flexibility

To assess the deformation of the helix, we defined two helix kinks as the crossing-angle between the N-terminal (res *i* to *j*) and middle (res *j* to *k*) helical axes together with the crossing-angle between the

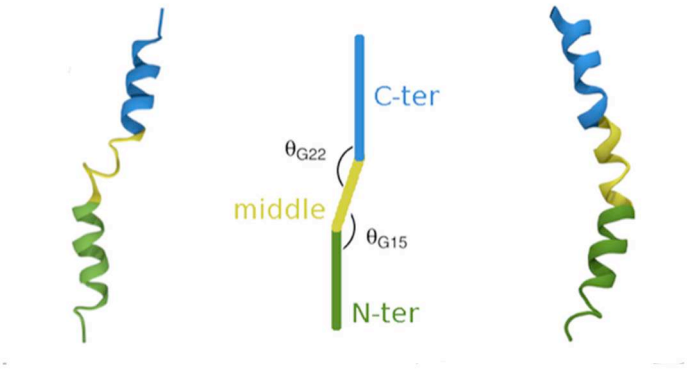

Figure 5.10: Kink angles

middle and the C-terminal (res *k* to *l*) axes. A non-zero crossing-angle means that a break is present between two axes (Fig.5.10). These angles are calculated at every time step.

In order to detect the most frequent conformation we performed a clustering analysis over a concatenated trajectory of all the replicas for each case. We used the algorithm of Daura et al., which counts the number of neighbors using a cut-off. Then it chooses the structure with the largest number of neighbors and with all these neighbors creates a cluster. Finally the program eliminates the structure from the pool of clusters. The method repeats the operation for the remaining structures in the pool. The cut-off is decided from an RMSd analysis. Each structure is assigned to exactly one cluster. The structure with the smallest average distance to the others, the average structure, or all the structures for each cluster, will be written in a trajectory file. It is then possible to obtain the cluster number as a function of time and the size of the cluster.

5.7.2.5 Helix orientation: tilt and azimuthal rotation

The tilt τ angle between the helix and the normal to the bilayer and the helix axis) and azimuthal rotation (angle between the direction of the tilt and a residue of reference) were calculated as in (Ozdirekcan *et al.*, 2007) (Fig.5.11) . The normal to the membrane was taken as the *z-axis*.

In the case of the tilt, we calculated the helix axis by taking the first eigenvector of the inertia matrix (defined by all heavy atoms of the backbone). As the peptide is interfacial, its tilt fluctuates around 90° (the value 90° refers to a perfect horizontal peptide at the interface of the membrane), thus it was more convenient to express the tilt within the range [0-180°]. This could be easily achieved by just orienting the helix axis from C to N before calculating the angle.

For the azimuthal rotation (which describes the rotation of the peptide about its helix axis), we used as reference residues A8 as for the N-terminal helix, residue F16 for middle helix and residue A30 for the C-terminal helix. The tools for evaluating the tilt and azimuthal rotation are freely available at http://www.dsimb.inserm.fr/~fuchs.

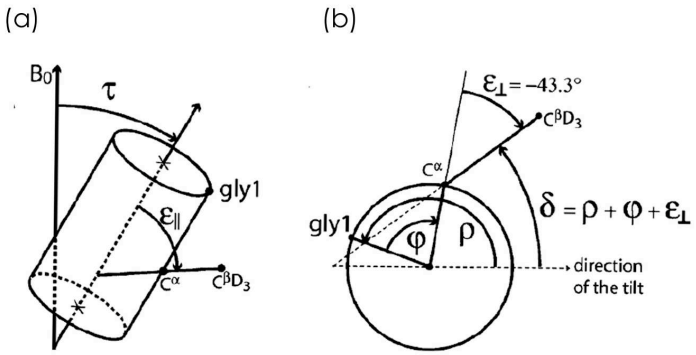

Figure 5.11: Schematics of (a) Tilt and (b) azimuthal rotation

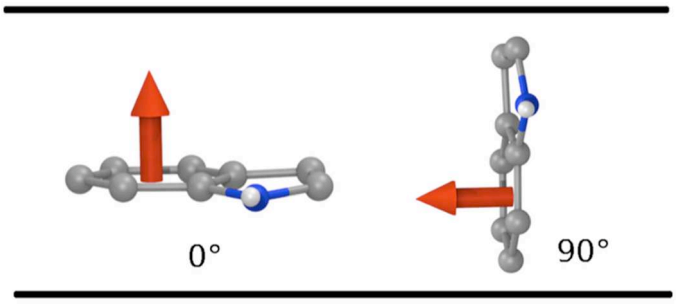

Figure 5.12: Aromatic ring orientations with respecto to the bilayer normal (perpendicular to the plane of the bilayer represented with black lines)

5.7.3 Aromatic side-chain orientation

We assessed the orientations of aromatic residues by calculating the tilt angle of the normal to the plane of the aromatic ring, with respect to the membrane normal. The plane is defined by all the heavy atoms of the ring and the membrane normal is taken as the z-axis (Fig.).

5.7.4 Analysis of lipid-peptide interactions

5.7.4.1 Radial Distribution function (RDF)

Either neutron or X-ray scattering can study the structure of liquids. The most common way to describe liquid structure is by a radial distribution function. To assess the radial distribution function (rdf) gAB(r) of A with respect to B, we have to calculate:

$$4\pi r^2 gAB\,(r) = V \sum_{i \epsilon A}^{N_A} \sum_{j \epsilon B}^{N_B} P\,(r) \tag{5.10}$$

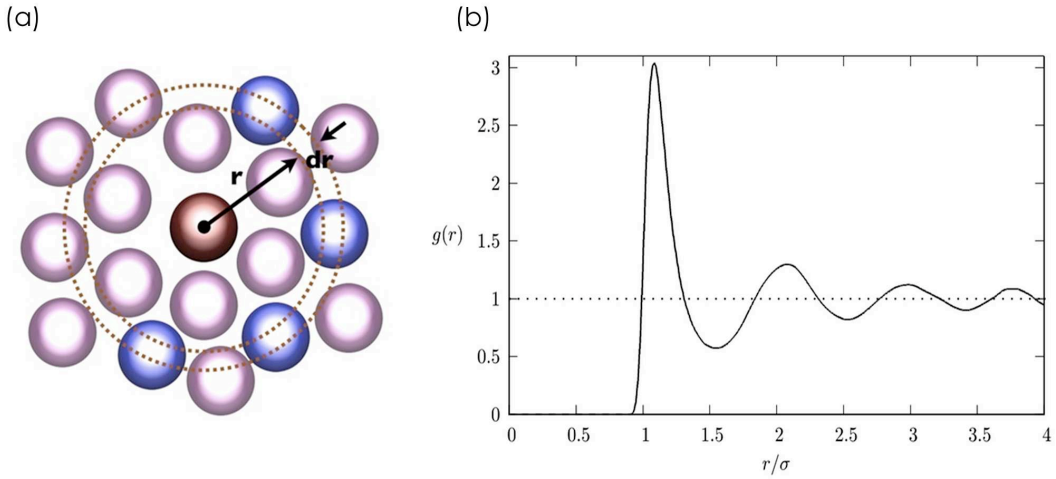

Figure 5.13: (a) Schematics of the Radial distribution function (RDF), (b) Example of the RDF of a pure liquid

where V is the volume and $P(r)$ is the probability to find a B atom at a distance r from an A atom.

To evaluate the repartition of lipids around the peptide (as well as between them), we computed some radial distribution functions g(r) (RDF) of suitable chosen pairs of atoms. For a given pair of particles A and B (e.g. phosphorous of phosphate / nitrogen of choline), g(r) is calculated as the ratio between the local (particle) density of B at distance r from any particle A with respect to the global particle density of B in the medium. The value thus varies around one and we obtain peaks that give the position of the different shells of particles B around A. The height of these peaks is directly proportional to the amount of particles in the corresponding shell (Fig.5.13) . Since a membrane/water system is highly inhomogeneous compared to a pure liquid, all RDF are not expected to tend to 1 at long distances (due to the normalization over an inhomogeneous medium) or go above and below 1 like in a pure liquid.

In general, averaged properties were calculated over the 120 ns of each simulation minus the time of equilibration (position restraints MD). For some properties (when explicitly stated) we computed averages over the three replica concatenated as a single trajectory which allowed to improve statistics. All the snapshots of the membrane systems were generated using VMD (Humphrey *et al.*, 1996).

Chapter 6

Deciphering the structural attributes of ALPS

We offered in chapter 4 an overview about the mechanism implicated in membrane shape control, generation and sensing. We pointed out the membrane features that hake to be taken into account to understand the membrane deformation processes, and the role of many proteins and lipid-binding domains in the control and sensing of those features. The capacity to sense the membrane curvature has been attributed to every interfacial amphipathic helix, based on some shape (of the helix "tube" and the shape factor of different lipids) and space (the defects created between lipids in function of the increase in the curvature) criteria. An helix in principle will fit to that defects in packing created by the curvature. The aim of this work is to show that the question is not as simple as that. The membranes are very maleable and dynamic and an important role in the process must be attributed to their particular properties. On the other hand, most of the interfacial amphipathic helices have positively charged polar faces that help the binding to the membranes. That is not the case for ALPS. Hence, other mechanisms must exit related to the curvature sensing. The fact that curvature sensors with mostly uncharged residues on their polar face and with mostly aromatic hydropbobic residues on their hydrophobic face, such as ALPS, may exist in a wide range of proteins, makes ALPS a very interesting and challenging research subject. Understanding the atomic details of ALPS and membrane interactions may provide unvaluable insights about ALPS properties and its way of action, as well as how the membranes respond to ALPS.

In this context our research aimed to adresse the question of ALPS lipid-packing recognition from two perspectives:

1. the sense of the amino acid composition and peptide structure in ALPS lipid-packing sensors
2. the effects that different lipid-packing defects can exert in ALPS structure

From these two perspectives, that will help us to recognize the contribution of each component of the peptide-membrane system in the lipid-packing recognition process, we aimed at :

1. Explain how ALPS structure is influenced by the lipid environment and which kind of interactions are favor between a Set/Thr rich polar face and the lipid polar heads, and between the aromatic hydrophobic residues and the acyl chains.
2. Elucidate ALPS strcuture and lipid-peptide interactions relevance for the lipid-packing recognition
3. Recognize the effect of ALPS in the bilayer properties
4. Propose how the ALPS-mediated bilayer responses could be of relevance in the context of the curvature recognition.
5. Incorporate all these information in a comprehensive dynamic model that could complete the actual knowledge about ALPS and its curvature sensing capacities.

Our first objective was then to reveal the impact of the lipidic environment on ALPS structural properties. We aimed to describe, at atomic detail, the experimentally-detected features ALPS, as well as offer insights about ALPS role on lipid-packing recognition. In this chapter I will discuss how the comparisons of ALPS and the mutant LWF-A behaviors in DOPC bilayers allowed us to unravel some key questions about the importance of aromatic hydrophobic and Ser/Thr residues in the constitution of ALPS-like sensors. Additionally, I will present a new notion about ALPS flexibility and deformability, which are two relevant features that a protein should have in order to adapt to the lipid-packing defects. Finally, I will describe important differences concerning how the DOPC lipids react to the presence of both peptides.The results summarized in this chapter have been submitted to the Journal of Molecular Biology as a paper entitled *"Novel atomistic view of ALPS curvature sensor lipid-packing recognition"*.

6.1 Interfacial partitioning of ALPS and LWF-A

The starting configuration of the ALPS-DOPC and LWF-A-DOPC systems was an interfacial partitioning of the peptides at the level between the phosphate and the glycerol moeities in one leaflet of the DOPC bilayer. During all the length of the simulation the partitioning of both is stabilized at the level of the glycerol (Fig.5.9).

6.2 ALPS structure and conformational diversity

In order to understand how DOPC lipids influence ALPS structural properties, we followed the evolution of ALPS secondary structure during the 120 ns simulated in the three different replicas of ALPS-DOPC system (Fig.6.1). We then compared with LWF-A peptide secondary structure evolution on simulations of the same length (Fig.6.1). The discussion of the results is based on the averaged properties over all the replicas. You can refer to the starting configuration of these systems is in section 5.5 (Figures 5.7 and 5.9).

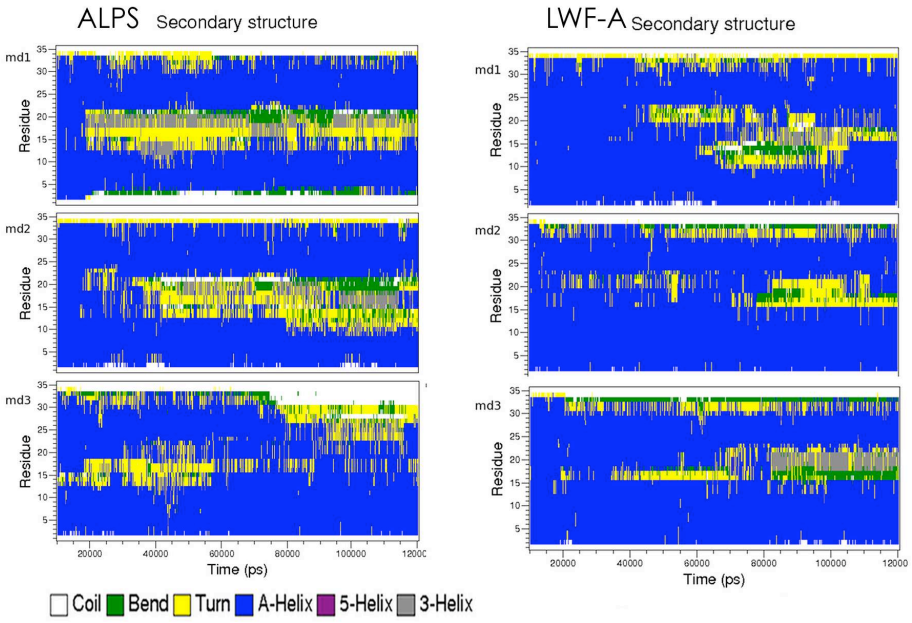

Figure 6.1: Secondary structure evolution of ALPS and LWF-A in DOPC bilayers simulations

6.2.1 ALPS secondary structure and deformation

In Fig. 3a, we observe that starting from an ideal α—helical structure, ALPS rapidly evolved (from 20 ns and so forth) to an altered state. Most residues in the middle region adopt a turn or 3_{10}-helix conformation, while in the N-terminal and C-terminal region, the α—helical structure is globally maintained. The peptide lingers in that state for the remaining 100 ns (Fig.6.1 (left panels)).

We assessed the helicity content along the sequence, which was averaged over all the configurations using ALPS three replica (Fig.6.2). By doing so, the helicity content drops to zero at residues Gly15 and Gly22 suggesting two breaking points and three well distinct regions. This effect is not surprising, since it is known that glycines are helix breakers that accordingly disrupt helices in water (Pace and Scholtz, 1998; Chakrabarty *et al.*, 1991) and modulate the peptide structure in hydrophobic environments (Li and Deber, 1992c,a).

The highest helicity content is around 60% (Fig. 6.2), which mostly concerns the first and last segments of the sequence. Both segments have a combination of residues with high and low propensities to form helices in hydrophobic environments (Liu and Deber, 1998b). In turn, the segment flanked by the glycines has a more variable helicity content (Fig. 6.2). The residues in this segment (Ser, Thr, Trp) (Fig.5.7) have intermediate propensities to form helices in hydrophobic environments (see table 2.9)). However, glycines, Ser and Thr have, nonetheless been also described as stabilizers of TM helices. It is possible that in an interfacial environment they play a dual role.

Then we looked at the conformations ALPS could adopt during the secondary structure changes

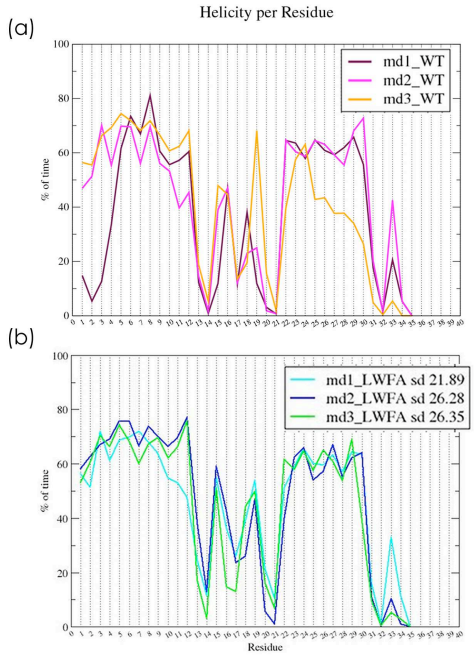

Figure 6.2: Helicity content of ALPS and LWF-A in DOPC in three different replica

(Fig.6.3). A clustering analysis provided three main conformations (78% of the conformations). The most populated cluster (46%) represents a "Z-shaped" bended-helix conformation, which clearly shows the three segments with different helicity content. Two other conformers were found (16% each one) corresponding to a curved helix and a more restrained "Z-shaped" structure (Fig. 6.3).

Consistently with the helicity and the clustering analysis, our results allowed us to define three different segments which we use for all further analyses (see Fig. 5.7 for the sequence of these segments):

- the N-terminal segment comprising Asp2 to Ser14,
- the middle segment consisting of residues Gly15 to Gly22, and
- the C-terminal segment covering Ala23 to Lys36

In one of the ALPS-DOPC replica we observed that in the last half of the simulation, the peptide recovers its original helical structure in the middle segment leading to instability of the C-terminal helical structure (Fig. 6.1(bottom panel of left)). These data may suggest that an unwinding process has occurred at the C-terminal that might be due to the fact that Lys35 does not cap correctly to neutralize the helix dipole (Viguera and Serrano, 1999; Petukhov *et al.*, 2002; Chakrabartty *et al.*, 1993a). Moreover, this residue and the Glu32 have low propensities to form helices in hydrophobic environments (Liu and Deber, 1998b) (see table 2.9). The resulting coil/bend/turn is therefore able to reach Ala30, which may contribute to stabilize the rest of the helix in that region (Chou and Fasman, 1974; Chakrabartty *et al.*, 1994).

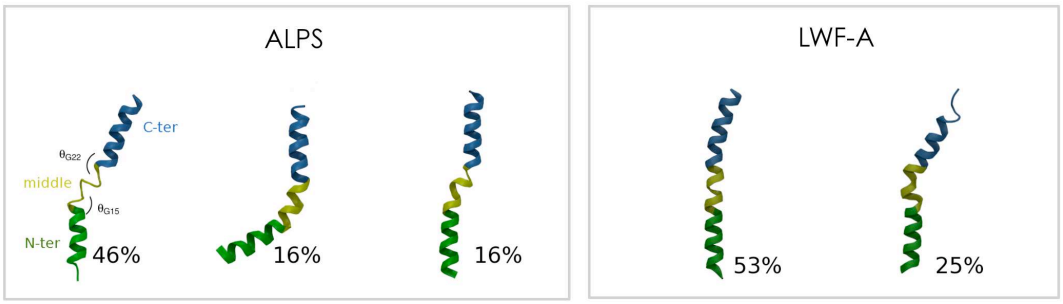

Figure 6.3: Clustering analysis of ALPS and LWF-A in DOPC. N-ter segment is in green, middle segment in yellow and C-ter segment in bleu.

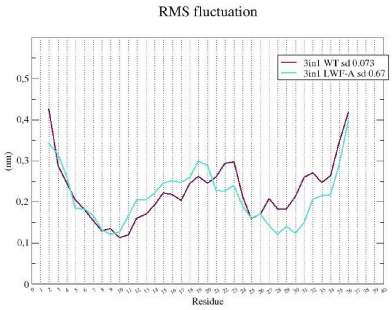

Figure 6.4: Root means square fluctuations (RMSF) of ALPS and LWF-A in DOPC

In both peptides, a coil structure affects the first residues of the N-terminal during all the simulations that we attribute to an end-effect. Nonetheless, the presence of two Asp and one Asn, which are less prone residues to form helices in aqueous solution (Pace and Scholtz, 1998) and in hydrophobic environments (Liu and Deber, 1998b; Li and Deber, 1994a)(see table 2.9), may have played an important role to create the initial coil structure.

6.2.1.1 Mutant LWF-A limited deformation

In LWF-A the secondary structure evolves differently (Fig. 6.1(right)). Although Gly15 and Gly22 still alter the α−helical structure in its middle segment, they do not do it simultaneously as in ALPS. In consequence, the deformation and turn/3_{10}-helix transitions are limited to a few residues. The alanine inserted at expenses of Trp16 enhance the stability of the helix, but the alanines that substitute Leu12 and Phe19 destabilize the helix. These effects could come from the fact that alanine is more prone to form helices than Trp, but less prone to do so than Leu and Phe, according to the propensities of Deber in hydrophobic environment (Liu and Deber, 1998b; Deber *et al.*, 1993) (see table 2.9). Hence, the helicity content of both peptides is very similar (Fig. 6.2), as well as their RMSF (Fig. 6.4). However, from the clustering analysis we determined that in LWF-A only two conformers were representative,

covering 78% of the conformations (same number of conformations as the three clusters of ALPS presented above). The first cluster (53 %) is a slightly curved helix (Fig. 6.3 (left panel)), whereas the second (25 %) reminds the ALPS curved helix conformer.

Overall, the force-field (Tieleman *et al.*, 2006) used for our simulations, successfully explores the possible conformational transitions of an α−helix. Moreover, we found an important correlation of our results and the propensities measured experimentally. These results show that LWF-A is less deformable than ALPS. LWF-A presents frequent conformational transitions between similar conformers, whereas ALPS has a stronger conformational diversity with fewer transitions.

6.2.2 Characterization of helix deformations

ALPS conformational diversity clearly reflects the segmentation in three distinct parts, whereas in LWF-A, the conformational population does not correspond to the segmentation suggested by the helicity content. Therefore, we decided to characterize these differences in terms of the different segments reciprocal orientation by examining two kink angles of the helix around the flexible glycine hinges (θGly15 and θGly22, see Fig. 6.3(schematisc in cluster 1 of ALPS in right panel)).

The kinked helices are described in terms of crossing-angles between the N-terminal and middle segments (θGly15 in blue) the crossing-angle between the middle and the C-terminal segments (θGly22 in red). At a first glance, the first thing that was evident from this data was that the kink distribution are considerably larger for ALPS compared to the mutant, and the average values are larger for ALPS (θGly15 = 36° and θGly22 = 25°) in the Z-bended conformation, compared to the slightly curved conformation of the mutant (20° for both angles). Moreover, we observed that the fluctuations of these angles are also higher for ALPS than for LWF-A. These results illustrate and confirm the greater conformational diversity of ALPS over LWF-A. Overall, these data bring a dynamic view of ALPS conformation and suggest that when ALPS binds to the membrane, it does not fold into a "perfect" rigid α-helix.

6.3 Peptide orientation relative to the membrane

We have showed so far that the mutations of LWF-A have caused major changes in the structural flexibility. They can also modify the hydrophobic moment and hydrophobicity (Table 6.1). In order to understand the conformational changes in the context of these modifications of the physicochemical properties, we analyzed the relative positioning of the peptide within the membrane. We examined the relative orientation of each segment with two descriptors, the tilt (angle between the helix axis and the membrane normal) (Fig.6.5) and azimuthal rotation (rotation about the helix axis) (Fig. 6.6). We observed that in ALPS, the N-terminal and C-terminal tilt slightly deviates from the position parallel to

	hydrophobicity		μH		azimuthal rotation		tilt	
segments	ALPS	LWF-A	ALPS	LWF-A	ALPS	LWF-A	ALPS	LWF-A
N-term	0.415	0.308	0.413	0.307	48 (10)	41 (10)	84 (4)	89 (6)
middle	0.493	0.113	0.385	0.061	24 (15)	-33 (18)	76 (10)	83 (7)
C-term	-0.006	-0.006	0.300	0.300	18 (16)	17 (18)	83 (5)	89 (6)

Table 6.1: ALPS and LWF-A segments properties. The table shows for each segment the hydrophobicity, hydrophobic moment (μH calculated with the program Heliquest (Gautier *et al.*, 2008), azimuthal rotation and tilt angles averaged over the 3 simulations). For the angles, the values in parentheses represent the standard deviation. Azimuthal rotation and Tilt assesed as specified in methods section. In both cases the value in parentheses represent the fluctuations.

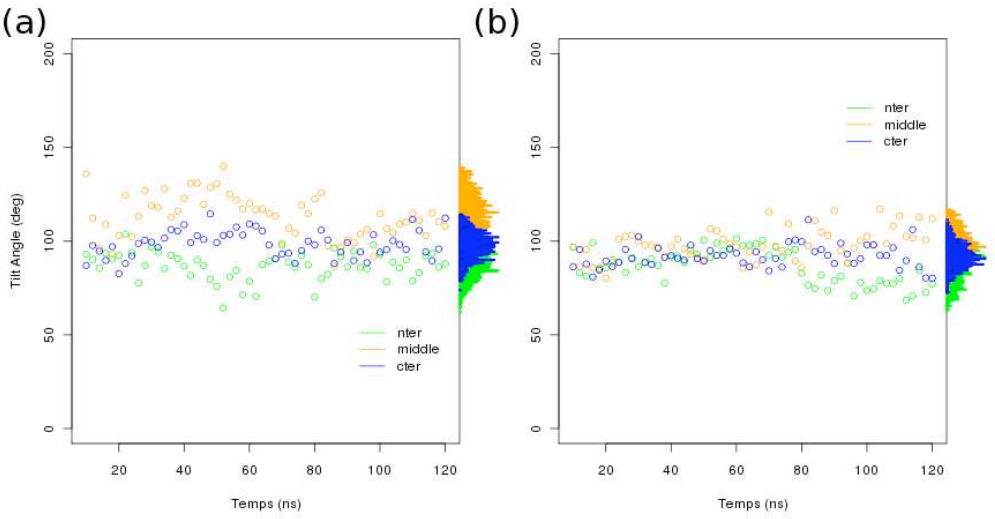

Figure 6.5: Tilt of ALPS (a) and LWF-A (b) segments as a funtion of time

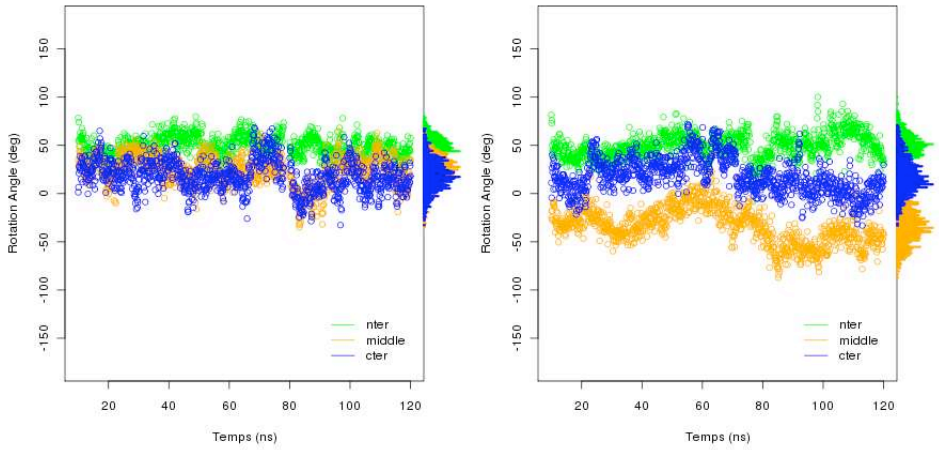

Figure 6.6: Azimuthal rotation of ALPS (a) and LWF-A (b) segments as a function of time

the membrane plane (90°), whereas in the middle segment the tilt changes more pronouncedly (Fig.6.5 (a)). In the case of LWF-A, the three segments remain parallel to the membrane plane (Fig.6.5 (b)). Manifestly, conformational changes for both peptides take place principally in the XY plane.

Concerning the azimuthal rotation, the fluctuations of this rotation are lower for ALPS compared to LWF-A. Moreover, the comparison between ALPS and LWF-A segments indicates that ALPS does not display a significant rotational variation, contrary to LWF-A (Fig.6.6). This can be explained by the change on the hydrophobic moment in LWF-A with respect to ALPS (Table 6.1). Additionally, the lack of bulky hydrophobic residues in LWF-A makes its backbone less sensitive to rotation. In contrast, the bulky hydrophobic residues in ALPS forces the backbone to adapt, anchoring the peptide to the membrane.

We also qualitatively evaluated the peptide diffusion as the trajectory in the plane XY of the center of mass of the peptide. This showed that, in turn, the peptides display different diffusion inside their respective membranes (Fig.6.7), the mutant being the one that diffuses the most of both peptides in DOPC.

6.4 ALPS and LWF-A partitioning inside the membrane

We showed that the mutations of LWF-A impairs the structural deformability of the peptide and modify its orientation with respect to the membrane related with the hydrophobicity and hydrophobic moment changes (Table 6.1). These changes have several implications on the partitioning of the peptide inside the membrane (see section 2.5 as reference). We evaluated this effect using the average density profile of the different segments of ALPS and LWF-A.

The prevailing structures of ALPS-DOPC and LWF-A-DOPC systems illustrate that the partitioning

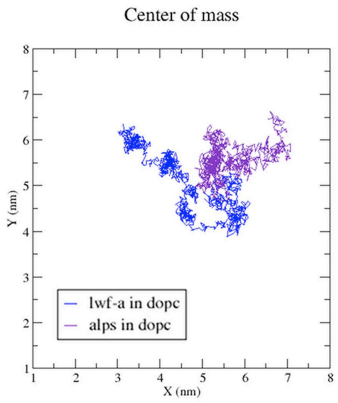

Figure 6.7: ALPS and LWF-A diffusion in the XY plane of the membrane

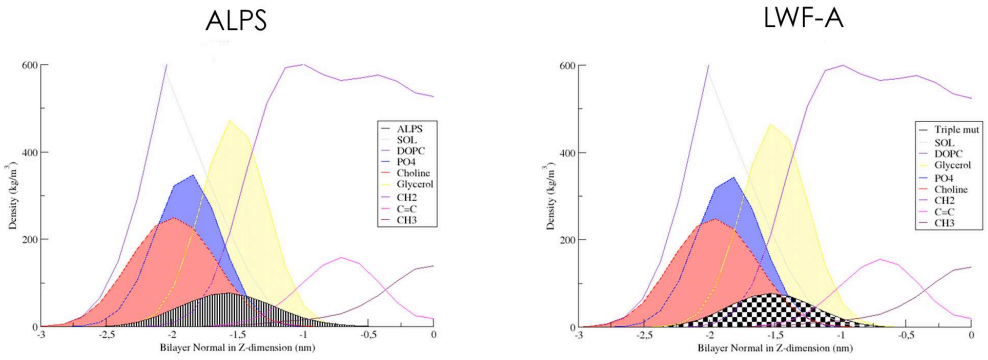

Figure 6.8: Partitioning of ALPS (left) and LWF-A (right) amphipathic helices at the level of the phosphate(bleu)/glycerol(yellow)groups. The water (grey) reach the limits of the interface at the bilayer interior. The acyl chains (purple) can be in contact with the peptides.

takes place at the level of the phosphate/glycerol region between the polar headgroups and the acyl chains, during the entire simulations, as we mentioned before (Fig.6.8). The partitioning of ALPS and LWF-A seems globally the same when it is calculated over the entire peptide. However we can see that LWF-A has a slightly more deeper partitioning (the center of the Gaussian that represents the peptide density at the level of the glycerol has shifted towards the center of the bilayer; Fig. 6.8 (right)).

If we make a zoom in this partitioning, taking for instance the density profiles of each helix segment in ALPS, we observe a slightly shift with respect to each other segment (Fig.6.9). That is, the helix as a whole does not have the same partitioning: while the middle and C-terminal segments colocalize, the N-terminal segment is shifted towards the phosphates. In contrast, in LWF-A the three segments conserve the same partitioning position (the center of their Gaussians colocalize) (Fig. 6.9 (b)). The differential partitioning of ALPS is favored by Gly15 and Gly22 hinges (see previous sections), and

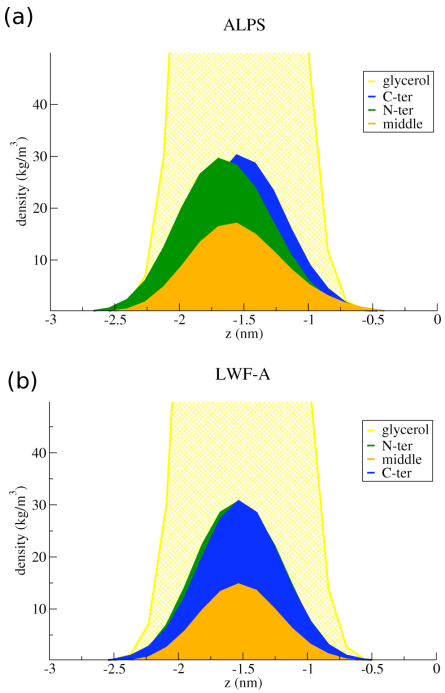

Figure 6.9: Partitioning of each peptide segment separately in (a) ALPS-bound system and (b) LWF-A-bound system.

principally by the higher tilt fluctuations of its middle segment, which pull the adjacent segments with it. This is the result of the concomitant effect of ALPS N-terminal and middle segments tilt and secondary structure variations.

When we compared the Gaussian distribution of each segment density profile of ALPS against their respective segments in LWF-A, we realized that the mutated segments, N-terminal and middle segment, are more compacted in LWF-A than in ALPS. The green and yellow areas in the plots in Figure 6.9, show the distribution of the density of this segments respectively. This result is in agreement with conformational changes that are more significant in ALPS than in LWF-A. In the C-terminal which is the non mutated segment, the size of the Gaussian density is the same for both peptides (the blue areas in the plots correspond to the density profiles).

A second zoom-in, now to the residues on each segment, allowed us to infer some important features (Fig.6.10). We sought to analyze the residues partitioning in order to correlate this parameter with their contribution to the global conformational changes. We observed that between ALPS and LWF-A, several interesting differences appeared regarding the amin oacids, in the N-terminal and the middle segments. The smaller areas in different colors on each plot (Fig.6.10), represent the density profile for each type of amino acid. In ALPS N-terminal segment (Fig.6.10 (a and b)), we observed an evident segregation in the Z-dimension between the polar and hydrophobic residues. The partitioning of the conserved Serines, Asn6, Leu5, residues in the two sequences is almost unchanged. However a small

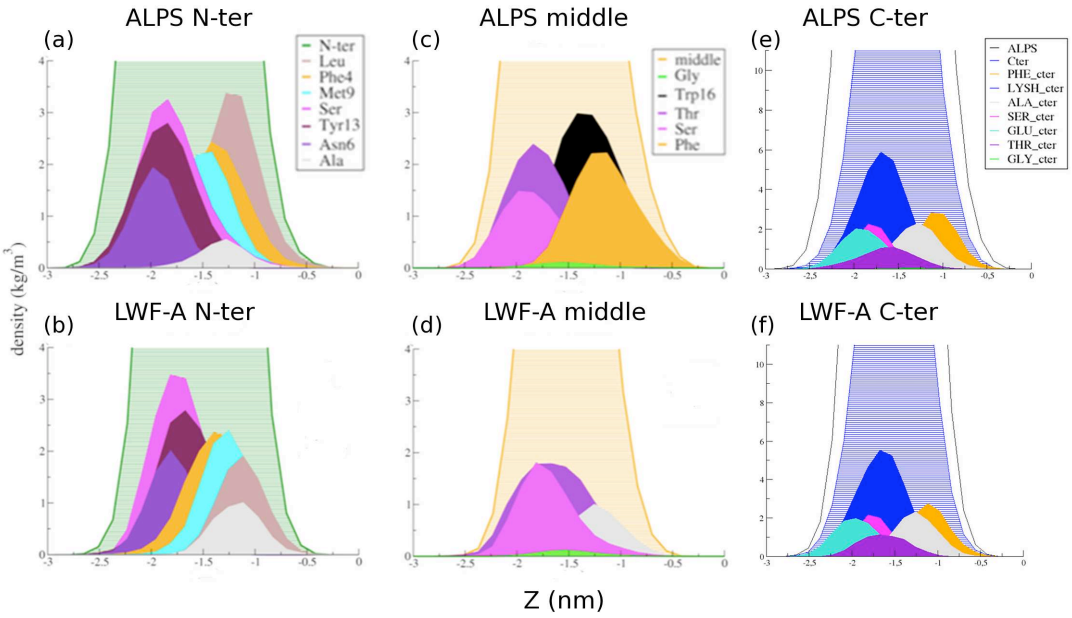

Figure 6.10: Density plots of zoom view of ALPS (upper panels) and LWF-A (lower panels) different residues partitioning. N-terminal segment (green), middle segment (orange) and C-terminal segment (blue) partitioning with respect to the glycerol position (yellow area). Each residue color follows the color code use in other figures.

shift is detected on LWF-A towards the hydrophobic core (Fig.6.10 (b)). These results illustrate the long-range effect of the mutations. In ALPS, Tyr13 (darkred) or Met9 (cyan) are mainly in contact with acyl chains, and in LWF-A, they have shifted about 2.5 Å towards the center of the bilayer (Fig.6.10 (a and b)). These results are correlated with the orientation of the side-chains and the lipid-peptide and intra-peptide interactions as I will discuss in the sections 6.5and 6.6. In the middle segment of LWF-A, the partitioning of conserved serines and threonines has also shifted towards the bilayer center (Fig.6.10 (d)). Regarding the non-mutated C-terminal segment, LWF-A and ALPS have the same partitioning behavior and we can therefore exclude any outside influence from the other segments (Fig.6.10 (e and f)).

The partitioning observed in our simulations is in agreement with the calculations of the free energy transfer from solvent to membrane medium (MacCallum, Tieleman, 2008) (see Fig.2.6) of section 2.2.2). The residues with very favorable energies for an interfacial partitioning (Leu, Met, Leu, Tyr, Trp, Phe) flank the serines and threonines (not very prone to be at the interface) and make possible their partitioning at the interface. The Ala present in LWF-A have more favorable free energies of partitioning at the center of the bilayer than at the interface. This could explain why we observe the shift of almost all residues of the N-terminal and middle segments in LWF-A towards the hydrophobic core.

6.5 Lipid-peptide interactions

In order to obtain detailed structural information about the lipid-peptide association at the membrane interface, we performed an analysis of the radial distribution function (RDF) of the peptide-bound systems. We explored the arrangement of the lipids around the peptide by calculating their repartition at different distances of key atoms of specific ALPS residues (Fig.6.11). For clarity purposes only chosen RDF plots of relevant pairs of atoms are shown and discussed in the next paragraphs.

We first analyzed the representative small polar residues in ALPS (conserved in LWF-A) (Fig. 6.11 (a-c)). The narrow peaks located at 0.25 nm for the serine and threonine residues indicate that they are involved in H-bond formation with the glycerol and phosphate oxygens. The RDF plot of Fig. 5a indicates that Thr21 can interact with the phosphate oxygens, whereas Thr20 interacts with the glycerol oxygens (Fig. 6.11 (b). In the case of the serines, they can concurrently interact with both phosphate and glycerol oxygens (Fig. 6.11 (c)). In all cases, a second peak (major some times) appears at 0.5 nm showing no direct and specific interaction but the extent of the peptide influence on the lipids. Both kinds of residues do not display significant interactions with the solvent. It is important to underline that the lipid organization around the small polar residues is different from that of charged residues, which are more prone to interact with the solvent, even if they can also establish polar interactions with different polar moieties of the lipids. Thus, the abundance of serine/threonine residues in ALPS assures the occurrence of H-bonds between the peptide and the crowded membrane interface.

Considering the hydrophobic face, the different curves observed in Fig.6.11 (d) describe the arrangement that the acyl chains maintain with the hydrophobic residues. The major peaks located at

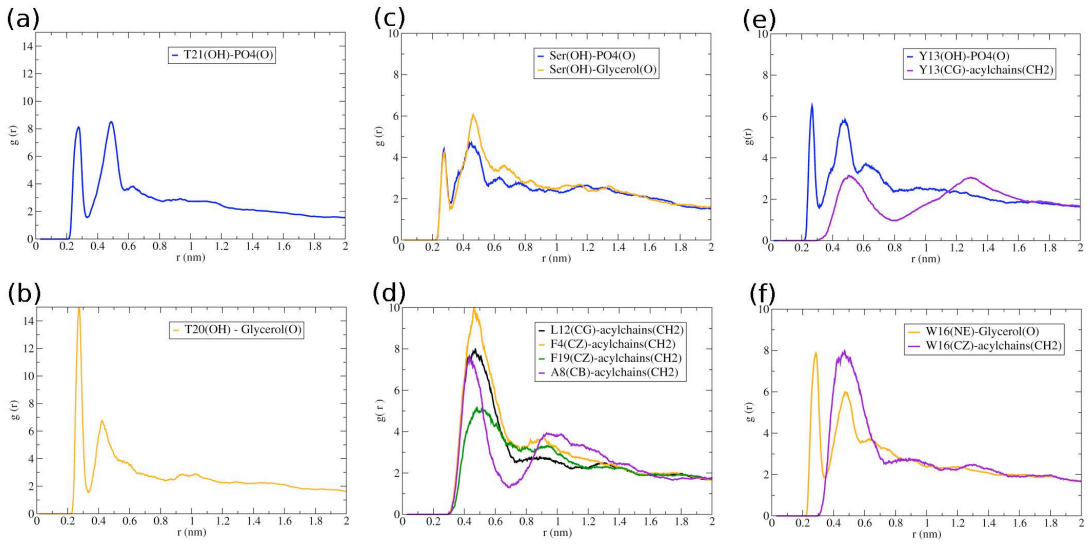

Figure 6.11: Radial distribution function plots between characteristic atoms from representative residues in ALPS and atoms from the different lipid moieties (PO4(O) (blue), Glycerol(O) (yellow), acyl chains(CH2) (purple). (a) T21(OH)-Glycerol(O) RDF plot. (b) T20(OH)- PO4(O) RDF plot. (c) serines(OH)-PO4(O) and serines(OH)-Glycerol(O) RDF plots. The first peak at 0.25 nm represents a first shell of interaction with the lipids, representative of H-bond interactions. The second peak at 0,5 nm represent long distance effects of peptide-lipid interactions. (d) RDF plots of representative atoms from hydrophobic residues and carbon atoms from the acyl chains; one can see two shells of interaction with the acyl chains (at 0.5 and 1 nm). All the curves present the same first peak although they have different g(r) value and some small shifts on the distances are evident. (e) Y13(OH)-PO4(O) (blue) and Y13(CG)- acylchains(CH2) (purple) RDF plots; Y13 establishes H-bond interactions with phosphates and hydrophobic interactions with the acyl chains. (f) W16(NH)-Glycerol(O) (yellow) and W16(CZ)-acylchains(CH2) RDF plots; W16 forms H-bond interactions with glycerol oxygens and establishes hydrophobic interactions with the acyl chains.

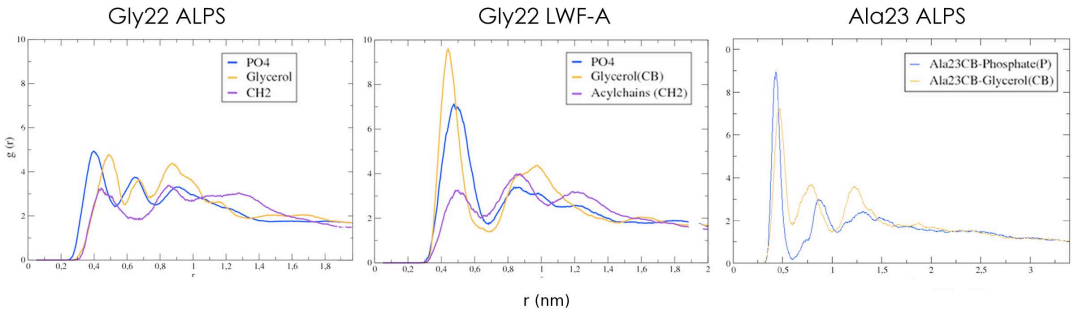

Figure 6.12: Radial distribution function plots between characteristic atoms from glycines (Cα) and alanines (Cβ) in ALPS and LWF-A and atoms from the different lipid moieties (PO4(O) (blue), Glycerol(Cβ) (yellow), acyl chains(CH2) (purple).

0.45-0.5 nm indicate a favorable distance for peptide-lipid (methylene) hydrophobic interactions. However, depending on the nature of the residue, i.e. aromatic or aliphatic, significant differences in curves width and height are observed. This illustrates a slightly different organization of the lipid acyl chains around these residues. The more evident effect is for Phe19 (in green) (in this position LWF-A has an alanine), compared to Phe4 (in yellow) (conserved between ALPS and LWF-A). Interestingly, the curve corresponding to the acyl chains distribution around alanine residues presents a first narrower peak and a second larger peak located approximately at 1 nm. The organization of acyl chains of lipids around alanines in ALPS is identical to that in the mutated positions of LWF-A.

Two aromatic residues in ALPS, Tyr13 and Trp16 have hydrophobic and polar properties, and are suitable for interfacial interactions. In Fig.6.11 (e) the first peak located at 0.25 nm shows that Tyr13-OH can form H-bonds preferentially with the lipid phosphate oxygens and Trp16-NH with the glycerol oxygens (Fig. 6.11(f), in yellow). The second peak observed in both cases is centered at 0.5 nm. These distributions of the polar headgroups are similar to what was observed for serines and threonines (see above). The violet curves in both panels correspond to the distribution of the aromatic rings with respect to the acyl chains. Both curves show the typical distance between an acyl chain and a hydrophobic group (i.e. 0.5 nm, see above). In LWF-A, H-bonds can be preferentially formed between Tyr13-OH group and glycerol oxygen and the first peak observed corresponding to the acyl chains around the aromatic ring increases. This is due to the preferential positioning of Tyr13 close to the glycerol.

From the RDF plots and from the visual inspection of the trajectory we were able to determine that the structural deformability of ALPS and the fluidity of the membrane make possible the interactions of ALPS residues with several lipid moieties and with more than one lipid. Consistently, the RDF of ALPS Gly22 shows a complex interaction with the surrounding lipids (Fig.6.12 (left))). The RDF distribution of the lipids around the Gly22-Cα showed more order than the RDF of lipids around other residues. This behavior is not observed in the Gly22 of LWF-A (Fig. 6.12 (center)). Moreover, in ALPS, the Gly22 (region of flexibility) promotes the contiguous Ala23 to take a partitioning that privileges the

interactions with the headgroups (Fig. 6.12 (right)). Phosphate(P) and Glycerol (Cβ) showed a first peak of preferential distribution around Ala23-Cβ at 0.4 nm and their curves display some degree of periodicity. In the contrary, in LWF-A Ala23 displays the partitioning of the other alanines that are rather embebed in the hydrophobic core (as in Fig.6.11(d)), and therefore display the usual hydrophobic interactions. Another example of the reciprocal influence of peptide deformation and membrane fluidity is the RDF of phosphate(P) and glycerol(Cβ) around Ser17-OH, residue in the center of the middle segment, for which the weigth of the peaks of these RDF is lower than for other serines.

To summarize, the RDF analysis indicates that all the lipid moieties are packed close to the peptide (0.25-0.6 nm). Sequence differences between ALPS and LWF-A impact the lipid organization around different key residues, notably aromatic residues. However, a long distance effect is also detected on lipid organization around serine/threonine and therefore on their H-bond formation with lipids. The Trp16A mutation in LWF-A abolishes the dual (H-bonds and hydrophobic) interfacial interactions that this residue is able to establish, but still maintain that of Tyr13. Furthermore, the conformational flexibility can influence changes of the lipid-peptide interations in the vicinity of certains aminoacids (i.e. glycines), as well as impact the order of the lipids (I will discuss this aspects in the next chapter).

6.6 Side chains flexibility and intra-peptide interactions

We observed that there exist an effect of conformers on side chain orientation. The backbone conformational changes are clearly a consequence of the peptide sequences. However, the membrane interface environment influences the way these changes take place. The sequence-dependence and the lipid-environment effect are strongly imbricated. I will consider first the sequence-dependence effect, mainly governed by the peptide side chains, and subsequently I will introduce the lipid-environment effect that will be developed in the next chapter. I will begin by discussing the role of side chains on the peptide conformation stability, and then I will consider their relative orientation with respect to the membrane interface.

ALPS conformational changes and its partitioning showed an adaptation of each segment of the Z-shaped structure to the membrane interface. The change on partitioning of different amino-acids in LWF-A suggested that this latter also tries to display the more adaptable orientation inside the membrane. Therefore, we analyzed in more detail the role of side chains on the peptide conformation (Fig.6.13). illustrates some representative orientations of ALPS hydrophobic and aromatic residues located in the proximity of (the mutated residue Leu12 and Tyr13) or within the middle region (the residues Trp16, Phe19, the two other mutated positions). In the starting conformer (Fig. 6.13(a)), the aromatic side chains of Trp16 and Phe19 are in a parallel orientation but rather distant from each other and in phase with Leu12, while Tyr13 is perpendicular to the position of these hydrophobic residues mentioned. In Fig. 6.13(b), Trp16 and Phe19 get closer in a more favorable parallel stacking interaction, while Tyr13 side chain approaches the helical axis. Moreover, thanks to the glycine hinges, the middle region rotates as a rigid body with respect to the N-terminal and C-terminal flanking segments. This orientation corresponds to the Z-shaped bended-helix (see left snapshot of Fig. 6.13(b))

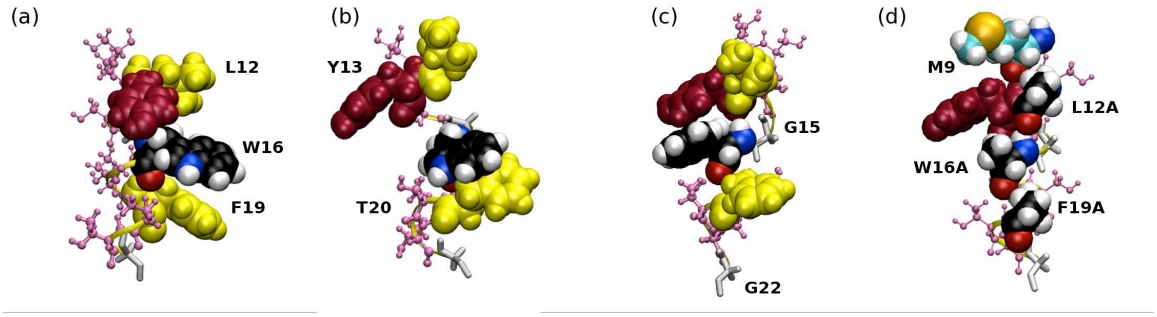

Figure 6.13: Structural transition in ALPS and LWF-A middle region. (a) Snapshot of the initial configuration of ALPS in a perfect a—helix structure, where L12(yellow up), W16(black), F19 (yellow down) are pointing to the hydrophobic core and Y13 (dark-red) lies at the interface. (b) Snapshot of an extended configuration of ALPS obtained by the stacking between W16 and F19. (c) Snapshot of a compact form of ALPS produced by the stacking between Y13- W16 and the hydrophobic interaction between the T20 methyl group (in pink) and the W16 indole ring. (d) Snapshot of LWF-A illustrating the interaction of Y13 and M9 in the absence of L12 and W16. L12A, W16A and F19A mutations are shown in black. In all the snapshots the hinges G15 and G22 that favor the transition between compact and extended configurations are shown in a gray licorice representation. All the serines and theorines of the region are in a pink CPK representation.

but some alternative orientations exist where Trp16 switches to privilege a favorable offset-parallel stacking interaction with Tyr13 (Fig. 6.13(c)) (see left snapshot of Fig. 6.13(b)). In this last case, Leu12 tends to be in phase with and gets closer to Phe19. In the case of LWF-A conformers, in the absence of Trp16 and Phe19, Tyr13 adopts a conformation perpendicular to the helical axis that in absence of Leu12 allows a favorable interaction with Met9 (Fig. 6.13(d)).

In summary, aromatic side chains display many stabilizing interactions, such as parallel or T-stacking, that are modified or lacking in LWF-A. However, some other intra-peptide interactions that stabilize ALPS and LWF-A conformers take place, such as those involving Ser/Thr residues.

The middle segment sequence-composition and hence the interactions we just described in ALPS lead to the transition between a compact and a more extended structure: many aromatic side chain orientations occur that may contribute to both kind of structures. In the case of the compact structure (Fig.6.14), it is possible thanks to:

- the hydrophobic interaction between the aromatic ring of Tyr13 with the Thr20 methyl group that have several serines between them (Fig. 6.14(a)) and by the parallel stacking or T-stacking interactions of Phe19 with Trp16 (Fig. 6.14(b)).

- or by the offset-parallel interaction of Tyr13 and Trp16 at the same time that Leu12 get closer to Phe19 (Fig. 6.14(b)) when the latter benzene ring is pointing to the center of the bilayer in almost perpendicular position with respect to the membrane plane (as I will explain in the next section).

In turn, the extended structure is possible thanks to:

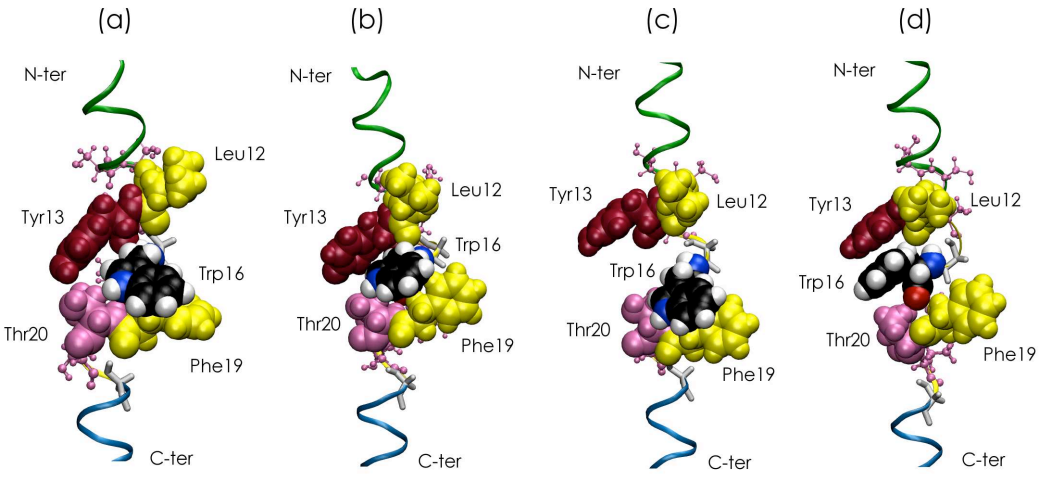

Figure 6.14: Compacted (a and b) and extended (c and d) conformations and intra-peptide interactions in ALPS. (same color code as in the precedent figure and Leu (yellow). The N-ter segment (green) and C-ter (bleu) are represented in ribbons for reference).

- the offset-parallel stacking of Trp16 and Phe19 with Tyr13 pointing to the solvent (Fig. 6.14(c)) and getting closer to Ser17 (residue not visible in this orientation of the snapshot).
- or only the offset-parallel stacking of Trp16 and Phe19
- when all these aromatic residues are completely out of phase from each other and Trp16 interacts with Thr20 (Fig.6.14(d)).

As I mentioned before, the absence of Trp16 and Phe19 in LWF-A impedes the formation of these transitive structures. Besides Tyr13 and Met9 interaction, in LWF-A C-terminal segment, the Lys25 can establish H-bonds with the threonines of the middle segment capping the small residues between them or can form a parallel stacking with its long aliphatic chain with the benzene ring of Phe26. This interaction contributes to the first curved conformer of LWF-A.

6.7 Aromatic residues side-chain orientations with respect to the membrane

The last analysis about the intrapeptide interactions prompted us to study in a greater detail the dynamic and flexibility of the aromatic side-chains. We evaluated the preferential orientation of all the aromatic residues present in ALPS and LWF-A sequence. Briefly, this was defined as the angle formed between the normal of the aromatic ring and the normal to the membrane (see section 5.7.3). We focused on the middle region discussed above. The distribution described in Fig.6.15 shows that Phe19

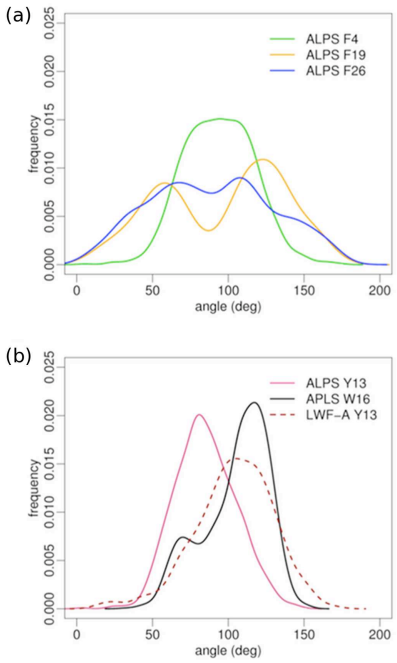

Figure 6.15: Orientations of aromatic residues. (a) Schematics showing the vector we defined to assess the orientation of the aromatic ring with respect to the normal of the membrane. If the vector is parallel to the normal of the membrane (represented by two black lines) the orientation of the ring is of 0º, if its perpendicular its orientation is of 90º. (b) Phenylalanines present in ALPS sequence with the color code of the segment that harbors them; F4 (green), F19 (yellow) and F25 (blue). (c) Other aromatic residues in ALPS: W16 (black) and Y13 (red). The Y13 of LWF-A (red dashed line) is shown for comparison.

(yellow line) can adopt two distinct orientations (120° and 60°). In the first one, the aromatic ring is perpendicular to the membrane plane facing towards the hydrophobic core whereas in the second one, the ring gets closer to the membrane interface. Trp16 has mostly a preferred orientation (120°), parallel to the first Phe19 orientation. In this orientation, the rings are in a parallel/offset-parallel stacking interaction whereas in the 60° orientation, the rings are in T-stacking. To a less extent Trp16 (75°) (Fig.6.15) orients the aromatic ring closer to the membrane interface, for interacting with Tyr13 (Fig. 6.14(d)). In turn, Tyr13 preferential orientation is 90° with the aromatic plane perpendicular to the membrane plane but pointing towards the solvent (Fig.6.14(c)). Interestingly, in LWF-A Tyr13 prefers the orientation that in ALPS is adopted by Trp16 (Fig.6.15dotted darkred line).

Then, we compared these orientations with the other segments in ALPS. Each phenyalanine residue has a different preferential orientation according to their peptide location and the neighboring residues. It is possible that the orientations of Phe4 and Phe26 (Fig.6.15(gree and blue respectively) are the result of the loss of helicity in those regions (see section 6.2.1) in both peptides. In LWF-A, its higher azimuthal rotation significantly contributes to this wider range of orientations of these phenylalanines.

In summary, the flexibility of the aromatic rings is restricted or favored by the sequence context. For instance, Gly15 breaks the helix and in consequence Tyr13 and Trp16 adopt orientations that favor their mutual interactions. Gly 22 breaks the helix further and in consequence Phe19 adopts an orientation that makes it interact with Trp16 and Thr20 gets closer to Tyr13. We shall not forget, however, that these aromatic residues can also establish hydrophobic-hydrophobic interaction (and in some cases polar interactions) with the lipids that contributes to these panoply of orientations.

6.8 Synchronized Intra-peptide and lipid-peptide interactions determine ALPS deformability

The lipid-peptide interactions and intra-peptide interactions we described in the last sections occur at the same time and have an impact on each other. This means that a conformational transition can favor or avoid certain interactions between the peptide and the lipids. This also implies that the orientations of, for instance, the aromatic residues and the involvement of Ser/Thr residues in H-bonds with the phosphate/glycerol moeities of the lipids, play an important role in how this balance between intra-peptide and lipid-peptide interactions take place. Figure 6.16 illustrate some of these synchronized interactions. I consider important to discuss in the next chapter some of the effects the peptide can cause to the membrane. This chapter will give us the bases to further discuss the ensemble of the results regarding ALPS structure in the context of the lipidic environment.

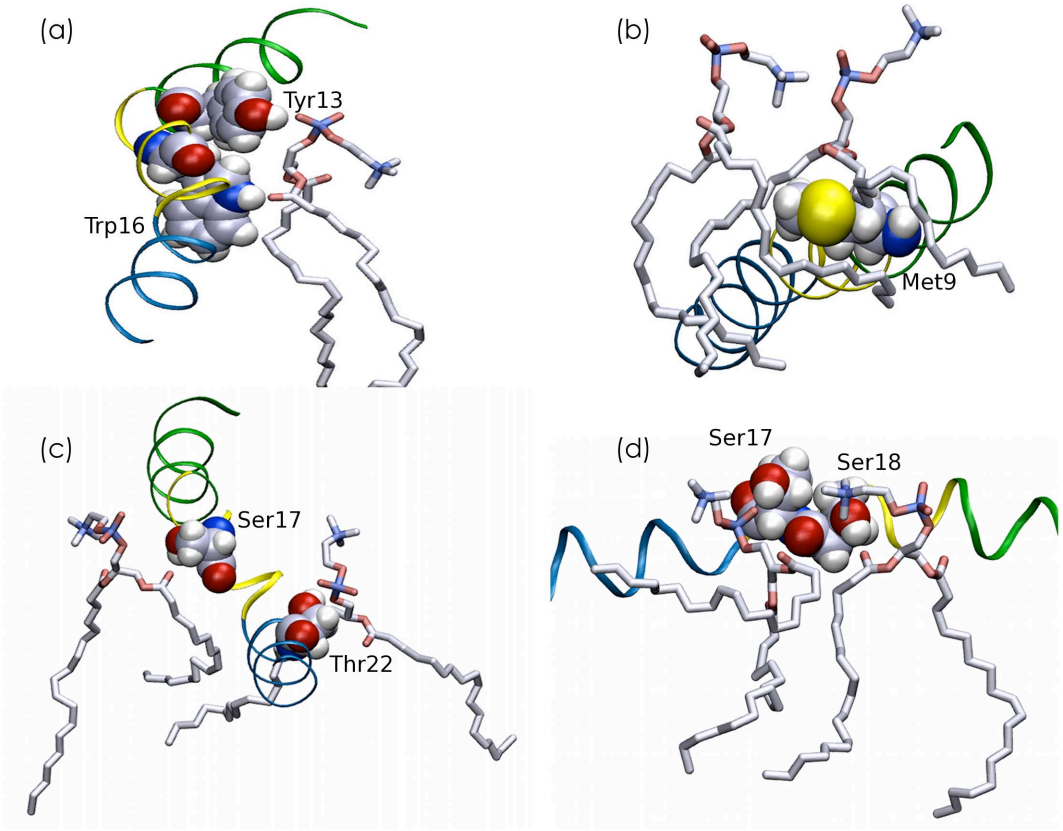

Figure 6.16: Synchronized intra-peptide and lipid-peptide interactions (a) offset-stacking between Tyr13 and Trp16 exhibiting their correspondent polar interactions with the phosphate and glycerol groups and hydrophobic interactioons with the oleoyl chains.(b) Met9 anchored between oleoyl chains. (c) Interactions of Ser17 and DOPC-glycerol and Thr22 and DOPC-phosphate and (d) between Ser18 and DOPC-choline as exemples of the interactions this residues can establish with the glycerol and phosphate groups.

Chapter 7

Membrane-peptide reciprocal adaptation

In the present section, I will focus on the membrane properties and main changes it undergoes due to the peptide presence. I will describe the effects that ALPS has on the global structure of the bilayer and the lipid-lipid packing, followed by a description of the main changes in the principal properties of the bilayer: order parameter, lipid diffusion and bilayer thickness. I will explain these results in the context of membrane fluidity and plasticity (i.e local membrane deformations).

7.1 Lipid-lipid interactions

In order to obtain detailed structural information about the lipid-lipid associations in the presence of the peptide at the membrane interface, we analyzed the RDF of the peptide-free systems. The impact of the peptide on lipid-lipid interactions was evaluated by comparing the lipid-lipid RDF of both with and without the peptide (Fig.7.1). We observed that the main effect of the peptide is to increase the probability of short-range interactions. The packing of lipids in the peptide surroundings is manifestly increased compared to the bulk lipids. Moreover, the RDF analysis of lipid-lipid interactions and of lipid-peptide interactions in section 6.5, indicates that all the lipid moieties are packed closer to the peptide (0.25-0.6 nm) than between the lipids themselves (0.5-0.8 nm) (Fig.7.4 (a and b)).

7.2 Lipids diffusion

We decided to examine how the increase of lipid packing affected the fluidity of the lipids. As a qualitative measure we assessed the MSD (Fig.7.2) which gives some insights about the dynamics of the bilayer at long timescale and long-range level. These data reveals that the diffusion of lipids in the bound-leaflet diminishes in the presence of both interfacial peptides with respect of the non-bound

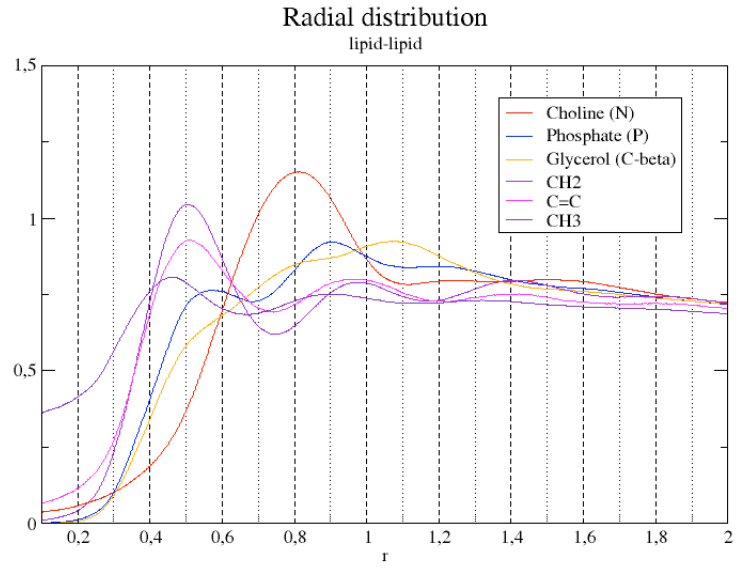

Figure 7.1: Radial distribution function plot of characteristic atoms of different lipid-moieties between them. Represents DOPC packing

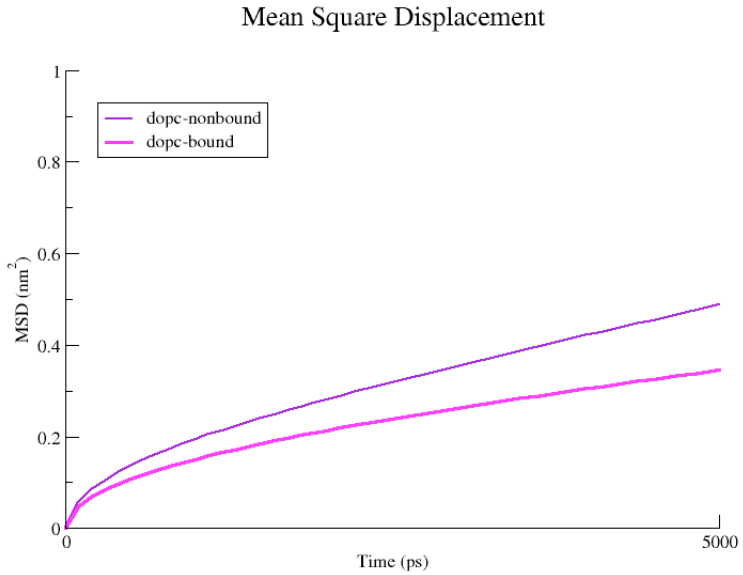

Figure 7.2: Mean square displacement of DOPC in the presence of ALPS

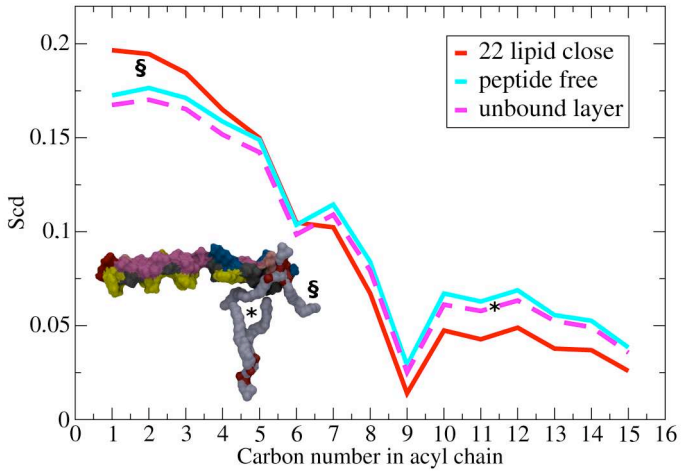

Figure 7.3: Order parameter averaged over all ALPS trajectories. The three curves correspond to associated lipids (red line; lipids that are closer than 1 nm from the peptide in the same leaflet), lipids from the non-bound leaflet (magenta dashed line) and lipids from a peptide-free system (cyan). The variation of order parameter of each group is represented as a function of the carbon position, with C15 corresponding to the methyl end group. The snapshot illustrates one of the possible configurations that cause the observed effect in lipids order. The symbols guide the reader to the appropriate region where this occurs: §proximities of the polar heads, *center of the hydrophobic core.

leaflet and the peptide-free system. This means that the presence of the peptide limits the diffusion of the lipids in both leaflets of the bilayer.

7.3 Order parameter

The peptide-lipid adaptation process largely depends on the dynamics and orientation of the hydrocarbon chains, which can be assessed by calculating the order parameter (see section 5.7.1.2). This parameter is related to the average orientation of each acyl C-C bond with respect to the normal to the membrane plane. The variation of order parameter for each group is represented as a function of the carbons position, with C15 corresponding to the methyl end group (Fig.7.3). High values reflect an ordered system whereas values close to 0 are representative of a disordered system (see section 5.7.1.2). We compared the order parameter of three groups of lipids: the associated lipids (lipids closer than 10A to the peptide in the monolayer that contains the peptide), the non-associated lipids (lipids far from the peptide in the same monolayer), and the non-bound monolayer lipids. Then we compared these three groups with the peptide-free system (Fig.7.3).

As expected, in the peptide-free system, the order parameter of the lipids of both leaflets is the same. The curve that describes both the order parameter of the DOPC peptide-free bilayer corresponds to the values observed experimentally and in other simulations (represented in cyan in Fig.7.3).

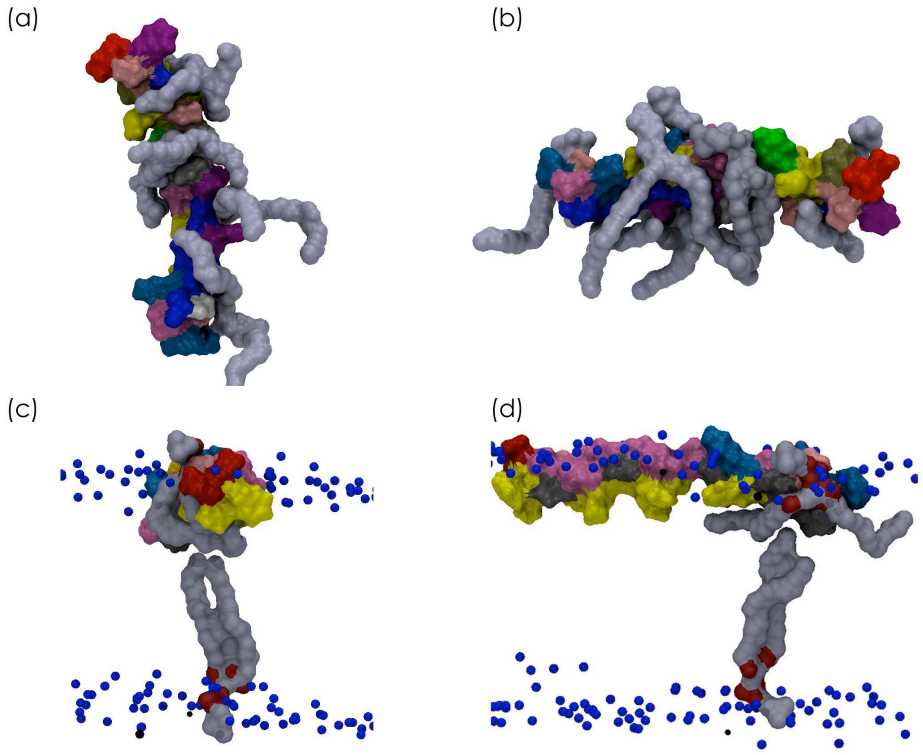

Figure 7.4: Snapshots of DOPC oleoyl chaisn conformations around the peptide (a) and (b) show the knob-ito holes arrangement between the bulky hydrophobic residues of ALPS and the oleoyl chains. (c) and (d) Show the bend around the peptide of the oleoyl chains of the associated lipids and the partial-transversal diffusion (and or extension) of the oleoyl chains from the non-bound layer to fill the spaces leaf by the bended oleoyl chains just above.

In the case of the ALPS-DOPC system, in the monolayer that contains the peptide, the associated-lipids show a significant increase of order near the interfacial region compared to the peptide-free system. This observation is directly related to the changes in the lipid-lipid interactions, which increase in this region. These changes are related to the increase in packing induced by the peptide. In contrast, the order parameter near the methyl group decreases because of the excess of volume generated by the presence of the peptide just above. This behavior creates some space at the center of the hydrophobic core, which produces the disorder near the methyl group (in the center of the bilayer). Other contributions for the high order near the interfacial region come from some methyl groups that can approach the region near the interface when the acyl chains bends to fill the spaces below the peptide (Fig.7.4 (c and d)). The order parameter of the non-associated-lipids (Fig.7.3), even if it is very close to that of the peptide-free system, shows that they have a tendency to become more ordered near the methyl groups. It may be because the disorder created at this region in the proximities of the peptide push the distal lipids to get more packed between them as a result of the lateral pressure

induced by the changes in lipid packing and lipid order.

Compared to the peptide-free bilayer, the order of the leaflet that does not contain the peptide (non-bound monolayer), decreases all along the acyl chain (Fig.7.3 (dotted line)). However, if we compare these results with those of the bound-monolayer, we observe that the non-bound monolayer shows the opposite behavior: a higher order is observed near the methyl groups (in the center of the bilayer), while the order near the headgroups is smaller (Fig.7.3 (red)). One possible explanation is that the spaces left by the new conformations adopted by the acylchains around the peptides, are filled by the extension of the acyl chains from the non-bounded layer lipids (increasing the order of their acylchains distal regions (see inset in Fig.7.3 and Fig. 7.4(c and d)). At the same time, this displacement toward the opposite monolayer produces an immersion of the headgroup into the hydrophobic core (a semi-transversal diffusion as described in section 2.1.4). The immersion generates a space at the polar head region that would increase the disorder in the non-bounded layer. This process can lead to a thinning effect of the bilayer in the proximities of the peptide (as we will see in the next section). Globally, the behavior observed on the order parameter of the bound and unbound-monolayer is correlated with the bilayer-coupling effect described in section 3.4.2 (see Fig.3.3(d)), which is a natural response of the membrane to the interfacial insertion of an amphipathic helix. A similar behavior for both leaflets is also observed in the LWF-A-bound system.

7.4 Bilayer thickness in the presence of the peptides

In the peptide-DOPC system, when we evaluated the bilayer thickness in the proximity of the peptides there is a difference with respect to the lipids non-associated to the peptide; the portion of the bilayer near the peptide shows a reduction of its thickness. More importantly, the fluctuations of the bilayer thickness are larger near the peptide than in those portions of the membrane that are not in direct contact with the peptide (Fig.7.5). This means that some invaginations are produced as a consequence of this thinning effect, which is more pronounced as the peptide gets deeper inside the bilayer (Fig.7.6). The opposite effect is observed when the peptide becomes more superficial. An explanation of this behavior can be that during the simulation the position of the peptide at the interface fluctuates (with the fluctuations of the membrane (the reason the strcuture of the bilayer is represented as Gaussian curves. See section 2.2.1). The middle segment of ALPS can tilt and shift the position of the other segments with respect to each other following the membrane fluctuations (Fig.7.7 (b)). Moreover since the bilayer thickness is correlated with the bending of the membranes, the thinning effect observed here, suggest a degree of curvature.

In summary, the peptide-lipid interactions that determine the structural behavior of ALPS depend on the partitioning, the bilayer fluidity and plasticity. We clearly observed an orchestrated peptide-lipid adaptation. The membrane dynamics reflects the wide range of conformations lipids adopt. As a consequence, instantaneous lipid packing is inhomogeneous (Fig. 7.7(a)). ALPS deformability allows it to adapt to these local "defects" in lipid packing at the membrane interface displaying H-bonds between its polar residues and the lipids polar moieties, while the hydrophobic residues display knobs-into-holes

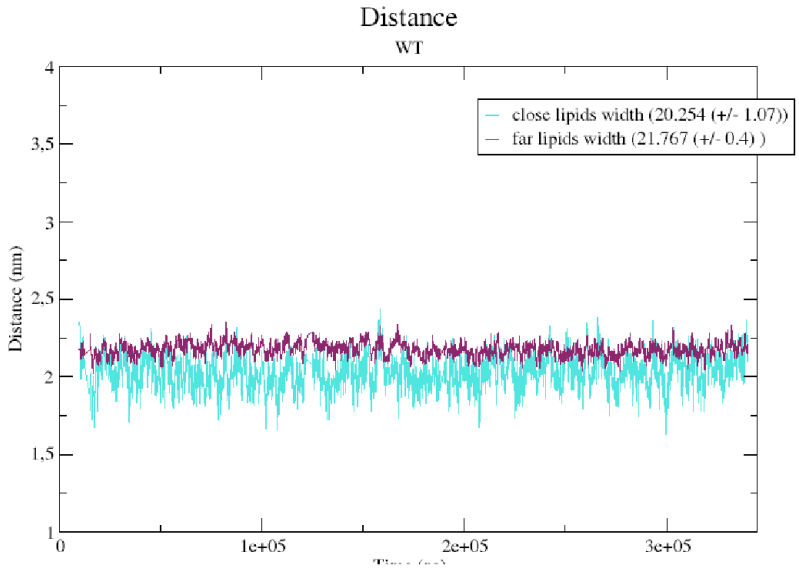

Figure 7.5: Bilayer thickness of surrounding lipids (close) and the rest of the bilayer (far lipids) as a function of time. Measured as the distance between the first acyl carbon from the oleoyl chains of both leaflets.

arrangements with the acyl chains (Fig. 7.4(a) and Fig.7.7(c)). In consequence, these interactions limit ALPS diffusion in the membrane. Reciprocally, the partitioning of ALPS in the interfacial region of the membrane influences the packing of the lipids: the membrane adapts to the presence of ALPS by modifying the lipid-lipid interactions and their dynamics. In this way, the conformational adaptability of the acyl chains allows the lipid shape to follow the peptide changes. Hence, the acyl chains can remain attached to the peptide a long time during the simulations, affecting the lipids diffusion (as we described in section 7.2).

From the analysis of the order parameter, which provides which lipids are associated as a function of time, we indeed detected that most of them stay in close contact with the peptide during long periods of time in the simulations. Unexpectedly, we saw that ALPS and LWF-A possess the same number of associated lipids during the simulations, which would mean that the restricted deformability of LWF-A caused by the mutations does not affect the number of peptide-lipid interactions. This result is correlated with the order parameter and the diffusion coefficient, which show the same tendencies in both peptides-bilayer systems.

I will now discuss the possible reason why these tendencies are similar in both peptide-DOPC systems and their effect in the peptide-lipid association. From the visual inspection of the peptide trajectory, we determined that in the case of ALPS, its lower diffusion can be explained due to the intricate adaptation between the peptide and the lipid conformations. The acyl chain conformations that lipids might adopt near the lipid hydrophobic face, can get blocked between the bulky hydrophobic residues

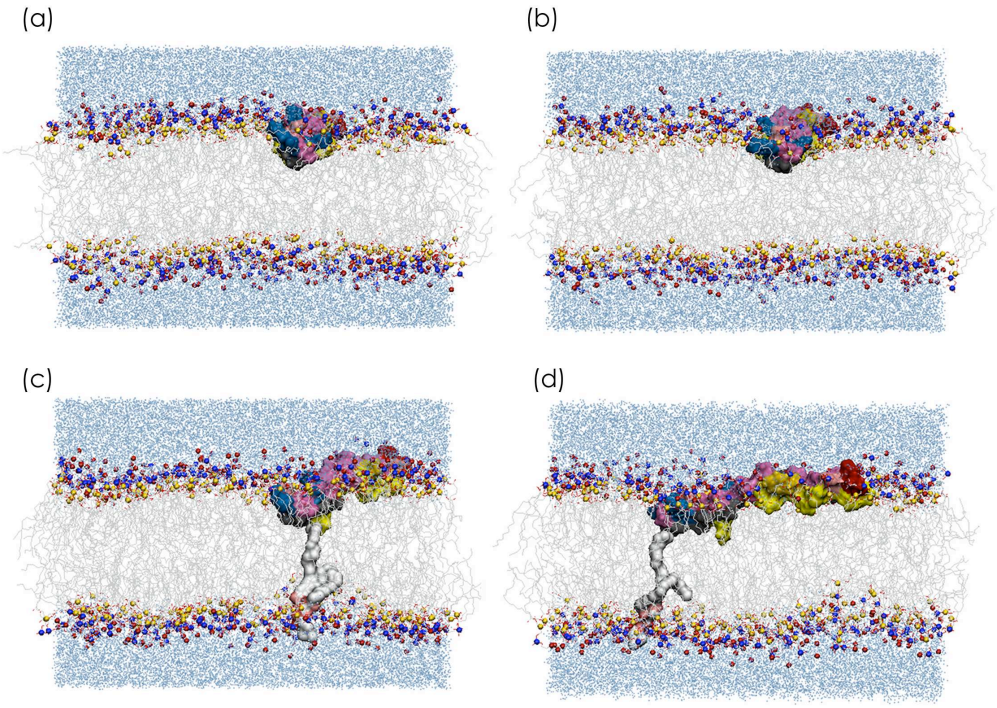

Figure 7.6: Snapshots of the invaginations consequence of the bilayer thickness variations in the vicinity of the pepetide.

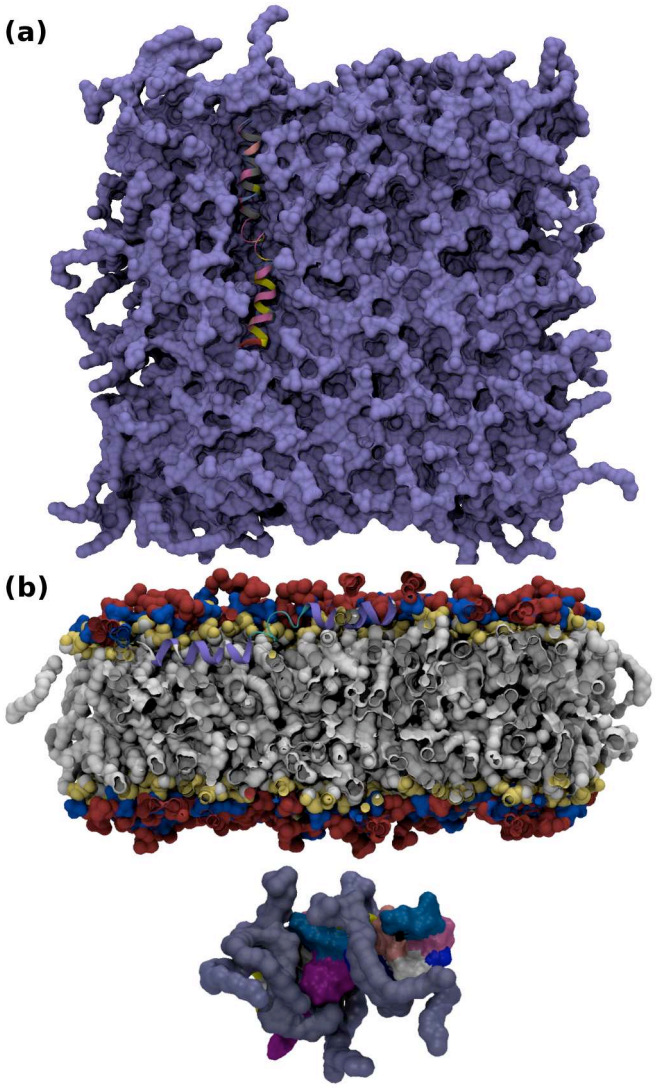

Figure 7.7: Reciprocal ALPS-membrane adaptation. (a) ALPS-bound system top view of the xy plane, showing the adaptation of ALPS (ribbons in same color code than before) to the roughness of the membrane. (b) Snapshot of the Z-bended conformation of ALPS at the membrane interface (middle segment in cyan and N-ter and C-ter segments in purple, acyl chains in gary, glycerol level represented by yellow spheres, phosphate in bleu and choline in red). (c) Examples of configurations adopted by the lipids (gray surface representation) in the proximity of ALPS (colored by residue name, with lysines in blue, phenylalanines in violet, glycine in white and serines in pink) that adapt by filling the spaces below it and favor the interactions between the polar residues and the glycerol moieties.

of ALPS in the knob-into-holes arrangement (described just above). We explained in section 7.3, how this interactions can induce a decrease in the order near the methy groups. The order parameters in the case of LWF-A have the same tendency but the inspection of the trajectory let us observe different conformations of the acyl chains compared to the system ALPS-DOPC. In the LWF-A-DOPC system acyl chains cannot display the knob-into-holes arrangement, and therefore these acyl chains can either tilt in order to interact with the hydrophobic Ala of the peptide or get packed against each other (i.e, the acyl chain of a flanking lipid in one side of the peptide with the acyl chain of a lipid flanking the opposite side) just beneath the peptide. These differences in conformations around the vicinity of the peptide decrease the order near the methyl group. Therefore, the transversal diffusion of some acyl chains from the non-bound layer is accentuated. Additionally, in both LWF-A-DOPC and ALPS-DOPC systems the lipids establish H-bond interactions with the peptide polar face. This implies that in both systems some lipids will remain longer period of time near the peptide.

The results obtained here show that ALPS and LWF-A adapt differently to the bilayer rough surface, displaying different orientations and conformations. This suggests that the lipid-packing recognition is an orchestrated process between the peptide and the membrane lipids with mutual effects that strongly depends on the peptide sequence-specific conformational deformability.

Chapter 8

Elucidating lipid-packing influence on ALPS structure

Our second main objective was to determine the influences of different lipids on ALPS structural properties. Hence, as I will develop in the present chapter, the comparison of ALPS in different lipid environments permitted us to unravel some of the effects that the lipid-packing exert in ALPS structure. We performed simulations using two bilayers with a non favorable lipid content and one more favorable than DOPC (according to the experimental data). I will present first the results obtained with those bilayers that experimentally avoid ALPS function (DMPC and POPC), and particularly I will focus on the effects of changing the acyl chain nature of the lipids. At the end of the chapter I will describe the simulations on the most favorable bilayer (DOPC-DOG), and I will concentrate on the effects produced by the introduction of lipids with smaller headgroups.

The description of these results is based on the same kind of analysis used for the results described in chapter 6 and I will do a constant comparison with those results all along the chapter.

8.1 ALPS in DMPC and POPC membranes: Role of the acyl chains nature

I performed simulations of ALPS embedded in a DMPC bilayer and POPC bilayer where only one acyl chain changes with respect to DOPC. We performed three replicas of 120ns of these systems. The analyses were performed on all the replicas and sometimes averaged over the concatenated trajectories of all three together. For clarity purposes I will present only some of the most representative figures and plots.

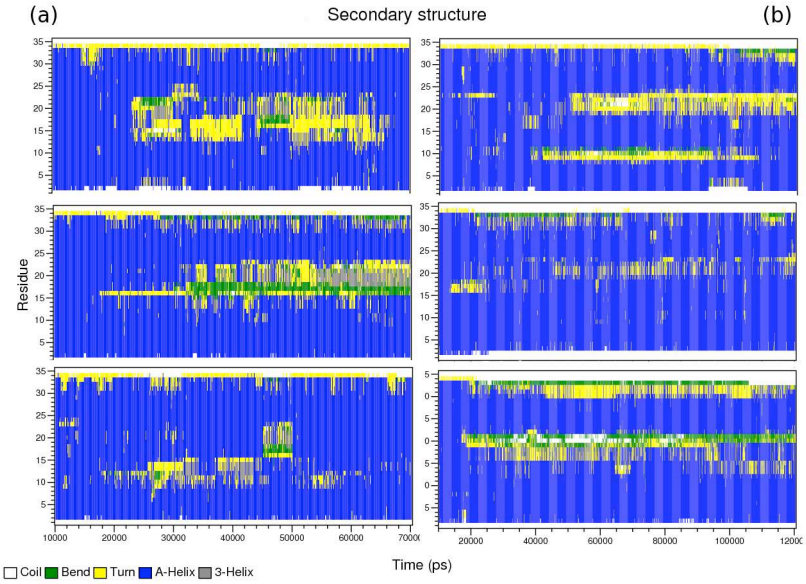

Figure 8.1: Secondary structure evolution in the three replicas from (a) ALPS in DMPC and (b) ALPS in POPC

8.1.1 ALPS secondary structure and deformability in DMPC and POPC

In order to understand how these new lipid contexts influence ALPS structural properties, we followed the evolution of ALPS secondary structure during the simulations (in the three different replicas) of ALPS-DMPC and ALPS-POPC systems (Fig.8.1). The discussion of the results is based on the averaged properties over all replicas.

In DMPC, ALPS structural transitions in the middle segment remind LWF-A in DOPC (see chapter 6). In the case of ALPS-POPC, the changes in secondary structure are significantly more limited, sometimes affecting other regions than the middle segment. In both systems, the main secondary changes take place in the regions of residues with lower propensities. In consequence the helicity content of ALPS in DMPC and POPC system is also very similar to ALPS and LWF-A helicity content in DOPC (Fig.8.2)

8.1.1.1 ALPS structure deformation and orientation

Afterwards, we decided to look at those conformations that ALPS could adopt during the secondary structure changes in these new lipid environments. In the case of ALPS-DMPC system, the clustering analysis provided two main populated conformers (96% of the conformations). The most populated cluster (75%) represents an almost unperturbed straight helix (Fig.8.3). The second conformer (21%) correspond to a slightly bended-helix conformation, that reminds us of the first curved helix conformer of LWF-A in DOPC.

In the case of ALPS-POPC system three main populated conformers were detected (88% of the

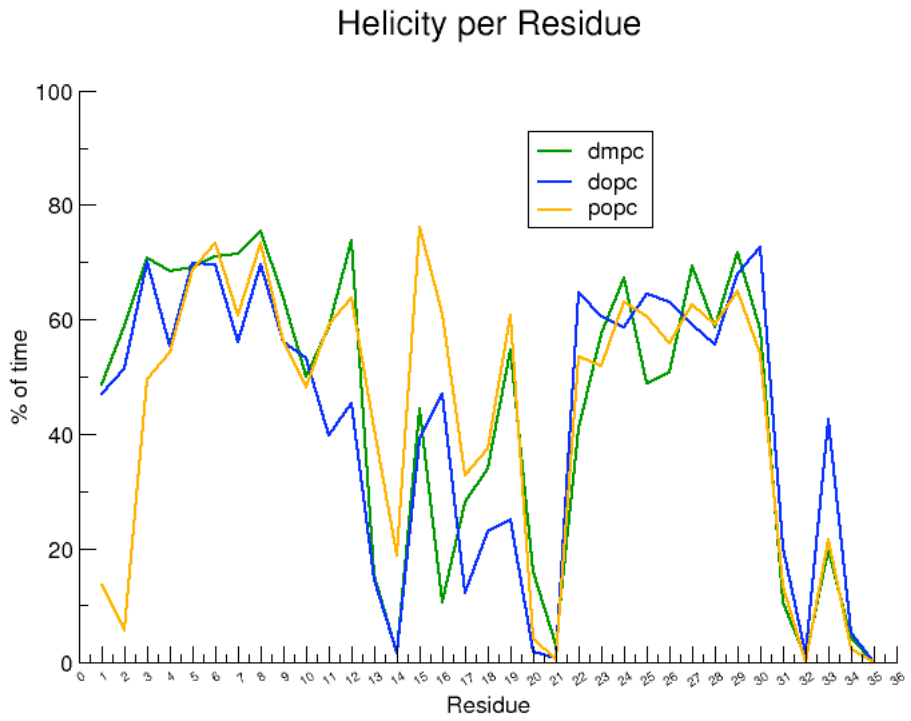

Figure 8.2: Helicity content of ALPS in DMPC and POPC bilayers compared to ALPS_DOPC system.

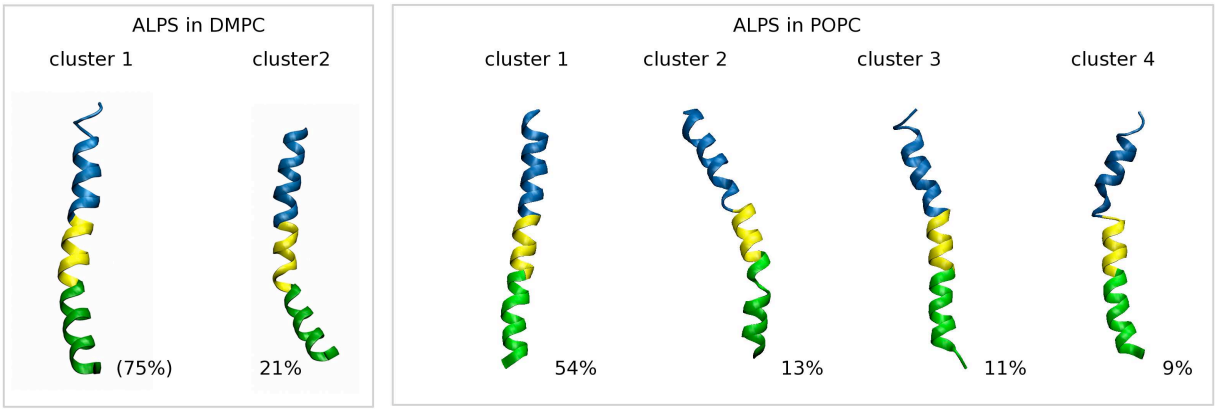

Figure 8.3: Clustering analysis of ALPS in DMPC and POPC bilayers.

conformations) (Fig.8.3). The first one (it covers 54% of the conformations) represents an almost unperturbed straight helix as ALPS in DMPC (Fig. 8.3). The second one and the third one, which cover 13% and 11% of the conformations respectively, represent a slightly curved helix (reminding LWF-A), in the thirth case we observe the amino and carboxyl extremities in coil and in the third case we see break points in Ser11 and Gly22). Finally, a fourth cluster (9% of the conformations) represents a structure that starts to resseamble the Z-bended structure of ALPS in DOPC.

Overall, these structural results showed that ALPS in DMPC bilayers is even less deformable than LWF-A mutant. In POPC ALPS is as deformable as LWF-A in DOPC but with less secondary structure transitions. Thence DMPC favors secondary structure transitions and POPC favors the deformability, but neither of these bilayer environments favor both at the same time. Interestingly, in neither of these bilayers ALPS middle segment tilts as it does in DOPC bilayer

8.1.2 Intra-peptide interactions and aromatic side-chains orientations with respect to the membrane

The analysis of the intra-peptide interactions showed that in ALPS-DMPC system, the most populated conformer of the peptide exhibits the residues, Tyr13, Trp16 and Phe19, completely out of phase and is unable to establish stacking interactions. However, in the second conformer, we observe an offset-parallel stacking between the Trp16 and Phe19. Moreover, Thr20 methyl group is in contact with the aromatic rings of Trp16 in the first conformer and with the Tyr13 in the second conformer.

In ALPS-POPC system, the aromatic residues are also out of phase in all the conformers and the Thr20 methyl group is in contact with the Trp16. These results are confirmed by the orientations the aromatic residues can take with respect to the membrane interface. This last analysis also showed that the phenylalanines can either have only one preferential orientation or display more flexibility, as in the cases of Phe4 and Phe26 from the N-terminal and C-terminal regions, respectively.

The results shown here confirm that ALPS in DMPC and POPC does not display the same intra-peptide interactions that are observed in ALPS-DOPC system, interactions that favor and at the same time are a consequence of the deformability of the peptide in the bilayer.

8.1.3 Interfacial partitioning and orientation of ALPS in DMPC and POPC

The partitioning of ALPS at the membrane interface is also maintained all along ALPS-DMPC and ALPS-POPC simulations. Comparing ALPS-DOPC system and ALPS-POPC system, the partitioning of ALPS seems the same. However, if we compare ALPS partitioning in DMPC we can see a shift from the Gaussian curve representing ALPS density, towards the hydrophobic core (Fig.8.4). That means that the Gaussian of ALPS and the Gaussian of the glycerol moiety do not colocalize. ALPS partitioning in DOPC and POPC bilayers is found between the phosphate and the glycerol, whereas in DMPC it is slightly shifted from the glycerol position towards the acyl chains. As we will see, this has major consequences.

When we made a zoom-in to individual partitioning of ALPS N-terminal, middle and C-terminal

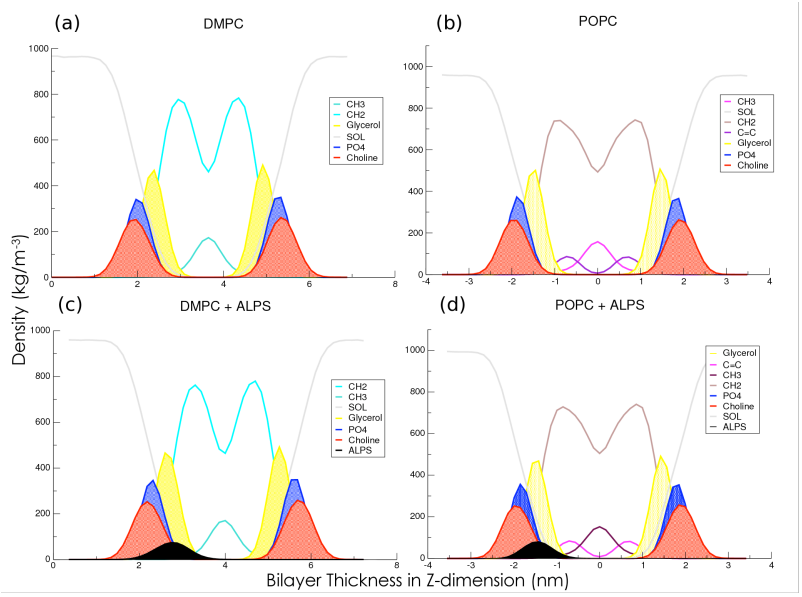

Figure 8.4: General partitioning

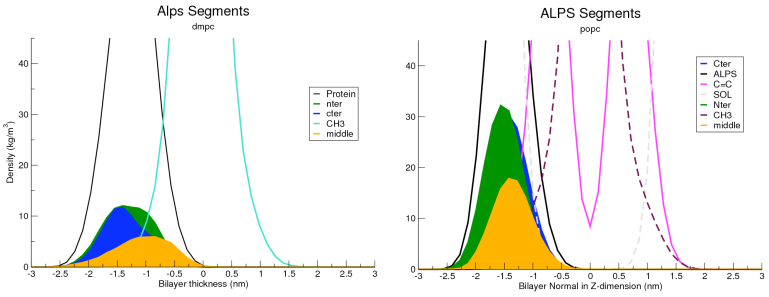

Figure 8.5: ALPS Segments in DMPC and POPC

segments (Fig.8.5), in both bilayers an important difference became evident: in DMPC ALPS segments densities are wider and smaller in height than in POPC. This observation is congruent with the more numerous secondary structure transitions of ALPS in DMPC than in POPC. Furthermore, in DMPC the N-terminal and C-terminal Gaussians curves almost colocalize with each other (C-terminal is slightly biased towards the phosphates), whereas the middle segment shifts towards the center of the bilayer entering in contact with the last methyl group of the myristoyl acyl chains (CH3) (Fig.8.5(a)).

In POPC, the density profiles of ALPS segments show the same tendency observed in ALPS-DOPC system: the middle and C-terminal segments colocalize, whereas the N-terminal is shifted towards the phosphates.

Interestingly, the analysis at the level of the residues on each segment (Fig.8.6) showed that in DMPC, in ALPS N-terminal and middle segment all the residues have a bias towards the hydrophobic

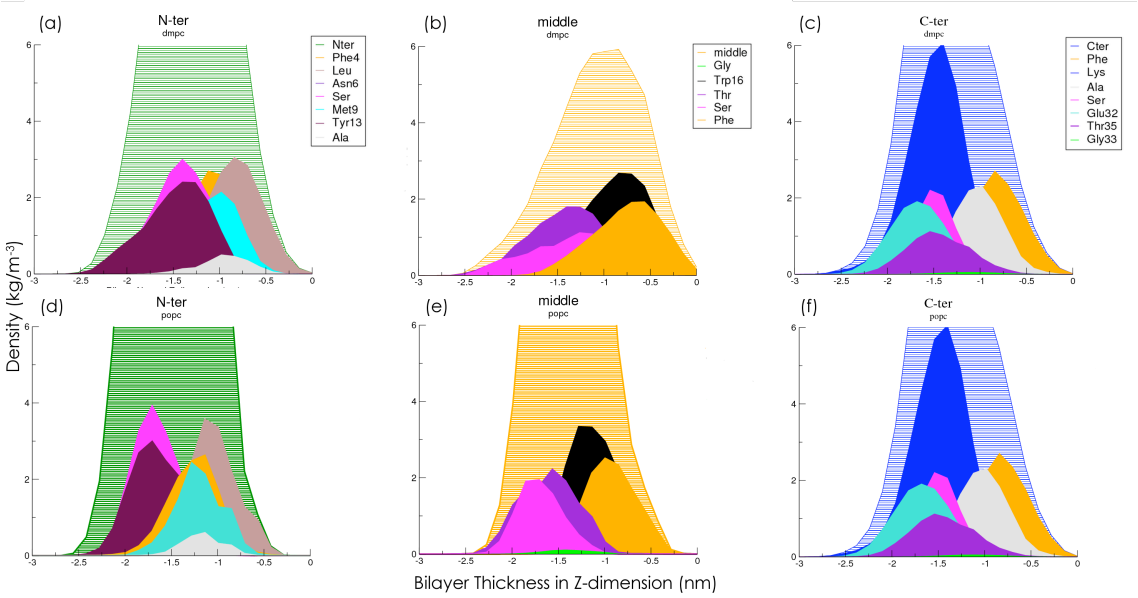

Figure 8.6: Segments residues partitioning

core, whereas the C-terminal segment maintains a normal segregation between its polar and hydrophobic residues. In POPC, the zoom-in to the residues density profiles showed the same partitioning behavior than that of the ALPS-DOPC system.

The behavior on partitioning of ALPS in DMPC also reminds the changes in partitioning in LWF-A with respect to ALPS in a DOPC bilayer.

8.1.4 Response of DMPC and POPC membranes to ALPS presence

We saw that DMPC is not favourable for ALPS deformability and POPC affects the possibilty of secondary structures transitions. Both effects affect the global flexibility properties we described in the last chapter, impacting the intra-peptide interactions, and as can be deduced from the density plots, also impacting the lipid-peptide interactions. At a first glance, an ordered bilayer such as DMPC abolishes ALPS deformability. The lipid-packing defects created by the mixture of monounsaturated and unsaturated acyl chains in POPC allow some deformable adaptability of ALPS but without secondary structure rearrengements. In order to discuss properly this effect and elucidate the influence of membrane properties on ALPS sensitivity on the lipid-packing, it is important to analyse what is the effect of ALPS on those membranes, acording to some of their intrinsic properties.

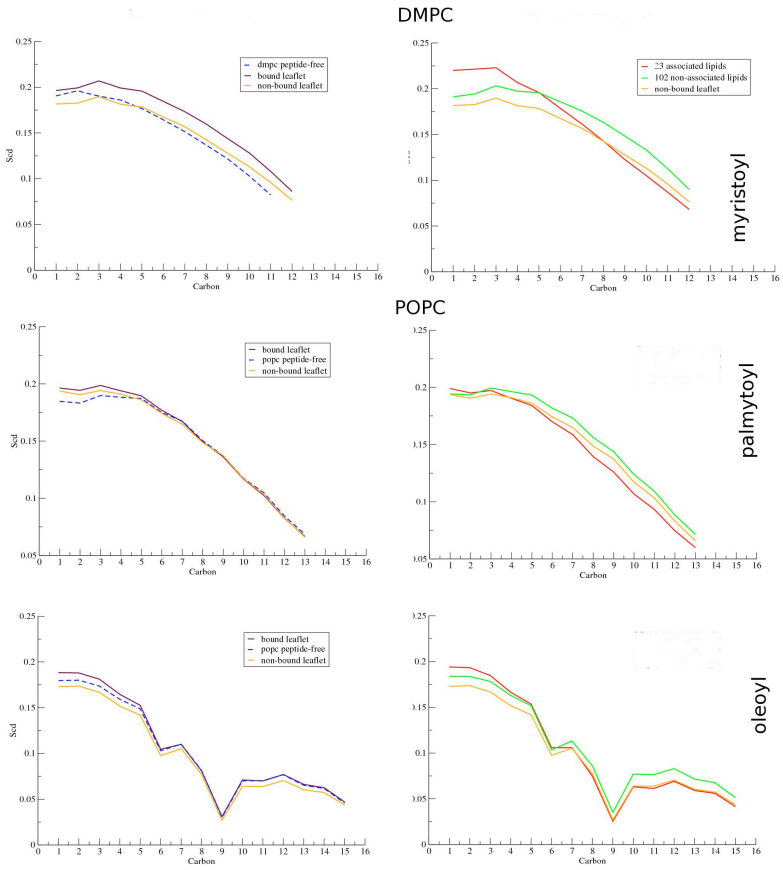

Figure 8.7: Order parameter of DMPC and POPC

8.1.4.1 Order Parameter [1]

The order parameter of our DMPC and POPC peptide-free bilayers is consistent with the values observed both experimentally and during simulations (Fig.8.7). As expected, DMPC bilayers are normally more ordered than DOPC bilayers, and hence, in the POPC bilayers the palmitoyl chains display greater order than the oleoyl chains. From the order parameter analysis we were able to determine that in response to the presence of ALPS in DMPC and POPC bilayers in general, with respect to the peptide-free system (left panels, blue lines in Fig.8.7), the order increases in the bound leaflet (darkred lines in Fig.8.7) whereas it decreases in the non-bound leaflet (yellow lines in Fig.8.7). If we decompose the effect on the bound leaflet in the contribution of associated lipids and non-associated lipids (right panels, red and green lines respectively) the response of the lipids to the presence of ALPS has the same tendency than that observed in ALPS-DOPC system. That is, an increase in order near the headgroups and

[1] Since these results will be explained making reference to the results in ALPS-DOPC system, I refer you to the section 7.3.

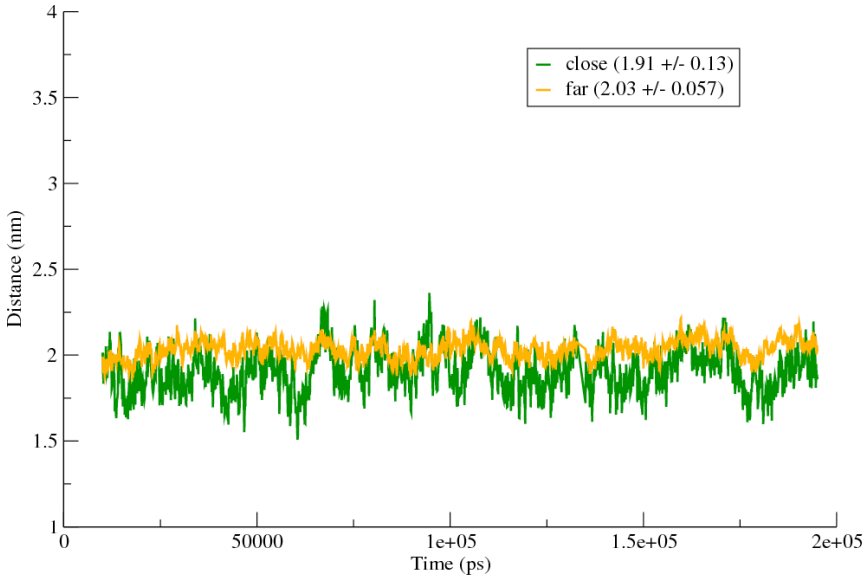

Figure 8.8: Bilayer thickness near and far away from the peptide in DMPC

disorder near the acyl chains of the associated lipids, whereas the non-associated lipids display the very opposite reaction due to the lateral pressure (see section 7.3) created in the monolayer. However the impact of ALPS in the order of each bilayer is different: the increase of order near the headgroups of the associated lipids does not have the same magnitude. Moreover, the order of DMPC saturated myristoyl chains is higher than the palmytoyl chains of POPC. When ALPS is in the bilayer, the increase induced in DMPC is higher than in the palmyoyl chains of POPC where the order is increased in only few carbon atoms. The effect on the oleoyl chains of POPC is almost the same as in DOPC.

8.1.4.2 Bilayer thickness

DOPC, DMPC and POPC bilayers have a different thickness. The divergence of the thickness of these bilayers with respect to DOPC bilayer is more evident from the density plots (Fig. 8.4). As in the case of ALPS-DOPC system the presence of ALPS in DMPC and POPC bilayers affects their thickness. In the ALPS-DMPC and ALPS-POPC systems, in the surroundings of the peptide, a thinning effect is observed with respect to the distal regions of the bilayer (Fig.8.8). Interestingly, in both systems the fluctuations of both measures (distal thickness vs close thickness) are bigger than in ALPS-DOPC system. An explanation for this could be that ALPS and the DMPC bilayer or ALPS and POPC bilayer cannot efficiently adapt to each other. ALPS limited deformability or structural flexibility on each respective case, leave more free the lipids on its vicinity than in the case of DOPC where ALPS and lipids are well attached to each other.

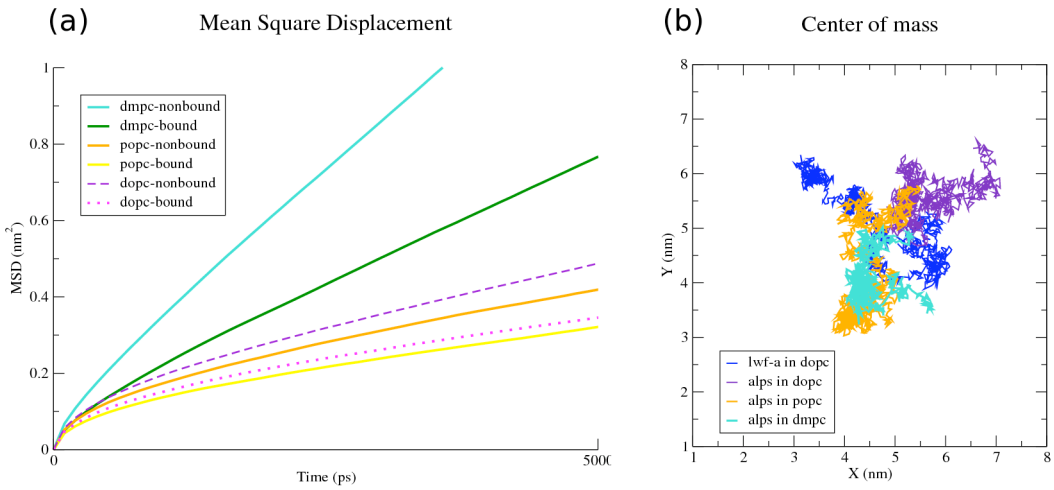

Figure 8.9: Diffusion of ALPS, DMPC and POPC lipids.

8.1.4.3 Lipids diffusion

The mean square displacement calculated for DMPC and POPC in the presence of ALPS (Fig.8.9 left) shows that DMPC lipids (green and cyan curves) diffusion is higher than POPC (Yellow and orange curves) or DOPC (magenta and violet dashed curves)) lipids. However, the same tendency than the lipid diffusion of ALPS-DOPC system is observed. That is, the diffusion of lipids in the bound-monolayer is lower than in the non-bound monolayer. Furthermore, the difference between leaflets is more remarkable in DMPC bilayer than in the cases of ALPS-POPC and ALPS-DOPC, which are about of the same magnitude. This suggets that ALPS considerably reduce DMPC lipids diffusion in the bound leaflet (green curve). In turn, ALPS diffusion[2] in DMPC is more limited (similar to ALPS in DOPC) (Fig.8.9 right, in cyan) than in POPC (in orange), and the diffusion of ALPS in POPC reminds the diffusion of LWF-A in DOPC. To summarize, the ordered short and saturate myristoyl chains of DMPC, avoid

ALPS deformability. The thin width of the DMPC bilayer induces ALPS to take a more hydrophobic partitioning that, firstly, pack and order even more the acyl chains, and secondly, limits ALPS-DMPC polar interactions such as the Ser/Thr mediated H-bonds with the phosphates. However, since all the hydrophobic interactions take place with the more "rigid" myristoyl chains, some lipids might get attached to the peptide and therefore lipids and peptide, reciprocally, limit their diffusions. It is possible that in this process the secondary structure transitions can play a role in lipid-peptide interactions.

[2]Recall that this was evaluated as a function of the trajectory of the peptide center of mass in the XY plane, and is a qualitative approximation

The POPC bilayer is apparently less sensitive to the presence of ALPS, since the order parameter in both monolayers is just slightly affected. The lipid packing defects created by the combination of a monounsaturated oleoyl chain with a saturated palmitoyl chain, favor ALPS deformability but do not seem to favor the anchoring of ALPS to the acyl chains since the diffusion of the peptide in this bilayer is more important than in DOPC and DMPC. In consequence ALPS on each one of these bilayers exihibit the structural behavior of an inefficient curvature sensor.

Furthermore, our results showed that there is a less important reciprocal adaptation process between ALPS and DMPC nor with POPC, as it was seen for the DOPC membrane. They also show that the same amphipathic helix, inserted at the interface of membranes of different compositions, does not induce the same bilayer coupling response of the membrane to the inserted molecules. Therefore, the bilayer thickness and the differential dynamics of lipids of different nature contribute to the membrane behaviour faced to an amphipathic helix inserted at the interface.

8.2 ALPS in a DOPC-DOG membrane: Role of the size of polar heads

We also performed simulations of ALPS embedded in a DOPC-DOG bilayer where 15% of the lipids are DOG (conical, with only and hydroxyl group as polar head (see Fig. 5.8). As in all the other simulations, we performed three replicas of 120ns of this system and the analysis were carried out as in the previous cases.

8.2.1 ALPS secondary structure and deformability in DOPC-DOG

The effect of DMPC and POPC on ALPS deformability and structural properties, as we have seen previously, is very unfavorable to ALPS since it reproduces a behavior that reminds that of LWF-A. As we did before we analyzed for this new system the effect of lipid-packing defects at the level of the polar groups on ALPS deformability and flexibility properties. We followed again, the evolution of ALPS secondary structure during the simulations (in the three different replicas) (Fig.8.10).

In DOPC-DOG, ALPS also shows a 3_{10}/turn/bend structural transitions in the middle segment in a similar way it does in DOPC. However, in this new system the transitions extend to the N-terminal segment reaching Ala8 (this is confirmed in the helicity content plot in Fig.8.11). The transitions in the C-terminal segment reach the Ala30 as happens in ALPS-DOPC system. The first residues of the N-terminal segment, and the residues 23 to 30 from the C-terminal segment remain helical (the former more than the latter), manifestly because these Ala contribute to stabilize the helix in both regions.

The clustering analysis in Fig.8.12 show that the most populated conformers cover 93% of the total conformers of the simulation, in 6 principal clusters that exhibit more curved variations from the Z-bended structure of ALPS in DOPC (cluster 3[18%] and cluster 4 [8%] and other significantly curved conformers, cluster 1 [31%], cluster 2 [22%], cluster 5 [7%] and cluster 6 [7%]).

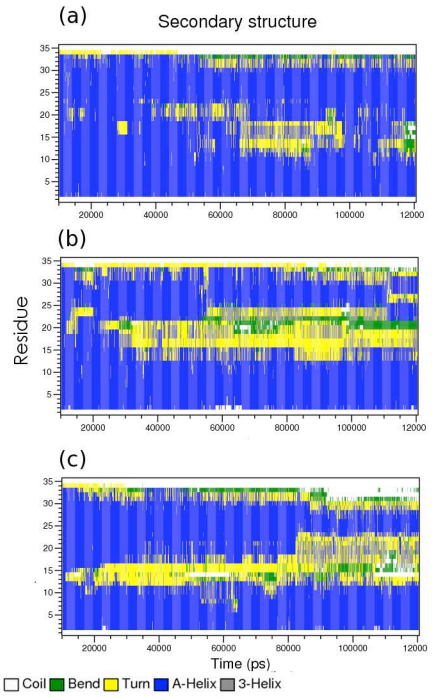

Figure 8.10: ALPS Secondary Structure evolution in DOPC-DOG

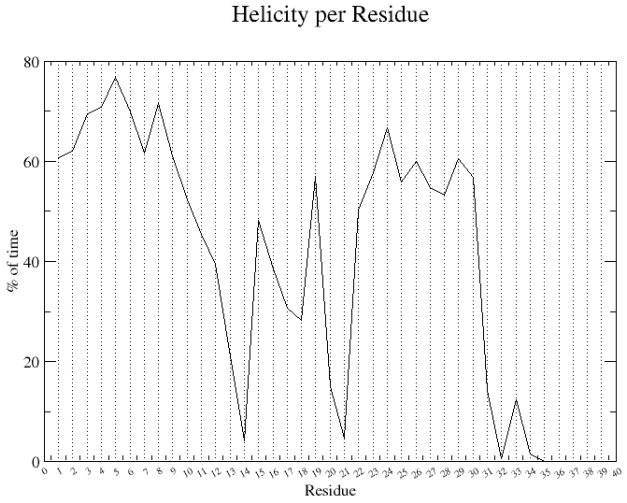

Figure 8.11: Helicity content of ALPS in DOPC-DOG

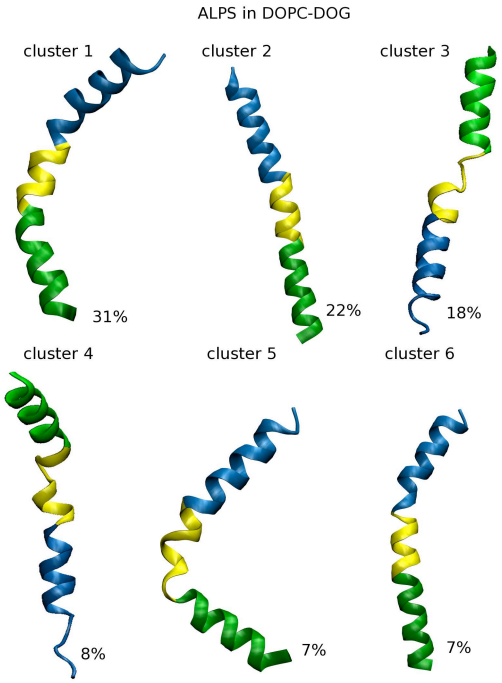

Figure 8.12: Clusters of ALPS conformers in DOPC-DOG. N-ter segment is in green, middle segment in yellow and C-ter segment in bleu.

Concerning the azimuthal rotation of ALPS segments in DOPC-DOG, we observed that the N-terminal and middle segment do not display a significant change, whereas the C-terminal does. On the other hand, N-terminal and C-terminal segments do not tilt with respect to the normal of the bilayer, whereas the middle segment moves significantly more from its horizontal position.

Manifestaly, the mixed bilayer DOPC-DOG favors simultaneously the secondary structure flexibility and deformability of ALPS.

8.2.2 Intra-peptide interactions and aromatic side-chains orientations with respect to the membrane

It is not surprising then that a lot of different intrapeptide interactions takes place in all the conformers. However, the most favored interactions are mostly Tyr13-Trp16 stacking (parallel or offset-parallel) (Fig.8.13 in clusters 1,3 and 4). The Trp16-Phe19 staking (Fig.8.13cluster 2) and a triple-stacking involving the three aromatic residues (Fig. 8.13cluster 5) were also observed. In cluster 6 all these residues were out of phase . Its is also possible to observed that Thr20 its involved in the network of intrapeptide interactions as it was in ALPS-DOPC system (Snapshots from Fig. 8.13). The preferential orientations of the aromatic residues with respect to the membrane are consistent with the favorable Tyr13 and Trp16 orientations for stacking interactions. The possibility of orientations of Phe4 and Phe26 in ALPS is wider in the DOPC-DOG membrane than in DOPC (Fig.8.13). This is not surprising

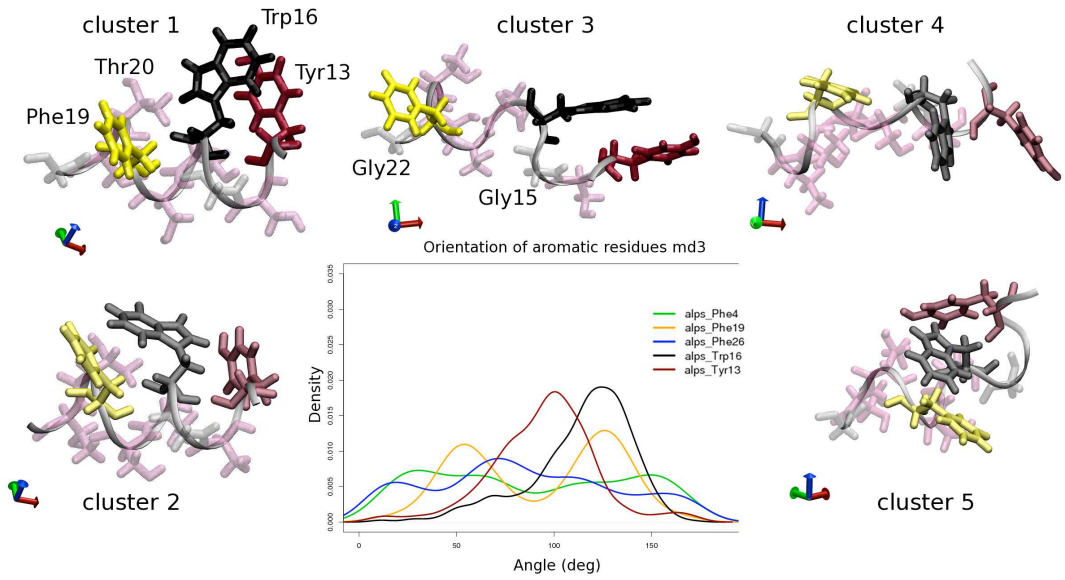

Figure 8.13: Intrapeptide interactions and aromatic orientations. In the snapshots Ser/Thr in pink, glycines in grey, Tyr13 in red, Trp16 in black and Phe19 in yellow. The axis on each snapshot represent the orientation of the peptide with respect to the normal to the bilayer (z-axis in bleu) (xy plane between red and green axis represent the plain of the membrane. The central plot show the orientation of the aromatic residues with the same color code used before, plus Phe26 in bleu and Phe4 in green.

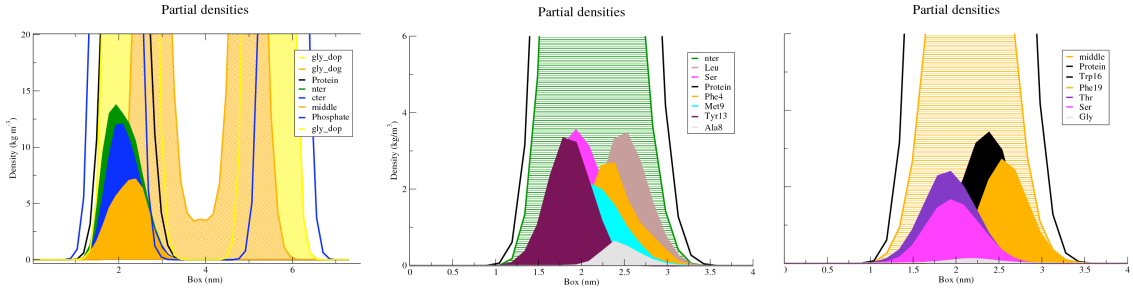

Figure 8.14: ALPS partitioning in DOPC-DOG (a) shows ALPS segments partitioning (N-ter, green solid area; middle, orange solid area; and C-ter bleu solid area) with respect to lipids phosphate (bleu lines), DOPC glycerol (yellow) and DOG glycerol (orange). (b) and (c) represnet zoom view of the N-ter segment and middle segment partitioning, respectively with their residues.

since in the latter case Phe4 and Phe26 regions showed a more important loss of secondary structure. Regarding the aromatic residues of the middle segment, their preferential orientations confirm that those orientations that favor stacking interactions between them are privileged. It is important to mention that the triple-stacking between the aromatic residues in cluster 5 disposes ALPS in a particular conformation in the bilayer where the three residues Tyr13, Trp16 and Phe19 establish interactions with lipids phosphate, glycerol and acyl chains, respectively at almost the same XY position, aligned in the Z-axis.

8.2.3 Interfacial partitioning and orientation of ALPS in DOPC-DOG

The partitioning of ALPS at the membrane interface is also maintained all along ALPS-DOPC-DOG simulations. ALPS in a DOPC-DOG bilayer privileges a partitioning between the phosphate and the glycerol, the Gaussian density distribution is slightly shifted to the phosphates (Fig.8.14 bleu lines), but still between the glycerol groups of DOPC and DOG (big yellow and orange areas behind the segments densities in the plot of the left). From the zoom-in perspective of different segments (N and C terminal and middle section) partitioning, we observed that all the segments density Gaussians colocalize. The N-terminal and C-terminal are slightly biased towards the phosphates and the middle segment Gaussian is biased towards the hydrophobic core. In the zoom-in of the residues, they showed the same segregation as in ALPD-DOPC system (Fig.8.14 (a and c)).

8.2.4 Lipid-peptide interactions

Performing the same RDF analysis that we did on ALPS-DOPC system, we observed some interesting differences and many similarities with respect to the control system.

These results are illustrated in Figure8.15 . Based on the distribution of different lipid moeities around the hydroxyl groups of serine and threonine residues we were able to determine that these residues, as in the case of ALPS-DOPC system, can establish H-bonds either with DOPC phosphate or

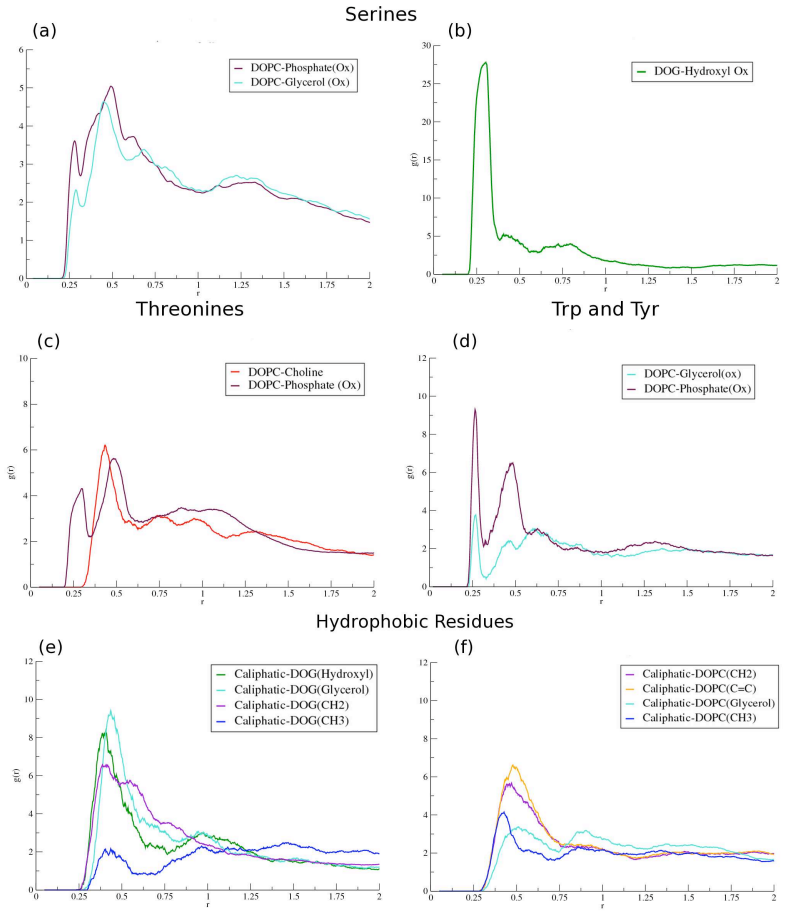

Figure 8.15: DOPC-DOG-ALPS interactions base on RDF analysis. (a) and (b) RDF of characteristic atoms from different lipid moieties with repsetc to the Ser-OH group. (c) with respect to Thr-OH, (d) with respect to Tyr-OH and Trp-NH, (e) and (f) RDF between aliphatic atoms from hydrophobic residues and DOG and DOPC respectively.

the glycerol groups. In some cases, the interactions with the phosphates are favored and sometimes those with the threonines are favored (in particular the interactions with the choline group). Interestingly, the hydroxyl group of DOG lipids showed a first and predominant peak at a distance of 0.25 nm from the serine and threonine hydroxyl groups (Fig.8.15 (a-c)), suggesting that these small polar residues can establish H-bond interactions with the hydroxyl group of DOG. However, the RDF of DOG-glycerol group does not show a favorable distance for this kind of interactions with these residues indicating that serine/threonine do not for H-bonds with DOG-glycerol oxygens.

In the case of the residue Tyr13 and Trp16, the RDF analysis with respect to the different lipid moieties (Fig.8.15(d)) allowed us to determine that in DOPC-DOG bilayers, as in the case of ALPS-DOPC interactions , the disposition of DOPC lipids around them favor H-bonds interactions between their polar groups at a distance of 0.25 nm. Also there are hydrophobic-hydrophobic interactions at a distance of 0.5 nm (Fig. 8.15(e)) as shown in the case of ALPS/DOPC system. In consequence, Tyr13 and Trp16 display a dual role of polar-hydrophobic interactions in the interface. Concerning DOG moeities, their RDF distribution around different reference atoms from these two residues showed that Tyr13 does not show close distance interactions and it seems that the DOG can only favor long distance interactions (~0.8 and 1nm). However, in the case of Trp16, the RDF shows favorable hydrophobic-hydrophobic interactions at 0.5 nm (Fig. 8.15(e)), and a first peak the low magnitude concerning the distribution of DOG-hydroxyl group around Trp16 (Fig.8.15(d)). These interactions are correlated with the intra-peptide interactions and the orientations of the aromatic side chains discussed in section 8.2.2 and Fig. 8.13.

With respect to the hydrophobic residues, such as Phe19 and Leu12, the RDF reveals interesting data: The RDF of DOPC moieties around these two hydrophobic residues shows that the preferential distance for interactions is exhibited by the acyl carbons of the lipids at a distance of 0.5 nm. However, in this case the interactions with the terminal acylchain methyl group become more evident. On the other hand, the RDF of DOG atoms around these hydrophobic residues shows that the DOG are closer from these residues than DOPC lipids, this can be inferred from the curves that present a peak at closer distances (~0.35nm instead of 0.5nm) (Fig.8.15). The first peak seen in Figure 8.15(e), corresponds to a close (0.35 nm) interaction of the aliphatic carbons of Phe19 and Leu12 with DOG hydroxyl group. The second peak corresponds to the interaction of these residues with the glycerol moiety. The other RDF curves, more wider (covering distances from 0.35 to 0.5 nm or more), correspond to the hydrophobic interactions between the aliphatic carbons of Phe19 and Leu12 residues and the acyl chains.

In summary, the oxygen atoms from the DOPC and DOG lipids are disposed at favorable distances from ALPS serine and threonine residues, in order to establish H-bonds. The Tyr13 and Trp16 can display a dual role as hydrophobic and polar residues favoring both kind of interactions with both types of lipids (this is particularly true for Trp16). An interesting detail obtained thanks to this analysis was that DOG have a distribution around the aliphatic carbons of Phe16 and Leu12 that enhance their hydrophobic interactions and the interaction with DOG-hydroxyl group.

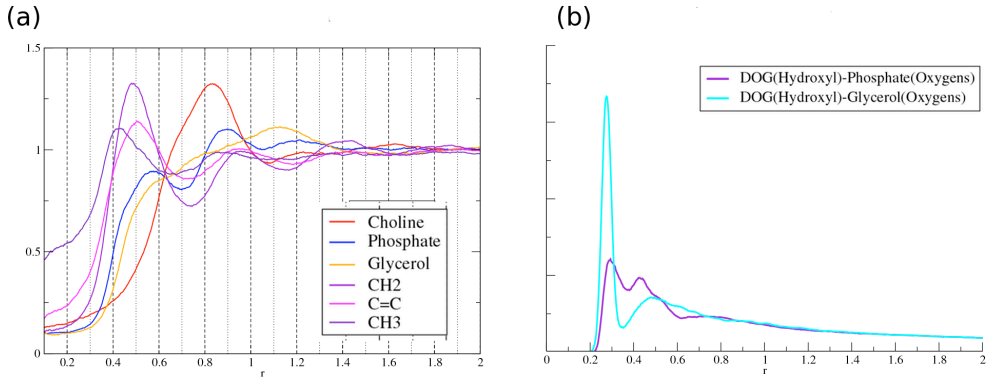

Figure 8.16: DOPC-DOG interactions from RDF analysis

8.2.5 Response of DOPC-DOG membrane to ALPS presence

A DOPC-DOG bilayer completely favors ALPS deformability and flexibility properties. It also produces a tight packing of the lipids towards the peptide, which favors in consequence short distance interactions. At a first glance, the lipid-packing defects created by the conical lipids with smaller headgroups induces ALPS to adopt different conformers that contributs to its better adaptation to the inhomogeneities found at this level. The intrinsic properties of ALPS and the response of the DOPC-DOG membrane to its presence should contribut to this favorable effect.

8.2.5.1 Lipid-lipid interactions

With respect to the packing between lipids, the RDF analysis of DOPC-DOPC interactions shows that DOPC lipids in the DOPC-DOG bilayer display the same distribution as in the DOPC membrane favoring the packing. This can be inferred because the height of the peaks is higher and the width of these peaks thinner (Fig.8.16 (a)), than in the DOPC pure (Fig.7.1). When we calculated DOG-DOPC interactions, we observed that the distances between both lipid acyl chains are the same than between DOPC-DOPC. Moreover, the distribution of DOPC moeities around DOG-hydroxyl group showed that the DOG-hydroxyl group can manifestly establish H-bond interactions with DOPC-glycerol oxygens and, in a less measure, with DOPC-phosphate oxygens (Fig.8.16 (b)).

8.2.5.2 DOPC-DOG membrane lateral and transversal dynamics

We calculated the diffusion of DOPC lipids in the membrane and observed that ALPS did not reduce lipid diffusion as it happens in ALPS-DOPC system: both leaflets display the same mean square displacement very close from the non-bound monolayer in ALPS-DOPC system (Fig.8.17 left). It was not possible, however, to determine accurately, the mean square displacement of the DOG due to methodological constraints, i.e. the limited number of molecules and the time scale. The introduction of DOG in a DOPC membrane induces different dynamic effects, for instance, we observed a spontaneous flip-flop

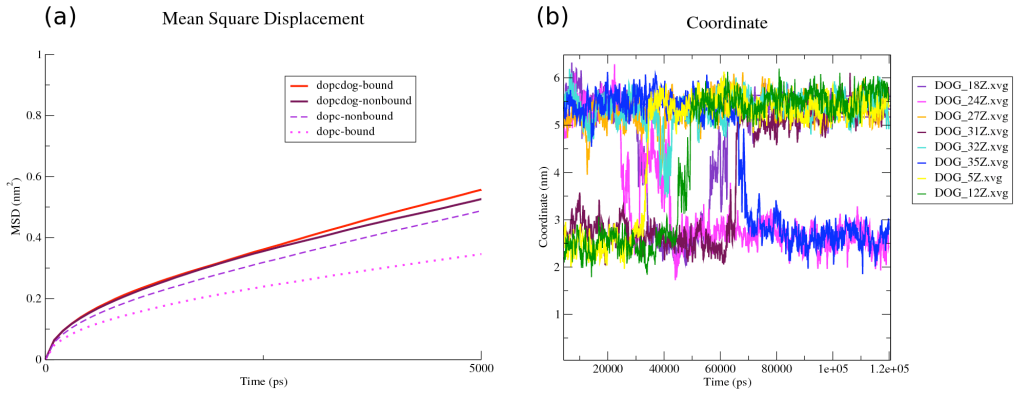

Figure 8.17: DOPC-DOG dynamics (left) lateral diffusion and (right) flip-flop

of the DOG lipids during all the simulations. We measure it as the trajectory in z-axis of the center of mass of the DOG molecule (Fig.8.17, right). Associated with this flip-flop, the thickness of the DOPC-DOG bilayer showed more significant variations caused by the presence of the peptide (Fig.8.18). Both the thickness of the bilayer close to the peptide and far away from it fluctuate stroingly than in ALPS-DOPC system. This is particularly the case for the close regions, where maybe there exists a contribution of both: the thinning effect induced by the peptide (as in the case of ALPS-DOPC system explained in section 7.4, a partial DOPC transversal diffusion) and the that induce by the DOG flip-flop.

8.2.5.3 Order parameter

Because of the DOG flip-flop it was difficult to calculate the order parameter for the DOG and been sure of having the same number of DOG molecuales in both leaflets all along the simulation. Thats why we assessed the order parameter solely for the DOPC lipids in both the pure system and the peptide-bound system (Fig.8.19). In the DOPC-DOG peptide-free system, the order of the DOPC-DOG lipids in the upper leaflet is higher than in the lower leaflet, may be because of the flip-flop of DOG. Other contribution to this behavior could be that, the cylindrical lipids in DOPC bialyer can be organized in a perfectly flat bilayer, whereas in a DOPC-DOG bilayer, the conical DOG lipids are maybe inducing a local negative spontaneous curvature of the bilayer, packing and ordering the upper leaflet lipids.

When the order parameter of DOPC in the ALPS-DOPC-DOG system is measure, ALPS present at the interface of this bilayer in the upper(bound) leaflet, interestingly, the difference in order between the bound and non-bound leaflet dissapears. When we assesed the order parameter of associated and non associated lipids (DOPC) the order parameter tendencies are the same as in ALPS-DOPC system: ALPS increase the order near the headgroups but reduce th order of the distal parts of the acyl chains. Somehow the effect ALPS induce in DOPC-DOG membrane (DOPC order in particular) in the bound leaflet, could counteract the effect of the DOG (that result from the flip-flop and/or its shape), inducing a local positive spontaneous curvature, that results in the lateral pressure generated by the presence of the peptide. When we evaluate the order of the DOG separetly in the peptide-free system and in the

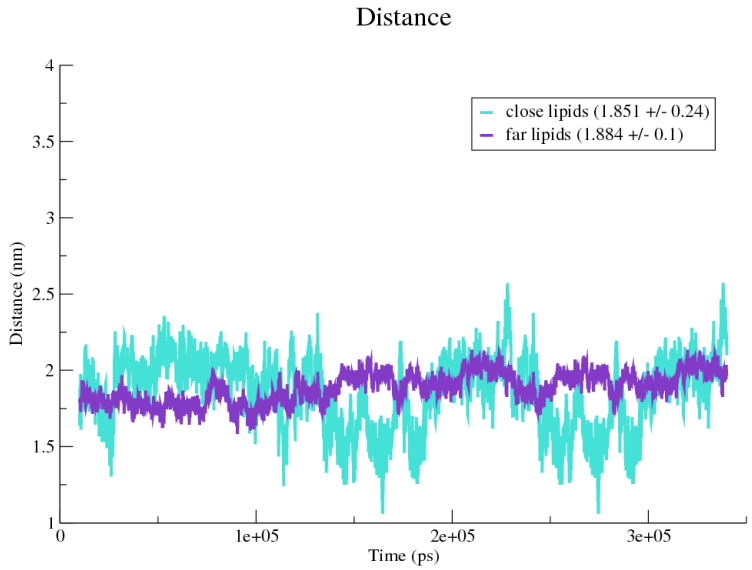

Figure 8.18: DOPC-DOG Bilayer thickness variations

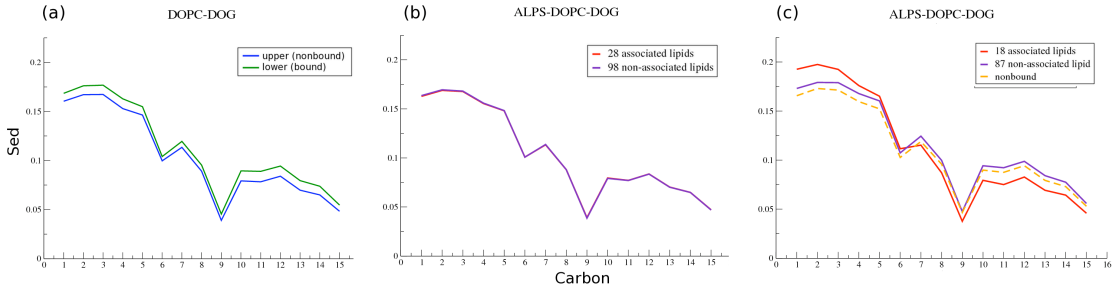

Figure 8.19: Order parameter of DOPC-DOG

ALPS-bound system it always showed the same order parameter, more disordered than DOPC. As we mentioned, it is difficult to assure that the claculations is considering the same amount of lipids in both monolayer, due to the flip-flop assymetry generated.

Manifestly ALPS adapts to the lipid-packing defects created by the conical and more dynamic DOG.

8.3 Effect of the lipid-packing on ALPS deformability

Overall, the lipid-packing defects created in a mixed DOPC-DOG bilayer sustantialy contribute to ALPS deformability and flexibility, four important properties of the DOPC-DOG bilayer contribute to this :

1. DOG induces DOPC-DOPC packing and increases their order.
2. DOG can interact by making H-bonds either with DOPC lipids oxygens or with ALPS residues.
3. DOPC-DOG membrane exhibits spontaneous local negative curvature cause by the conical DOG lipids.
4. Besides its shape, DOG transversal dynamics, also contributes to the inhomogeneities of the membrane. Therefore this property should be an element to take in consideration to understand ALPS lipid-packing recognition.

Moreover the presence of ALPS:

1. ALPS insertion induce a bilayer coupling response that induce positive curvature of whole the system and its able tu adapt to lipid-packing defects generated by both the shape and the lipids dynamics.
2. The intra-peptide interactions (stacking) between aromatic residues favored by the environment-induced deformability, allow ALPS to span the z-dimension at the membrane interface. In consequence ALPS establish interactions at three levels, the phosphate, the glycerol and the acyl chains, with residues than can establish polar and hydrophobic interactions simultaneously (as Trp and Tyr).

In contrast, in the absence of lipid-packing defects, as in DMPC, ALPS deformability is avoid. In this case the secondary structure changes produce by the lipid environment are not by their own able to contribute to deform ALPS. In consequence many intrapeptide interactions are avoid, as well as lipid-peptide interactions. The introduction of some degree of inhomogeneity in the membrane by the inclusion of unsaturated chains can contribute, in some degree, to deform ALPS but favoring less secondary structure changes in differnt places than the middle segment, and in consequence the intrapeptide and lipid-peptide interactions that we observe in ALPS-DOPC and ALPS-DOPC-DOG systems are not present anymore.

These results show that the deformability and structural flexibility of ALPS and the presence of lipid-packing defects in the membrane are correlated. They also showed that this deformability is not

only sequence-dependent but respond to the environment. Therefore, this plasticity of ALPS must be of relevance for its curvature sensitivity.

Chapter 9

Novel atomistic view of ALPS curvature sensor lipid-packing recognition

This is the first time that an ALPS motif is simulated; it therefore represents a landmark in the simulation field of membrane-shape related proteins, as well as in the field of interfacial amphipathic peptides. Although the simulation conditions, i.e. an already folded peptide interacting with a small membrane patch, did not permit to directly elucidate the curvature sensor mechanism, the present comparison between two peptides with different affinities for small liposomes yields indirect but valuable information about this mechanism. It allows revisiting the simplistic vision of the peptide as a simple tube with two opposite faces, one in contact with the membrane interior and the opposite one facing the solvent. Thus, the present study clearly emphasizes the importance of the peptide conformational flexibility and deformability, as well as the intricate role of small polar and aromatics residues to drive and stabilize the anchoring of the peptide in the membrane. In particular, it allowed us to clarify the role of the intrinsic lipid-packing defaults in the properties of the ALPS recognition motif and extend our explainations to other ALPS-like sequences previously identified. In the next sections, these different aspects are discussed at the light of experimental data and prevailing models.

9.1 Importance of the local 3_{10} motif in ALPS helix deformation and adaptation to the membrane

Our results show for the first time the molecular details and the importance of the sequence-specific conformational deformability of ALPS peptide over LWF-A. ALPS peptide within the membrane remains globally α-helical in our simulations, a result that is fully consistent with CD experiments of ALPS incubated with liposomes (Bigay *et al.*, 2003; Drin *et al.*, 2007). Nonetheless, our work also showed

that ALPS helix undergoes local deformations that are untraceable with a low-resolution technique such as CD. We could also assess the stability of LWF-A helix within the membrane, which is difficult to do experimentally because of the lower affinity of LWF-A binding to liposomes compared to ALPS (Bigay *et al.*, 2005). We found that LWF-A only exhibits light natural helix bending (as frequently observed in MD simulations) with numerous small transitions. In contrast, ALPS adopts distinct stable conformations, the dominant one being a deformable helix-turn/3_{10}-helix "Z-shaped" conformation. This latter result is consistent with the experimental data that showed this S/T rich region induces a drop in the probability of α-helical content (Drin *et al.*, 2007; Bigay *et al.*, 2005). This 3_{10}-helix structural motif, whose periodicity and twist differ from a pure α-helical motif, is stabilized by the Ser/Thr residues that lie in the proximities and which favor the stabilization of interactions between aromatic residues, as well as interactions between the peptide and the lipid chains. Interestingly, NMR and CD experiments, as well as MD simulations have shown other examples of membrane interacting peptides that present a small 3_{10} helix portion (Freitas *et al.*, 2007; Gao and Wong, 2001; Marty *et al.*, 2009; Okuda *et al.*, 2008) on their membrane-binding domains. This may suggest a role for these local and small 3_{10} motifs in the correct partitioning of those proteins. The case of annexins is of particular interest since Annexin II has a membrane-binding domain that presents a 3_{10} helix segment (Hong *et al.*, 2003) and Annexin B12 has been proven to be a membrane curvature sensor (Fischer *et al.*, 2007). Whether the curvature sensitivity could be correlated with the 3_{10} helix is still unclear but the present study brings new insights into the potential role of this motif. It would be interesting to perform NMR experiments to validate this hypothesis.

We also were able to determine that different lipid bilayers can impair secondary structure transitions and deformability. These different membranes can even produce that ALPS behaves as LWF-A, that is, as an indeformable or inflexible motif. For instance, in DMPC ALPS undergoes limited helix-turn/3_{10}-helix transitions in an indeformable state, whereas in POPC ALPS undergoes more significant deformations forming turns and bends in other regions. In neither of both cases a 3_{10}-helix structural motif that could stabilize aromatic residues interactions can be observed. Interestingly, a mixed DOPC-DOG bilayer, enhances both the helix-turn/3_{10}-helix transitions and the deformability, inducing ALPS to adopt a wider panoply of curved and Z-shape conformations and intra-peptide interactions particularly favorable to span the interface z-dimension in order to optimaly detect the lipid-packing defaults. These results are consistent with the experimental data that shows that the mono-unsaturated acyl chains and the small headgroups enhance ALPS binding to the liposomes, whereas unsaturated lipids are unfavorable for this binding (Antonny *et al.*, 1997b) (see section 4.3.4). Thus, our results suggest an environment dependence of ALPS conformational deformability and sequence-specific structural flexibility. This implies that the optimal environment for ALPS curvature sensitivity is that one where there is a synchronic potentiation between the sequence-specific effects and environment-dependent effects. I will develop this explanation in the further sections of this chapter starting with a discussion on the environment dependent effects, and then I will continue with the details about the sequence properties dependent effects.

9.2 Dynamic lipid-packing defaults as mayor potentiators of ALPS deformability and adaptability

The prevailing model about ALPS curvature sensor attributes to ALPS the capacity to recognize the lipid-packing defaults created by the curvature of the membrane. Our results complement this view analyzing the intrinsic lipid-packing defaults in different lipid composition membranes. These inhomogeneities, when they are present, are not static and depend on the lipid dynamics. The bilayer fluidity and its plasticity determine the peptide-lipid interactions that affect ALPS structural behavior. ALPS partitioning at the interface represents an optimal orientation to simultaneously detect the inhomogeneities created at the level of the acyl chains and to those formed at the level of the polar headgroups. ALPS deformability and structural flexibility are the perfect strategy to adapt its structure to these lipid-packing defaults while inducing adaptative dynamic response of the membrane that leads to a bilayer-coupling effect and a reciprocal orchestrated adaptation process.

ALPS and LWF-A adapt differently to the DOPC bilayer rough surface, displaying different orientations and conformations. The change in the hydrophobic moment of LWF-A with respect to ALPS and their differences in hydrophobicity, contribute to this difference. For instance, ALPS bulky hydrophobic residues (absent in LWF-A) are anchored in the membrane and limit its rotational liberty. Moreover, this anchoring limits ALPS diffusion in the membrane and simultaneously reduces the lipid diffusion. On the other hand, LWF-A diffuse more in the membrane because it has a limited anchoring. These behaviors are clearly sequence-specific responses to the lipid environment.

As I mentioned before, the lipid context can drastically affect ALPS structural properties. For example, the lipid context can make ALPS behave as the inefficient curvature sensor such as LWF-A, as we saw inr DMPC and POPC bilayers. Moreover, these membranes abolish the mutual adaptation process. In DMPC the ordered saturated myristoyl chains do not leave enough space for ALPS to be freely deformed nor to anchoring the membrane by knob-into-holes of its bulky aromatic residues to the acyl chains. In DMPC membrane ALPS does not significantly diffuse because the lipids are distributed too tightly. Moreover, even if the POPC membrane possess spaces created by the oleoyl chains that allow ALPS to slightly deform, the order imposed by the palmitoyl chains limits ALPS secondary structure transitions and avoid the knob-into-holes anchoring of ALPS to the oleoyl chains, which therefore reduces its diffusion.

In DOPC and DOPC-DOG membranes, the circumstances are entirely opposed. Here we clearly observe an orchestrated peptide-lipid adaptation. The membrane dynamics reflect the lipids adaptation to a wide range of conformations. Moreover, the cavities formed by the headgroup-lack DOGs and their transversal dynamics, create an interfacial landscape in constant change. In consequence, instantaneous lipid packing is inhomogeneous. ALPS deformability and structural flexibility is enhanced in this membrane due to these local defaults in lipid packing at the membrane interface. ALPS display H-bonds between its polar residues and the lipids polar moieties. Moreover ALPS hydrophobic residues can make knobs-into-holes arrangements with the oleoyl chains, as it was observed in DOPC. Manifestly, all these are environment-dependent deformability responses of ALPS structure.

In response to the presence of the peptide, the DOPC and DOPC-DOG membrane can adapt by modifying the lipid-lipid interactions and dynamics. Indeed, the partitioning of ALPS in the interfacial region of the membrane influences the packing of the lipids. The partitioning of the amphipathic peptides at the level of the glycerol in one monolayer of the membrane produces an asymmetry in the system, which accordingly to the monolayer asymmetry model (Devaux, 2000), produces an expansion of the bound leaflet. This induces a stress in the non-bound leaflet curvature leading to positive membrane curvature (Bechinger, 2009) (see section 3.4.2 and Fig. 3.3(d)), which may counteract the negative spontaneous curvature of the DOG. The space occupied by ALPS in the bilayer interface increases the density of an already crowded environment. In this context, the complex behavior of the order parameters reported in chapter 7 and 8, and the effects of the peptide on the order parameter of the non-bound leaflet, may reflect an induced local curvature of the system that increase the defaults of the flat membrane. However, since we are using periodic boundary conditions it is difficult to assess the amount of curvature generated. Interestingly, in the particular case of DOPC-DOG bilayer, where the combined effect of DOPC partial transversal diffusion (in response to the presence of the peptide) and DOG flip-flop induce the formation of larger invaginations of the bilayer (changements in the bilayer thickness). This clearly suggests that the binding/lipid-packing recognition is an orchestrated process between the peptide and the membrane lipids nature and dynamics.

9.3 ALPS sequence: an optimal synergy between polar and hydrophobic steric interactions

In the orchestrated scenario of environment-dependent and sequence-specific conformational deformability, which are the main sequence features than make possible the lipid-packing sensing of ALPS? We detected a sequence pattern Bulky-small&polar-Bulky in its amphipathic α—helix that provides important insights to answer this question. This pattern achieves such a task thanks to its residues that exhibit specific (1) partitioning, (2) propensities to form α-helices, (3) steric effects and (4) conformational liberty.

1. According to interface-partitioning energies assessed experimentally (Wimley and White, 1996; White and Wimley, 1998) and by *in silico* calculations (MacCallum *et al.*, 2007, 2008) (see Fig.2.6), the most favorable interfacial partitioning energies in ALPS correspond to Leu, Met, Tyr, Trp, Phe and Lys. These residues (with the exception of Lys) flank the serines/threonines (residues with less favorable interface-partitioning energies) and favor their partitioning at the interface. Their absence in LWF-A could disfavor the peptide interface-partitioning and thus impairs its binding to the membrane.

2. According to the propensities to form helices (explained in section 2.3.2, Fig.2.9), 51% of ALPS residues, principally concentrated in the middle segment (Trp, Tyr, Ser, Thr, Gly, Met), have intermediary propensities to form helices in hydrophobic environments and very low propensities to do so in aqueous environment. The latter would favor the emergence of helix-turn/3_{10}-

helix. In turn, Phe, Leu[1] and Ala (30% of ALPS residues) have high propensities in hydrophobic environments, and in aqueous solution, they can either have high propensities (Ala, Leu and Ile) or low propensities (Phe and Val) (Liu and Deber, 1998b). In TM proteins, the helical propensity of hydrophobic segments with different compositions, decrease in the following order: Ala-Leu-rich> Gly-Leu-rich> Gly-Ile-Val-rich (Li and Deber, 1992b). This suggests that Gly and β-branched residues may provide, partially, the structural basis for conformational transitions. Moreover, serines and threonines have a modulator role of the helical structures in TM proteins, stabilizing local distortions (Deupi *et al.*, 2009; Ballesteros *et al.*, 2000; Deupi *et al.*, 2004). It is therefore possible that these amino acids also play a similar role in interfacial proteins. Thus, in ALPS, Ser/Thr flanked by residues with high helical propensities would favor an helical arrangement of the residues while maintaining the ability to deform.

3. The hydrophobic residues in the N-terminal and middle segment of ALPS are mostly bulky and aromatic. As we showed, the shape and geometry of these aromatic residues favors their steric and hydrophobic interaction. The amphipathic character of ALPS must be guaranteed, and at the same time, must limit the obstacles for the hydrophobic interactions. Serines have been shown to decrease the mean hydrophobicity without creating steric clashes (Jonson and Petersen, 2001). Moreover, the polar character of these residues makes them ideal candidates to be between the bulky hydrophobic residues and establish polar interactions with the lipids.

4. The organization of the hydrophobic and polar residues based on the steric and hydrophobic effects is an important feature of ALPS motifs. In this context, the neighboring serines/threonines provide the perfect hydrophilic and steric balance needed to maintain the H-bond contacts that allow ALPS to explore the lipid-packing defects at the level of the headgroups, while the multiple conformations of the bulky residues explore the lipid-packing defects at the level of the acyl chains. In this respect, the presence of aromatic residues with potential dual roles (as Tyr and Trp for instance, but also Met) could represent and advantageous feature.

We propose that a synergy between the bulky hydrophobic anchor to the membranes and small polar residues-lipids H-bond network, improves the affinity of ALPS to bind highly curved membranes, acquiring a helical arrangement. The deformable helix-turn/3_{10}-helix represents the perfect strategy to correctly dispose the hydrophobic residues in their most favorable orientation with respect to the membrane interface, in order to specifically anchor the peptide in a dynamic and adaptative manner.

The pattern in ALPS consists of a series of Bulky-small&polar-Bulky motifs (BssB) (Fig. 9.1), where the 's' stands for small polar and neutral residues (as serines are the most frequent one, then threonines and glutamines/asparagines) or glycines; and 'B' stands for bulky hydrophobic residues. ALPS exhibits a central pattern with three consecutive BssB motifs covering Met9 to Phe19 (MssLYsgWssF) (Fig.9.1). In fact, it is in this region where the transitions turn-3_{10}/helix are observed. The bulky aromatic residues Tyr, Trp and Phe are very close to each other, hence flexible small and neutral polar residue should separate them thus allowing stacking interactions and the performance of dual polar and hydrophobic

[1] and β-branched residues, such as Ile and Val

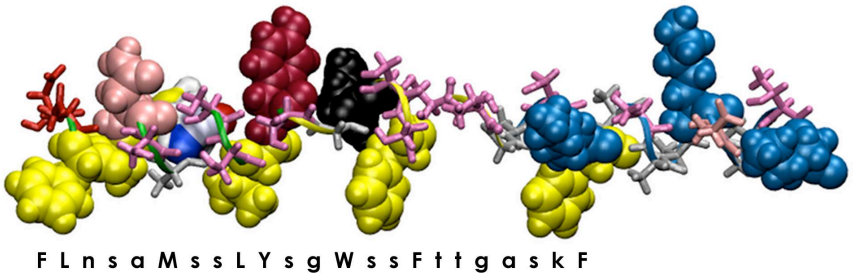

Figure 9.1: Bulky-small&polar-Bulky motifs in ALPS sequence. Snapshot of ALPS structure, showing VDW representations of Bulky hydrophobic residues in yellow , the Bulky aromatic residues Tyr13 (Y) and Trp16 (W) in red and black respectively. Lysines (K) from the C-terminal segment in bleu VDW representation. Ser/Thr (small and polar residues (S/T)) in pink licorice representation, alanines (A) and glycines (G) gray licorice representations. ALPS helix is represented as a ribbon colored N-terminal segment in green, middle segment in yellow, and C-terminal segment in bleu. Asn6 (N) and Met9 (M) in lightpink and and atom-name color VDW representations, respectively.

interactions of Tyr and Trp with the lipidic environement. The BssB pattern described above supposes that two small polar and neutral residues separating two neighboring bulky hydrophobic residues allows these latter to freely adopt a greater number of orientations. These "s" intermediary residues avoid the possibility of forming an intrapeptide hydrophobic-hydrophobic rigid structure, and stabilize favorable secondary structure for the exploration of the rough interface.

This BssB motif allows us to explain (i) the relevance of ALPS conformational deformability, (ii) how the small polar residues could contribute to the lipid-packing recognition and (iii) why the aromatic anchors in ALPS sequence could be one of its most important attributes. The following part of the discussion will focus on these aspects.

9.4 Sensing properties of the Bulky-small&polar-Bulky motif at the light of experiments

Antonny and coworkers first discovered ALPS sequence sensitivity to curved membrane thanks to its ability to sense lipid packing defects. They tested experimentally a number of mutants that allowed them to understand the role played by the different residues (Bigay *et al.*, 2005; Drin *et al.*, 2007). They found two particularly important features, i) the presence of bulky hydrophobic residues which contribute to the affinity of ALPS binding to membranes; ii) the presence of small polar residues (serines/threonines) and the concomitant paucity of charged residues that contribute to the specificity of ALPS for curved membranes. Our interpretation at the molecular level described above fully complements and improves the model of Antonny and coworkers. In the following, we discuss in more details the relevance of the BssB motif into ALPS lipid-packing recognition properties at the light of the experimental results of Antonny and co-workers.

We described that serine/threonine residues are important H-bond partners of lipid oxygens. The charged residues can, in a way, also establish this kind of interactions with the lipids. If a small charged residue, such as the aspartate, is introduced at the expense of serine/threonine residues, the effects may not be so notorious, but if the bulky lysines are placed between the bulky hydrophobic residues, the steric hindrance prevents the conformational freedom of the bulky hydrophobic residues and the possibility of interactions between them. Indeed, this is likely what happens in some of the mutants Antonny and co-workers worked on, when lysines are introduced at the expense of Ser18 and Thr20, which are known to produce key intrapeptide interactions in ALPS middle segment structure. On the other hand, a lysine at the place of Tyr13 may favor dual hydrophobic-polar roles as described in this work for Tyr13 and Trp16. It would be very interesting to create mutants in order to isolate the possibility of this effect.

Consistently with the BssB hypothesis, LWF-A presents a completely disturbed BssB pattern, a bulky residue, Met9 and Phe24 flank some small polar residues but also alanines over a long part of the sequence (MssaYsgassattgaskF) (Table 9.1). Therefore, even if it still exhibits the organization of an amphipathic α—helix, it is no longer able to form the network of intrapeptide interactions that we observe in ALPS. The absence of Trp16 and Phe19 in LWF-A avoids the conformational diversity and the adaptative anchor to the membranes. Indeed, the hydrophobic interactions with the lipids are not the same, and the dual-role of Trp16 interaction with both polar and hydrophobic lipid moieties is abolished. It is worth mentioning that since the polar residues in ALPS and LWF-A are conserved, some of the roles attributed to these residues remain unchanged, like the H-bonds they can display with the oxygen atoms of the lipids. The presence of Tyr13 and the remaining bulky residues in LWF-A contribute to maintain a weak specificity to small liposomes. On the other hand, the interactions established by S/T residues with the lipids at the interface of the membrane, may allow LWF-A to maintain certain degree of affinity.

With respect to the lipid-packing, our BssB hypothesis would also explain why ALPS is sensitive to cone-shaped lipids (Antonny *et al.*, 1997b) as DOG (with only a hydroxyl group as polar head). The Ser/Thr rich regions can either make interactions with the DOG hydroxyl group or with DOPC glycerol oxygens. Moreover, the conformational liberty of the bulky hydrophobic residues allow tight contacts with DOG and DOPC oleoyl acyl chains. Interestingly, in DOPC-DOG membranes, the increased in lipid-packing defauts by lipids shape and dynamics also favor the ALPS adoption of a 3_{10}-helix structure. Helped by ALPS vast deformability in this environment, this secondary structure can anchor to the membrane disposing the aromatic residues in favorable stacking orientations to span the Z-dimension of the interface, from the acylchains (Phe19 at this level), passing throught the glycerol (Trp16 interacting with it by polar and hydrophobic interactions), reaching the phosphate level (thanks to the more polar Tyr13).

Finally, we propose that in those membranes without flexible acyl chains and showing less packing defects at the level of the hydrophobic core, (DMPC and POPC membranes), the bulky hydrophobic residues of ALPS would not be able to adapt so easily because of impared deformability and structural flexibility.

protein	ALPS motif	start	Bulky-small&polar-Bulky Pattern	end
ARFG1	*ALPS1*	198	DDFLNSAMSSLYSGWSSFTTGASKFASAAKEGATK	226
		2	..BBsssBssBBssBssBssssss-B..........	35
			AssAssAssssss-A..........	
	ALPS2	270	SGVSQLASKVQGVGSKGWRDVTTFFSG	296
			..BssBss-BssBss-sB..BssBB..	
			..-ss-ss--ss-ssssA.--ssAA..	
GCS1	*AL_gcs1*	240	ADPLGTLSRGWGLFSSAVTKSFE	262
			...BssBsssB..BsssBsssB.	
			...-ss-sssA..Asss-sssA.	
TRIPB	*AL_tripb*	1	MSSWLGGLGSGLGQSLGQVGGSLASLTGQISNFTKDML	38
			BssBBssBsssBsssBssBsssBssBsssBssB.....	
			-ssA-ss-sss-sss-ss-sss-ss-sss-ssA.....	
NU133	*AL_nup133*	245	LPQGQGMLSGIGRKVSSLFGILS	267
			.......BssB...s--BssBB....	
			.......-ss-s---ss-A....	
KES1	*AL_kes1*	7	SSSWTSFLKSIASFNGDLSSLSA	29
			...BssBB-sBssBss-BssB..	
			...AssA--s-ssAss--ss-..	

Table 9.1: Bulky-small&polar-Bulky motif patterns found on ALPS and other ALPS-like sensors. First the pattern is highlighted on the sensor motif sequence with uppercase (bulky residues) and lowercase (the rest of the residues). Charged residues (in BspspspB motifs or bigger) are marked in gray or with a slash. Below, the sizes of the patterns are represented: BspspB is the smallest motif (green), and BspspspB (yellow). Longer motifs are in black. In BspspB, B= L, T, W, Y, I, V (bulky residues with favorable interfacial partitioning); sp= small polar and neutral residues S, T, N or G in the case B is aromatic (alanine can be sometimes present). The third representation of the pattern, highlights the preponderance of aromatic residues in ALPS sensor motif.When only the aromatics are considered as Bulky hydrophobic residues, an A is marked at the place of B in the table patterns (if other hydrophobic residue in B position, then a slash is found. For each protein ALPS-like motif, "AL" states for ALPSlike and then the name of the protein is given.

9.5 Bulky-small&polar-Bulky pattern in other ALPS-like motifs: ALPS the paradigm

The Bulky-small&polar-Bulky pattern we proposed for ALPS is also present in the second ALPS motif of ArfGAP1 and in the Gcsp1 yeast homologue (Table 9.1). Two important differences with respect to ALPS are highlighted. The first one corresponds to the nature of the hydrophobic residues in the Bulky positions (valine overrepresented), the second one is related to the number of sp in the BssB motif. Val and Ile are overrepresented in soluble β-sheets and thus considered to be helix breakers (Doig, 2005; Dahl *et al.*, 2008), suggesting less helical content in ALPS2. However we mentioned before that β-branched residues may partially provide the structural basis for conformational transitions. Indeed, CD experiments showed that ALPS2 helicity content was lower than in ALPS because it binds less efficiently to small liposomes (Mesmin *et al.*, 2007) and acts in a cooperative way with ALPS to increase the sensibility to high curvature (Mesmin *et al.*, 2007). Nonetheless, even if ALPS2 have more helix-breaking residues, its specificity and affinity for small liposomes is better than LWF-A (where alanines, which are helix-former, are overepresented). This implies that the helical arrangement is only the perfect strategy to correctly dispose the hydrophobic residues in their most favorable orientation with respect to the membrane interface, but does not improve the curvature sensing capacities.

Remarkably, the Bulky-small&polar-Bulky pattern is also present in other ALPS-like motifs that have been confirmed to sense the curvature (see Table 9.1) (Drin *et al.*, 2007; Gautier *et al.*, 2008). However, it presents on each case different important variations concerning the nature of the Bulky residues as well as the distribution of the BssB pattern along the curvature sensor motif. For instance, in the ALPS-like motif of GMAP-210, an uninterrupted pattern of BssB repetitions all over the sequence is manifest. In the case of Nup133 ALPS-like motif, its specificity for small liposomes is evident but it binds them with less affinity than ALPS (Drin *et al.*, 2007), the BssB motif is found two times with a gap between them. In both ALPS-like motifs, the first intriguing characteristic is that the proportion of aromatic residues is considerably smaller (Nup133 only has one F). In GMAP-210 the Trp and the Phe are in the borders of the pattern and recognize the curvature binding to the membrane as a dimer. As we described, ALPS motif YsgWssF favors stacking interactions between the aromatic residues and stabilize the helix-turn/3_{10}-helix structure. This suggests that the aromatic-aromatic interactions probably represent an important feature that improves the anchor and recognition of the lipid packing defects on highly curved membranes. In GMAP-210 due to the low content of aromatic hydrophobic residues, it could be thta the strength of the binding and the recognition capability need the formation of a dimer in order to sense the curvvature.

In all these ALPS-like peptides, we can also consider that the positively and negatively charged residues surrounding the patterns could be important to create a balance between the interactions with the membrane and the solvent, and at the same time they would limit the charged interactions with the membrane to maintain the binding to flat membranes at the minimal level as suggested by Drin, *et al.*

9.6 Delimiting ALPS sensor

The precise size of ALPS is not well defined (it can cover from 25 to 36 residues). The secondary structure analysis and the coil formation at the N and C terminal ends suggest that ALPS could cover from Ala8 to Ala30. Nevertheless, the identification of the Bulky-small&polar-Bulky ALPS pattern will be useful to delimit ALPS and ALPS-like motifs boundaries with more precision. If we explain ALPS limits on the bases of the BssB hypothesis (Fig. 9.1 and Table 9.1): in the N-terminal segment we found a long hydrophobic Met9 and an interfacial orientation-bulky branched Leu12 that always adopt the most hydrophobic orientation, that is, away from the intrapeptide interactions; these two residues flank two serines. Further in the sequence, two other serines are flanked by two bulky aromatic residues, the aromatic big polar residue Tyr13 and the aromatic Trp16. Both display interfacial orientations that make them establish stacking interactions and hydrophobic and polar interactions with the lipids. Finally, between Trp16 and Phe19, which orientations are mostly hydrophobic, we found two flanking serines. Phe19 can also establish stacking interactions with the Trp, and both residues perform knob-into-holes arrangements with the lipid acylchains. This shows the importance of steric and hydrophobic effects in the organization of the hydrophobic residues as an important feature of the ALPS motifs. In this context, the neighboring serines and threonines seem to provide the perfect hydrophilic and steric balance needed to maintain the contacts with the polar heads, while the multiple conformations of the bulky residues explore the interface in the three-dimensions. In other areas of ALPS, away from the pattern, the conformational freedom is lost. For instance, the N-terminal Phe4 has limited preferential orientations because Leu5 imposes a steric resistance. This Leu5 is involved with Met9 in a Bulky-small&polar-Bulky pattern that includes an Asn and an Ala (LnsaM). It is possible that in motifs like this one, the presence of a "s" residue bigger than Ser/Thr impose the necessity of an extra "s" residue, as would be the case of Ala, in order to avoid clashes between the bulky hydrophobic residues. This possibility is also observed in the BsssB patterns in other ALPS-like motifs. On the other hand, in the C-terminal segment, Phe26 has a broad range of orientations because it does not have a big surrounding hydrophobic residue with the same partitioning that limits its movements. It is also important to notice that in this region, the BssB pattern is not well defined, and it contains a lysine in what would be a large Bulky-small&polar-Bulky motif (FttgasaKF). Indeed, the presence of this lysine (Lys25) allows different kind of steric and planar interactions between Lys25 hydrophobic sidechain and the benzene ring of Phe26, which influences Phe26 orientations.

Based on our results we suggest that the curvature sensor motif in ALPS comprises from Met9 to Thr20 (residues 200 to 215 in ArfGAP1 protein sequence) (Table 9.1) where the structural 3_{10}helix/turn transitions take place. The other remaining residues (Leu5 to Ala8 and Thr21 to Ala30) would play animportant role in the correct partitioning of the peptide in the bilayer interface (see Fig.9.1) and a contribution to deformability.

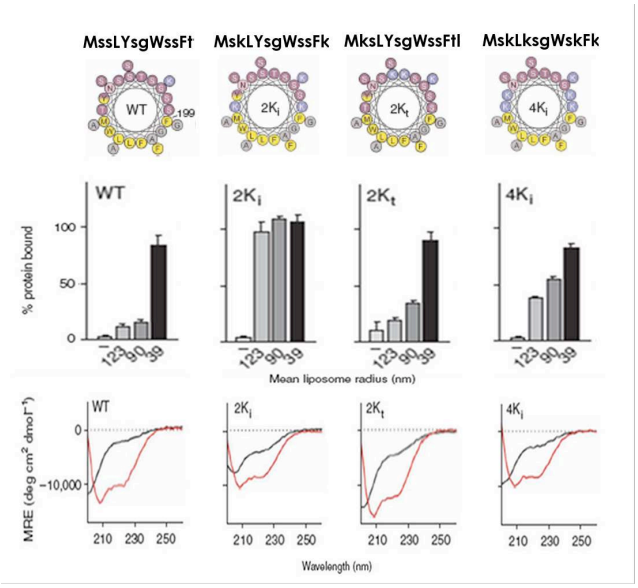

Figure 9.2: Polar face mutant of ALPS with the reference of the disrupted BssB patterns in their sequences (Modified from (Drin *et al.*, 2007)).

9.7 Understanding other ALPS mutants in the BssB context

In chapter 4 section 4.3.3 I described the experiments that indicated that ALPS binding is independent of the charged electrostatic interactions. I also pointed out that these mutations were difficult to interpret. I would therefore like to discuss in this section Drin *et al* results on the bases of the BssB hypothesis in order to complement this hypothesis and propose further experiments.

Drin *et al* tested four mutants where Ser/Thr residues were replaced by charged residues (mostly Lys). These mutants are explained in the section just referred and are illustrated in Fig.4.6. For clarity purposes, I will refer from now on to the mutants using the numbers illustrated in the ALPS model (Fig.9.2):

1. Mutant 2Ki (S11K and T20K)
2. Mutant 4Ki (S11K, Y13K, S18K and T20K)
3. Mutant 2Kt (S10K and T21K)
4. Mutant 4Ki/4Et (S11K, Y13K, S18K, T20K plus S10E, T21E, S14E and S17E)

For the four mutants, it is not just the electrostatic nature of the residues that has been changed, but also other important properties that are in agreement with the BssB hypothesis. For instance, the change to a bulky Lys, whose steric effect is substantially bigger than those from Ser/Thr. Moreover, the propensity to form helices would also be affected by this change since lysines are less prone to form helices in hydrophobic environments than Ser/Thr, and more prone to do it in aqueous solution.

Additionally, the interfacial partitioning of lysine residues is more favorable than Ser/Thr partitioning, and the structural modulator role of Ser/Thr would also be affected. All these factors are being changed in the four mutants. However, in the light of the BssB hypothesis some interpretations could be put forward in order to address several new questions. The experiments of incubation of these mutant with liposomes of different sizes, showed that ALPS-2Ki mutant is no longer able to discriminate between high or low curvatures (Drin *et al.*, 2007) (Fig.9.2). This mutant has a changed (with respect of ALPS) **MskL**YsgWss**Fkt** pattern that affects the stabilizing interaction that Thr20 established with Trp16 and Tyr13 in ALPS. Four aspects could be acting here:

1. the favorable partitioning of the lysine in the interface increase the binding, which might be helped by
2. charged electrostatic interactions;
3. The structural modulator Thr20 is lost, as well as Ser11, which might play a similar role as Thr20 by establishing a stabilizing interaction between Tyr13 in ALPS MssL pattern;

In Drin's work, detailed in section 4.3.3, ALPS-2Kt shows only a small difference with respect to ALPS activity, although we observe a slight increase in the binding to big and small liposomes. Interestingly, in ALPS-2Kt the pattern has been changed to **MksL**YsgWss**Ftk** This would mean that Thr21 is not as important as Thr20 to ALPS curvature recognition. Furthermore, in this mutant there is not loss in the helicity content (see Fig.9.2). In the case of mutant 2Kt the 3_{10}helix/turn transitions are still possible stabilized by Thr20, whereas in the mutant 2Ki, they do not.

More importantly, the mutant 4Ki, where most of the polar residues in the middle segment are mutated, has a **MskLksgWskFkt** pattern with lower helicity content than $ALPS_{wt}$ (Fig.9.2). This mutant has attenuated binding to small liposomes and an increase in the binding to big ones (Drin *et al.*, 2007). Now again there are many aspects to take in consideration to explain this behavior: The increase of binding to big liposomes can be attributed to the lysines in Ser11 and Thr20 positions as in the case of the mutant 2Ki. However, the reduction of binding to small liposomes can be attributed to the mutation in Tyr13 and Ser18. This confirms the importance of the intrapeptide interactions we described involving Tyr13 as well as Tyr13 interaction with both the lipid headgroups and the acyl chains. Lysine, as we mentioned before, establishes hydrophobic interactions with its long aliphatic chain and charged interactions with its polar group. Lysines could therefore do as many interactions as Tyr13. Furthermore, if the bulky lysines are placed between the bulky hydrophobic residues, the steric hindrance prevents the conformational freedom of the bulky hydrophobic residues and the possibility of interactions between them. Indeed, this is likely what happens when lysines are introduced at the expense of S11, S18 and T20, which we showed produce key intrapeptide interactions in ALPS middle segment structure.

Many questions remain without clear answer, due, in part, to the structural low resolution of many of the experiments performed with ALPS mutants . However, our explanations of these mutants based on the BssB pattern hypothesis allowed us to provide some interesting conclusions and guidance for further design of experiments and analysis. First, Thr20 and the presence of aromatic-polar residues

such as Tyr13, are essential to for the curvature recognition. Secondly, the explanation exposed in the last paragraphs complement our view of sequence-specific deformability and structural flexibility to recognize the lipid-packing defaults:

1. 2Ki has lost lost helicity and the ability to stabilize deformable conformations in the absence of Thr20. It does not longer discriminate between high and low curvatures.
2. 2Kt remains helicoidal but maybe with the possibility of 3_{10}helix/turn transitions and it has become less specific to high curvatures.
3. 4Ki has lost its helical content and liberty to deform.

These experimental data, in the light of our results, show that effectively there is a sequence-specific deformability and structural flexibility that contributes to the recognition of the lipid-packing. They also sustain the possibility that the lysine-rich C-terminal region of ALPS, only contributes to the binding of the motif to the membrane, but without being part of the lipid-packing motif itself, which incidentally supports our proposal regarding the new ALPS borders. Overall this examination showed that the partitioning, the sgtructural propensities and the steric hyndrance are aspects that must be taken in account when designing mutants for the study of interfacial peptides.

Considering Hatzikis model for membrane curvature recognition, where every highly curved membrane would be able to recruit amphhipathic molecules, the experiments discussed above seems to provide more elements for this hypothesis. However, the case of mutant 2Ki that loose the possibility of stabilize the 3_{10}helix/turn transitions, concomintantly loosing the specificity for small liposomes, suggest that this structure could be relevant.

9.8 Conclusions

Here we propose that the flexibility and deformability of ALPS are essential for the efficient recognition of the lipid packing defects at the level of the acyl chains and polar heads. Curvature sensors like ALPS may display interactions with both the polar heads and the hydrophobic core that allow them to efficiently explore the interface surroundings. A perfect α-helix would result in an obstacle to explore the interface, but a deformable helical arrangement seems to be the most adapted solution to this problem. In this context, and since the membrane interface is a very crowded environment, the Bulky-small&polar-Bulky pattern suggests that ALPS explores the interface and senses lipid packing defects usingbulky residues that can be flexible enough thanks to the neighboring small and neutral residues. The bulky residues can either explore the hydrophobic core-glycerol region (Leu,Val, Ile, Met, Phe) or the headgroup-glycerol interface (Tyr, Trp). Moreover, the small neutral residues as glycines help the adoption of favorable conformations, while the small polar residues between the bulky ones can be useful for establishing H-bonds interactions with the lipids oxygens, at the same time that contribute to modulate the different peptide conformations.

We also suggest that ALPS can induce adaptative dynamic responses to the membrane that leads to bilayer-coupling effect and a reciprocal orchestrated adaptation process. We have shown how the

absence of lipid-packing defaults avoids ALPS deformability and structural flexibility, affecting in consequence important intra-peptide and lipid-peptide interactions. Our results highlight that deformability and structural flexibility of ALPS are correlated with the presence of lipid-packing defaults in the membrane. In consequence, the deformability is space-dependent from to perspectives : the available space in the bilayer interface for deformation, and the space available in the sequence vicinity to allow conformational liberty of ALPS side chains. Therefore, this plasticity of ALPS must be of great relevance for its curvature sensitivity. The partitioning of ALPS at the interfacial phosphate/glycerol level suggests an adaptive interplay between the peptide-sequence geometrical and space restrictions, the lipids conformations and the physical forces that shape the membranes.

We can imagine that in curved membranes the lipid dynamics contribute to in the formation of "dynamic" lipid-packing defaults. Thus, we can expect that the particularities of ALPS, with respect to other interfacial amphipathic helices, reside on its ability to be sufficiently deformable and structurally flexible to establish specific intra-peptide and lipid-peptide interactions that allow it to span all the dimensions of the interface to optimally recognize these "dynamic" inhomogeneities.Hatzakis *et al.* (2009) proposed that the curved membranes in generale, are responsable of the recruitment of different "adaptors" to their lipid-packing defaults. The fact that ALPS exhibit a particular amino acid composition, - that contrast with must of the interfacila amphipathic helix (that have charged residues on their polar face, for instance) - and as we shown peculiar structural behavior, suggest that there also exist molecules with special sensor capabilites, that sustantialy depend on the membrane that recrut them in a synchronic way. In this scenario, it is possible that not all the curved membranes would have the same "dynamic" lipid-packing defaults and that not all the interfacial amphipathic helices would be able to recognize all the curved membranes.

9.8.1 Completing ALPS curvature sensing model

We can imagine that the unfolded state of ALPS1 in the aqueous environment when approaches to the curved membrane surface thanks to hydrophobic forces, principally the aromatic residues. It start to be absorved by the membrane interface thanks to the formation of the 3_{10}helix/turn which are intermediates of a-helices folding. This structure allow the exploration and interaction at differents levels of the interface in the Z-dimension (acyl-chains, glycerol and phosphate). We suggest this is actually the driven force for the lipid-packing recognition. The 3_{10}helix get anchor to these defects while the rest of the sequence folds in an helical arrangement capable to dispose the hydrophobic in their favorable possition with respect to the acyl chains and with the serine/threonine residues disposed to stablish hydrogen bondings. Simultaneously these interactions would contribute to maintain the interaction the time needed, alleviating the stress created by the high curvature, and then favorizing the binding of ALPS2.

9.9 Perspectives

The study of the structural and dynamic roles of some ALPS sequence that we have highlighted in this work should guide further experiments as well as new molecular simulations. Form the perspective of the peptide it would be very interesting to introduce some mutations that allow distinguishing the charge effect, without perturbing the size of the amino-acids. Additionally it would be appealing to introduce small charged residues (such as aspartate) at expenses of threonines (both residues have similar sizes) or to replace serines for glutamines or asparangines (big, polar and not charged residues). These changes will give additional information about the precise role that the residue size has in ALPS function. With the same philosophy, replacement of aromatics amino acids by other kind of bulky hydrophobic residues will allow to understand the large possibilities of ALPS-like motifs to anchor the membrane. Our next step will be to simulate ALPS on curved membranes to corroborate our hypothesis on lipid-packing-recognition-dependence on conformational deformability and side chains flexibility. Moreover, these simulations will allow to corroborate the hypothesis of lipid-packing defaults dependence on the lipid dynamics and complete the interpretation of the creation of spaces in curved membranes for the recruitment of curvature sensors of different natures. On the other hand, it will be also very appealing to simulate more complicated mixtures of lipids. The success of these further researches will depend entirely on the tight collaboration between the experimentalist and the theoricians. For instance, it would be extreamly interesting to perform NMR experiments to corroborate the importance of the 3_{10}helix/turn transitions as a function of the curvature.

Finally, I consider of importance to recall that additionally to the ALPS-like sensors motifs analyzed by Drin et al, many others ALPS-like sequences were identified. It is highly possible that many of them are also curvature sensors. It would be suitable that the rich list of potential ALPS motifs is examined in detail using the structural information we provide here to discriminate the more probable candidates. Only using functional information it will be possible to corroborate these predictions. We have already started to look for the BssB pattern in those ALPS-like sequences, applying the criteria we used here to characterize ALPS sensor motif structural properties.

It would be also interesting to screen other organisms sequences databases, since in archea and gram (+) and gram (-) bacteria there also exist the formation of vesicles and some interesting curved forms are display. Maybe it would be possible to find ALPS motifs on that kind of organisms.

Bibliography

Ahumada H, Montecinos R, Tieleman DP, Weiss-Lopez BE, Aliste MP, MacCallum JL, et al. Molecular dynamics simulations of pentapeptides at interfaces: salt bridge and cation-pi interactions. J Phys Chem A 2003; 42: 8976–87. Eng.

Alder B, Wainwright T. Studies in Molecular Dynamics. I. General Method. Journal of Chemical Physics 1959; 31: 459. Studies in Molecular Dynamics. I. General Method.

Aliste MP, Tieleman DP. Computer simulation of partitioning of ten pentapeptides Ace-WLXLL at the cyclohexane/water and phospholipid/water interfaces. BMC Biochem 2005; 6: 30. Eng.

Allan VJ, Schroer TA. Membrane motors. Curr Opin Cell Biol 1999; 11: 476–82. Eng.

Amor JC, Harrison DH, Kahn RA, Ringe D. Structure of the human ADP-ribosylation factor 1 complexed with GDP. Nature 1994; 372: 704–8. Eng.

Anezo C, de Vries A, Holtje H, Tiueleman P, Marrink S. Methodological Issues in Lipid Bilayer Simulations. J Phys Chem B 2003; 107: 9424–9433.

Antonny B, Beraud-Dufour S, Chardin P, Chabre M. N-terminal hydrophobic residues of the G-protein ADP-ribosylation factor-1 insert into membrane phospholipids upon GDP to GTP exchange. Biochemistry 1997a; 36: 4675–84. Eng.

Antonny B, Gounon P, Schekman R, Orci L. Self-assembly of minimal COPII cages. EMBO Rep 2003; 4: 419–24. Eng.

Antonny B, Huber I, Paris S, Chabre M, Cassel D. Activation of ADP-ribosylation factor 1 GTPase-activating protein by phosphatidylcholine-derived diacylglycerols. J Biol Chem 1997b; 272: 30848–51. Eng.

Appelt C, Eisenmenger F, Kuhne R, Schmieder P, Soderhall JA. Interaction of the antimicrobial peptide cyclo(RRWWRF) with membranes by molecular dynamics simulations. Biophys J 2005; 89: 2296–306. Eng.

Ash WL, Zlomislic MR, Oloo EO, Tieleman DP. Computer simulations of membrane proteins. Biochim Biophys Acta 2004; 1666: 158–89. Eng.

Ayton GS, Blood PD, Voth GA. Membrane remodeling from N-BAR domain interactions: insights from multi-scale simulation. Biophysical Journal 2007; 92: 3595–3602. Http://www.ncbi.nlm.nih.gov/pubmed/17325001.

Bahatyrova S, Frese RN, Siebert CA, Olsen JD, Van Der Werf KO, Van Grondelle R, et al. The native architecture of a photosynthetic membrane. Nature 2004; 430: 1058–62. Eng.

Ballesteros J, Deupi X, Olivella M, Haaksma E, Pardo L. Serine and threonine residues bend alpha-helices in the chi(1) = g(-) conformation. Biophysical Journal 2000; 79(5): 2754–2760.

Baumgart T, Hess ST, Webb WW. Imaging coexisting fluid domains in biomembrane models coupling curvature and line tension. Nature 2003; 425: 821–4. Eng.

Bechinger B. Rationalizing the membrane interactions of cationic amphipathic antimicrobial peptides by their molecular shape. Current Opinion in Colloid & Interface Science 2009; 14: 349–355.

Bemporad D, Luttmann C, Essex JW. Computer simulation of small molecule permeation across a lipid bilayer: dependence on bilayer properties and solute volume, size, and cross-sectional area. Biophys J 2004; 87: 1–13. Eng.

Berendsen HJ, Van Gunsteren WF, Zwinderman HR, Geurtsen RG. Simulations of proteins in water. Annals of the New York Academy of Sciences 1986; 482: 269–286. Http://www.ncbi.nlm.nih.gov/pubmed/3471111.

Berendsen HJC, Postma ea. Molecular dynamics with coupling to an external bath. J Chem Phys 1984; 81: 3684–3690.

Berendsen vdSDVDR HJC. GROMACS : A message-passing parallel molecular dynamics implementation. Computer Physics Communications 1995; 91: 43–56. GROMACS : A message-passing parallel molecular dynamics implementation.

Berendsen WFvG, C HJ. Groningen Molecular Simulation (GROMOS) Library Manual. Groningen, 1987. Groningen Molecular Simulation (GROMOS) Library Manual.

Berger O, Edholm O, Jhnig F. Molecular dynamics simulations of a fluid bilayer of dipalmitoylphosphatidylcholine at full hydration, constant pressure, and constant temperature. Biophysical Journal 1997; 72: 2002–2013. Http://www.ncbi.nlm.nih.gov/pubmed/9129804.

Berneche S, Nina M, Roux B. Molecular dynamics simulation of melittin in a dimyristoylphosphatidylcholine bilayer membrane. Biophys J 1998; 75: 1603–18. Eng.

Bi X, Corpina RA, Goldberg J. Structure of the Sec23/24-Sar1 pre-budding complex of the COPII vesicle coat. Nature 2002; 419: 271–7. Eng.

Bigay J, Casella JF, Drin G, Mesmin B, Antonny B. ArfGAP1 responds to membrane curvature through the folding of a lipid packing sensor motif. EMBO J 2005; 24: 2244–53. Eng.

Bigay J, Gounon P, Robineau S, Antonny B. Lipid packing sensed by ArfGAP1 couples COPI coat disassembly to membrane bilayer curvature. Nature 2003; 426: 563–6. Eng.

Blood PD, Swenson RD, Voth GA. Factors influencing local membrane curvature induction by N-BAR domains as revealed by molecular dynamics simulations. Biophysical Journal 2008; 95: 1866–1876. Http://www.ncbi.nlm.nih.gov/pubmed/18469070.

Blood PD, Voth GA. Direct observation of Bin/amphiphysin/Rvs (BAR) domain-induced membrane curvature by means of molecular dynamics simulations. Proc Natl Acad Sci U S A 2006; 103: 15068–72. Eng.

Bonifacino JS, Glick BS. The mechanisms of vesicle budding and fusion. Cell 2004; 116: 153–66. Eng.

Bromley SK, Burack WR, Johnson KG, Somersalo K, Sims TN, Sumen C, et al. The immunological synapse. Annu Rev Immunol 2001; 19: 375–96. Eng.

Brooks BR, Bruccoleri RE, Olafson BD, States DJ, Swaminathan S, Karplus M. CHARMM: A program for macromolecular energy, minimization, and dynamics calculations. Journal of Computational Chemistry 1983; 4: 187–217.

Bucki R, Giraud F, Sulpice JC. Phosphatidylinositol 4,5-bisphosphate domain inducers promote phospholipid transverse redistribution in biological membranes. Biochemistry 2000; 39: 5838–44. Eng.

Buton X, Morrot G, Fellmann P, Seigneuret M. Ultrafast glycerophospholipid-selective transbilayer motion mediated by a protein in the endoplasmic reticulum membrane. J Biol Chem 1996; 271: 6651–7. Eng.

Campbell JBR Neil A, Mitchell LG. Biology. Addison Wesley Longman, Inc, 1999. Biology.

Campelo F, McHanon H, Kozlov M. The hydrophobic insertion Mechanism of membrnae curvature generation by proteins. Biophys J 2008; 95: 2325–2339.

Canutescu AA, Shelenkov AA, Dunbrack RL. A graph-theory algorithm for rapid protein side-chain prediction. Protein Science: A Publication of the Protein Society 2003; 12: 2001–2014. Http://www.ncbi.nlm.nih.gov/pubmed/12930999.

Carstanjen D, Yamauchi A, Koornneef A, Zang H, Filippi MD, Harris C, et al. Rac2 regulates neutrophil chemotaxis, superoxide production, and myeloid colony formation through multiple distinct effector pathways. J Immunol 2005; 174: 4613–20. Eng.

Chakrabartty A, Doig AJ, Baldwin RL. Helix capping propensities in peptides parallel those in proteins. Proc Natl Acad Sci U S A 1993a; 90: 11332–6. Eng.

Chakrabartty A, Kortemme T, Baldwin RL. Helix propensities of the amino acids measured in alanine-based peptides without helix-stabilizing side-chain interactions. Protein Sci 1994; 3: 843–52. Eng.

Chakrabartty A, Kortemme T, Padmanabhan S, Baldwin RL. Aromatic side-chain contribution to far-ultraviolet circular dichroism of helical peptides and its effect on measurement of helix propensities. Biochemistry 1993b; 32: 5560–5. Eng.

Chakrabartty A, Schellman JA, Baldwin RL. Large differences in the helix propensities of alanine and glycine. Nature 1991; 351: 586–588. Http://www.ncbi.nlm.nih.gov/pubmed/2046766.

Chandler DE, Hsin J, Harrison CB, Gumbart J, Schulten K. Intrinsic curvature properties of photosynthetic proteins in chromatophores. Biophys J 2008; 95: 2822–36. Eng.

Chandrasekhar I, Kastenholz M, Lins RD, Oostenbrink C, Schuler LD, Tieleman DP, et al. A consistent potential energy parameter set for lipids: dipalmitoylphosphatidylcholine as a benchmark of the GROMOS96 45A3 force field. Eur Biophys J 2003; 32: 67–77. Eng.

Chen CP, Kernytsky A, Rost B. Transmembrane helix predictions revisited. Protein Sci 2002; 11: 2774–91. Eng.

Chen CS, Mrksich M, Huang S, Whitesides GM, Ingber DE. Geometric control of cell life and death. Science (New York, NY) 1997; 276: 1425–1428.

Chipot C, Maigret B, Pohorille A. Early events in the folding of an amphipathic peptide: A multi-nanosecond molecular dynamics study. Proteins 1999; 36: 383–99. Eng.

Chiu SW, Jakobsson E, Mashl RJ, Scott HL. Cholesterol-induced modifications in lipid bilayers: a simulation study. Biophys J 2002; 83: 1842–53. Eng.

Chou PY, Fasman GD. Conformational parameters for amino acids in helical, beta-sheet, and random coil regions calculated from proteins. Biochemistry 1974; 13: 211–22. Eng.

Clementi C. Coarse-grained models of protein folding: toy models or predictive tools? Current Opinion in Structural Biology 2008; 18: 10–15. Http://www.ncbi.nlm.nih.gov/pubmed/18160277.

Cole NB, Sciaky N, Marotta A, Song J, Lippincott-Schwartz J. Golgi dispersal during microtubule disruption: regeneration of Golgi stacks at peripheral endoplasmic reticulum exit sites. Mol Biol Cell 1996; 7: 631–50. Eng.

Coorssen JR, Blank PS, Albertorio F, Bezrukov L, Kolosova I, Chen X, et al. Regulated secretion: SNARE density, vesicle fusion and calcium dependence. J Cell Sci 2003; 116: 2087–97. Eng.

Cornell RB, Taneva SG. Amphipathic helices as mediators of the membrane interaction of amphitropic proteins, and as modulators of bilayer physical properties. Curr Protein Pept Sci 2006; 7: 539–52. Eng.

Cornell WD, Cieplak P, Bayly CI, Gould IR, Merz KM, Ferguson DM, et al. A Second Generation Force Field for the Simulation of Proteins, Nucleic Acids, and Organic Molecules. Journal of the American Chemical Society 1995; 117: 5179–5197.

Cukierman E, Pankov R, Stevens DR, Yamada KM. Taking cell-matrix adhesions to the third dimension. Science 2001; 294: 1708–12. Eng.

D P, PJ L, RM G. The X-ray crystal structure of the membrane protein prostaglandin H2 synthase-1. Nature 1994; 367(6460): 243Ð249.

Dabora SL, Sheetz MP. The microtubule-dependent formation of a tubulovesicular network with characteristics of the ER from cultured cell extracts. Cell 1988; 54: 27–35. Eng.

Dahl DB, Bohannan Z, Mo Q, Vannucci M, Tsai J. Assessing side-chain perturbations of the protein backbone: a knowledge-based classification of residue Ramachandran space. Journal of Molecular Biology 2008; 378: 749–758. Http://www.ncbi.nlm.nih.gov/pubmed/18377931.

Darden T, York D, Pedersen L. Particle mesh Ewald: An N [center-dot] log(N) method for Ewald sums in large systems. The Journal of Chemical Physics 1993; 98: 10092, 10089–10092, 10089.

Dawson JC, Legg JA, Machesky LM. Bar domain proteins: a role in tubulation, scission and actin assembly in clathrin-mediated endocytosis. Trends Cell Biol 2006; 16: 493–8. Eng.

de Joannis J, Jiang FY, Kindt JT. Coarse-grained model simulations of mixed-lipid systems: composition and line tension of a stabilized bilayer edge. Langmuir 2006a; 22: 998–1005. Eng.

de Joannis J, Jiang Y, Yin F, Kindt JT. Equilibrium distributions of dipalmitoyl phosphatidylcholine and dilauroyl phosphatidylcholine in a mixed lipid bilayer: atomistic semigrand canonical ensemble simulations. J Phys Chem B 2006b; 110: 25875–82. Eng.

De Krujiff CAVAHMVECTT B. Lipid polymorphism and membrane function. In Martonosi, A, editors, The Enzyme of Biological Membranes. Plenum Press, 1985; pp. 131–204. Lipid polymorphism and membrane function.

de Planque MRR, Killian JA. Protein lipid interactions studied with designed transmembrane peptides: role of hydrophobic matching and interfacial anchoring (Review). Molecular Membrane Biology 2003; 20: 271–271.

De Vos KJ, Allan VJ, Grierson AJ, Sheetz MP. Mitochondrial function and actin regulate dynamin-related protein 1-dependent mitochondrial fission. Curr Biol 2005; 15: 678–83. Eng.

de Vries AH, Mark AE, Marrink SJ. Molecular dynamics simulation of the spontaneous formation of a small DPPC vesicle in water in atomistic detail. J Am Chem Soc 2004a; 126: 4488–9. Eng.

de Vries AH, Mark AE, Marrink SJ. Molecular dynamics simulation of the spontaneous formation of a small DPPC vesicle in water in atomistic detail. Journal of the American Chemical Society 2004b; 126: 4488–4489. Http://www.ncbi.nlm.nih.gov/pubmed/15070345.

Deber CM, Khan AR, Li Z, Joensson C, Glibowicka M, Wang J. Val–>Ala mutations selectively alter helix-helix packing in the transmembrane segment of phage M13 coat protein. Proc Natl Acad Sci U S A 1993; 90: 11648–52. Eng.

Debret G, Valadie H, Stadler AM, Etchebest C. New insights of membrane environment effects on MscL channel mechanics from theoretical approaches. Proteins 2008; 71: 1183–96. Eng.

DeLano W. The PyMOL Molecular Graphics System. 2002. Http://www.pymol.org.

Delaye L, Becerra A, Lazcano A. The last common ancestor: what's in a name? Origins of Life and Evolution of the Biosphere: The Journal of the International Society for the Study of the Origin of Life 2005; 35: 537–554.

Deupi X, Olivella M, Govaerts C, Ballesteros J, Campillo M, Pardo L. Ser and Thr Residues Modulate the Conformation of Pro-Kinked Transmembrane alpha-Helices. Biophysical Journal 2004; 86(1): 105–115.

Deupi X, Olivella M, Sanz A, Dolker N, Campillo L M Pardo. Influence of the g- conformation of Ser and Thr on the structure of transmembrane helices. Journal of Structural biology 2009; In press.

Devaux PF. Is lipid translocation involved during endo- and exocytosis? Biochimie 2000; 82: 497–509. Eng.

Doherty GJ, McMahon HT. Mechanisms of endocytosis. Annu Rev Biochem 2009; 78: 857–902. Eng.

Doig ENIT AJ. Stability and design of alpha-helices. In Wiley, editor, Protein Folding handbook, volume 1. Weinheim, Germany, 2005; pp. 247–313. Stability and design of alpha-helices.

Dolan EA, Venable RM, Pastor RW, Brooks BR. Simulations of membranes and other interfacial systems using P2(1) and Pc periodic boundary conditions. Biophys J 2002; 82: 2317–25. Eng.

Doyle DA, Morais Cabral J, Pfuetzner RA, Kuo A, Gulbis JM, Cohen SL, et al. The structure of the potassium channel: molecular basis of K+ conduction and selectivity. Science 1998; 280: 69–77. Eng.

Drin G, Bigay J, Antonny B. Regulation of the vesicular transport by the membrane curvature. Synthese Reviews (in french) 2009; 25: 483–488.

Drin G, Casella JF, Gautier R, Boehmer T, Schwartz TU, Antonny B. A general amphipathic alpha-helical motif for sensing membrane curvature. Nat Struct Mol Biol 2007; 14: 138–46. Eng.

Drin G, Morello V, Casella JF, Gounon P, Antonny B. Asymmetric tethering of flat and curved lipid membranes by a golgin. Science 2008; 320: 670–3. Eng.

Durrieu MP, Peter JB, Mark SPS, Richard L, Marc B. Coarse-Grain Simulations of the R-SNARE Fusion Protein in its Membrane Environment Detect Long-Lived Conformational Sub-States. ChemPhysChem 2009; 10: 1548–1552.

Edholm O, Berger O, Jahnig F. Structure and fluctuations of bacteriorhodopsin in the purple membrane: a molecular dynamics study. J Mol Biol 1995; 250: 94–111. Eng.

Edidin M. Lipids on the frontier: a century of cell-membrane bilayers. Nat Rev Mol Cell Biol 2003; 4: 414–8. Eng.

Efremov RG, Nolde DE, Konshina AG, Syrtcev NP, Arseniev AS. Peptides and proteins in membranes: what can we learn via computer simulations? Curr Med Chem 2004; 11: 2421–42. Eng.

Egea G, Lazaro-Dieguez F, Vilella M. Actin dynamics at the Golgi complex in mammalian cells. Curr Opin Cell Biol 2006; 18: 168–78. Eng.

Engelman D. Membranes are more mosaic than fluid. Nature 2005; 438: 578–580.

Engelman DM, Steitz TA, Goldman A. Identifying nonpolar transbilayer helices in amino acid sequences of membrane proteins. Annu Rev Biophys Biophys Chem 1986; 15: 321–53. Eng.

Essmann U, Perera L, Berkowitz M, Darden T, Lee H, Pedersen L. A smooth particle mesh Ewald method. The Journal of Chemical Physics 1995; 103: 8593, 8577–8593, 8577.

Everard-Gigot V, Dunn CD, Dolan BM, Brunner S, Jensen RE, Stuart RA. Functional analysis of subunit e of the F1Fo-ATP synthase of the yeast Saccharomyces cerevisiae: importance of the N-terminal membrane anchor region. Eukaryot Cell 2005; 4: 346–55. Eng.

Farsad K, De Camilli P. Mechanisms of membrane deformation. Curr Opin Cell Biol 2003; 15: 372–81. Eng.

Farsad K, Ringstad N, Takei K, Floyd SR, Rose K, De Camilli P. Generation of high curvature membranes mediated by direct endophilin bilayer interactions. J Cell Biol 2001; 155: 193–200. Eng.

Fath S, Mancias JD, Bi X, Goldberg J. Structure and organization of coat proteins in the COPII cage. Cell 2007; 129: 1325–36. Eng.

Feigenson GW. Phase behavior of lipid mixtures. Nat Chem Biol 2006; 2: 560–3. Eng.

Feller SE. Molecular dynamics simulations as a complement to nuclear magnetic resonance and X-ray diffraction measurements. Methods in Molecular Biology (Clifton, NJ) 2007; 400: 89–102. Http://www.ncbi.nlm.nih.gov/pubmed/17951729.

Feller SE, Gawrisch K. Properties of docosahexaenoic-acid-containing lipids and their influence on the function of rhodopsin. Curr Opin Struct Biol 2005; 15: 416–22. Eng.

Fischer T, Lu L, Haigler HT, Langen R. Annexin B12 Is a Sensor of Membrane Curvature and Undergoes Major Curvature-dependent Structural Changes. J Biol Chem 2007; 282: 9996–10004. Http://www.jbc.org/cgi/content/abstract/282/13/9996.

Ford MG, Mills IG, Peter BJ, Vallis Y, Praefcke GJ, Evans PR, et al. Curvature of clathrin-coated pits driven by epsin. Nature 2002; 419: 361–6. Eng.

Forterre P, Gribaldo S, Brochier C. [Luca: the last universal common ancestor]. Medecine Sciences: M/S 2005; 21: 860–865.

Fotin A, Cheng Y, Sliz P, Grigorieff N, Harrison SC, Kirchhausen T, et al. Molecular model for a complete clathrin lattice from electron cryomicroscopy. Nature 2004; 432: 573–9. Eng.

Fowler PW, Balali-Mood K, Deol S, Coveney PV, Sansom MS. Monotopic enzymes and lipid bilayers: a comparative study. Biochemistry 2007; 46: 3108–15. Eng.

Freitas MS, Gaspar LP, Lorenzoni M, Almeida FC, Tinoco LW, Almeida MS, et al. Structure of the Ebola fusion peptide in a membrane-mimetic environment and the interaction with lipid rafts. J Biol Chem 2007; 282: 27306–14. Eng.

Frese RN, Pamies JC, Olsen JD, Bahatyrova S, van der Weij-de Wit CD, Aartsma TJ, et al. Protein shape and crowding drive domain formation and curvature in biological membranes. Biophys J 2008; 94: 640–7. Eng.

Frese RN, Siebert CA, Niederman RA, Hunter CN, Otto C, van Grondelle R. The long-range organization of a native photosynthetic membrane. Proc Natl Acad Sci U S A 2004; 101: 17994–9. Eng.

Gallop JL, McMahon HT. BAR domains and membrane curvature: bringing your curves to the BAR. Biochem Soc Symp 2005; : 223–31Eng.

Gao X, Wong TC. Molecular dynamics simulation of adrenocorticotropin (1-10) peptide in a solvated dodecylphosphocholine micelle. Biopolymers 2001; 58: 643–59. Eng.

Gautier R, Camproux AC, Tuffery P. SCit: web tools for protein side chain conformation analysis. Nucleic Acids Research 2004; 32: W508–511–W508–511. Http://www.ncbi.nlm.nih.gov/pubmed/15215438.

Gautier R, Douguet D, Antonny B, Drin G. HELIQUEST: a web server to screen sequences with specific alpha-helical properties. Bioinformatics 2008; 24: 2101–2. Eng.

Giraud MF, Paumard P, Soubannier V, Vaillier J, Arselin G, Salin B, et al. Is there a relationship between the supramolecular organization of the mitochondrial ATP synthase and the formation of cristae? Biochim Biophys Acta 2002; 1555: 174–80. Eng.

Gortel E, Grendel F. On bimolecular layers of lipoid on the chromocytes of the blood. J Exp Med 1925; 41: 439–443. On bimolecular layers of lipoid on the chromocytes of the blood.

Gumbart J, Wang Y, Aksimentiev A, Tajkhorshid E, Schulten K. Molecular dynamics simulations of proteins in lipid bilayers. Curr Opin Struct Biol 2005; 15: 423–31. Eng.

Gurtovenko AA, Vattulainen I. Effect of NaCl and KCl on phosphatidylcholine and phosphatidylethanolamine lipid membranes: insight from atomic-scale simulations for understanding salt-induced effects in the plasma membrane. J Phys Chem B 2008; 112: 1953–62. Eng.

Gurtovenko AA, Vattulainen I. Intrinsic potential of cell membranes: opposite effects of lipid transmembrane asymmetry and asymmetric salt ion distribution. The Journal of Physical Chemistry B 2009; 113: 7194–7198. Http://www.ncbi.nlm.nih.gov/pubmed/19388690.

Han X, Gross RW. Global analyses of cellular lipidomes directly from crude extracts of biological samples by ESI mass spectrometry: a bridge to lipidomics. J Lipid Res 2003; 44: 1071–9. Eng.

Haney EF, Hunter HN, Matsuzaki K, Vogel HJ. Solution NMR studies of amphibian antimicrobial peptides: linking structure to function? Biochim Biophys Acta 2009; 1788: 1639–55. Eng.

Hatzakis NS, Bhatia VK, Larsen J, Madsen KL, Bolinger PY, Kunding AH, et al. How curved membranes recruit amphipathic helices and protein anchoring motifs. Nat Chem Biol 2009; Eng.

Hess B, Bekker H, Berendsen HJC, Fraaije JGEM. LINCS: A linear constraint solver for molecular simulations. Journal of Computational Chemistry 1997; 18: 1463–1472.

Hinshaw JE, Schmid SL. Dynamin self-assembles into rings suggesting a mechanism for coated vesicle budding. Nature 1995; 374: 190–2. Eng.

Hirokawa N. Kinesin and dynein superfamily proteins and the mechanism of organelle transport. Science 1998; 279: 519–26. Eng.

Holthuis JC, Levine TP. Lipid traffic: floppy drives and a superhighway. Nat Rev Mol Cell Biol 2005; 6: 209–20. Eng.

Hong YH, Won HS, Ahn HC, Lee BJ. Structural Elucidation of the Protein- and Membrane-Binding Properties of the N-Terminal Tail Domain of Human Annexin II. J Biochem 2003; 134: 427–432. Http://jb.oxfordjournals.org/cgi/content/abstract/134/3/427.

Hristova K, Dempsey CE, White SH. Structure, location, and lipid perturbations of melittin at the membrane interface. Biophys J 2001; 80: 801–11. Eng.

Humphrey W, Dalke A, Schulten K. VMD: visual molecular dynamics. Journal of Molecular Graphics 1996; 14: 33–8, 27–8–33–8, 27–8. Http://www.ncbi.nlm.nih.gov/pubmed/8744570.

Huttner WB, Zimmerberg J. Implications of lipid microdomains for membrane curvature, budding and fission. Curr Opin Cell Biol 2001; 13: 478–84. Eng.

Jang H, Ma B, Woolf TB, Nussinov R. Interaction of protegrin-1 with lipid bilayers: membrane thinning effect. Biophys J 2006; 91: 2848–59. Eng.

Janmey PA, Kinnunen PK. Biophysical properties of lipids and dynamic membranes. Trends Cell Biol 2006a; 16: 538–46. Eng.

Janmey PA, Kinnunen PKJ. Biophysical properties of lipids and dynamic membranes. Trends in Cell Biology 2006b; 16: 538–546.

Jao CC, Der-Sarkissian A, Chen J, Langen R. Structure of membrane-bound alpha-synuclein studied by site-directed spin labeling. Proc Natl Acad Sci U S A 2004; 101: 8331–6. Eng.

Jayasinghe SA, Langen R. Membrane interaction of islet amyloid polypeptide. Biochim Biophys Acta 2007; 1768: 2002–9. Eng.

Jekely G. Did the last common ancestor have a biological membrane? Biology Direct 2006; 1: 35–35. Http://www.ncbi.nlm.nih.gov/pubmed/17129384.

Jekely G. Origin of Eukaryotic Endomembranes: A Critical Evaluation of Different Model Scenarios. In Eukaryotic Membranes and Cytoskeleton. 2007; pp. 38–51.

Johnson RM, Hecht K, Deber CM. Aromatic and cation-pi interactions enhance helix-helix association in a membrane environment. Biochemistry 2007; 46: 9208–9214. Http://www.ncbi.nlm.nih.gov/pubmed/17658897.

Johnson RM, Rath A, Melnyk RA, Deber CM. Lipid solvation effects contribute to the affinity of Gly-xxx-Gly motif-mediated helix-helix interactions. Biochemistry 2006; 45: 8507–15. Eng.

Jonson PH, Petersen SB. A critical view on conservative mutations. Protein Eng 2001; 14: 397–402. Eng.

Jorgensen W, Maxwell DS, Tirado-Rives J. Development and Testing of the OPLS All-Atom Force Field on Conformational Energetics and Properties of Organic Liquids. Journal of the American Chemical Society 1996; 118: 11225–11236. 10.1021/ja9621760.

Jorgensen WL. Revised TIPS for simulations of liquid water and aqueous solutions. The Journal of Chemical Physics 1982; 77: 4156–4163. Http://link.aip.org/link/?JCP/77/4156/1.

Kabsch W, Sander C. Dictionary of protein secondary structure: Pattern recognition of hydrogen-bonded and geometrical features. Biopolymers 1983; 22: 2577–2637.

Kandasamy SK, Larson RG. Binding and insertion of alpha-helical anti-microbial peptides in POPC bilayers studied by molecular dynamics simulations. Chem Phys Lipids 2004; 132: 113–32. Eng.

Kandt C, Xu Z, Tieleman DP. Opening and closing motions in the periplasmic vitamin B12 binding protein BtuF. Biochemistry 2006; 45: 13284–92. Eng.

Karplus M, Petsko GA. Molecular dynamics simulations in biology. Nature 1990; 347: 631–9. Eng.

Khandelia H, Ipsen JH, Mouritsen OG. The impact of peptides on lipid membranes. Biochimica Et Biophysica Acta 2008; 1778: 1528–1536. Http://www.ncbi.nlm.nih.gov/pubmed/18358231.

Koonin EV, Martin W. On the origin of genomes and cells within inorganic compartments. Trends in Genetics: TIG 2005; 21: 647–654.

Kozlov MM. Dynamin: possible mechanism of "Pinchase" action. Biophys J 1999; 77: 604–16. Eng.

Kozlov MM. Fission of biological membranes: interplay between dynamin and lipids. Traffic 2001; 2: 51–65. Eng.

Kung C. A possible unifying principle for mechanosensation. Nature 2005; 436: 647–54. Eng.

Kusumi A, Suzuki K. Toward understanding the dynamics of membrane-raft-based molecular interactions. Biochim Biophys Acta 2005; 1746: 234–51. Eng.

La Rocca P, Biggin PC, Tieleman DP, Sansom MS. Simulation studies of the interaction of antimicrobial peptides and lipid bilayers. Biochim Biophys Acta 1999; 1462: 185–200. Eng.

Landolt-Marticorena C, Williams KA, Deber CM, Reithmeier RA. Non-random distribution of amino acids in the transmembrane segments of human type I single span membrane proteins. J Mol Biol 1993; 229: 602–8. Eng.

Lee JSMCGSK Eric H; Hsin. Discovery Through the Computational Microscope. Structure 2009; 17: 1295–1306.

Lee MC, Orci L, Hamamoto S, Futai E, Ravazzola M, Schekman R. Sar1p N-terminal helix initiates membrane curvature and completes the fission of a COPII vesicle. Cell 2005; 122: 605–17. Eng.

Li SC, Deber CM. Glycine and beta-branched residues support and modulate peptide helicity in membrane environments. FEBS Lett 1992a; 311: 217–20. Eng.

Li SC, Deber CM. Glycine and beta-branched residues support and modulate peptide helicity in membrane environments. FEBS Letters 1992b; 311: 217–220. Http://www.ncbi.nlm.nih.gov/pubmed/1397317.

Li SC, Deber CM. Influence of glycine residues on peptide conformation in membrane environments. Int J Pept Protein Res 1992c; 40: 243–8. Eng.

Li SC, Deber CM. A measure of helical propensity for amino acids in membrane environments. Nat Struct Biol 1994a; 1: 558. Eng.

Li SC, Deber CM. A measure of helical propensity for amino acids in membrane environments. Nat Struct Mol Biol 1994b; 1: 368–373.

Li SC, Goto NK, Williams KA, Deber CM. Alpha-helical, but not beta-sheet, propensity of proline is determined by peptide environment. Proc Natl Acad Sci U S A 1996; 93: 6676–81. Eng.

Lindahl E, Edholm O. Mesoscopic undulations and thickness fluctuations in lipid bilayers from molecular dynamics simulations. Biophys J 2000; 79: 426–33. Eng.

Lindahl HBvdSD E. Gromacs 3.0: A package for molecular simulation and trajectory analysis. Journal of Molecular Modeling 2001; 7: 306–317. Gromacs 3.0: A package for molecular simulation and trajectory analysis.

Lippincott-Schwartz J, Roberts TH, Hirschberg K. Secretory protein trafficking and organelle dynamics in living cells. Annu Rev Cell Dev Biol 2000; 16: 557–89. Eng.

Liu LP, Deber CM. Uncoupling Hydrophobicity and Helicity in Transmembrane Segments. alpha - HELICAL PROPENSITIES OF THE AMINO ACIDS IN NON-POLAR ENVIRONMENTS. J Biol Chem 1998a; 273: 23645–23648. Http://www.jbc.org/cgi/content/abstract/273/37/23645.

Liu LP, Deber CM. Uncoupling hydrophobicity and helicity in transmembrane segments. Alpha-helical propensities of the amino acids in non-polar environments. J Biol Chem 1998b; 273: 23645–8. Eng.

Lomize AL, Pogozheva ID, Lomize MA, Mosberg HI. The role of hydrophobic interactions in positioning of peripheral proteins in membranes. BMC Struct Biol 2007; 7: 44. Eng.

Lopez-Garcia P, Moreira D. The Syntrophy Hypothesis for the Origin of Eukaryotes. In Symbiosis. 2004; pp. 131–146.

Losev E, Reinke CA, Jellen J, Strongin DE, Bevis BJ, Glick BS. Golgi maturation visualized in living yeast. Nature 2006; 441: 1002–6. Eng.

Lukas D Schuler WFvG Xavier Daura. An improved GROMOS96 force field for aliphatic hydrocarbons in the condensed phase. Journal of Computational Chemistry 2001; 22: 1205–1218. An improved GROMOS96 force field for aliphatic hydrocarbons in the condensed phase.

M M, I N, A E, von Heijne G. Turns in transmembrane helices: determination of the minimal length of a 'helical hairpin' and derivation of a fine-grained turn propensity scale. Journal of Molecular Biolog 1999; 293 (4): 807–814.

M PJ, E JM, B HI. The C terminus of penicillin-binding protein 5 is essential for localisation to the E. coli inner membrane. EMBO J 1986; 5: 2399Ð2405.

MacCallum JL, Bennett WFD, Tieleman DP. Partitioning of Amino Acid Side Chains into Lipid Bilayers: Results from Computer Simulations and Comparison to Experiment. J Gen Physiol 2007; 129: 371–377. Http://jgp.rupress.org.

MacCallum JL, Bennett WFD, Tieleman DP. Distribution of amino acids in a lipid bilayer from computer simulations. Biophysical Journal 2008; 94: 3393–3404. Http://www.ncbi.nlm.nih.gov/pubmed/18212019.

MacCallum JL, Tieleman DP. Calculation of the water-cyclohexane transfer free energies of neutral amino acid side-chain analogs using the OPLS all-atom force field. J Comput Chem 2003; 24: 1930–5. Eng.

MacCallum JL, Tieleman DP. Computer simulation of the distribution of hexane in a lipid bilayer: spatially resolved free energy, entropy, and enthalpy profiles. J Am Chem Soc 2006; 128: 125–30. Eng.

Mackerell J A D. Empirical force fields for biological macromolecules: overview and issues. J Comput Chem 2004; 25: 1584–604. Eng.

Manneville JB, Casella JF, Ambroggio E, Gounon P, Bertherat J, Bassereau P, et al. COPI coat assembly occurs on liquid-disordered domains and the associated membrane deformations are limited by membrane tension. Proc Natl Acad Sci U S A 2008; 105: 16946–51. Eng.

Marrink SJ, de Vries AH, Tieleman DP. Lipids on the move: simulations of membrane pores, domains, stalks and curves. Biochim Biophys Acta 2009a; 1788: 149–68. Eng.

Marrink SJ, de Vries AH, Tieleman DP. Lipids on the move: simulations of membrane pores, domains, stalks and curves. Biochim Biophys Acta 2009b; 1788: 149–68. Eng.

Marrink SJ, Jahnig F, Berendsen HJ. Proton transport across transient single-file water pores in a lipid membrane studied by molecular dynamics simulations. Biophys J 1996; 71: 632–47. Eng.

Marrink SJ, Lindahl E, Edholm O, Mark AE. Simulation of the spontaneous aggregation of phospholipids into bilayers. J Am Chem Soc 2001; 123: 8638–9. Eng.

Marrink SJ, Mark AE. Molecular view of hexagonal phase formation in phospholipid membranes. Biophys J 2004; 87: 3894–900. Eng.

Marrink SJ, Risselada HJ, Yefimov S, Tieleman DP, de Vries AH. The MARTINI force field: coarse grained model for biomolecular simulations. The Journal of Physical Chemistry B 2007; 111: 7812–7824. Http://www.ncbi.nlm.nih.gov/pubmed/17569554.

Marrink SJ, Tieleman DP. Molecular dynamics simulation of a lipid diamond cubic phase. J Am Chem Soc 2001; 123: 12383–91. Eng.

Martinez-Seara H, Rog T, Karttunen M, Reigada R, Vattulainen I. Influence of cis double-bond parametrization on lipid membrane properties: how seemingly insignificant details in force-field change even qualitative trends. J Chem Phys 2008a; 129: 105103. Eng.

Martinez-Seara H, Rog T, Pasenkiewicz-Gierula M, Vattulainen I, Karttunen M, Reigada R. Interplay of unsaturated phospholipids and cholesterol in membranes: effect of the double-bond position. Biophys J 2008b; 95: 3295–305. Eng.

Marty NJ, Rajalingam D, Kight AD, Lewis NE, Fologea D, Kumar TK, et al. The membrane-binding motif of the chloroplast signal recognition particle receptor (cpFtsY) regulates GTPase activity. J Biol Chem 2009; 284: 14891–903. Eng.

Matthes D, de Groot BL. Secondary structure propensities in peptide folding simulations: a systematic comparison of molecular mechanics interaction schemes. Biophys J 2009; 97: 599–608. Eng.

McCammon JA, Karplus M. Internal motions of antibody molecules. Nature 1977; 268: 765–6. Eng.

McIntosh TJ. Overview of Membrane Rafts. In Lipid Rafts. 2007; pp. 1–7.

McMahon HT, Gallop JL. Membrane curvature and mechanisms of dynamic cell membrane remodelling. Nature 2005; 438: 590–6. Eng.

McMahon HT, Mills IG. COP and clathrin-coated vesicle budding: different pathways, common approaches. Curr Opin Cell Biol 2004; 16: 379–91. Eng.

Mesmin B, Drin G, Levi S, Rawet M, Cassel D, Bigay J, et al. Two lipid-packing sensor motifs contribute to the sensitivity of ArfGAP1 to membrane curvature. Biochemistry 2007; 46: 1779–90. Eng.

Miller S, Krijnse-Locker J. Modification of intracellular membrane structures for virus replication. Nature Reviews Microbiology 2008; 6: 363–374.

Mishra VK, Palgunachari MN. Interaction of model class A1, class A2, and class Y amphipathic helical peptides with membranes. Biochemistry 1996; 35: 11210–11220. Http://www.ncbi.nlm.nih.gov/pubmed/8780526.

Mishra VK, Palgunachari MN, Krishna R, Glushka J, Segrest JP, Anantharamaiah GM. Effect of leucine to phenylalanine substitution on the nonpolar face of a class A amphipathic helical peptide on its interaction with lipid: high resolution solution NMR studies of 4F-dimyristoylphosphatidylcholine discoidal complex. The Journal of Biological Chemistry 2008; 283: 34393–34402. Http://www.ncbi.nlm.nih.gov/pubmed/18845546.

Mishra VK, Palgunachari MN, Lund-Katz S, Phillips MC, Segrest JP, Anantharamaiah GM. Effect of the arrangement of tandem repeating units of class A amphipathic alpha-helixes on lipid interaction. The Journal of Biological Chemistry 1995; 270: 1602–1611. Http://www.ncbi.nlm.nih.gov/pubmed/7829491.

Mitra K, Ubarretxena-Belandia I, Taguchi T, Warren G, Engelman DM. Modulation of the bilayer thickness of exocytic pathway membranes by membrane proteins rather than cholesterol. Proc Natl Acad Sci U S A 2004; 101: 4083–8. Eng.

Miyamoto S, Kollman PA. SETTLE: an analytical version of the SHAKE and RATTLE algorithm for rigid water models. J Comput Chem 1992; 13: 952–962. Http://portal.acm.org/citation.cfm?id=148324.

Monticelli L Personal communication; .

Monticelli L, Kandasamy S, Periole X, Larson R, Tieleman P, Marrink SJ. The MARTINI Coarse-Grained Force Field: Extension to Proteins. J Chem Theory Comput 2008; .

Monticelli L, Robertson KM, MacCallum JL, Tieleman DP. Computer simulation of the KvAP voltage-gated potassium channel: steered molecular dynamics of the voltage sensor. FEBS Lett 2004; 564: 325–32. Eng.

Mossman KD, Campi G, Groves JT, Dustin ML. Altered TCR signaling from geometrically repatterned immunological synapses. Science 2005; 310: 1191–3. Eng.

MS S, H W. Hinges, swivels and switches: the role of prolines in signalling via transmembrane alpha-helices. Trends Pharmacol Sci 2000; 21(11): 445–451.

Mukhopadhyay S, Cho W. Interactions of annexin V with phospholipid monolayers. Biochim Biophys Acta 1996; 1279: 58–62. Eng.

Myers JK, Pace CN, Scholtz JM. Trifluoroethanol effects on helix propensity and electrostatic interactions in the helical peptide from ribonuclease T1. Protein Sci 1998; 7: 383–8. Eng.

Nelson D, Young K. Contributions of PBP 5 and dd-Carboxypeptidase Penicillin Binding Proteins to Maintenance of Cell Shape in Escherichia coli. Journal of Bacteriology 2001; 183(10): 3055–3064.

Niemela P, Hyvanen M, Vattulainen I. Atom-scale molecular interactions in lipid raft mixtures. Biochimica Et Biophysica Acta 2009; 1788: 122–135. Http://www.ncbi.nlm.nih.gov/pubmed/18817748.

Nina M, Berneche S, Roux B. Anchoring of a monotopic membrane protein: the binding of prostaglandin H2 synthase-1 to the surface of a phospholipid bilayer. Eur Biophys J 2000; 29: 439–54. Eng.

Norman KE, Nymeyer H. Indole localization in lipid membranes revealed by molecular simulation. Biophys J 2006; 91: 2046–54. Eng.

Nossal R, Zimmerberg J. Endocytosis: curvature to the ENTH degree. Curr Biol 2002; 12: R770–2. Eng.

Okuda S, Watanabe S, Tokuda H. A short helix in the C-terminal region of LolA is important for the specific membrane localization of lipoproteins. FEBS Lett 2008; 582: 2247–51. Eng.

Oloo EO, Fung EY, Tieleman DP. The dynamics of the MgATP-driven closure of MalK, the energy-transducing subunit of the maltose ABC transporter. J Biol Chem 2006; 281: 28397–407. Eng.

Oostenbrink C, Villa A, Mark AE, van Gunsteren WF. A biomolecular force field based on the free enthalpy of hydration and solvation: the GROMOS force-field parameter sets 53A5 and 53A6. J Comput Chem 2004; 25: 1656–76. Eng.

Ozdirekcan S, Etchebest C, Killian JA, Fuchs PFJ. On the Orientation of a Designed Transmembrane Peptide: Toward the Right Tilt Angle? Journal of the American Chemical Society 2007; 129: 15174–15181.

Pace CN, Scholtz JM. A helix propensity scale based on experimental studies of peptides and proteins. Biophys J 1998; 75: 422–7. Eng.

Pasenkiewicz-Gierula M, Subczynski WK, Kusumi A. Rotational diffusion of a steroid molecule in phosphatidylcholine-cholesterol membranes: fluid-phase microimmiscibility in unsaturated phosphatidylcholine-cholesterol membranes. Biochemistry 1990; 29: 4059–69. Eng.

Patel AJ, Lazdunski M, Honore E. Lipid and mechano-gated 2P domain K(+) channels. Curr Opin Cell Biol 2001; 13: 422–8. Eng.

Paumard P, Vaillier J, Coulary B, Schaeffer J, Soubannier V, Mueller DM, et al. The ATP synthase is involved in generating mitochondrial cristae morphology. EMBO J 2002; 21: 221–30. Eng.

Peter BJ, Kent HM, Mills IG, Vallis Y, Butler PJ, Evans PR, et al. BAR domains as sensors of membrane curvature: the amphiphysin BAR structure. Science 2004; 303: 495–9. Eng.

Petukhov M, Uegaki K, Yumoto N, Serrano L. Amino acid intrinsic alpha-helical propensities III: positional dependence at several positions of C terminus. Protein Sci 2002; 11: 766–77. Eng.

Petukhov M, Uegaki K, Yumoto N, Yoshikawa S, Serrano L. Position dependence of amino acid intrinsic helical propensities II: non-charged polar residues: Ser, Thr, Asn, and Gln. Protein Sci 1999; 8: 2144–50. Eng.

Ploeg P van der BH. Molecular dynamics simulation of a bilayer membrane. J Chem Phys 1982; 76: 3271–3276. Molecular dynamics simulation of a bilayer membrane.

Pohorille A, Wilson MA, New MH, Chipot C. Concentrations of anesthetics across the water-membrane interface; the Meyer-Overton hypothesis revisited. Toxicol Lett 1998; 100-101: 421–30. Eng.

Praefcke GJ, McMahon HT. The dynamin superfamily: universal membrane tubulation and fission molecules? Nat Rev Mol Cell Biol 2004; 5: 133–47. Eng.

Przestalski S, Sarapuk J, Kleszczynska H, Gabrielska J, Hladyszowski J, Trela Z, et al. Influence of amphiphilic compounds on membranes. Acta Biochim Pol 2000; 47: 627–38. Eng.

Rabouille C, Klumperman J. Opinion: The maturing role of COPI vesicles in intra-Golgi transport. Nat Rev Mol Cell Biol 2005; 6: 812–7. Eng.

Rajendran L, Simons K. Lipid rafts and membrane dynamics. Journal of Cell Science 2005; 118: 1099–1102.

Ramirez-Alvarado M, Kortemme T, Blanco FJ, Serrano L. Beta-hairpin and beta-sheet formation in designed linear peptides. Bioorg Med Chem 1999; 7: 93–103. Eng.

Resh MD. Trafficking and signaling by fatty-acylated and prenylated proteins. Nat Chem Biol 2006; 2: 584–90. Eng.

Risselada H, Marrink S. The molecular face of lipid rafts in model membranes. Proc Natl Acad Sci U S A 2008; 105: 17367–72. Eng.

Risselada H, Marrink S. Curvature effects on lipid packing and dynamics in liposomes revealed by coarse grained molecular dynamics simulations. Phys Chem Chem Phys 2009; 11: 2056–67. Eng.

Robertson J. The ultrastructure of cell membranes and their derivatives. Biochem Soc Symp 1959; 16: 3–43.

Robertson KM, Tieleman DP. Molecular basis of voltage gating of OmpF porin. Biochem Cell Biol 2002; 80: 517–23. Eng.

Roux A, Cuvelier D, Nassoy P, Prost J, Bassereau P, Goud B. Role of curvature and phase transition in lipid sorting and fission of membrane tubules. EMBO J 2005; 24: 1537–45. Eng.

Salnikov ES, Mason AJ, Bechinger B. Membrane order perturbation in the presence of antimicrobial peptides by (2)H solid-state NMR spectroscopy. Biochimie 2009a; Eng.

Salnikov ES, Zotti MD, Formaggio F, Li X, Toniolo C, O'Neil J D, et al. Alamethicin Topology in Phospholipid Membranes by Oriented Solid-state NMR and EPR Spectroscopies: a Comparison. J Phys Chem B 2009b; Eng.

Samatey FA, Xu C, Popot JL. On the distribution of amino acid residues in transmembrane alpha-helix bundles. Proc Natl Acad Sci U S A 1995; 92: 4577–81. Eng.

Sanderson JM. Peptide-lipid interactions: insights and perspectives. Org Biomol Chem 2005; 3: 201–12. Eng.

Sangiorgio V, Pitto M, Palestini P, Masserini M. GPI-anchored proteins and lipid rafts. Ital J Biochem 2004; 53: 98–111. Eng.

Sansom MS, Bond P, Beckstein O, Biggin PC, Faraldo-Gomez J, Law RJ, et al. Water in ion channels and pores–simulation studies. Novartis Found Symp 2002; 245: 66–78; discussion 79–83, 165–8. Eng.

Sapay N. Les peptides dacrages a linterace membranaire analyses structurales par RMN et dynamique moleculaire et developpement dune methode de prediction bioinformatique. PhD Thesis, 2006.

Sapay N, Guermeur Y, Delage G. Prediction of amphipathic in-plane membrane anchors in monotopic proteins using a SVM classifier. BMC Bioinformatics 2006a; 7: 255–255. Http://www.ncbi.nlm.nih.gov/pubmed/16704727.

Sapay N, Montserret R, Chipot C, Brass V, Moradpour D, Delage G, et al. NMR structure and molecular dynamics of the in-plane membrane anchor of nonstructural protein 5A from bovine viral diarrhea virus. Biochemistry 2006b; 45: 2221–2233. Http://www.ncbi.nlm.nih.gov/pubmed/16475810.

Sapay N, Tieleman DP, Scott EF. Chapter 4 Molecular Dynamics Simulation of Lipid-Protein Interactions. In Computational Modeling of Membrane Bilayers, volume Volume 60. Academic Press, 2008; pp. 111–130.

Sato H, Feix JB. Peptide-membrane interactions and mechanisms of membrane destruction by amphipathic alpha-helical antimicrobial peptides. Biochim Biophys Acta 2006; 1758: 1245–56. Eng.

Schindler M, Ahmed I, Kamal J, Nur EKA, Grafe TH, Young Chung H, et al. A synthetic nanofibrillar matrix promotes in vivo-like organization and morphogenesis for cells in culture. Biomaterials 2005; 26: 5624–31. Eng.

Schulz G. The structure of bacterial outer membrane proteins. Biochim Biophys Acta 2002; 1565(2): 3 08–317.

Seelig J. Thermodynamics of lipid-peptide interactions. Biochim Biophys Acta 2004; 1666: 40–50. Eng.

Sens P, Gov N. Force balance and membrane shedding at the red-blood-cell surface. Phys Rev Lett 2007; 98: 018102. Eng.

Sevcsik E, Pabst G, Jilek A, Lohner K. How lipids influence the mode of action of membrane-active peptides. Biochimica Et Biophysica Acta 2007; 1768: 2586–2595.

Shaitan K, Antonov M, Tourleigh Y, Levtsova O, Tereshkina K, Nikolaev I, et al. Comparative study of molecular dynamics, diffusion, and permeability for ligands in biomembranes of different lipid composition. Biochemistry (Moscow) Supplemental Series A: Membrane and Cell Biology 2008a; 2: 73–81.

Shaitan KV, Levtsova OV, Tereshkina KB, Orshanskii IA, Antonov M, Akimov MP, et al. [Molecular dynamics of oligopeptides. A comparative study of the interactions of amino acid residues in dipeptide structures]. Biofizika 2008b; 53: 550–5. Rus.

Sheetz MP, Painter RG, Singer SJ. Biological membranes as bilayer couples. III. Compensatory shape changes induced in membranes. J Cell Biol 1976; 70: 193–203. Eng.

Sheetz MP, Singer SJ. Biological membranes as bilayer couples. A molecular mechanism of drug-erythrocyte interactions. Proc Natl Acad Sci U S A 1974; 71: 4457–61. Eng.

Shepherd CM, Vogel HJ, Tieleman DP. Interactions of the designed antimicrobial peptide MB21 and truncated dermaseptin S3 with lipid bilayers: molecular-dynamics simulations. Biochem J 2003; 370: 233–43. Eng.

Singer SJ, Nicolson GL. The fluid mosaic model of the structure of cell membranes. Science 1972; 175: 720–31. Eng.

Smith CJ, Grigorieff N, Pearse BM. Clathrin coats at 21 A resolution: a cellular assembly designed to recycle multiple membrane receptors. EMBO J 1998; 17: 4943–53. Eng.

Sorre B, Callan-Jones A, Manneville JB, Nassoy P, Joanny JF, Prost J, et al. Curvature-driven lipid sorting needs proximity to a demixing point and is aided by proteins. Proceedings of the National Academy of Sciences 2009; 106: 5622–5626. Http://www.pnas.org/content/106/14/5622.abstract.

Sparr E, Ash WL, Nazarov PV, Rijkers DT, Hemminga MA, Tieleman DP, et al. Self-association of transmembrane alpha-helices in model membranes: importance of helix orientation and role of hydrophobic mismatch. J Biol Chem 2005; 280: 39324–31. Eng.

Spoel DVD, Lindahl E, Hess B, Groenhof G, Mark AE, Berendsen HJC. GROMACS: Fast, flexible, and free. Journal of Computational Chemistry 2005; 26: 1701–1718.

Sprong H, van der Sluijs P, van Meer G. How proteins move lipids and lipids move proteins. Nat Rev Mol Cell Biol 2001; 2: 504–13. Eng.

Stagg SM, LaPointe P, Razvi A, Gurkan C, Potter CS, Carragher B, et al. Structural basis for cargo regulation of COPII coat assembly. Cell 2008; 134: 474–84. Eng.

Stahelin RV, Long F, Peter BJ, Murray D, De Camilli P, McMahon HT, et al. Contrasting membrane interaction mechanisms of AP180 N-terminal homology (ANTH) and epsin N-terminal homology (ENTH) domains. J Biol Chem 2003; 278: 28993–9. Eng.

Stelzer W, Poschner BC, Stalz H, Heck AJ, Langosch D. Sequence-Specific Conformational Flexibility of SNARE Transmembrane Helices Probed by Hydrogen/Deuterium Exchange. Biophysical Journal 2008; 95: 1326–1335. Http://www.pubmedcentral.nih.gov/articlerender.fcgi?artid=2479619.

Stevens TJ, Arkin IT. Do more complex organisms have a greater proportion of membrane proteins in their genomes? Proteins 2000; 39: 417–20. Eng.

Subczynski WK, Markowska E, Gruszecki WI, Sielewiesiuk J. Effects of polar carotenoids on dimyristoylphosphatidylcholine membranes: a spin-label study. Biochim Biophys Acta 1992; 1105: 97–108. Eng.

Subczynski WK, Markowska E, Sielewiesiuk J. Spin-label studies on phosphatidylcholine-polar carotenoid membranes: effects of alkyl-chain length and unsaturation. Biochim Biophys Acta 1993; 1150: 173–81. Eng.

Sweitzer SM, Hinshaw JE. Dynamin undergoes a GTP-dependent conformational change causing vesiculation. Cell 1998; 93: 1021–9. Eng.

Takaoka Y, Pasenkiewicz-Gierula M, Miyagawa H, Kitamura K, Tamura Y, Kusumi A. Molecular dynamics generation of nonarbitrary membrane models reveals lipid orientational correlations. Biophys J 2000; 79: 3118–38. Eng.

Tarricone C, Xiao B, Justin N, Walker PA, Rittinger K, Gamblin SJ, et al. The structural basis of Arfaptin-mediated cross-talk between Rac and Arf signalling pathways. Nature 2001; 411: 215–9. Eng.

Tieleman DP. Computer simulations of transport through membranes: passive diffusion, pores, channels and transporters. Clin Exp Pharmacol Physiol 2006; 33: 893–903. Eng.

Tieleman DP, Berendsen HJ, Sansom MS. Voltage-dependent insertion of alamethicin at phospholipid/water and octane/water interfaces. Biophysical Journal 2001a; 80: 331–346. Http://www.ncbi.nlm.nih.gov/pubmed/11159406.

Tieleman DP, Biggin PC, Smith GR, Sansom MS. Simulation approaches to ion channel structure-function relationships. Q Rev Biophys 2001b; 34: 473–561. Eng.

Tieleman DP, Forrest LR, Sansom MS, Berendsen HJ. Lipid properties and the orientation of aromatic residues in OmpF, influenza M2, and alamethicin systems: molecular dynamics simulations. Biochemistry 1998; 37: 17554–61. Eng.

Tieleman DP, MacCallum JL, Ash WL, Kandt C, Xu Z, Monticelli L. Membrane protein simulations with a united-atom lipid and all-atom protein model: lipid protein interactions, side chain transfer free energies and model proteins. Journal of Physics: Condensed Matter 2006; 18: S1221–S1234–S1221–S1234. Http://www.iop.org/EJ/abstract/0953-8984/18/28/S07.

Tien A TH & Ottova-Leitmannova. Membrane Biophysics. 2000. Membrane Biophysics.

Tristram-Nagle S, Nagle JF. Lipid bilayers: thermodynamics, structure, fluctuations, and interactions. Chemistry and Physics of Lipids 2004; 127: 3–14. Http://www.ncbi.nlm.nih.gov/pubmed/14706737.

Tristram-Nagle S, Petrache HI, Nagle JF. Structure and interactions of fully hydrated dioleoylphosphatidylcholine bilayers. Biophys J 1998; 75: 917–25. Eng.

Turner MS, Sens P. Gating-by-tilt of mechanically sensitive membrane channels. Phys Rev Lett 2004; 93: 118103. Eng.

Ubarretxena-Belandia I, Engelman D. Helical membrane proteins: diversity of functions in the context of simple architecture. Curr Opin Struct Biol 2001; 11: 370–6376.

Ulmschneider JP. Peptide Partitioning and folding into lipid bilayers. J Chem Theory and Comput 2009; in press. Peptide Partitioning and folding into lipid bilayers.

Ulmschneider JP, Ulmschneider MB. Sampling efficiency in explicit and implicit membrane environments studied by peptide folding simulations. Proteins 2009; 75: 586–97. Eng.

Ulmschneider JP, Ulmschneider MB, Di Nola A. Monte Carlo vs molecular dynamics for all-atom polypeptide folding simulations. J Phys Chem B 2006; 110: 16733–42. Eng.

Ulmschneider JP, Ulmschneider MB, Di Nola A. Monte Carlo folding of trans-membrane helical peptides in an implicit generalized Born membrane. Proteins 2007; 69: 297–308. Eng.

Ulmschneider MB, Ulmschneider JP. Membrane adsorption, folding, insertion and translocation of synthetic trans-membrane peptides. Mol Membr Biol 2008; 25: 245–57. Eng.

Vale RD, Hotani H. Formation of membrane networks in vitro by kinesin-driven microtubule movement. J Cell Biol 1988; 107: 2233–41. Eng.

Varadi A, Johnson-Cadwell LI, Cirulli V, Yoon Y, Allan VJ, Rutter GA. Cytoplasmic dynein regulates the subcellular distribution of mitochondria by controlling the recruitment of the fission factor dynamin-related protein-1. J Cell Sci 2004; 117: 4389–400. Eng.

Veatch SL. Lipids out of order. Nature Chemical Biology 2008; 4: 225–226.

Veiga E, Cossart P. The role of clathrin-dependent endocytosis in bacterial internalization. Trends Cell Biol 2006; 16: 499–504. Eng.

Viguera AR, Serrano L. Stable proline box motif at the N-terminal end of alpha-helices. Protein Sci 1999; 8: 1733–42. Eng.

Voeltz GK, Prinz WA, Shibata Y, Rist JM, Rapoport TA. A class of membrane proteins shaping the tubular endoplasmic reticulum. Cell 2006; 124: 573–86. Eng.

Voeltz PW GK. Sheets, ribbons and tubules -how organelles get their shape. Nature 2007; 8: 258. Sheets, ribbons and tubules -how organelles get their shape.

Vogel V, Sheetz M. Local force and geometry sensing regulate cell functions. Nat Rev Mol Cell Biol 2006; 7: 265–75. Eng.

Wang Q, Kaan HYK, Hooda RN, Goh SL, Sondermann H. Structure and plasticity of Endophilin and Sorting Nexin 9. Structure (London, England: 1993) 2008; 16: 1574–1587. Http://www.ncbi.nlm.nih.gov/pubmed/18940612.

White S. Hydropathy plots and the prediction of membrane protein topology. New York: Oxford Univ. Press, 1994. Hydropathy plots and the prediction of membrane protein topology.

White SH. Membrane protein insertion: the biology-physics nexus. J Gen Physiol 2007; 129: 363–9. Eng.

White SH, Wimley WC. Hydrophobic interactions of peptides with membrane interfaces. Biochim Biophys Acta 1998; 1376: 339–52. Eng.

White SH, Wimley WC. Membrane protein folding and stability: physical principles. Annu Rev Biophys Biomol Struct 1999; 28: 319–65. Eng.

White SH, Wimley WC, Ladokhin AS, Hristova K. Protein folding in membranes: determining energetics of peptide-bilayer interactions. Methods Enzymol 1998; 295: 62–87. Eng.

White SH WM. The liquid-crystallographic structure of fluid lipid bilayer membranes. Boston: Birkh!auser, 1996. The liquid-crystallographic structure of fluid lipid bilayer membranes.

Wiener MC, King GI, White SH. Structure of a fluid dioleoylphosphatidylcholine bilayer determined by joint refinement of x-ray and neutron diffraction data. I. Scaling of neutron data and the distributions of double bonds and water. Biophys J 1991; 60: 568–76. Eng.

Wiener MC, White SH. Fluid bilayer structure determination by the combined use of x-ray and neutron diffraction. I. Fluid bilayer models and the limits of resolution. Biophys J 1991a; 59: 162–73. Eng.

Wiener MC, White SH. Fluid bilayer structure determination by the combined use of x-ray and neutron diffraction. II. "Composition-space" refinement method. Biophys J 1991b; 59: 174–85. Eng.

Wimley WC, Creamer TP, White SH. Solvation energies of amino acid side chains and backbone in a family of host-guest pentapeptides. Biochemistry 1996a; 35: 5109–24. Eng.

Wimley WC, Gawrisch K, Creamer TP, White SH. Direct measurement of salt-bridge solvation energies using a peptide model system: implications for protein stability. Proc Natl Acad Sci U S A 1996b; 93: 2985–90. Eng.

Wimley WC, Hristova K, Ladokhin AS, Silvestro L, Axelsen PH, White SH. Folding of beta-sheet membrane proteins: a hydrophobic hexapeptide model. J Mol Biol 1998; 277: 1091–110. Eng.

Wimley WC, White SH. Experimentally determined hydrophobicity scale for proteins at membrane interfaces. Nat Struct Biol 1996; 3: 842–8. Eng.

Woolf TB, Roux B. Molecular dynamics simulation of the gramicidin channel in a phospholipid bilayer. Proc Natl Acad Sci U S A 1994; 91: 11631–5. Eng.

Xiang TX, Anderson BD. Influence of chain ordering on the selectivity of dipalmitoylphosphatidylcholine bilayer membranes for permeant size and shape. Biophys J 1998a; 75: 2658–71. Eng.

Xiang TX, Anderson BD. Phase structures of binary lipid bilayers as revealed by permeability of small molecules. Biochim Biophys Acta 1998b; 1370: 64–76. Eng.

Yefimov S, van der Giessen E, Onck PR, Marrink SJ. Mechanosensitive membrane channels in action. Biophysical Journal 2008; 94: 2994–3002. Http://www.ncbi.nlm.nih.gov/pubmed/18192351.

Yesylevskyy S, Marrink SJ, Mark AE. Alternative mechanisms for the interaction of the cell-penetrating peptides penetratin and the TAT peptide with lipid bilayers. Biophysical Journal 2009; 97: 40–49. Http://www.ncbi.nlm.nih.gov/pubmed/19580742.

Yin Y, Arkhipov A, Schulten K. Simulations of membrane tubulation by lattices of amphiphysin N-BAR domains. Structure 2009; 17: 882–92. Eng.

Zimmerberg J, Kozlov MM. How proteins produce cellular membrane curvature. Nat Rev Mol Cell Biol 2006; 7: 9–19. Eng.

Zimmerberg J, McLaughlin S. Membrane curvature: how BAR domains bend bilayers. Curr Biol 2004; 14: R250–2. Eng.

Nomenclature

AC Acyl Chains

AH Amphipathic alpha-Helix

ALPS Amphipatic Lipid Packing Sensor

AMP Antimicrobial Peptides

BAR Bin/amphiphysin/Rvs

COPI and II Coat protein complex I and II

DAG diacylglycerol

DMPC Dimyristoylphosphatidylcholine

DOG dioleoylglycerol

DOPC Dioleoylphosphatidilcholine

ER Endoplamic Reticulum

GAP GTPase activating proteins

GUV Giant Unilamellar Vesicles

HC Hydrophobic Core

HG Headgroup

IMM Inner Mitochondrial Membranes

LH1-LH2 Light Harvesting Complexes I and II

LUCA Last Universal Common Ancestor

LWF-A ALPS L207A-W211A-F214A triple mutant

MD Molecular Dynamics

NMR Nuclear Magnetic Resonance

NPT A simulation where the number of particles, the pressure and the temperature are constant

ORFs Open Reading Frames

PA Phosphatidic Acid

PC Phosphatidylcholine

PDB Protein Database

PE Phosphatidylethanolamine

PI Phosphatidylinositol

POPC Dipalmitoylphosphatidilcholine

PP Packing Parameter

PS Phosphatidylserine

TFE Trifluoroethanol

TM Transmembrane